P.Ya. UFIMTSEV

METHOD OF EDGE WAVES IN THE PHYSICAL THEORY OF DIFFRACTION

P.Ya. UFIMTSEV

METHOD OF EDGE WAVES IN THE PHYSICAL THEORY OF DIFFRACTION

TABLE OF CONTENTS

The book is a monograph written as a result of research by the author. The diffraction of plane electromagnetic waves by ideally conducting bodies, the surface of which have discontinuities, is investigated in the book. The linear dimensions of the bodies are assumed to be large in comparison with the wavelength. The method developed in the book takes into account the perturbation of the field in the vicinity of the surface discontinuity and allows one to substantially refine the approximations of geometric and physical optics. Expressions are found for the fringing field in the distant zone. A numerical calculation is performed of the scattering characteristics, and a comparison is made with the results of rigorous theory and with experiments.

The book is intended for physicists and radio engineers who are interested in diffraction phenomena, and also for students of advanced courses and aspirants who are specializing in antennas and the propagation of radio waves.

FOREWORD

First of all, one should explain the term "physical theory of diffraction". In order to do this, let us discuss briefly the historical development of diffraction theory.

If one investigates, for example, the incidence of a plane electromagnetic wave on a body which conducts well, all the dimensions of which are large in comparison with the wavelength, then the simplest solution of this problem may be obtained by means of geometric optics. It is known that in a number of cases one must add to geometric optics the laws of physical optics which are connected with the names of Huygens, Fresnel, Kirchhoff and Cotler. Physical optics uses, together with the field equations, the assumption that in the vicinity of a reflecting body geometric optics is valid.

At the start of the Twentieth Century, a new division of mathematical physics appeared — the mathematical theory of diffraction. Using it, rigorous solutions to the problem of diffraction by a wedge, sphere, and infinite cylinder were obtained. Subsequently, other rigorous solutions were added; however, the total number of solutions was relatively small. For sufficiently short waves (in comparison with the dimensions of the body or other characteristic distances) these solutions, as a rule, are ineffective. Here the direct numerical methods also are unsuitable.

Hence, an interest arose in approximation (asymptotic) methods which would allow one to investigate the diffraction of sufficiently short waves by various bodies, and would lead to more precise and reliable quantitative results than does geometric or physical optics. Obviously, these methods must in some way be considered the most important results extracted from the mathematical theory of diffraction.

In the "geometric theory of diffraction" proposed by Keller, the results obtained in the mathematical theory of diffraction of short waves were exactly the ones which were used and generalized. Here, the concept of diffraction rays advanced to the forefront. This concept was expressed rather as a physical hypothesis and was not suitable for representing the field in all of space: it was not usable where the formation of the diffraction field takes place (at the caustic, at the boundary of light and shadow, etc.). Here it is impossible to talk about rays, and one must use a wave interpretation.

What has been said above makes it clear why a large number of works appeared in which the diffraction of short waves was investigated by other methods. Among those applied to reflecting bodies with abrupt surface discontinuities or with sharp edges (strip, disk, finite cylinder or cone, etc.) one should first of all mention the works of P. Ya. Ufimtsev. These works began to appear in print in 1957, and it is on the basis of them that this book was written.

P. Ya. Ufimtsev studied the scattering characteristics by such bodies by taking into account, besides the currents being excited on the surface of the body according to the laws of geometric optics (the "uniform part of the current" according to his terminology), the additional currents arising in the vicinity of the edges or borders which have the character of edge waves and rapidly attenuate with increasing distance from the edge or border (the "nonuniform part of the current"). One may find the radiation field created by the additional currents by comparing the edge or border with the edge of an infinite wedge or the border of a half-plane. In certain cases, one is obliged to consider the diffraction interaction of the various edges — that is, the fact that the wave created by one edge and propagated past another edge is diffracted by it (secondary diffraction).

Such an approach to the diffraction of short waves has great physical visualizability and allows one to obtain rather simple approximation expressions for the field scattered by various metal bodies. This approach may be called the physical theory of diffraction.

This name is applied to many works on the diffraction of short waves in which the mathematical difficulties are bypassed by means of physical considerations.

It is clear that the physical theory of diffraction is a step forward in comparison with physical optics, which in general neglects the additional (edge) currents. The results obtained in this book show that with a given wavelength the physical theory of diffraction gives a better precision than physical optics, and with a given precision the physical theory of diffraction allows one to advance into the longer wave region and, in particular, to obtain a number of results which are of interest for radar where the ratios of the dimensions of the bodies to the wavelength do not reach such large values as in optics.

In addition, the physical theory of diffraction encompasses a number of interesting phenomena which are entirely foreign to physical optics. Thus, in a number of cases the additional currents give, not a small correction to the radiation field, but the main contribution to this field (see especially Chapters IV and V). If a plane wave is diffracted by a thin straight wire (a passive vibrator), then the additional current falls off very slowly as one goes further from the end of the wire. Therefore, the solution is obtained by summing the entire array of diffraction waves (secondary, tertiary, etc.) which successively arise as a consequence of the reflection of the currents from the ends of the wires. It has a resonance character. Thus, the problem of the scattering of the plane wave by a finite length wire which is a diffraction problem of a slightly unusual type is solved in Chapter VII. The resulting solution is applicable under the condition that the diameter of the wire is small in comparison with the wavelength and length of the wire, and the ratio of the length of the wire to the wavelength is arbitrary.

The final equations which are derived in this book and are used for calculations are not asymptotic in the strict sense of the word.

Therefore, it is natural to pose the question: in what way will the subsequent asymptotic equations differ from them when at last one obtains them in the mathematical theory of diffraction? One can say beforehand that the main term of the asymptotic expansion will not, in the general case, agree with the solution obtained on the basis of physical considerations: other (as a rule more complicated) slowly varying functions which determine the decay of the fields and currents as one goes further from the edges and borders, and also the diffraction interaction of the edges and the shadowing of the edge waves will figure in the main term. However, the refinement of the slowly varying functions in the expression for the diffraction field is not able to seriously influence the quantitative relationships. This is seen from a comparison of the results obtained in this book with calculations based on rigorous theory and other approximation equations, and also with the results of measurements.

The relationships obtained in this book also should help the development of asymptotic methods in the mathematical theory of diffraction, since they suggest the character of the approximations and the structure of the desired solution.

L. A. Vaynshteyn

INTRODUCTION

In recent years, there has been a noticeable increase of interest in the diffraction of electromagnetic waves by metal bodies of complex shape. Such diffraction problems with a rigorous methematical formulation reduce to an interpretation of the wave equation or Maxwell equations with consideration of the boundary conditions on the body's surface. However, one cannot succeed in finding solutions in the case of actual bodies of a complicated configuration. This may be done only for bodies of the simplest geometric shape — such as an infinitely long cylinder, a sphere, a disk, etc. It turns out that the resulting solutions permit one to effectively calculate the diffraction field only under the condition that the wavelength is larger than, or comparable to, the finite dimensions of the body. In the "quasi-optical"case, when the wavelength is a great deal less than the dimensions of the body, the rigorous solutions usually lose their practical value, and it is necessary to add to them laborious and complicated asymptotic studies. Here, the numerical methods for the solution of boundary value problems also become ineffective. Therefore, in the theory of diffraction the approximation methods which allow one to study the diffraction of sufficiently short waves by various bodies acquire great importance.

The field scattered by a given body may be calculated approximately by means of geometric optics laws (the reflection equations, see,for example [1-3]), from the principles of Huygens-Fresnel and from the equations of Kirchhoff and Cotler [3-6].

The most common method of calculation in the quasi-optic case is the principle of Huygens-Fresnel in the formulation of Kirchhoff and Cotler — the so-called physical optics approach. The essence of this method may be summarized as follows.

Let a plane electromagnetic wave fall on some ideally conducting body which is found in free space. In the physical optics approach, the surface current density which is induced by this wave on the irradiated part of the body's surface is (in the absolute system of units) equal to

$$j^0 = \frac{c}{2\pi}[nH_0]. \qquad (A)$$

where c is the speed of light in a vacuum, **n** is the external normal to the body's surface, H_0 is the magnetic field of the incident wave. On the darkened side of the body the surface current is assumed to be equal to zero ($j^0 = 0$). Equation (A) means that on each element of the body's irradiated surface the same current is excited as on an ideally conducting surface of infinite dimensions tangent to this element. The scattered field created by the current (A) is then found by means of Maxwell's equations.

It is obvious that in reality the current induced on the body's surface will differ (as a consequence of the curve of the surface) from the current j^0. The precise expression for the surface current density has the form

$$j = j^0 + j^1. \qquad (B)$$

where j^1 is the surface density of the additional current which results from the curve of the surface. By the curve of the surface, we mean any of its deviations from an infinite plane (a smooth curve, a sharp bend, a bulge, a hole, etc.). If the body is convex and smooth and its dimensions and radii of curvature are large in comparison with the wavelength, then the additional current is concentrated mainly in the vicinity of the boundary between the illuminated and shadowed parts of the body's surface. But if the body has an edge, bend, or point, then the additional current also arises near them. The additional current density is comparable to the density j^0, as a rule, only at distances of the order of a wavelength from the corresponding edge, bend, or point. Thus, if the body's dimensions

significantly exceed the wavelength, the additional currents occupy a comparatively small part of its surface.

Since the current excited by the plane wave on an ideally conducting surface is distributed uniformly over it (the absolute magnitude of its surface density is constant) then the vector j^0 may be called the "uniform" part of the surface current. The additional current j^1 which is caused by the curve of the body's surface we will henceforth call the "nonuniform" part of the current. In the physical optics approach, only the uniform part of the current is considered. Therefore, it is no wonder that in a number of cases it gives unsatisfactory results. For a more precise calculation, it is necessary to also take into account the nonuniform part of the current.

In this book, the results of the author relating to the approximation solution of diffraction problems are discussed and systematized. Essentially, these results were briefly discussed in a number of papers [7-14]. Roughly at the same time, the works of other authors devoted to similar problems appeared. We will discuss them in more detail (in §25) after the reader becomes accustomed to the concepts being used in diffraction problems of this type. For the present, let us only note that in these works, as a rule, other methods are used.

In the book, problems of the diffraction of plane electromagnetic waves by complex metal bodies, the surfaces of which have discontinuities (edges), are investigated. The dimensions of the bodies are assumed to be large in comparison with the wavelength, and their surface is assumed to be ideally conducting.

Obviously, if the edges are sufficiently far from one another, then the current flowing on a small element of the body's surface in the vicinity of its discontinuity may be approximately considered to be the same as on a corresponding infinite dihedral angle (a wedge). In fact, in Chapter I it is shown (see also [5] §20) that the nonuniform part of the current on a wedge has the character of an edge

wave which rapidly decreases with the distance from the edge. Therefore, one may consider that the nonuniform part of the current is concentrated mainly in the vicinity of the discontinuity. By means of this physically obvious assumption, the field scattered by a strip (Chapter I), by a disk (Chapter II), by a finite length cylinder (Chapter III) and by certain other bodies of rotation (Chapter IV) is calculated.

For a more precise calculation, however, it is necessary to keep in mind that the actual current distribution in the vicinity of the body's edges differs from the current distribution near the edge of the wedge. Actually, the edge wave corresponding to the nonuniform part of the current, propagated along the body's surface, reaches the adjacent edge and undergoes diffraction by it, exciting secondary edge waves. The latter in turn produce new edge waves, etc. If all the dimensions of the body are large in comparison with the wavelength, then as a rule it is sufficient to consider only the secondary diffraction. This phenomenon is studied in Chapter V using the example of a strip and disk.

In the case of a narrow cylindrical conductor of finite length, the edge waves of the current decrease very slowly with the distance from each end. Therefore, here it is impossible to limit oneself to a consideration only of secondary diffraction, and it is necessary to investigate the multiple diffraction of edge waves. Chapter VII is devoted to this problem.

The uniform and nonuniform parts of the current are more than auxiliary concepts which are useful in solving diffraction problems. In Chapter VI it is shown that one is able experimentally to separate from the total fringing field that part of it which is created by the nonuniform part of the current. There, it is also shown that the depolarization phenomenon of the reflected signal is caused only by the nonuniform part of the current.

Let us note the following feature of the method discussed in the book. A physical representation of the nonuniform part of the current is widely used in the book, but nowhere are its explicit mathematical expressions cited. This part of the current is generally not expressed in terms of well-known functions. Obviously a direct integration of the currents when calculating the fringing field is able to lead only to very complicated and immense equations. Therefore, we will find the fringing field created by the nonuniform part of the current on the basis of indirect considerations without direct integration of it (see especially Chapters I - IV).

The method by which the diffraction problems are solved in this book may be briefly summarized as follows. We will seek an approximate solution of the diffraction problem for a certain body by first having studied diffraction by its separate geometric elements. For example, for a finite cylinder such elements are: the lateral surface as part of an infinite cylindrical surface, each base as part of a plane, each section of the base rim as the edge of a wedge (the curvature of the rim in the first approximation may be neglected). Having studied the diffraction by the separate elements of the body, we will obtain a representation of the nonuniform part of the current and of the field which is radiated by it. Then secondary, tertiary, etc. diffraction is studied — that is, the diffraction interaction of the various elements of the body is taken into account.

This method appeals to physical considerations, not only when formulating the problem but also in its solution process, and in this way differs from the methods of the mathematical theory of diffraction. Therefore, such a method may be referred to as the physical theory of diffraction.

A whole series of other diffraction studies which appeared in the last five to ten years also are able to relate to the physical theory of diffraction. The first work which contained the idea of the physical theory of diffraction is evidently the paper of Schwarzschild [15] which was published at the beginning of this century and was devoted to diffraction by a slit.

One should note that approximate solutions of diffraction problems would be impossible without the use of the results obtained in the mathematical theory of diffraction. In particular, the rigorous solution to the problem of diffraction by a wedge which is attributed to Sommerfeld [16] is widely used in this book. In Chapter I this solution is obtained by another method. The works of Fok [17, 18] served as the starting point for numerous studies on diffraction by smooth convex bodies. The rigorous solution of the problem of diffraction at the open end of a wave guide [19] revealed the mechanism for the formation of primary diffraction waves, and their shadowing by the opposite end of the wave guide. The rigorous theory as applied to a strip and disk allows us to examine the precision of the approximation theory (see Chapter V).

CHAPTER I

DIFFRACTION BY A WEDGE

As was already said in the Introduction, the field scattered by a body may be investigated in the form of the sum of the fields being radiated by the uniform and nonuniform parts of the surface current. The uniform part of the current is completely determined by the geometry of the body and the magnetic field of the incident wave. The nonuniform part generally is unknown. However, one may approximately assume that in the vicinity of the discontinuity of a convex surface it will be the same as on a corresponding wedge. Therefore, it is necessary for us to begin by studying the diffraction of a plane electromagnetic wave by a wedge. This chapter will be devoted to this problem. First we will investigate the rigorous solution of this problem (§ 1 and 2). Then we will find its solution in the physical optics approach (§ 3). The difference of these solutions determines the field created by the nonuniform part of the current (§ 4).

§ 1. The Rigorous Solution

The rigorous solution to the problem of diffraction of a plane wave by a wedge was first obtained by Sommerfeld by the method of branching wave functions [16]. Later, the diffraction of cylindrical and spherical waves by a wedge also was studied. A rather extensive bibliography on these problems may be found, for example, in the

paper of Oberhettinger [20]. Since the problem of diffraction by a wedge lies at the base of our studies, we considered it advisable not only to present the results of its rigorous solution, but also to give them a new more graphic derivation. The idea for this derivation follows directly from the work of Sommerfeld. Sommerfeld found the solution to the problem in the form of a contour integral, and then he transformed it to a series. However, one may proceed in the opposite direction: first find the solution in the form of a series and then give its integral representation. Such a path seems to us more graphic, and is discussed in this section. The necessity for a detailed derivation is caused by the fact that the results of Sommerfeld [16] are not represented in a sufficiently clear form, which hinders their use.

Let us assume there is in free space (a vacuum) an ideally conducting wedge and a cylindrical wave source Q parallel to its edge (Figure 1). Let us introduce the cylindrical coordinate system r, ϕ, z in such a way that the z axis coincides with the wedge edge, and the angle ϕ is measured from the irradiated surface. The external wedge angle will be designated by the letter α, so that $0 \leqslant \varphi \leqslant \alpha$. The coordinates of the source Q we will designate by r_0, ϕ_0.

Let us investigate two particular cases for the excitation of an electromagnetic field. In the first case, it is excited by a "filament of electric current"

$$j_z^e = -i\omega p_z \delta(r - r_0, \varphi - \varphi_0). \tag{1.01}$$

in the second case, it is excited by a "filament of magnetic current"

$$j_z^m = -i\omega m_z \delta(r - r_0, \varphi - \varphi_0). \tag{1.02}$$

The quantities p_z and m_z here designate, respectively, the electric and magnetic moments of the filament per unit length along the z axis, ω is the cyclic frequency $\left(\omega = ck = c\frac{2\pi}{\lambda}\right)$, $\delta(r - r_0, \varphi - \varphi_0) = \delta(r - r_0)\delta[r(\varphi - \varphi_0)]$ is a two-dimensional delta function which satisfies the condition

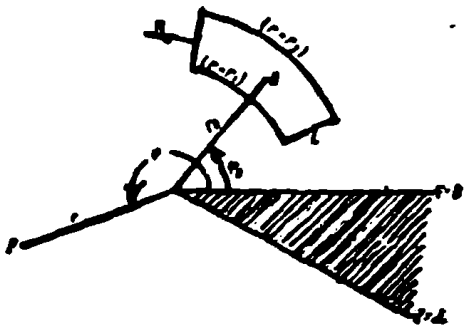

Figure 1. The excitation of a wedge-shaped region by a linear source.

Q - source; P - the observation point;
L - the integration contour in Equation (1.10).

$$\iint \delta(r - r_0,\ \varphi - \varphi_0)\, r\,dr\,d\varphi = 1$$

with integration over the neighborhood of the point r_0, ϕ_0.

Here and henceforth, we will use the absolute system of units (the Gauss system), and we will assume the dependence on time is in the form $e^{-i\omega t}$.

In the first case, the "electric" vector potential A_z^e satisfies the equation (see, for example, [4])

$$\Delta A_z^e + k^2 A_z^e = -\frac{4\pi}{c} j_z^e \qquad (1.03)$$

and the boundary condition

$$A_z^e = 0 \quad \text{with} \quad \varphi = 0 \ \text{and} \ \varphi = \alpha \qquad (1.04)$$

In the second case, the "magnetic" vector potential A_z^m satisfies the equation

$$\Delta A_s^m + k^2 A_s^m = -\frac{4\pi}{c} j_s^m \tag{1.05}$$

and the boundary condition

$$\frac{\partial A_z^m}{\partial \varphi} = 0 \quad \text{with} \quad \varphi = 0 \text{ and } \varphi = a. \tag{1.06}$$

It is natural to seek the solution of the nonhomogeneous Equations (1.03) and (1.05) in the form

$$A_s^e = \begin{cases} \sum_{s=1}^{\infty} a_s J_{\nu_s}(kr) H_{\nu_s}^{(1)}(kr_0) \sin^2 \nu_s \varphi_0 \sin \nu_s \varphi \text{ with } r < r_0, \\ \sum_{s=1}^{\infty} a_s J_{\nu_s}(kr_0) H_{\nu_s}^{(1)}(kr) \sin \nu_s \varphi_0 \sin \nu_s \varphi \text{ with } r > r_0; \end{cases} \tag{1.07}$$

$$A_s^m = \begin{cases} \sum_{s=0}^{\infty} b_s J_{\nu_s}(kr) H_{\nu_s}^{(1)}(kr_0) \cos \nu_s \varphi_0 \cos \nu_s \varphi \text{ with } r < r_0, \\ \sum_{s=0}^{\infty} b_s J_{\nu_s}(kr_0) H_{\nu_s}^{(1)}(kr) \cos \nu_s \varphi_0 \cos \nu_s \varphi \text{ with } r > r_0, \end{cases} \tag{1.08}$$

$$\nu_s = s\frac{\pi}{a}.$$

The products

$$\begin{matrix} J_{\nu_s}(kr)\sin \nu_s \varphi & J_{\nu_s}(kr)\cos \nu_s \varphi \\ \text{and} & \\ H_{\nu_s}^{(1)}(kr)\sin \nu_s \varphi & H_{\nu_s}^{(1)}(kr)\cos \nu_s \varphi \end{matrix} \tag{1.09}$$

are the partial solutions of Equations (1.03) and (1.05) without the right-hand member which satisfy the boundary conditions (1.04) and (1.06). The remaining factors entering into Equations (1.07) and (1.08) ensure the observance of the reciprocity principle and the continuity of the field on the arc $r = r_0$. The Bessel function $J_{\nu_s}(kr)$ enters these equations when $r < r_0$, because it remains finite when $r \to 0$, and the Hankel function $H_{\nu_s}^{(1)}(kr)$ is taken when $r > r_0$ in order that the solution satisfies the radiation condition.

The coefficients a_s and b_s may be determined by means of Green's theorem

$$\int_L \frac{\partial u}{\partial n} dl = \int \Delta u dS, \quad dS = r dr d\varphi \tag{1.10}$$

for the contour L in the plane z = const which is shown in Figure 1. Here, the external normal to the contour L is designated by the letter n. Applying Equation (1.10) to the functions A_z^e and A_z^m and performing the limiting transitions $r_1 \to r_0$ and $r_2 \to r_0$ in it, we obtain

$$\int \left(\frac{\partial A_z^e}{\partial r}\bigg|_{r_0+0} - \frac{\partial A_z^e}{\partial r}\bigg|_{r_0-0} \right) r_0 d\varphi = i \frac{4\pi k}{r_0} p_z \int \delta(\varphi - \varphi_0) r_0 d\varphi,$$

$$\int \left(\frac{\partial A_z^m}{\partial r}\bigg|_{r_0+0} - \frac{\partial A_z^m}{\partial r}\bigg|_{r_0-0} \right) r_0 d\varphi = i \frac{4\pi k}{r_0} m_z \int \delta(\varphi - \varphi_0) r_0 d\varphi.$$

Since here the integration limits are arbitrary, it follows from the equality of the integrals that the integrands are equal:

$$\frac{\partial A_z^e}{\partial r}\bigg|_{r_0+0} - \frac{\partial A_z^e}{\partial r}\bigg|_{r_0-0} = i \frac{4\pi k p_z}{r_0} \delta(\varphi - \varphi_0), \tag{1.11}$$

$$\frac{\partial A_z^m}{\partial r}\bigg|_{r_0+0} - \frac{\partial A_z^m}{\partial r}\bigg|_{r_0-0} = i \frac{4\pi k m_z}{r_0} \delta(\varphi - \varphi_0). \tag{1.12}$$

Now let us substitute Expressions (1.07) into Equality (1.11) and multiply both members of the latter by $\sin \nu_s \varphi$. Then integrating the resulting equality over ϕ in the limits from 0 to α, we find

$$a_s = -\frac{4\pi^2}{\alpha} k p_z. \tag{1.13}$$

In a similar way, let us determine the coefficients

$$b_s = \varepsilon_s \frac{4\pi^2}{\alpha} k m_z, \tag{1.14}$$

where

$$\varepsilon_0 = \frac{1}{2}, \quad \varepsilon_1 = \varepsilon_2 = \ldots = 1. \tag{1.15}$$

Consequently, the electric current filament excites, in the space outside the wedge, the field

$$E_z = ikA_z^e =$$

$$= \begin{cases} i\frac{4\pi^2}{e} k^2 p_z \sum_{s=1}^{\infty} H_{\nu_s}^{(1)}(kr_0) J_{\nu_s}(kr) \sin \nu_s \varphi_0 \sin \nu_s \varphi \\ \qquad \text{with } r < r_0, \\ i\frac{4\pi^2}{e} k^2 p_z \sum_{s=1}^{\infty} J_{\nu_s}(kr_0) H_{\nu_s}^{(1)}(kr) \sin \nu_s \varphi_0 \sin \nu_s \varphi \\ \qquad \text{with } r > r_0, \end{cases}$$

$$E_r = E_\varphi = 0, \quad \mathbf{H} = \frac{1}{ik} \operatorname{rot} \mathbf{E}, \tag{1.16}$$

and the magnetic current filament excites, outside the wedge, the field

$$H_z = ikA_z^m =$$

$$= \begin{cases} i\frac{4\pi^2}{e} k^2 m_z \sum_{s=0}^{\infty} \varepsilon_s H_{\nu_s}^{(1)}(kr_0) J_{\nu_s}(kr) \cos \nu_s \varphi_0 \cos \nu_s \varphi \\ \qquad \text{with } r < r_0, \\ i\frac{4\pi^2}{e} k^2 m_z \sum_{s=0}^{\infty} \varepsilon_s J_{\nu_s}(kr_0) H_{\nu_s}^{(1)}(kr) \cos \nu_s \varphi_0 \cos \nu_s \varphi \\ \qquad \text{with } r > r_0, \end{cases}$$

$$H_r = H_\varphi = 0, \quad \mathbf{E} = -\frac{1}{ik} \operatorname{rot} \mathbf{H}. \tag{1.17}$$

Now using the asymptotic equation for the Hankel function when $kr_0 \to \infty$ [21], we have

$$H_{\nu_s}^{(1)}(kr_0) = \sqrt{\frac{2}{\pi kr_0}} e^{i\left(kr_0 - \frac{\pi}{2}\nu_s - \frac{\pi}{4}\right)} = H_0^{(1)}(kr_0) e^{-i\frac{\pi}{2}\nu_s}. \tag{1.18}$$

Then Expressions (1.16) and (1.17) in the region $r < r_0$ take the form

$$E_z = i\frac{4\pi^2}{e} k^2 p_z H_0^{(1)}(kr_0) \times$$

$$\times \sum_{s=1}^{\infty} e^{-i\frac{\pi}{2}\nu_s} J_{\nu_s}(kr) \sin \nu_s \varphi_0 \sin \nu_s \varphi,$$

(equation continued on next page)

$$H_z = i\frac{4\pi^2}{a}k^2 m_z H_0^{(1)}(kr_0)\times$$
$$\times\sum_{s=0}^{\infty}\varepsilon_s e^{-i\frac{\pi}{2}\nu_s}J_{\nu_s}(kr)\cos\nu_s\varphi_0\cos\nu_s\varphi$$

or

$$\left.\begin{aligned}E_z &= i\pi k^2 p_z H_0^{(1)}(kr_0)[u(r,\ \varphi-\varphi_0)-u(r,\ \varphi+\varphi_0)],\\ H_z &= i\pi k^2 m_z H_0^{(1)}(kr_0)[u(r,\ \varphi-\varphi_0)+u(r,\ \varphi+\varphi_0)],\end{aligned}\right\} \qquad (1.19)$$

where

$$u(r,\ \varphi)=\frac{2\pi}{a}\sum_{s=0}^{\infty}\varepsilon_s e^{-i\frac{\pi}{2}\nu_s}J_{\nu_s}(kr)\cos\nu_s\psi \qquad (1.20)$$

$(\psi=\varphi\pm\varphi_0)$.

Let us note, furthermore, that in free space the field of the electric filament with a moment p_z is determined by the relationship

$$E_z = i\pi k^2 p_z H_0^{(1)}(kr_0), \qquad (1.21)$$

and the field of the magnetic filament with the moment m_z is determined by the relationship

$$H_z = i\pi k^2 m_z H_0^{(1)}(kr_0). \qquad (1.22)$$

Therefore, the expressions in front of the square brackets in Equations (1.19) may be regarded as the primary field of the filament — the cylindrical wave arriving at the wedge edge. Now removing the filament of current to infinity ($r_0 \to \infty$), let us proceed to the incident plane waves

$$E_z = E_{0z}\cdot e^{-ikr\cos(\varphi-\varphi_0)},\quad E_r = E_\varphi = 0 \qquad (1.23)$$

and

$$H_z = H_{0z} \cdot e^{-ikr\cos(\varphi - \varphi_0)}, \quad H_r = H_\varphi = 0. \tag{1.24}$$

The field arising with the diffraction of these waves by the wedge will obviously have the component

$$E_z = E_{0z}[u(r, \varphi - \varphi_0) - u(r, \varphi + \varphi_0)] \tag{1.25}$$

and

$$H_z = H_{0z}[u(r, \varphi - \varphi_0) + u(r, \varphi + \varphi_0)]. \tag{1.26}$$

Let us find the integral representation for the function u (r, ψ). For this purpose, let us use the equation (see [16], p. 866)

$$J_{\nu_s}(kr) = \frac{1}{2\pi} \int_{I}^{III} e^{i\left[kr\cos\beta + \nu_s\left(\beta - \frac{\pi}{2}\right)\right]} d\beta, \tag{1.27}$$

where the limits I - III mean that the integration contour goes from region I to region III (Figure 2). The cross-hatched sections in the plane of the complex variable β (β') shown in Figure 2 are regions in which $\mathrm{Im}\cos\beta > 0$ ($\mathrm{Im}\cos\beta' < 0$). Therefore, in the sections of the contour extending to infinity the integrand strives to zero, ensuring the convergence of the integral. Substituting Expression (1.27) into Equation (1.20), we obtain

$$u(r, \psi) = \frac{1}{2\pi} \int_{I}^{III} e^{ikr\cos\beta} \left[1 + \sum_{s=1}^{\infty} e^{i\nu_s(\beta - \alpha + \psi)} + \sum_{s=1}^{\infty} e^{i\nu_s(\beta - \alpha - \psi)}\right] d\beta.$$

After summing the infinite geometric progressions and replacing the variable β by $\beta' = \beta - \pi$, the function u (r, ψ) acquires the form

$$u(r, \psi) = \frac{1}{2\pi} \int_{I'}^{III'} e^{-ikr\cos\beta'} \left[\frac{1}{1 - e^{i\frac{\pi}{\alpha}(\beta' + \psi)}} - \frac{1}{1 - e^{-i\frac{\pi}{\alpha}(\beta' - \psi)}}\right] d\beta'.$$

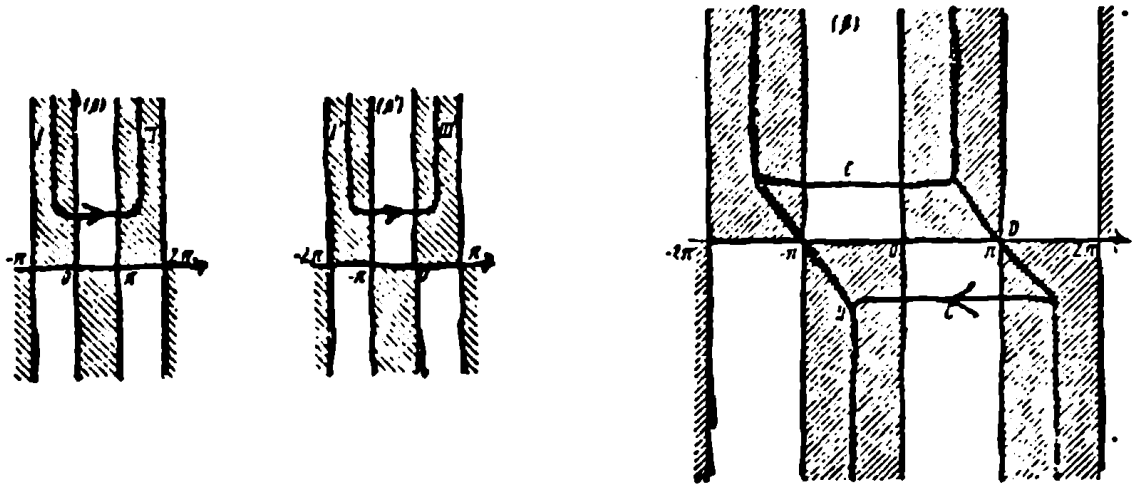

Figure 2. The integration contours in the complex plane β.

Figure 3. The integration contour in Equation (1.28).

As a result, we obtain the well-known integral of Sommerfeld

$$u(r,\ \psi)=\frac{1}{2\pi}\int_{C}\frac{e^{-ikr\cos\beta}}{1-e^{i\frac{\pi}{\alpha}(\beta+\psi)}}d\beta. \tag{1.28}$$

The integration contour C is shown in Figure 3 and consists of two infinite branches. Since the integrand expression has poles at the points $\beta_m=2\alpha m-\psi\ (m=0,\pm 1,\pm 2,\ldots)$, then for the values of ϕ corresponding to the space outside the wedge $(0<\varphi<\alpha)$ the function u (r, ψ) may be represented (with $\pi<\alpha\leq 2\pi$, $0\leq\varphi_0\leq\pi$) in the following way:

$$\left.\begin{aligned} u(r,\ \psi)&=v(r,\ \psi)+e^{-ikr\cos\psi} && \text{with } -\pi<\psi<\pi,\\ u(r,\ \psi)&=v(r,\ \psi) && \text{with } \pi<\psi<2\alpha-\pi,\\ u(r,\ \psi)&=v(r,\ \psi)+e^{-ikr\cos(2\alpha-\psi)} && \text{with } 2\alpha-\pi<\psi<2\alpha, \end{aligned}\right\} \tag{1.29}$$

where

$$v(r,\ \psi)=\frac{1}{2\pi}\int_{\gamma}\frac{e^{-ikr\cos\beta}}{1-e^{i\frac{\pi}{\alpha}(\beta+\psi)}}d\beta,$$

or

$$v(r, \psi) = \frac{i}{2\alpha} \sin\frac{\pi^2}{\alpha} \int_{D_0} \frac{e^{ikr\cos\zeta}\,d\zeta}{\cos\frac{\pi^2}{\alpha} - \cos\frac{\pi}{\alpha}(\psi + \zeta)}. \tag{1.30}$$

The integration contours D and D_0 are shown, respectively, in Figures 3 and 4.

With an arbitrary incidence of a plane wave on a wedge, one of two cases may occur: (1) the plane wave "illuminates" only one face of the wedge $(0 < \varphi_0 < \alpha - \pi)$, and (2) the plane wave "illuminates" both faces of the wedge $(\alpha - \pi < \varphi_0 < \pi)$. Let us write out in more detail the functions $u(r, \psi)$ corresponding to these cases. In the case $\varphi_0 < \alpha - \pi$ (Figure 5), we have

$$\left.\begin{array}{l}
\left.\begin{array}{l} u(r, \varphi - \varphi_0) = \\ = v(r, \varphi - \varphi_0) + e^{-ikr\cos(\varphi - \varphi_0)} \\ u(r, \varphi + \varphi_0) = \\ = v(r, \varphi + \varphi_0) + e^{-ikr\cos(\varphi + \varphi_0)} \end{array}\right\} \text{with } 0 < \varphi < \pi - \varphi_0, \\
\left.\begin{array}{l} u(r, \varphi - \varphi_0) = \\ = v(r, \varphi - \varphi_0) + e^{-ikr\cos(\varphi - \varphi_0)} \\ u(r, \varphi + \varphi_0) = v(r, \varphi + \varphi_0) \end{array}\right\} \text{with } \pi - \varphi_0 < \varphi < \pi + \varphi_0, \\
\left.\begin{array}{l} u(r, \varphi - \varphi_0) = v(r, \varphi - \varphi_0) \\ u(r, \varphi + \varphi_0) = v(r, \varphi + \varphi_0) \end{array}\right\} \text{with } \pi + \varphi_0 < \varphi < \alpha,
\end{array}\right. \tag{1.31}$$

and in the case $\alpha - \pi < \varphi_0 < \pi$ (Figure 6) we have

$$\left.\begin{array}{l}
\left.\begin{array}{l} u(r, \varphi - \varphi_0) = \\ = v(r, \varphi - \varphi_0) + e^{-ikr\cos(\varphi - \varphi_0)} \\ u(r, \varphi + \varphi_0) = \\ = v(r, \varphi + \varphi_0) + e^{-ikr\cos(\varphi + \varphi_0)} \end{array}\right\} \text{with } 0 < \varphi < \pi - \varphi_0, \\
\left.\begin{array}{l} u(r, \varphi - \varphi_0) = \\ = v(r, \varphi - \varphi_0) + e^{-ikr\cos(\varphi - \varphi_0)} \\ u(r, \varphi + \varphi_0) = v(r, \varphi + \varphi_0) \end{array}\right\} \text{with } \pi - \varphi_0 < \varphi < 2\alpha - \pi - \varphi_0, \\
\left.\begin{array}{l} u(r, \varphi - \varphi_0) = \\ = v(r, \varphi - \varphi_0) + e^{-ikr\cos(\varphi - \varphi_0)} \\ u(r, \varphi + \varphi_0) = \\ = v(r, \varphi + \varphi_0) + e^{-ikr\cos(2\alpha - \varphi - \varphi_0)} \end{array}\right\} \text{with } 2\alpha - \pi - \varphi_0 < \varphi < \alpha.
\end{array}\right. \tag{1.32}$$

The direction $\phi = \pi - \phi_0$ corresponds to the ray reflected in a specular fashion from the first face (we will consider as the first face that face from which the angles are calculated), and the direction $\varphi = 2\alpha - \pi - \varphi_0$ corresponds to the ray reflected specularly from the second face (Figure 5 and 6). The functions $e^{-ikr\cos\phi}$ describe plane waves of unit amplitude: $e^{-ikr\cos(\varphi-\varphi_0)}$ describes the incident wave, $e^{-ikr\cos(\varphi+\varphi_0)}$ describes the wave reflected from the first face, and $e^{-ikr\cos(2\alpha-\varphi-\varphi_0)}$ — the wave reflected from the second face.

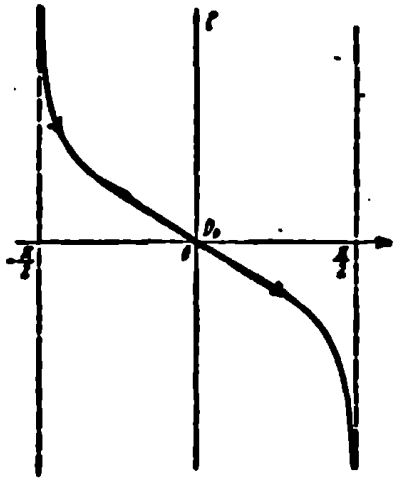

Figure 4. The integration contour in Equation (1.30).

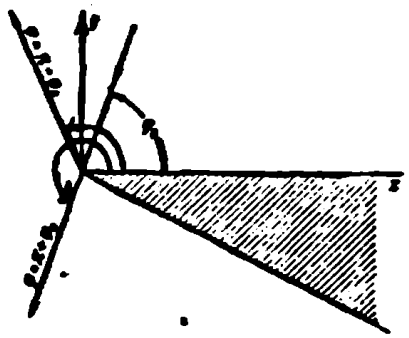

Figure 5. Diffraction of a plane wave by a wedge. The plane wave irradiates only one face of the wedge. ϕ_0 is the angle of incidence. The line $\phi = \pi - \phi_0$ is the boundary of the reflected plane wave, and the line $\phi = \pi + \phi_0$ is the boundary of the shadow.

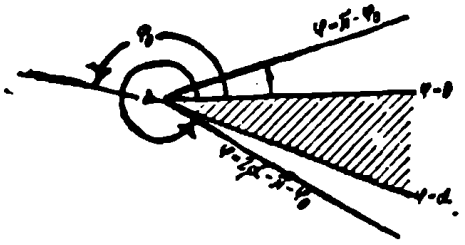

Figure 6. Diffraction by a wedge. The plane wave irradiates both faces. The line $\phi = 2\alpha - \pi - \phi_0$ is the boundary of the plane wave reflected from the second face ($\phi = \alpha$).

§ 2. Asymptotic Expressions

The integral

$$v(r,\psi)=\frac{i}{2\pi}\sin\frac{\pi^0}{a}\int_{L_0}\frac{e^{ikr\cos\zeta}d\zeta}{\cos\frac{\pi^0}{a}-\cos\frac{\pi}{a}(\psi+\zeta)}, \tag{2.01}$$

in Equations (1.31) and (1.32) generally is not expressed in terms of well-known functions. However, when kr >> 1 it may be calculated approximately by the method of steepest descents [21]. In integral (2.01), changing for this purpose to a new integration variable

$$s=\sqrt{2}e^{i\frac{\pi}{4}}\sin\frac{\zeta}{2},\quad s^0=i(1-\cos\zeta),$$

we obtain

$$v(r,\psi)=\frac{\sin\frac{\pi}{n}}{\sqrt{2}n}e^{i\left(kr+\frac{\pi}{4}\right)}\int_{-\infty}^{\infty}\frac{e^{-krs^0}ds}{\left(\cos\frac{\pi}{n}-\cos\frac{\psi+\zeta}{n}\right)\cos\frac{\zeta}{2}}, \tag{2.02}$$

where

$$n=\frac{a}{\pi}. \tag{2.03}$$

It is not difficult to see that the point s = 0 is a saddle point: as one goes further from it along the imaginary axis (Re s = 0) in the plane of the complex variable s, the function e^{-krs^0} most rapidly increases, and as one goes along the real axis (Im s = 0) it decreases most rapidly. Therefore, when kr >> 1 the main contribution to the integral (2.02) is given by the integrand in the section of the contour in the vicinity of the saddle point (s = 0).

The method of steepest descents is carried out by expanding the integrand (except for the factor e^{-krs^0}) into a Taylor series in powers of s. This series is then integrated term by term. If the integrand

expansion converges only on part of the integration contour, the resultant series obtained after the integration will be semiconvergent (asymptotic). Limiting ourselves to the first term in it, we obtain:

$$v(r,\psi)\approx\frac{\sin\frac{\pi}{n}}{\sqrt{2\pi n}}\frac{e^{i\left(kr+\frac{\pi}{4}\right)}}{\cos\frac{\pi}{n}-\cos\frac{\psi}{n}}\int_{-\infty}^{\infty}e^{-krs^2}ds=$$
$$=\frac{\frac{1}{n}\sin\frac{\pi}{n}}{\cos\frac{\pi}{n}-\cos\frac{\psi}{n}}\frac{e^{i\left(kr+\frac{\pi}{4}\right)}}{\sqrt{2\pi kr}}. \qquad (2.04)$$

The remaining terms of the asymptotic series have a value on the order of $\frac{1}{(kr)^{3/2}}$ and higher.

Expression (2.04) is valid with the condition $\left(\cos\frac{\pi}{n}-\cos\frac{\psi}{n}\right)\sqrt{kr}\gg 1$ and describes that part of the diffraction field which has the character of cylindrical waves diverging from the wedge edge. With the incidence of the plane wave (1.23) on a wedge, the electric vector of which is parallel to the wedge edge, the cylindrical wave is determined in accordance with (1.25) and (2.04) by the equation

$$E_z=-H_\varphi=E_{0z}\cdot[v(r,\varphi-\varphi_0)-v(r,\varphi+\varphi_0)]=$$
$$=E_{0z}f\frac{e^{i\left(kr+\frac{\pi}{4}\right)}}{\sqrt{2\pi kr}}. \qquad (2.05)$$

where

$$f=\frac{\sin\frac{\pi}{n}}{n}\left(\frac{1}{\cos\frac{\pi}{n}-\cos\frac{\varphi-\varphi_0}{n}}-\frac{1}{\cos\frac{\pi}{n}-\cos\frac{\varphi+\varphi_0}{n}}\right). \qquad (2.06)$$

When the wedge is excited by the plane wave (1.24), in which the magnetic vector is parallel to the wedge edge, the cylindrical wave has the form

$$H_z=E_\varphi=H_{0z}\cdot[v(r,\varphi-\varphi_0)+v(r,\varphi+\varphi_0)]=$$
$$=H_{0z}g\frac{e^{i\left(kr+\frac{\pi}{4}\right)}}{\sqrt{2\pi kr}}, \qquad (2.07)$$

where

$$g=\frac{\sin\frac{\pi}{n}}{n}\left(\frac{1}{\cos\frac{\pi}{n}-\cos\frac{\varphi-\varphi_0}{n}}+\frac{1}{\cos\frac{\pi}{n}-\cos\frac{\varphi+\varphi_0}{n}}\right). \tag{2.08}$$

In the vicinity of the shadow boundary ($\phi \tilde{\approx} \pi + \phi_0$) and near the directions of the mirror-reflected rays ($\varphi\approx\pi-\varphi_0$, $\varphi\approx 2\alpha-\pi-\varphi_0$) Expressions (2.04) - (2.08) are not valid, since the poles

$$s_1=\sqrt{2}e^{i\frac{\pi}{4}}\sin\frac{\pi-\phi}{2},\quad s_2=\sqrt{2}e^{i\frac{\pi}{4}}\sin\left(n\pi-\frac{\pi+\phi}{2}\right)$$

of the integrand in (2.02) are close to s = 0 and, consequently, its expansion in a Taylor series loses meaning. Physically, this result means that in the indicated region the diffraction wave does not reduce to plane and cylindrical waves, but has a more complicated character. An asymptotic representation of the function v (r, ψ) in this region was obtained in 1938 by Pauli [22]; here we will present the derivation of the first term of the asymptotic series obtained in [22].

Let us multiply and divide the integrand expression in Equation (2.02) by the quantity

$$\cos\psi+\cos\zeta=i(s^2-is_0^2)\quad\left(s_0^2=2\cos^2\frac{\psi}{2}\right) \tag{2.09}$$

and let us expand into a Taylor series in powers of s the function

$$\frac{\cos\psi+\cos\zeta}{\left(\cos\frac{\pi}{n}-\cos\frac{\psi+\zeta}{n}\right)\cos\frac{\zeta}{2}},$$

which no longer has a pole at the saddle point (s = 0) when $\psi = \phi \pm \pm \phi_0 = \pi$. Limiting ourselves in this series to the first term, we obtain

$$v(r,\phi)=\frac{\sqrt{2}}{\pi}\cdot\frac{\sin\frac{\pi}{n}}{n}\frac{1+\cos\phi}{\cos\frac{\pi}{n}-\cos\frac{\phi}{n}}e^{i\left(kr-\frac{\pi}{4}\right)}\int_0^\infty\frac{e^{-kr_0s^2}}{s^2-is_0^2}ds. \tag{2.10}$$

The integral here may be represented in the form

$$\int_0^\infty \frac{e^{-krs^2}}{s^2 - is_0^2}\,ds = e^{-ikrs_0^2}\int_0^\infty ds \int_{ks_0^2}^\infty e^{-(t-ks_0^2)t}\,dt.$$

Changing the order of integration here, we find

$$\int_0^\infty \frac{e^{-krs^2}}{s^2 - is_0^2}\,ds = e^{-ikrs_0^2}\int_{ks_0^2}^\infty e^{ts_0^2 t}\,\frac{dt}{\sqrt{t}}\int_0^\infty e^{-x^2}\,dx =$$

$$= \frac{\sqrt{\pi}}{|s_0|}\,e^{-ikrs_0^2}\int_{\sqrt{kr}\,|s_0|}^\infty e^{iq^2}\,dq \qquad (2.11)$$

and finally

$$v(r,\psi) = \frac{2}{n}\,\frac{\sin\frac{\pi}{n}\left|\cos\frac{\psi}{2}\right|}{\cos\frac{\pi}{n} - \cos\frac{\psi}{n}}\,e^{-ikr\cos\psi}\cdot\frac{e^{-i\frac{\pi}{4}}}{\sqrt{\pi}}\times$$

$$\times \int_{\sqrt{2kr}\left|\cos\frac{\psi}{2}\right|}^\infty e^{iq^2}\,dq. \qquad (2.12)$$

The next term of the asymptotic expansion for the function v (r, ψ) has a value, whose order of magnitude depends on the observation direction: in the vicinity of the border of the plane waves ($\varphi \approx \pi \pm \varphi_0$) its order of magnitude is $\frac{1}{\sqrt{kr}}$, but far from it the order of magnitude is 1/kr in comparison with the term written in (2.12).

It is convenient to represent Expression (2.12) in the following form:

$$v(r,\psi) = -\frac{2}{n}\,\frac{\sin\frac{\pi}{n}\cos\frac{\psi}{2}}{\cos\frac{\pi}{n} - \cos\frac{\psi}{n}}\,e^{-ikr\cos\psi}\cdot\frac{e^{-i\frac{\pi}{4}}}{\sqrt{\pi}}\times$$

$$\times \int_{\infty\cos\frac{\psi}{2}}^{\sqrt{2kr}\cos\frac{\psi}{2}} e^{iq^2}\,dq. \qquad (2.13)$$

Here the absolute value of the lower limit of the Fresnel integral always equals infinity, and its sign is determined by the sign of cos $\psi/2$. Therefore, when passing through the boundary of the plane waves ($\psi = \phi \pm \phi_0 = \pi$) the lower limit changes sign and the Fresnel integral undergoes a finite discontinuity, ensuring at this boundary the continuity of the function u (r, ψ) and consequently of the diffraction field. Actually, by means of the well-known equation

$$\int_0^\infty e^{ikq^2} dq = \frac{\sqrt{\pi}}{2} e^{i\frac{\pi}{4}} \tag{2.14}$$

it is not difficult to show that

$$v(r, \pi + 0) = \frac{e^{ikr}}{2}, \quad v(r, \pi - 0) = -\frac{e^{ikr}}{2} \tag{2.15}$$

and consequently

$$u(r, \pi \pm 0) = \frac{1}{2} e^{ikr}. \tag{2.16}$$

In view of the asymptotic relationships

$$\int_0^p e^{ikq^2} dq = \frac{e^{ikp^2}}{2ikp}, \quad \int_{-\infty}^{-p} e^{ikq^2} dq = -\frac{e^{ikp^2}}{2ikp} \text{ (with } p \gg 1) \tag{2.17}$$

Pauli's Equation (2.13) is transformed with $\sqrt{2kr}\left|\cos\frac{\psi}{2}\right| \gg 1$ to the Expression (2.04). As was already indicated above, it determines the cylindrical waves diverging from the wedge edge.

By means of Equation (2.13), one may also calculate the field in the vicinity of the direction $\phi = 2\alpha - \pi - \phi_0$ — that is, near the boundary of the plane wave reflected from the face $\phi = \alpha$; for this purpose, it is sufficient to replace ϕ by $\alpha - \phi$ and ϕ_0 by $\alpha - \phi_0$.

It is also interesting to note that in the case of a half-plane (n = 2) Equation (2.13) gives the expression

$$v(r,\psi)=e^{-ikr\cos\psi}\frac{e^{-i\frac{\pi}{4}}\sqrt{2kr}\cos\frac{\psi}{2}}{\sqrt{\pi}}\times\int_{\infty\cos\frac{\psi}{2}}^{0}e^{iq^2}dq, \tag{2.18}$$

which completely agrees with the rigorous solution. Actually, with $\alpha = 2\pi$, when the wedge is transformed to a half-plane, integral (1.30) equals

$$v(r,\psi)=-\frac{i}{4\pi}\int_{D_0}\frac{e^{ikr\cos\zeta}}{\cos\frac{\psi+\zeta}{2}}d\zeta \tag{2.19}$$

and it may be reduced to a Fresnel integral. For this purpose, let us divide the contour D_0 into two parts by the point $\zeta = 0$. Summing the integrals over these parts of the contour, we find that

$$v(r,\psi)=-\frac{i}{4\pi}\int_{0}^{\frac{\pi}{2}-i\infty}e^{ikr\cos\zeta}\left(\frac{1}{\cos\frac{\psi+\zeta}{2}}+\frac{1}{\cos\frac{\psi-\zeta}{2}}\right)d\zeta=$$

$$=-\frac{i}{\pi}\cos\frac{\psi}{2}\int_{0}^{\frac{\pi}{2}-i\infty}\frac{e^{ikr\cos\zeta}\cos\frac{\zeta}{2}}{\cos\psi+\cos\zeta}d\zeta$$

Now changing to a new integration variable $s=\sqrt{2}e^{i\frac{\pi}{4}}\sin\frac{\zeta}{2}$ and taking into account Equation (2.09), we obtain

$$v(r,\psi)=-\frac{\sqrt{2}}{\pi}\cos\frac{\psi}{2}e^{i\left(kr-\frac{\pi}{4}\right)}\int_{0}^{\infty}\frac{e^{-krs^2}}{s^2-is_0^2}ds. \tag{2.20}$$

The integral here was already calculated by us. Turning to Equation (2.11), we arrive at Expression (2.18) which — together with relationships (1.25), (1.26) and (1.31) — give us the rigorous solution to the problem of the diffraction of plane waves by an ideally conducting half-plane.

§ 3. The Physical Optics Approach

In the physical optics approach, the fringing field is sought as the electro-magnetic field created by the uniform part of the surface current

$$\mathbf{j}^0 = \frac{c}{2\pi}[\mathbf{n}\mathbf{H}_0]. \tag{3.01}$$

Let us recall that here n designates the external normal to the body's surface, and $\mathbf{H}_0$ designates the magnetic vector of the incident wave. First let us investigate the case $0 < \varphi_0 < \alpha = \pi$, when the incident plane wave irradiates only one face of the wedge (Figure 5).

From Equation (3.01) it follows that the density of the uniform part of the current being excited on the irradiated face by plane waves (1.23) and (1.24) has the following components, respectively

$$j_z^0 = \frac{c}{2\pi} E_{0z} \cdot \sin\varphi_0 e^{-ikx\cos\varphi_0}, \quad j_x^0 = j_y^0 = 0 \tag{3.02}$$

and

$$j_x^0 = \frac{c}{2\pi} H_{0z} e^{-ikx\cos\varphi_0}, \quad j_y^0 = j_z^0 = 0. \tag{3.03}$$

For the purpose of calculating the field radiated by this current, we will use the following integral representation of the Hankel function (see [16], p. 866)

$$H_0^{(1)}(\rho) = \frac{1}{\pi}\int_{-\delta+i\infty}^{\delta-i\infty} e^{i\rho\cos\beta}d\beta = \frac{1}{i\pi}\int_{-\infty}^{\infty} e^{i\rho\operatorname{ch} t}dt \quad (0 < \delta < \pi). \tag{3.04}$$

Assuming here $\rho = kd$ and changing to a new integration variable $\zeta = d \operatorname{sh} t$, we obtain

$$H_0^{(1)}(kd) = \frac{1}{i\pi}\int_{-\infty}^{\infty} \frac{e^{ik\sqrt{d^2+\zeta^2}}}{\sqrt{d^2+\zeta^2}}\,d\zeta. \tag{3.05}$$

It is easy to show by means of Equations (3.02), (3.03) and (3.05) that the vector potential

$$\mathbf{A}(x, y, 0) = \frac{1}{c}\int_0^{\infty} J^0(\xi)\,d\xi \int_{-\infty}^{\infty} \frac{e^{ik\sqrt{y^2+(x-\xi)^2+\zeta^2}}}{\sqrt{y^2+(x-\xi)^2+\zeta^2}}\,d\zeta \tag{3.06}$$

has the components

$$A_z = \frac{I}{2} E_{0z} \sin\varphi_0 \cdot I_1, \quad A_x = A_y = 0, \tag{3.07}$$

if the wedge is excited by plane wave (1.23), and

$$A_x = \frac{I}{2} H_{0x} \cdot I_1, \quad A_y = A_z = 0, \tag{3.08}$$

if the wedge is excited by plane wave (1.24). Here, I_1 designates the integral

$$I_1 = \int_0^{\infty} e^{-ik\xi\cos\varphi_0} H_0^{(1)}(k\sqrt{y^2+(x-\xi)^2})\,d\xi. \tag{3.09}$$

Let us transform it by using the relationship

$$H_0^{(1)}(k\sqrt{d^2+z^2}) = \frac{1}{\pi}\int_{-\infty}^{\infty} \frac{e^{i(vd-wz)}}{v}\,dw$$
$$(v = \sqrt{k^2-w^2},\ \operatorname{Im} v > 0,\ d > 0), \tag{3.10}$$

It is not difficult to establish the correctness of this relationship by verifying that it changes into Expression (3.04) with the substitution w = k sin t, v = k cos t and $k\sqrt{d^2+z^2} = \rho$. As a result

$$I_1 = \frac{1}{i\pi}\int_{-\infty}^{\infty} \frac{e^{i(v|y|-wx)}}{v(k\cos\varphi_0 - w)}\,dw, \tag{3.11}$$

where the integration contour passes above the pole $w = k \cos \phi_0$.

Let us note that integral (3.11) is a function of $|y|$, and let us change to polar coordinates according to the equations

$$\left.\begin{aligned} x &= r\cos\varphi, \\ |y| &= r\sin\varphi \text{ with } \varphi < \pi, \\ |y| &= -r\sin\varphi \text{ with } \varphi > \pi. \end{aligned}\right\} \tag{3.12}$$

Furthermore, by carrying out the substitution

$$w = -k\cos\xi \quad (v = k\sin\xi), \tag{3.13}$$

we obtain

$$\left.\begin{aligned} I_1 &= \frac{1}{i\pi k}\int_F \frac{e^{ikr\cos(\xi-\varphi)}}{\cos\varphi_0+\cos\xi}\,d\xi \text{ with } \varphi < \pi, \\ I_2 &= \frac{1}{i\pi k}\int_F \frac{e^{ikr\cos(\xi+\varphi)}}{\cos\varphi_0+\cos\xi}\,d\xi \text{ with } \varphi > \pi. \end{aligned}\right\} \tag{3.14}$$

The integration contour F is shown in Figures 7a and 7b. In Figure 7a the cross-hatched areas indicate the sections in the plane of the complex variable ξ in which $\operatorname{Im}\cos(\xi-\varphi) > 0$; in Figure 7b, the cross-hatched areas indicate the sections where $\operatorname{Im}\cos(\xi+\varphi) > 0$. Now let us deform the contour F into the contour G_1 (G_2) for the values $\varphi < \pi (\varphi > \pi)$, and let us change to a new integration variable

$$\left.\begin{aligned} \zeta &= \xi - \varphi \qquad \text{with } \varphi < \pi, \\ \zeta &= \xi - (2\pi - \varphi) \text{ with } \varphi > \pi. \end{aligned}\right\} \tag{3.15}$$

As a result, we obtain the following expressions:

$$I_1 = \frac{1}{i\pi k}\int_{D_0} \frac{e^{ikr\cos\zeta}d\zeta}{\cos\varphi_0+\cos(\zeta+\varphi)} + \begin{cases} 0 \text{ with } \varphi > \pi - \varphi_0, \\ \dfrac{2}{k\sin\varphi_0}\, e^{-ikr\cos(\varphi+\varphi_0)} \\ \quad \text{with } \varphi < \pi - \varphi_0, \end{cases} \tag{3.16}$$

if $\phi < \pi$ and

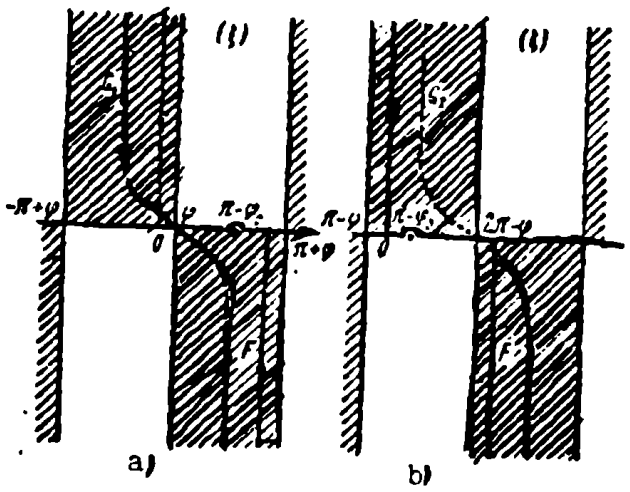

Figure 7. The integration contour in Equations (3.14).

$$I_s=\frac{1}{ikA}\int_{D_0}\frac{e^{ikr\cos\zeta}d\zeta}{\cos\varphi_0+\cos(\zeta-\psi)}+\begin{cases}0 \text{ with } \varphi<\pi+\varphi_0,\\ \frac{2}{k\sin\varphi_0}e^{-ikr\cos(\varphi-\varphi_0)}\\ \text{with } \varphi>\pi+\varphi_0,\end{cases} \tag{3.17}$$

if $\phi > \pi$. The integration contour D_0 is shown in Figure 4.

By means of Equation (3.06) and the equality

$$E_s=ikA_s \tag{3.18}$$

let us find the field which is radiated by the uniform part of the current excited on the face $\phi = 0$ by the plane wave (1.23)

$$\frac{E_0}{E_{0s}}=\begin{cases}v_1^+(\varphi,\varphi_0)-e^{-ikr\cos(\zeta+\varphi_0)} & \text{with } 0<\varphi<\pi-\varphi_0,\\ v_1^+(\varphi,\varphi_0) & \text{with } \pi-\varphi_0<\varphi<\pi,\\ v_1^-(\varphi,\varphi_0) & \text{with } \pi<\varphi<\pi+\varphi_0,\\ v_1^-(\varphi,\varphi_0)-e^{-ikr\cos(\zeta-\varphi_0)} & \text{with } \pi+\varphi_0<\varphi<\alpha,\end{cases} \tag{3.19}$$

where

$$v_1^{\pm}(\varphi, \varphi_0) = \frac{i}{2\pi} \sin\varphi_0 \int_{L_0} \frac{e^{ikr\cos\zeta} d\zeta}{\cos\varphi_0 \mp \cos(\zeta \pm \varphi)}. \tag{3.20}$$

It is not difficult to see that with $\alpha - \pi < \varphi_0 < \pi$, when both faces of the wedge are illuminated, the field excited by the second face ($\phi = \alpha$) will be described by the same equations if one replaces ϕ by $\alpha - \phi$, and ϕ_0 by $\alpha - \phi_0$ in them.

Adding the field being radiated by the uniform part of the current with the incident plane wave (1.23), we obtain the diffraction field in the physical optics approach. It equals

$$\frac{E_z}{E_{0z}} = \begin{cases} v_1^+(\varphi, \varphi_0) + e^{-ikr\cos(\varphi-\varphi_0)} - e^{-ikr\cos(\varphi+\varphi_0)} \\ \qquad \text{with } 0 < \varphi < \pi - \varphi_0, \\ v_1^+(\varphi, \varphi_0) + e^{-ikr\cos(\varphi-\varphi_0)} \\ \qquad \text{with } \pi - \varphi_0 < \varphi < \pi, \\ v_1^-(\varphi, \varphi_0) + e^{-ikr\cos(\varphi-\varphi_0)} \\ \qquad \text{with } \pi < \varphi < \pi + \varphi_0, \\ v_1^-(\varphi, \varphi_0) \qquad \text{with } \pi + \varphi_0 < \varphi < 2\pi, \end{cases} \tag{3.21}$$

if one face of the wedge ($0 < \varphi_0 < \alpha - \pi$) is illuminated, and

$$\frac{E_z}{E_{0z}} = \begin{cases} v_1^+(\varphi, \varphi_0) + v_1^-(\alpha-\varphi, \alpha-\varphi_0) + \\ + e^{-ikr\cos(\varphi-\varphi_0)} - e^{-ikr\cos(\varphi+\varphi_0)} \\ \qquad \text{with } 0 < \varphi < \pi - \varphi_0, \\ v_1^+(\varphi, \varphi_0) + v_1^-(\alpha-\varphi, \alpha-\varphi_0) + \\ + e^{-ikr\cos(\varphi-\varphi_0)} \quad \text{with } \pi - \varphi_0 < \varphi < \alpha - \pi, \\ v_1^+(\varphi, \varphi_0) + v_1^+(\alpha-\varphi, \alpha-\varphi_0) + \\ + e^{-ikr\cos(\varphi-\varphi_0)} \quad \text{with } \alpha - \pi < \varphi < \pi, \\ v_1^-(\varphi, \varphi_0) + v_1^+(\alpha-\varphi, \alpha-\varphi_0) + \\ + e^{-ikr\cos(\varphi-\varphi_0)} \quad \text{with } \pi < \varphi < 2\alpha - \pi - \varphi_0, \\ v_1^-(\varphi, \varphi_0) + v_1^+(\alpha-\varphi, \alpha-\varphi_0) + \\ + e^{-ikr\cos(\varphi-\varphi_0)} - e^{-ikr\cos(2\alpha-\varphi-\varphi_0)} \\ \qquad \text{with } 2\alpha - \pi - \varphi_0 < \varphi < \alpha, \end{cases} \tag{3.22}$$

if both faces of the wedge ($\alpha - \pi < \varphi_0 < \pi$) are illuminated.

Now let us calculate the field arising during diffraction by a wedge of a plane wave (1.24). The field scattered by the first face ($\phi = 0$) is determined by the relationship

$$\left.\begin{aligned} H_z &= -\frac{\partial A_z}{\partial y}, \\ H_x &= H_y = 0. \end{aligned}\right\} \tag{3.23}$$

One may write the component H_z in the form

$$H_z = -\frac{i}{2} H_{0z} \frac{\partial}{\partial y} I_1 \tag{3.24}$$

or

$$\left.\begin{aligned} H_z &= -\frac{i}{2} H_{0z} \cdot I_2 \text{ with } \varphi < \pi, \\ H_z &= \frac{i}{2} H_{0z} \cdot I_2 \text{ with } \varphi > \pi. \end{aligned}\right\} \tag{3.25}$$

The quantity I_2 introduced here is the integral

$$I_2 = \frac{1}{\pi} \int_{-\infty}^{\infty} \frac{e^{i(w|y| - \alpha x)}}{k \cos \varphi_0 - w} dw \tag{3.26}$$

along the infinite contour which passes above the pole $w = k \cos \phi_0$. This integral, precisely the same as integral I_1, is transformed to an integral along the contour D_0. As a result, we obtain

$$\frac{H_z}{H_{0z}} = \begin{cases} v_2^+(\varphi, \varphi_0) + e^{-ikr\cos(\zeta + \varphi_0)} & \text{with } 0 \leqslant \varphi < \pi - \varphi_0, \\ v_2^+(\varphi, \varphi_0) & \text{with } \pi - \varphi_0 < \varphi < \pi, \\ v_2^-(\varphi, \varphi_0) & \text{with } \pi < \varphi < \pi + \varphi_0, \\ v_2^-(\varphi, \varphi_0) - e^{-ikr\cos(\zeta - \varphi_0)} & \text{with } \pi + \varphi_0 < \varphi \leqslant \pi, \end{cases} \tag{3.27}$$

where

$$v_2^{\pm}(\varphi, \varphi_0) = \mp \frac{i}{2n} \int_{D_0} \frac{\sin\left(\frac{\zeta \pm \varphi}{n}\right) e^{ikr\cos\zeta}}{\cos\frac{\varphi_0}{n} + \cos\left(\frac{\zeta \pm \varphi}{n}\right)} d\zeta. \tag{3.28}$$

In the case when both faces of the wedge are illuminated, the field scattered by the second face also is determined by Equations (3.27) and (3.28) in which one need only replace ϕ_0 by $\alpha - \phi_0$, and ϕ by $\alpha - \phi$.

Then adding the field radiated by the nonuniform part of the current with the incident wave (1.24), we find the diffraction field in the physical optics approach. This equals

$$\frac{H_z}{H_{0z}} = \begin{cases} v_3^+(\varphi, \varphi_0) + e^{-ikr\cos(\varphi-\varphi_0)} + e^{-ikr\cos(\varphi+\varphi_0)} \\ \qquad \text{with } 0 < \varphi < \pi - \varphi_0, \\ v_3^+(\varphi, \varphi_0) + e^{-ikr\cos(\varphi-\varphi_0)} \\ \qquad \text{with } \pi - \varphi_0 < \varphi < \pi, \\ v_2^-(\varphi, \varphi_0) + e^{-ikr\cos(\varphi-\varphi_0)} \\ \qquad \text{with } \pi < \varphi < \pi + \varphi_0, \\ v_2^-(\varphi, \varphi_0) \qquad \text{with } \pi + \varphi_0 < \varphi < \alpha, \end{cases} \tag{3.29}$$

if one face of the wedge is illuminated, and

$$\frac{H_z}{H_{0z}} = \begin{cases} v_2^+(\varphi, \varphi_0) + v_2^-(\alpha-\varphi, \alpha-\varphi_0) + \\ + e^{-ikr\cos(\varphi-\varphi_0)} + e^{-ikr\cos(\varphi+\varphi_0)} \\ \qquad \text{with } 0 < \varphi < \pi - \varphi_0, \\ v_2^+(\varphi, \varphi_0) + v_2^-(\alpha-\varphi, \alpha-\varphi_0) + \\ + e^{-ikr\cos(\varphi-\varphi_0)} \quad \text{with } \pi - \varphi_0 < \varphi < \alpha - \pi, \\ v_2^+(\varphi, \varphi_0) + v_2^+(\alpha-\varphi, \alpha-\varphi_0) + \\ + e^{-ikr\cos(\varphi-\varphi_0)} \quad \text{with } \alpha - \pi < \varphi < \pi, \\ v_2^-(\varphi, \varphi_0) + v_2^+(\alpha-\varphi, \alpha-\varphi_0) + \\ + e^{-ikr\cos(\varphi-\varphi_0)} \quad \text{with } \pi < \varphi < 2\alpha - \pi - \varphi_0, \\ v_2^-(\varphi, \varphi_0) + v_2^+(\alpha-\varphi, \alpha-\varphi_0) + \\ + e^{-ikr\cos(\varphi-\varphi_0)} + e^{-ikr\cos(2\alpha-\varphi-\varphi_0)} \\ \qquad \text{with } 2\alpha - \pi - \varphi_0 < \varphi < \alpha, \end{cases} \tag{3.30}$$

if both of its faces are illuminated.

The integrals $V_1^{\pm}$, $V_2^{\pm}$ generally are not expressed in terms of well-known functions. However, by using the method of steepest descents, it is not difficult to obtain their asymptotic expansion when $kr >> 1$. Far from the directions $\phi = \pi \pm \phi_0$ and $\phi = 2\alpha - \pi - \phi_0$, the first term of the asymptotic expansion gives us the cylindrical wave diverging from the wedge edge. In the case of wedge excitation by a plane wave (1.23), these cylindrical waves are determined by the equation

$$\left.\begin{aligned} E_z = -H_\varphi = E_{0z} \cdot f^0 \cdot \frac{e^{i\left(kr + \frac{\pi}{4}\right)}}{\sqrt{2\pi kr}}, \\ E_\varphi = H_z = 0, \end{aligned}\right\} \tag{3.31}$$

and with the excitation of the wedge by a plane wave (1.24) they are determined by the equation

$$\left.\begin{aligned} H_z = E_\varphi = H_{0z} \cdot g^0 \cdot \frac{e^{i\left(kr + \frac{\pi}{4}\right)}}{\sqrt{2\pi kr}}, \\ H_\varphi = E_z = 0. \end{aligned}\right\} \tag{3.32}$$

The functions f^0 and g^0 have the form

$$\left.\begin{aligned} f^0 = \frac{\sin\varphi_0}{\cos\varphi + \cos\varphi_0}, \\ g^0 = -\frac{\sin\varphi}{\cos\varphi + \cos\varphi_0}, \end{aligned}\right\} \tag{3.33}$$

if one face of the wedge $(0 < \varphi_0 < \alpha - \pi)$, and

$$\left.\begin{aligned} f^0 = \frac{\sin\varphi_0}{\cos\varphi + \cos\varphi_0} + \frac{\sin(\alpha - \varphi_0)}{\cos(\alpha - \varphi) + \cos(\alpha - \varphi_0)}, \\ g^0 = -\frac{\sin\varphi}{\cos\varphi + \cos\varphi_0} - \frac{\sin(\alpha - \varphi_0)}{\cos(\alpha - \varphi) + \cos(\alpha - \varphi_0)}, \end{aligned}\right\} \tag{3.34}$$

if both of its faces $(\alpha - \pi < \varphi_0 < \pi)$ are illuminated. The index "0" for the functions f^0 and g^0 means that the cylindrical waves (3.31) and (3.32) are radiated by the uniform part of the surface current (j^0).

§ 4. The Field Radiated by the Nonuniform Part of the Current

In § 1 and 3 we represented the rigorous and approximate expressions for the diffraction field by integrals along the same contour in the complex variable plane. By subtracting the approximate expression from the rigorous expression, we find the field created by the nonuniform part of the current. It is determined by integrals of the type

$$\int_{L_0} p(a, \varphi, \varphi_0, \zeta)\, e^{ikr\cos\zeta}\, d\zeta, \tag{4.01}$$

which, with the replacement of the variable ζ by $s=\sqrt{2}e^{i\frac{\pi}{4}}\sin\frac{\zeta}{2}$, are transformed to the form

$$e^{ikr}\int_{-\infty}^{\infty} q(a, \varphi, \varphi_0, s)\, e^{-krs^2}\, ds \tag{4.02}$$

and may be approximately calculated by the method of steepest descents.

For this purpose, let us expand the function q(s) into a Taylor series

$$q(a, \varphi, \varphi_0, s)=q_0+q_1\cdot s+q_2\cdot s^2+\ldots \tag{4.03}$$

Let us note that expansion (4.03) does not have meaning only in the particular case

$$\left.\begin{aligned}&\varphi=\pi\pm\varphi_0 \qquad \text{with } \varphi_0=0;\ \pi,\\ &\varphi=2\pi-\pi-\varphi_0 \text{ with } \varphi_0=a-\pi,\end{aligned}\right\} \tag{4.04}$$

when the observation direction (ϕ) coincides with the direction of propagation of the incident wave glancing along one of the wedge faces.

Substituting series (4.03) into Equation (4.02) and then performing a term by term integration, we find the asymptotic expansion for the field radiated by the nonuniform part of the current. We limit ourselves to the first term of the asymptotic expansion, omitting terms of the order $(kr)^{-3/2}$ and higher. As a result, the required field from the nonuniform part of the current will equal

$$\left.\begin{aligned} E_z &= -H_\varphi = E_{0z} f^1 \frac{e^{i\left(kr+\frac{\pi}{4}\right)}}{\sqrt{2\pi kr}}, \\ E_\varphi &= H_z = 0 \end{aligned}\right\} \tag{4.05}$$

with wedge excitation by plane wave (1.23), and

$$\left.\begin{aligned} H_z &= E_\varphi = H_{0z} g^1 \frac{e^{i\left(kr+\frac{\pi}{4}\right)}}{\sqrt{2\pi kr}}, \\ H_\varphi &= E_z = 0 \end{aligned}\right\} \tag{4.06}$$

with wedge excitation by plane wave (1.24).

By calculating, with the help of Equations (4.05) and (4.06), the nonuniform part of the current, it is not difficult to see that it is concentrated mainly in the vicinity of the wedge edge. But the field created in the region kr >> 1 by this part of the current has the form of cylindrical waves, the angular functions of which are determined by the relationships[1]

$$f^1 = f - f^0, \quad g^1 = g - g^0, \tag{4.07}$$

where in accordance with § 1 and 3 we have

$$\left.\begin{matrix} f \\ g \end{matrix}\right\} = \frac{\sin\frac{\pi}{n}}{n}\left(\frac{1}{\cos\frac{\pi}{n} - \cos\frac{\varphi-\varphi_0}{n}} \mp \frac{1}{\cos\frac{\pi}{n} - \cos\frac{\varphi+\varphi_0}{n}}\right) \quad \left(n=\frac{\alpha}{\pi}\right) \tag{4.08}$$

---

(1) Footnote appears on page 42.

and

$$\left.\begin{aligned} f^0 &= \frac{\sin\varphi_0}{\cos\varphi+\cos\varphi_0}, \\ g^0 &= -\frac{\sin\varphi}{\cos\varphi+\cos\varphi_0}. \end{aligned}\right\} \tag{4.09}$$

if one face of the wedge is illuminated (that is, when $0<\varphi_0<\alpha-\pi$), and

$$\left.\begin{aligned} f^0 &= \frac{\sin\varphi_0}{\cos\varphi+\cos\varphi_0}+\frac{\sin(\alpha-\varphi_0)}{\cos(\alpha-\varphi)+\cos(\alpha-\varphi_0)}, \\ g^0 &= -\frac{\sin\varphi}{\cos\varphi+\cos\varphi_0}-\frac{\sin(\alpha-\varphi)}{\cos(\alpha-\varphi)+\cos(\alpha-\varphi_0)}. \end{aligned}\right\} \tag{4.10}$$

if both faces of the wedge are illuminated (that is, when $\alpha-\pi<\varphi_0<\pi$). Let us recall that the functions f and g describe the cylindrical waves radiated by the total current — that is, the sum of the uniform and nonuniform parts, and the functions f^0 and g^0 refer to the cylindrical waves radiated only by the uniform part of the current (j^0).

Let us note certain properties of the functions f^1 and g^1. The function $f^1 = f^1(\alpha, \phi, \phi_0)$ is continuous, whereas the function $g^1 = g^1(\alpha, \phi, \phi_0)$ undergoes a finite discontinuity when $\phi_0 = \alpha - \pi$. The reason for this discontinuity is that the uniform part of the current differs from zero on the face along which plane wave (1.24) is propagated (with $\phi_0 = \alpha - \pi$). In the case of radar, when the direction to the observation point coincides with the direction to the source ($\phi = \phi_0$), both functions f^1 and g^1 are continuous. There is no discontinuity of the function g^1 with $\phi = \phi_0 = \alpha - \pi$, because the current element does not radiate in the longitudinal direction.

On the boundary of the plane waves (that is, when $\varphi=\pi\pm\varphi_0$ and $\varphi=2\alpha-\pi-\varphi_0$) the functions f, f^0 and g, g^0 become infinite, whereas the functions f^1 and g^1 remain finite. In accordance with Equations (4.07) - (4.10), they take the following values

$$\left.\begin{matrix} f^1 \\ g^1 \end{matrix}\right\} = \frac{\frac{1}{n}\sin\frac{\pi}{n}}{\cos\frac{\pi}{n}-\cos\frac{\varphi-\varphi_0}{n}} + \frac{1}{2}\operatorname{ctg}\varphi_0 \mp \frac{1}{2n}\operatorname{ctg}\frac{\pi}{n}. \tag{4.11}$$

if $\phi = \pi - \phi_0$, and $\phi_0 < \alpha - \pi$,

$$\left.\begin{aligned} f^1 &= \frac{\frac{1}{n}\sin\frac{\pi}{n}}{\cos\frac{\pi}{n}-\cos\frac{\varphi-\varphi_0}{n}} + \frac{1}{2}\operatorname{ctg}\varphi_0 + \frac{1}{2n}\operatorname{ctg}\frac{\pi}{n} - \\ &\quad - \frac{\sin(\alpha-\varphi_0)}{\cos(\alpha-\varphi)+\cos(\alpha-\varphi_0)}. \\ g^1 &= \frac{\frac{1}{n}\sin\frac{\pi}{n}}{\cos\frac{\pi}{n}-\cos\frac{\varphi-\varphi_0}{n}} + \frac{1}{2}\operatorname{ctg}\varphi_0 - \frac{1}{2n}\operatorname{ctg}\frac{\pi}{n} + \\ &\quad + \frac{\sin(\alpha-\varphi)}{\cos(\alpha-\varphi)+\cos(\alpha-\varphi_0)}. \end{aligned}\right\} \tag{4.12}$$

if $\phi = \pi - \phi_0$ and $\alpha - \pi < \phi_0 < \pi$, and

$$\left.\begin{matrix} f^1 \\ g^1 \end{matrix}\right\} = \mp \frac{\frac{1}{n}\sin\frac{\pi}{n}}{\cos\frac{\pi}{n}-\cos\frac{\varphi+\varphi_0}{n}} \mp \frac{1}{2}\operatorname{ctg}\varphi_0 - \frac{1}{2n}\operatorname{ctg}\frac{\pi}{n}, \tag{4.13}$$

if $\phi = \pi + \phi_0$, and $\phi_0 < \alpha - \pi$. The value $\phi = \pi + \phi_0$ with $\alpha - \pi < \phi_0 < \pi$ corresponds to the angle inside the wedge, and therefore is not of interest. In the direction of the mirror-reflected ray $\phi = 2\alpha - \pi - \phi_0$, the functions f^1 and g^1 are determined (with $\alpha - \pi < \phi_0 < \pi$) by the following equation:

$$\begin{aligned} f^1 &= \frac{\frac{1}{n}\sin\frac{\pi}{n}}{\cos\frac{\pi}{n}-\cos\frac{\varphi-\varphi_0}{n}} - \frac{\sin\varphi_0}{\cos\varphi+\cos\varphi_0} + \\ &\quad + \frac{1}{2}\operatorname{ctg}(\alpha-\varphi_0) + \frac{1}{2n}\operatorname{ctg}\frac{\pi}{n}. \\ g^1 &= \frac{\frac{1}{n}\sin\frac{\pi}{n}}{\cos\frac{\pi}{n}-\cos\frac{\varphi-\varphi_0}{n}} + \frac{\sin\varphi}{\cos\varphi+\cos\varphi_0} + \\ &\quad + \frac{1}{2}\operatorname{ctg}(\alpha-\varphi_0) - \frac{1}{2n}\operatorname{ctg}\frac{\pi}{n}. \end{aligned} \tag{4.14}$$

The functions f^1 and g^1 have a finite value everywhere, except for the particular values ϕ and ϕ_0 enumerated in Equation (4.04). The graphs of the functions f^1 and g^1 (Figures 8 - 13) drawn in polar coordinates give a visual representation of the effect of the nonuniform part of the current which is concentrated near the wedge edge. In particular, they show that this effect may be usbstantial for the fringing field not only in the shadow region $(\pi+\varphi_0<\varphi\leq\alpha)$, but also in the region of light $(0\leq\varphi<\pi+\varphi_0)$. The continuous lines in the figures correspond to the functions f^1 ($f^1 < 0$). The dashed and dash-dot lines correspond to the functions g^1 — the dash lines refer to the case $g^1 < 0$, and the dash-dot lines refer to the case $g^1 > 0$.

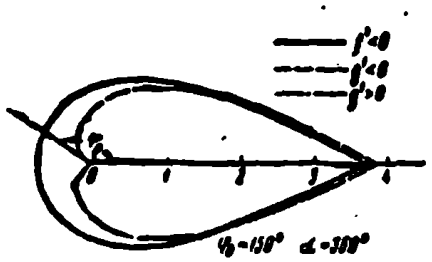

Figure 8. The diagram of the field from the nonuniform part of the current excited by a plane wave on a half-plane. The function f^1 (or g^1) corresponds to the case when the electric (or magnetic) vector of the incident wave is parallel to the wedge edge.

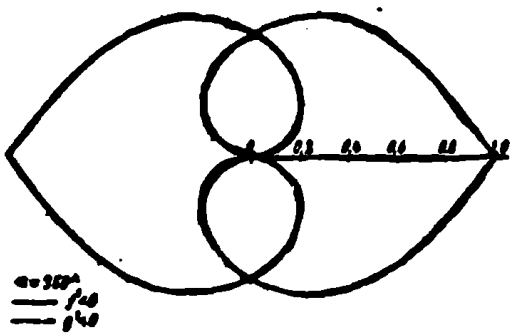

Figure 9. The same as Figure 8 for the case $\phi = \phi_0$.

Let us turn our attention to the next important aspect. As is seen from § 1 and 3, the nonuniform part of the current on the wedge is described by a contour integral which is generally not expressed in terms of well-known functions. But in order to calculate the field scattered by some convex, ideally conducting surface with discontinuities (edges), the indicated expression still must be integrated over the given surface. Obviously, such a path is able to lead only to very cumbersome equations. Therefore, henceforth, when calculating

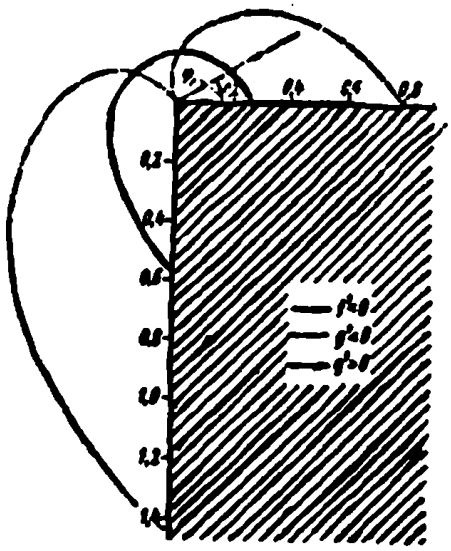

Figure 10. The functions f^1 and g^1 for a wedge ($\phi_0 = 30°$, $\alpha = 270°$).

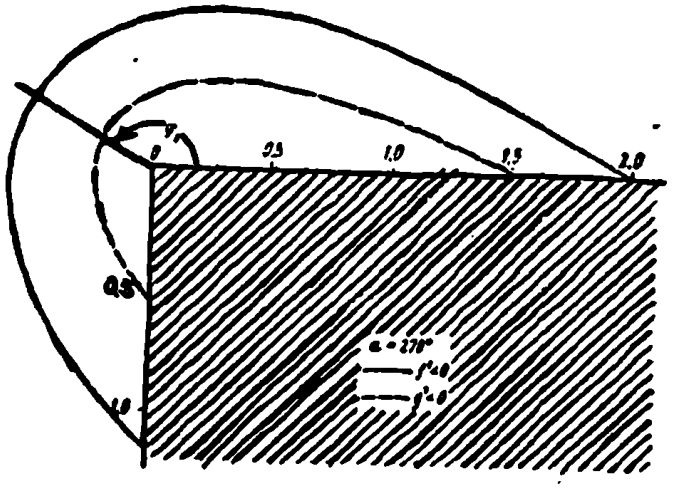

Figure 11. The same as Figure 10 when $\phi_0 = 150°$.

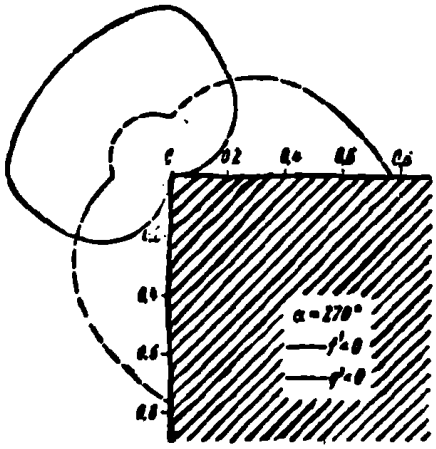

Figure 12. The same as Figure 10 for the case $\phi = \phi_0$.

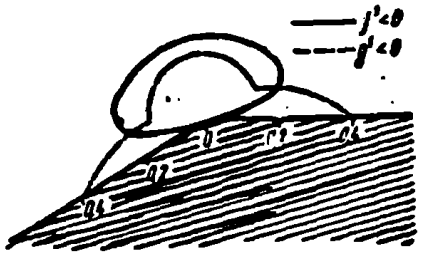

Figure 13. The functions f^1 and g^1 for a wedge ($\phi = \phi_0$, $\alpha = 210°$).

the field scattered by composite bodies, we will not integrate the explicit expressions for the nonuniform part of the current, but we will endeavour to express these integrals directly in terms of the functions f^1 and g^1 which have been found.

§ 5. The Oblique Incidence of a Plane Wave on a Wedge

Above, the diffraction was studied of a plane wave incident on a wedge perpendicular to its edge. Now let us investigate the case when the plane wave

$$\mathbf{E} = \mathbf{E}_0 e^{ik(x\cos\alpha + y\cos\beta + z\cos\gamma)} \tag{5.01}$$

falls on the wedge at an oblique angle $\gamma \left(0 < \gamma < \frac{\pi}{2}\right)$ to the wedge edge (Figure 14).

From the geometry of the problem, it follows that the diffraction field must have that same dependence on the z coordinate as the field of the incident wave, that is

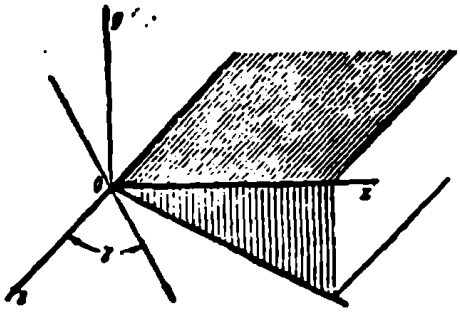

Figure 14. Diffraction by a wedge with oblique incidence of a plane wave. γ is the angle between the normal to the incident wave front and the z axis.

$$\left.\begin{aligned}\mathbf{E}&=\mathbf{E}(x, y)\,e^{ikz\cos\gamma},\\ \mathbf{H}&=\mathbf{H}(x, y)\,e^{ikz\cos\gamma}.\end{aligned}\right\} \tag{5.02}$$

Using Maxwell's equations

$$\operatorname{rot}\mathbf{H}=-ik\mathbf{E},\ \operatorname{rot}\mathbf{E}=ik\mathbf{H}, \tag{5.03}$$

one is able to obtain the following expressions for the radial and azimuthal components of the field:

$$\begin{aligned}E_r&=-\frac{1}{ik\sin^2\gamma}\left(\frac{1}{r}\frac{\partial H_z}{\partial\varphi}+\cos\gamma\frac{\partial E_z}{\partial r}\right),\\ H_r&=\frac{1}{ik\sin^2\gamma}\left(\frac{1}{r}\frac{\partial E_z}{\partial\varphi}-\cos\gamma\frac{\partial H_z}{\partial r}\right),\\ E_\varphi&=\frac{1}{ik\sin^2\gamma}\left(\frac{\partial H_z}{\partial r}-\frac{\cos\gamma}{r}\frac{\partial E_z}{\partial\varphi}\right),\\ H_\varphi&=-\frac{1}{ik\sin^2\gamma}\left(\frac{\partial E_z}{\partial r}+\frac{\cos\gamma}{r}\frac{\partial H_z}{\partial\varphi}\right).\end{aligned} \tag{5.04}$$

The functions E_z and H_z in turn satisfy the wave equations

$$\Delta E_z+k_1^2E_z=0,\ \Delta H_z+k_1^2H_z=0, \tag{5.05}$$

where

$$\Delta=\frac{\partial^2}{\partial x^2}+\frac{\partial^2}{\partial y^2}\ \text{and}\ k_1=k\sin\gamma. \tag{5.06}$$

In § 4 we found the fields (4.05) and (4.06) which satisfy the equations

$$\Delta E_z+k^2E_z=0,\quad \Delta H_z+k^2H_z=0 \tag{5.07}$$

and which are created by the nonuniform part of the current excited on the wedge by the plane wave

$$\mathbf{E} = \mathbf{E}_0 e^{-ik(x\cos\varphi_0 + y\sin\varphi_0)}. \tag{5.08}$$

Representing Expression (5.01) in the form

$$\mathbf{E} = \mathbf{E}_0 e^{ikz\cos\gamma - ik_1(x\cos\varphi_0 + y\sin\varphi_0)} \tag{5.09}$$

and comparing Equations (5.05) and (5.07), we easily find the field created by the nonuniform part of the current with the irradiation of the wedge by plane wave (5.01). For this purpose, it is sufficient to replace in Equations (4.05) and (4.06) k by k_1, and E_{0z} and H_{0z} by $E_{0z}e^{ikz\cos\gamma}$ and $H_{0z}e^{ikz\cos\gamma}$. As a result, we obtain

$$\left.\begin{aligned} E_z = -H_\gamma &= E_{0z} f^1(\varphi, \varphi_0) \frac{e^{i\left(k_1 r + \frac{\pi}{4}\right)}}{\sqrt{2\pi k_1 r}} e^{ikz\cos\gamma}, \\ H_z = E_\gamma &= H_{0z} g^1(\varphi, \varphi_0) \frac{e^{i\left(k_1 r + \frac{\pi}{4}\right)}}{\sqrt{2\pi k_1 r}} e^{ikz\cos\gamma}. \end{aligned}\right\} \tag{5.10}$$

The angle ϕ_0 introduced here is determined by the condition

$$e^{ik(x\cos\alpha + y\cos\beta)} = e^{-ik_1(x\cos\varphi_0 + y\sin\varphi_0)}, \tag{5.11}$$

hence

$$\operatorname{tg}\varphi_0 = \frac{\cos\beta}{\cos\alpha}. \tag{5.12}$$

The remaining components of the field created by the nonuniform part of the current with the oblique incidence of a plane wave are found from relationships (5.04), and when kr >> 1 they equal

$$\begin{aligned} E_r &= -\operatorname{ctg}\gamma E_z \quad H_r = -\operatorname{ctg}\gamma H_z \\ E_\varphi &= \frac{1}{\sin\gamma} H_z \quad H_\varphi = -\frac{1}{\sin\gamma} E_z. \end{aligned} \tag{5.13}$$

The equiphase surfaces for these waves have the form

$$r\sin\gamma + z\cos\gamma = \text{const} \tag{5.14}$$

and are conical surfaces, the generatrices of which form the angle $\pi/2 + \gamma$ with the positive direction of the z axis. Thus, with oblique irradiation of the wedge by a plane wave, the field created by the nonuniform part of the current is a set of conical waves diverging from the wedge edge. The normals to the phase surfaces of these waves form an angle γ with the positive direction of the z axis and are shown in Figure 15. These waves may be represented in a more graphic form if one introduces the components (see Figure 15):

$$\left.\begin{aligned} E_1 &= E_r \cos\gamma - E_z \sin\gamma, \\ H_1 &= H_r \cos\gamma - H_z \sin\gamma. \end{aligned}\right\} \tag{5.15}$$

Then the final expressions for the fringing field in the far zone will have the form

$$\left.\begin{aligned} E_1 = H_\varphi &= -\frac{1}{\sin\gamma} E_z, \\ H_1 &= -E_\varphi = -\frac{1}{\sin\gamma} H_z. \end{aligned}\right\} \tag{5.16}$$

Now we are able to proceed to the application of the results which have been obtained for the solution of specific diffraction problems. The simplest of them is the problem of diffraction by an infinitely long strip which has a rigorous solution [23] in the form of Mathieu function series. However, in the quasi-optical region when the width of the strip is large in comparison with the wavelength, these series have a poor convergence and are not suitable for numerical calculations. Therefore, the requirement arises for approximation equations which are useful in the quasi-optical region. The derivation of such equations for a field scattered by a strip will be given in the following section.

§ 6. Diffraction by a Strip

Let us investigate diffraction by an infinitely thin, ideally conducting strip which has a width of 2a and an unlimited length. The orientation of the strip in space is shown in Figure 16.

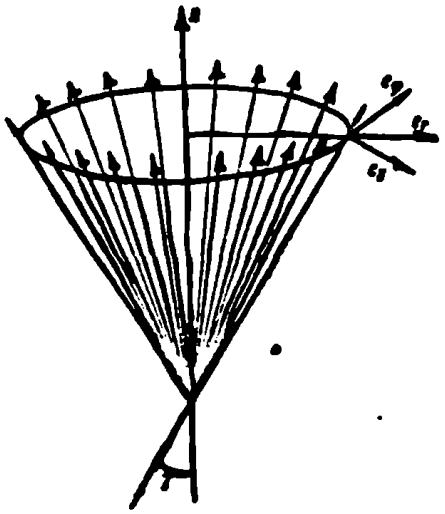

Figure 15. The cone of diffracted rays.

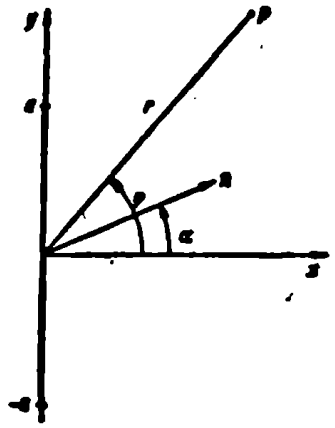

Figure 16. Diffraction of a plane wave by an infinitely long strip. The section of the axis y (-a $\leq$ y $\leq$ a) shows the transverse cross section of the strip with the plane z = 0; α is the angle of incidence.

Let a plane, electromagnetic wave strike the strip perpendicular to the edges. Let the direction of propagation of this wave form an angle $\alpha\left(|\alpha|<\frac{\pi}{2}\right)$ with the plane y = 0. The field of this wave is represented in the form

$$\mathbf{E}=\mathbf{E}_0 e^{ik(x\cos\alpha+y\sin\alpha)},\quad \mathbf{H}=\mathbf{H}_0 e^{ik(x\cos\alpha+y\sin\alpha)}. \tag{6.01}$$

The uniform part of the current excited by the plane wave on the strip has the components

$$\left.\begin{aligned} j_x^0&=0,\\ j_y^0&=\frac{c}{2\pi}H_{0z}e^{iky\sin\alpha},\\ j_z^0&=\frac{c}{2\pi}E_{0z}\cos\alpha\, e^{iky\sin\alpha}. \end{aligned}\right\} \tag{6.02}$$

Substituting these values into the equation for the vector potential

$$A=\frac{1}{c}\int_{-a}^{a}J^{0}(\eta)\,d\eta\int_{-\infty}^{\infty}\frac{e^{ik\sqrt{x^{2}+(y-\eta)^{2}+\zeta^{2}}}}{\sqrt{x^{2}+(y-\eta)^{2}+\zeta^{2}}}\,d\zeta. \tag{6.03}$$

and taking into account relationships (3.05) and (1.18), we obtain the following expressions in the region $r \gg ka^2$:

$$\left.\begin{aligned}A_x&=0,\\ A_y&=\frac{2}{k}H_{0z}\frac{\sin[ka(\sin\alpha-\sin\varphi)]}{\sin\alpha-\sin\varphi}\frac{e^{i\left(kr+\frac{\pi}{4}\right)}}{\sqrt{2\pi kr}},\\ A_z&=\frac{2}{k}E_{0z}\cos\alpha\frac{\sin[ka(\sin\alpha-\sin\varphi)]}{\sin\alpha-\sin\varphi}\frac{e^{i\left(kr+\frac{\pi}{4}\right)}}{\sqrt{2\pi kr}}.\end{aligned}\right\} \tag{6.04}$$

The components of the fringing field in the cylindrical coordinate system equal

$$E_z=-H_\varphi=ikA_z,\quad H_z=E_\varphi=ikA_\varphi, \tag{6.05}$$

where

$$A_\varphi=A_y\cos\varphi-A_x\sin\varphi. \tag{6.06}$$

Substituting Expressions (6.04) here, let us determine the field radiated by the uniform part of the current

$$\left.\begin{aligned}E_z&=-H_\varphi=2E_{0z}\cos\alpha\frac{\sin[ka(\sin\alpha-\sin\varphi)]}{\sin\alpha-\sin\varphi}\frac{e^{i\left(kr+\frac{3\pi}{4}\right)}}{\sqrt{2\pi kr}},\\ E_\varphi&=H_z=2H_{0z}\cos\varphi\frac{\sin[ka(\sin\alpha-\sin\varphi)]}{\sin\alpha-\sin\varphi}\frac{e^{i\left(kr+\frac{3\pi}{4}\right)}}{\sqrt{2\pi kr}}.\end{aligned}\right\} \tag{6.07}$$

This field may be represented in the form of cylindrical waves diverging from the strip edges

$$\left.\begin{aligned} E_\theta = -H_\varphi = E_{0z}\cdot[f^0(1)\,e^{ika(\sin\theta-\sin\varphi)}+ \\ +f^0(2)\,e^{-ika(\sin\theta-\sin\varphi)}]\frac{e^{i\left(kr+\frac{\pi}{4}\right)}}{\sqrt{2\pi kr}}, \\ E_\varphi = H_\theta = H_{0z}\cdot[g^0(1)\,e^{ika(\sin\theta-\sin\varphi)}+ \\ +g^0(2)\,e^{-ika(\sin\theta-\sin\varphi)}]\frac{e^{i\left(kr+\frac{\pi}{4}\right)}}{\sqrt{2\pi kr}}. \end{aligned}\right\} \tag{6.08}$$

Here the first terms correspond to the waves from edge 1 (y = a), and the second terms correspond to the waves from edge 2 (y = -a). The functions f^0 and g^0 are determined in the right half-plane $\left(|\varphi|<\frac{\pi}{2}\right)$ by the equations

$$\left.\begin{aligned} f^0(1) = -f^0(2) = \frac{\cos\varphi}{\sin\theta-\sin\varphi}, \\ g^0(1) = -g^0(2) = \frac{\cos\varphi}{\sin\theta-\sin\varphi}. \end{aligned}\right\} \tag{6.09}$$

Now let us find the field radiated by the nonuniform part of the current. Assuming the strip is sufficiently wide ($ka \gg 1$), one is able to approximately consider that the current near its upper edge is the same as on the ideally conducting half-plane $-\infty<y<a$, and near the lower edge it is the same as on the half-plane $-a<y<\infty$. Therefore, in accordance with § 4, the field from the nonuniform part of the current flowing on the strip may be represented in the form of the sum of the edge cylindrical waves.

$$\left.\begin{aligned} E_\theta = -H_\varphi = E_{0z}\cdot[f^1(1)\,e^{ika(\sin\theta-\sin\varphi)}+ \\ +f^1(2)\,e^{-ika(\sin\theta-\sin\varphi)}]\frac{e^{i\left(kr+\frac{\pi}{4}\right)}}{\sqrt{2\pi kr}}, \\ E_\varphi = H_\theta = H_{0z}\cdot[g^1(1)\,e^{ika(\sin\theta-\sin\varphi)}+ \\ +g^1(2)\,e^{-ika(\sin\theta-\sin\varphi)}]\frac{e^{i\left(kr+\frac{\pi}{4}\right)}}{\sqrt{2\pi kr}}, \end{aligned}\right\} \tag{6.10}$$

where the functions f^1 and g^1 are determined in the right half-plane $\left(|\varphi|<\frac{\pi}{2}\right)$ by the equations

$$\left.\begin{aligned} f^1(1)=f(1)-f^0(1),\quad f^1(2)=f(2)-f^0(2),\\ g^1(1)=g(1)-g^0(1),\quad g^1(2)=g(2)-g^0(2). \end{aligned}\right\} \tag{6.11}$$

in connection with which

$$\left.\begin{aligned} f(1)&=-\frac{\cos\frac{\alpha+\varphi}{2}-\sin\frac{\alpha-\varphi}{2}}{\sin\alpha-\sin\varphi},\\ f(2)&=-\frac{\cos\frac{\alpha+\varphi}{2}+\sin\frac{\alpha-\varphi}{2}}{\sin\alpha-\sin\varphi},\\ g(1)&=\frac{\cos\frac{\alpha+\varphi}{2}+\sin\frac{\alpha-\varphi}{2}}{\sin\alpha-\sin\varphi},\\ g(2)&=-\frac{-\cos\frac{\alpha+\varphi}{2}+\sin\frac{\alpha-\varphi}{2}}{\sin\alpha-\sin\varphi}. \end{aligned}\right\} \tag{6.12}$$

The functions f^0 and g^0 are described by the relationships (6.09).

As a result, the fringing field (the sum of the fields radiated by the uniform and nonuniform parts of the current) will equal

$$\left.\begin{aligned} E_z=-H_\varphi=E_{0z}\cdot[f(1)e^{ika(\sin\alpha-\sin\varphi)}+\\ +f(2)e^{-ika(\sin\alpha-\sin\varphi)}]\frac{e^{i\left(kr+\frac{\pi}{4}\right)}}{\sqrt{2\pi kr}},\\ E_\varphi=H_z=H_{0z}\cdot[g(1)e^{ika(\sin\alpha-\sin\varphi)}+\\ +g(2)e^{-ika(\sin\alpha-\sin\varphi)}]\frac{e^{i\left(kr+\frac{\pi}{4}\right)}}{\sqrt{2\pi kr}}. \end{aligned}\right\} \tag{6.13}$$

Consequently, the resulting field is expressed only in terms of the functions f and g which determine the cylindrical wave in the rigorous solution (see § 2). The field is the superposition of two such waves which diverge from the edges 1 (y = a) and 2 (y = -a).

Substituting into Equations (6.13) the explicit Expressions (6.12) for the functions f and g, we obtain

$$\left.\begin{aligned} E_z = -H_\varphi = E_{0z}\left\{-\frac{\cos[ka(\sin\alpha-\sin\varphi)]}{\cos\frac{\alpha+\varphi}{2}}+\right.\right. \\ \left.+i\frac{\sin[ka(\sin\alpha-\sin\varphi)]}{\sin\frac{\alpha-\varphi}{2}}\right\}\frac{e^{i\left(kr+\frac{\pi}{4}\right)}}{\sqrt{2\pi kr}}, \\ E_\varphi = H_z = H_{0z}\left\{\frac{\cos[ka(\sin\alpha-\sin\varphi)]}{\cos\frac{\alpha+\varphi}{2}}+\right. \\ \left.\left.+i\frac{\sin[ka(\sin\alpha-\sin\varphi)]}{\sin\frac{\alpha-\varphi}{2}}\right\}\frac{e^{i\left(kr+\frac{\pi}{4}\right)}}{\sqrt{2\pi kr}}.\right| \end{aligned} \tag{6.14}$$

These equations are valid when $r >> ka^2$ and $|\varphi| < \frac{\pi}{2}$. Moreover, it is assumed that $ka >> 1$, since only under this condition is one able to consider the nonuniform part of the current in the vicinity of the strip's edge to be approximately the same as on the corresponding half-plane. In the case of normal incidence of a plane wave ($\alpha = 0$), Equations (6.14) change into expressions corresponding to the first approximation of Schwarzschild [15].

From relationships (6.03) and (6.05), it follows that the electric field is an even function, and the magnetic field an odd function, of the x coordinate measured perpendicular to the plane $x = 0$ (in which the current flows)

$$E_z(x) = E_z(-x), \quad H_z(x) = -H_z(-x). \tag{6.15}$$

Therefore, on the basis of Equations (6.14) and (6.15) one is able to write the expressions for the fringing field in the region $x < 0$ (where $\frac{\pi}{2} < |\varphi| < \pi$)

$$\left.\begin{aligned} E_z = -H_\varphi = \pm E_{0z}\left\{\frac{\cos[ka(\sin\alpha-\sin\varphi)]}{\sin\frac{\alpha-\varphi}{2}}-\right.\right. \\ \left.-i\frac{\sin[ka(\sin\alpha-\sin\varphi)]}{\cos\frac{\alpha+\varphi}{2}}\right\}\frac{e^{i\left(kr+\frac{\pi}{4}\right)}}{\sqrt{2\pi kr}}, \\ E_\varphi = H_z = \pm H_{0z}\cdot\left\{\frac{\cos[ka(\sin\alpha-\sin\varphi)]}{\sin\frac{\alpha-\varphi}{2}}+\right.\left.\right| \end{aligned} \tag{6.16}$$

$$+i\frac{\sin\left[\frac{1}{2}ka(\sin\alpha-\sin\varphi)\right]}{\cos\frac{\alpha+\varphi}{2}}\Bigg\}\frac{e^{i\left(kr+\frac{\pi}{4}\right)}}{\sqrt{2\pi kr}}. \Bigg| \qquad (6.16)$$

Here one must select the upper sign in front of the braces when $\phi > 0$, and one must select the lower sign when $\phi < 0$.

The resulting Equations (6.14) and (6.16), in contrast to Equations (6.07), satisfy the reciprocity principle. It is not difficult to establish this by verifying that Equation (6.14) is not changed with the simultaneous replacement of α by ϕ and of ϕ by α, and Equation (6.16) is not changed with the replacement of α by $\pi + \phi$ and of ϕ by $\alpha - \pi$ (if $-\pi<\varphi<-\frac{\pi}{2}$) and with the replacement of α by $\pi - \phi$ and of ϕ by $\pi - \alpha$ (if $\frac{\pi}{2}<\varphi<\pi$).

However, the indicated equations lead to a discontinuity of the magnetic vector tangential component H_z on the plane $x = 0$. This is connected with the fact that, by considering the nonuniform part of the current in the vicinity of the strip's edge to be the same as on the corresponding half-plane, we actually assume the presence of currents on the entire plane containing the strip. In order to refine the resulting expressions, it is necessary to solve the problem of secondary diffraction — that is, diffraction of the wave travelling from one edge of the strip to its other edge. In other words, it is necessary to take into account the diffraction interaction of the strip's edges. As we see, it is also necessary to take into account the secondary diffraction in the case $\alpha=\pm\frac{\pi}{2}$ when the H_z component of the fringing field must equal zero.

In Chapter V, we will return to the problem of diffraction by a strip, and together with the investigation of the secondary diffraction, we will present the results of the numerical calculation based on Equations (6.07), (6.14) and (6.16).

FOOTNOTE

Footnote (1) on page 27

The designations used here differ slightly from those used in the papers [7 - 11]. The functions f and f^1 there were designated by f_1 and f, respectively.

CHAPTER II

DIFFRACTION BY A DISK

The problem of diffraction by a disk has a rigorous solution [24-26]; however, it is not suitable for numerical calculations in the quasi-optical region when the dimensions of the disk are large in comparison with the wavelength. The physical optics approach used in such cases sometimes gives erroneous results. In particular, the fringing field calculated in this approach does not satisfy the reciprocity principle.

In this Chapter a refinement of the physical optics approach is carried out. First the diffraction of a plane electromagnetic wave by a disk with normal incidence (§ 7-9) is investigated, and then (§ 10-12) diffraction by a disk with oblique incidence of a plane electromagnetic wave is investigated.

Normal Irradiation

§ 7. The Physical Optics Approach

Let an ideally conducting, infinitely thin disk of radius a (Figure 17) be irradiated by plane wave

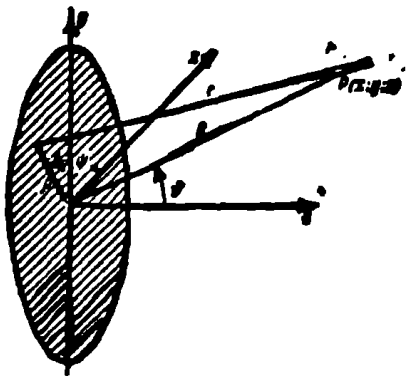

Figure 17. Diffraction by a disk of a plane wave propagated along the z axis.

$$\left.\begin{aligned} E_y &= -H_x = -H_{0x}e^{ikz}, \\ E_z &= H_y = 0. \end{aligned}\right\} \quad (7.01)$$

The uniform part of the current excited on the disk by wave (7.01) is determined by Equation (3.01) and has the components

$$j_y^0 = -\frac{c}{2\pi}H_{0x}, \quad j_x^0 = j_z^0 = 0. \quad (7.02)$$

Let us find the field created by this current.

Since the diffraction field in the far zone ($R >> ka^2$) is of interest to us, the vector potential

$$\mathbf{A}(x, y, z) = \frac{1}{c}\int_0^a \rho d\rho \int_0^{2\pi} \mathbf{j}(\rho, \psi)\frac{e^{ikr}}{r}d\psi \quad (7.03)$$

may be simplified by using the relationship

$$r = \sqrt{R^2 + \rho^2 - 2\rho R\cos\Omega} \approx R - \rho\cos\Omega, \quad (7.04)$$

where Ω is the angle between ρ and R, and

$$\cos\Omega = \sin\vartheta\cos(\psi - \varphi). \quad (7.05)$$

As a result, we obtain the simpler equation

$$\mathbf{A}(x, y, z) = \frac{1}{c}\frac{e^{ikr}}{R}\int_0^a \rho d\rho \int_0^{2\pi} \mathbf{j}(\rho, \psi)\, e^{-ik\rho\cos\Omega}\, d\psi. \quad (7.06)$$

Continuing by using the equations

$$\mathbf{H} = \mathrm{rot}\,\mathbf{A}, \quad \mathrm{rot}\,\mathbf{H} = -ik\mathbf{E}, \quad (7.07)$$

it is easy to show that in the spherical coordinate system the fringing field components with $R >> ka^2$ equal

$$\left.\begin{aligned} E_\theta &= H_\varphi = ikA_\theta, \\ E_\varphi &= -H_\theta = ikA_\varphi, \\ E_R &= H_R = 0, \end{aligned}\right\} \tag{7.08}$$

where

$$\left.\begin{aligned} A_\theta &= A_x \cos\varphi - A_y \sin\varphi, \\ A_\theta &= (A_x \cos\varphi + A_y \sin\varphi)\cos\theta - A_z \sin\theta. \end{aligned}\right\} \tag{7.09}$$

Substituting here the values

$$\left.\begin{aligned} A_y &= -H_{0x} \cdot \frac{a}{k \sin\theta} J_1(ka \sin\theta) \frac{e^{ikR}}{R}, \\ A_x &= A_z = 0, \end{aligned}\right\} \tag{7.10}$$

which result from Equations (7.02) and (7.06), let us find the field radiated by the uniform part of the current in the form

$$\left.\begin{aligned} E_\theta = H_\varphi &= -iaH_{0x} \cdot \frac{\sin\varphi}{\sin\theta} \cos\theta J_1(ka \sin\theta) \frac{e^{ikR}}{R}, \\ E_\varphi = -H_\theta &= -iaH_{0x} \cdot \frac{\cos\varphi}{\sin\theta} J_1(ka \sin\theta) \frac{e^{ikR}}{R}. \end{aligned}\right\} \tag{7.11}$$

The function $J_1(ka \sin\theta)$ is a first order Bessel function. By using its asymptotic expression

$$J_1(ka \sin\theta) = \sqrt{\frac{2}{\pi ka \sin\theta}} \cos\left(ka \sin\theta - \frac{3\pi}{4}\right), \tag{7.12}$$

which is applicable when $ka \sin\theta \gg 1$, one is able to rewrite Equations (7.11) in the following form:

$$\left.\begin{aligned} E_\theta = H_\varphi &= -iH_{0x} \sqrt{\frac{a}{2\pi k \sin\theta}} \cos\theta \frac{\sin\varphi}{\sin\theta} \times \\ &\times \left[e^{-i\left(ka \sin\theta - \frac{3\pi}{4}\right)} + e^{i\left(ka \sin\theta - \frac{3\pi}{4}\right)}\right] \frac{e^{ikR}}{R}, \\ E_\varphi = -H_\theta &= -iH_{0x} \sqrt{\frac{a}{2\pi k \sin\theta}} \frac{\cos\varphi}{\sin\theta} \times \\ &\times \left[e^{-i\left(ka \sin\theta - \frac{3\pi}{4}\right)} + e^{i\left(ka \sin\theta - \frac{3\pi}{4}\right)}\right] \frac{e^{ikR}}{R}. \end{aligned}\right\} \tag{7.13}$$

The resulting equations show that in the region $R \gg ka^2$, $ka \sin\theta \gg 1$ the fringing field may be investigated as the sum of the spherical waves from two "luminous" points on the rim of the disk, the polar angles of which respectively equal $\psi = \phi$ and $\psi = \pi + \phi$. It is not difficult to see that these waves satisfy the Fermi principle. Actually, of all the points on the disk's surface, the point $\rho = a$, $\psi = \phi$ is the closest to the observation point (R, θ, φ), and the point $\rho = a$, $\psi = \pi + \phi$ is the furthest from it.

However, Equations (7.13) describe the radiation not only from the two "luminous" points, but they determine the field radiated by the entire "luminous" region which is adjacent to the line connecting the points $\rho = a$, $\psi = \phi$ and $\rho = a$, $\psi = \pi + \phi$.

Let us show that the luminous region actually makes the main contribution to the fringing field. For this purpose, let us calculate the field radiated by the currents which flow inside the sector encompassing the line $\psi = \phi$ (Figure 18). Let us take the angular dimensions of the sector in such a way that its arc, which equals $2a\phi_0$, would occupy the first Fresnel zone. When this is done, the angle ϕ_0 will satisfy the equation

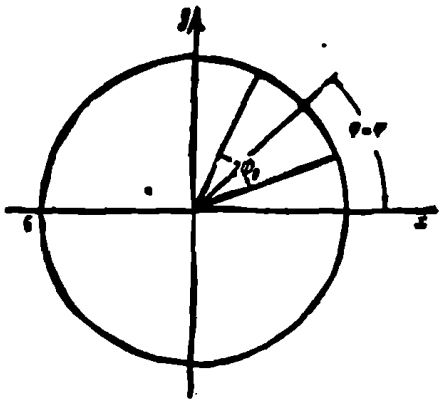

Figure 18. Calculation of the field radiated by the "luminous" region of the disk.

$$a(1-\cos\Phi_0)\sin\theta = \frac{\lambda}{4}. \qquad (7.14)$$

In the case being investigated by us, when the condition $ka \sin\theta \gg 1$ is fulfilled, we have from Equation (7.14)

$$\cos\Phi_0 = 1 - \frac{\lambda}{4a\sin\theta} \approx 1 - \frac{\Phi_0^2}{2}, \qquad (7.15)$$

hence

$$\Phi_0 = \sqrt{\frac{\pi}{ka\sin\theta}}. \qquad (7.16)$$

The vector potential of the currents flowing in the indicated sector is determined by the equation

$$\left.\begin{aligned} A_\varphi &= -\frac{1}{2\pi} H_{0x} \cdot \frac{e^{ikR}}{R} \int_{-\varphi_0}^{\varphi_0} d\psi \int_0^a e^{-ikp\sin\vartheta\cos\psi} p\, dp, \\ A_R &= A_\vartheta = 0. \end{aligned}\right| \tag{7.17}$$

Taking into account the condition $ka\sin\vartheta \gg 1$, one may show that the field created by the currents of this sector will equal

$$\left.\begin{aligned} E_\vartheta = H_\varphi &\sim H_{0x} \sqrt{\frac{a}{\pi k \sin\vartheta}} \cos\vartheta \times \\ \times \frac{\sin\varphi}{\sin\vartheta} \frac{e^{ikR}}{R} e^{-ika\sin\vartheta + i\frac{\pi}{4}} &+ 0\left(\frac{1}{\sqrt{ka\sin\vartheta}}\right). \\ E_\varphi = -H_\vartheta &\sim H_{0x} \sqrt{\frac{a}{\pi k \sin\vartheta}} \times \\ \times \frac{\cos\varphi}{\sin\vartheta} \frac{e^{ikR}}{R} e^{-ika\sin\vartheta + i\frac{\pi}{4}} &+ 0\left(\frac{1}{\sqrt{ka\sin\vartheta}}\right). \end{aligned}\right| \tag{7.18}$$

The amplitude of the expressions which have been found is approximately $\sqrt{2}$ times larger than the amplitude of the first terms in Equation (7.13). Moreover, expressions (7.18) and the corresponding terms in Equation (7.13) differ slightly in their phases: the first have the factor $e^{i\frac{\pi}{4}}$, and the latter — the factor $-e^{i\frac{\pi}{4}}$. The result obtained is similar to the well-known thesis in optics that the effect of a wave is equal to the effect of half of the first Fresnel zone (see, for example [27], p. 132).

In the vicinity of the directions $\vartheta=0$ and $\vartheta=\pi$, when the azimuthal components lose their meaning, for the purpose of studying the fringing field it is more convenient to use the Cartesian components

$$\left.\begin{aligned} E_x &= (E_\vartheta\cos\vartheta + E_R\sin\vartheta)\cos\varphi - E_\varphi\sin\varphi, \\ E_y &= (E_\vartheta\cos\vartheta + E_R\sin\vartheta)\sin\varphi + E_\varphi\cos\varphi. \end{aligned}\right| \tag{7.19}$$

Turning to Equations (7.11), we find that when $\vartheta=0$ and $\vartheta=\pi$

$$E_x = 0, \quad E_y = -iH_{0x} \cdot \frac{ka^2}{2} \cdot \frac{e^{ikR}}{R}. \tag{7.20}$$

Consequently, in the physical optics approach the field scattered in the directions $\theta = 0$ and $\theta = \pi$ preserves the polarization of the incident wave.

§ 8. The Field From the Uniform Part of the Current

Let us proceed to calculation of the field created by the nonuniform part of the current with normal irradiation of the disk. Since the latter is concentrated mainly in the vicinity of the disk's edge ($\rho = a$), the vector potential corresponding to it will equal, in accordance with Equation (7.06),

$$\mathbf{A} = \frac{a}{c}\frac{e^{ikR}}{R}\cdot\int_0^a d\rho\int_0^{2\pi} j^1(\rho, \psi)\, e^{-ik\rho\sin\theta\cos(\psi-\varphi)}\, d\psi. \tag{8.01}$$

The inner integral is calculated with $ka\sin\theta \gg 1$ based on the stationary phase method (see, for example [21], p. 256), and Equation (8.01) is transformed to the form

$$\mathbf{A}(x, y, z) = \frac{a}{c}\sqrt{\frac{2\pi}{ka\sin\theta}}\frac{e^{ikR}}{R}e^{i\frac{\pi}{4}}\times$$
$$\times\left[\int_0^a j^1(\rho, \psi_1)\, e^{-ik\rho\sin\theta}\, d\rho - i\int_0^a j^1(\rho, \psi_2)\, e^{ik\rho\sin\theta}\, d\rho\right], \tag{8.02}$$

which allows one to interpret the fringing field as the field from a luminous line on the disk. This line is a diameter, the polar angle ψ of the points on which equals

$$\psi_1 = \varphi \text{ and } \psi_2 = \pi + \varphi. \tag{8.03}$$

Assuming the diameter of the disk is sufficiently large in comparison with the wavelength ($ka \gg 1$), one may approximately assume that the nonuniform part of the current near the disk's edge will be the same as on the corresponding half-plane (Figure 19). On the basis of § 4, the field from the nonuniform part of the current flowing on the half-plane $-\infty < y_1 < a$ may be represented in the form

$$\left.\begin{aligned} E_{x_1}(1) &= ikA_{x_1}(1) = E_{0x_1}\cdot f^1(1)\frac{e^{i\left(kR+\frac{\pi}{4}\right)}}{\sqrt{2\pi kR}}e^{-ikx_1\sin\theta}, \\ H_{x_1}(1) &= -ikA_{y_1}(1)\cos\theta = \\ &= H_{0x_1}\cdot g^1(1)\frac{e^{i\left(kR+\frac{\pi}{4}\right)}}{\sqrt{2\pi kR}}e^{-ikx_1\sin\theta}. \end{aligned}\right\} \qquad (8.04)$$

and similarly the field from the current flowing on the half-plane $-a<y_1<\infty$, may be represented in the form

$$\left.\begin{aligned} E_{x_1}(2) &= ikA_{x_1}(2) = E_{0x_1}\cdot f^1(2)\frac{e^{i\left(kR+\frac{\pi}{4}\right)}}{\sqrt{2\pi kR}}e^{ikx_1\sin\theta}, \\ H_{x_1}(2) &= -ikA_{y_1}(2)\cos\theta = H_{0x_1}\cdot g^1(2)\frac{e^{i\left(kR+\frac{\pi}{4}\right)}}{\sqrt{2\pi kR}}e^{ikx_1\sin\theta}. \end{aligned}\right\} \qquad (8.05)$$

Here

$$\left.\begin{aligned} A(1) &= \frac{1}{c}\sqrt{\frac{2\pi}{kR}}e^{i\left(kR+\frac{\pi}{4}\right)}\int_{-a}^{\infty} f^1(\eta)e^{-ikx_1\sin\theta}d\eta, \\ A(2) &= \frac{1}{c}\sqrt{\frac{2\pi}{kR}}e^{i\left(kR+\frac{\pi}{4}\right)}\int_{-a}^{\infty} f^1(\eta)e^{ikx_1\sin\theta}d\eta, \end{aligned}\right\} \qquad (8.06)$$

and the functions f^1 and g^1 are determined for the right half-space $\left(0<\theta<\frac{\pi}{2}\right)$ by the equations

$$\left.\begin{aligned} f^1(1) &= f(1)+\frac{1}{\sin\theta}, \quad f(1) = -\frac{\cos\frac{\theta}{2}+\sin\frac{\theta}{2}}{\sin\theta}, \\ f^1(2) &= f(2)-\frac{1}{\sin\theta}, \quad f(2) = \frac{\cos\frac{\theta}{2}-\sin\frac{\theta}{2}}{\sin\theta}; \end{aligned}\right\} \qquad (8.07)$$

$$\left.\begin{aligned} g^1(1) &= g(1)+\frac{\cos\theta}{\sin\theta}, \quad g(1) = -\frac{\cos\frac{\theta}{2}-\sin\frac{\theta}{2}}{\sin\theta}, \\ g^1(2) &= g(2)-\frac{\cos\theta}{\sin\theta}, \quad g(2) = \frac{\cos\frac{\theta}{2}+\sin\frac{\theta}{2}}{\sin\theta}. \end{aligned}\right\} \qquad (8.08)$$

From relationships (8.04) - (8.06), it follows that

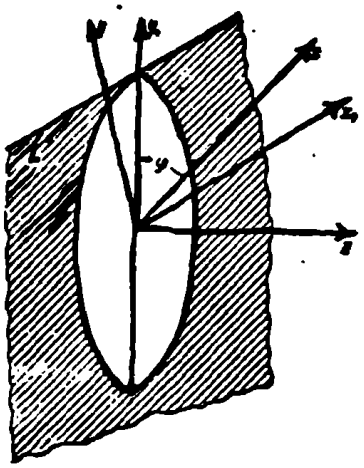

Figure 19. Diffraction by a disk. The half-plane L lies in the plane of the disk. The edge of the half-plane is tangent to the circumference of the disk at the point $y_1 = a$, $x_1 = 0$ (a is the radius of the disk).

$$\left.\begin{aligned}
&\int_{-\infty}^{a} f^1_{x_1}(\eta)\, e^{-ik\eta \sin\theta}\, d\eta = \\
&= -\frac{ic}{2\pi R} E_{0x_1} \cdot f^1(1)\, e^{-ika\sin\theta}, \\
&\int_{-\infty}^{a} f^1_{x_1}(\eta)\, e^{ik\eta \sin\theta}\, d\eta = \\
&= -\frac{ic}{2\pi R} E_{0x_1} \cdot f^1(2)\, e^{ika\sin\theta}
\end{aligned}\right\} \quad (8.09)$$

and

$$\left.\begin{aligned}
&\int_{-\infty}^{a} f^1_{y_1}(\eta)\, e^{-ik\eta \sin\theta}\, d\eta = \\
&= \frac{ic}{2\pi k \cos\theta} H_{0x_1} \cdot g^1(1)\, e^{-ika\sin\theta}, \\
&\int_{-\infty}^{a} f^1_{y_1}(\eta)\, e^{ik\eta \sin\theta}\, d\eta = \\
&= \frac{ic}{2\pi k \cos\theta} H_{0x_1} \cdot g^1(2)\, e^{ika\sin\theta}.
\end{aligned}\right\} \quad (8.10)$$

In accordance with the assumption of equal currents on the disk and on the half-plane, one may consider the following equalities to be valid:

$$\left.\begin{aligned}
&\int_{a}^{a} f^1(\rho, \varphi_1)\, e^{-ik\rho \sin\theta}\, d\rho = \int_{-\infty}^{a} f^1(\eta)\, e^{-ik\eta \sin\theta}\, d\eta, \\
&\int_{a}^{a} f^1(\rho, \varphi_2)\, e^{ik\rho \sin\theta}\, d\rho = \int_{-\infty}^{a} f^1(\eta)\, e^{ik\eta \sin\theta}\, d\eta.
\end{aligned}\right\} \quad (8.11)$$

Therefore, the field from the nonuniform part of the current flowing on the disk will equal

$$\left.\begin{aligned}
E_\varphi = -H_\theta &= \frac{iaE_{0\varphi}}{\sqrt{2\pi ka\sin\theta}} \left[f^1(2)\, e^{i\left(ka\sin\theta - \frac{3\pi}{4}\right)} - \right. \\
&\left. - f^1(1)\, e^{-i\left(ka\sin\theta - \frac{3\pi}{4}\right)} \right] \frac{e^{ikR}}{R}, \\
E_\theta = H_\varphi &= \frac{iaH_{0\varphi}}{\sqrt{2\pi ka\sin\theta}} \left[g^1(2)\, e^{i\left(ka\sin\theta - \frac{3\pi}{4}\right)} - \right. \\
&\left. - g^1(1)\, e^{-i\left(ka\sin\theta - \frac{3\pi}{4}\right)} \right] \frac{e^{ikR}}{R},
\end{aligned}\right\} \quad (8.12)$$

where in view of (7.01)

$$E_{0\varphi} = -H_{0x}\cos\varphi, \quad H_{0\varphi} = -H_{0x}\sin\varphi. \quad (8.13)$$

For the direction $\vartheta=0$, we have according to Equation (8.01)

$$A=\frac{a}{c}\cdot\frac{e^{ikR}}{R}\cdot\int_0^{2\pi}d\psi\int_0^a J^1(\rho,\ \psi)\,d\rho, \tag{8.14}$$

but in accordance with equalities (8.09) - (8.11)

$$\left.\begin{aligned}\int_0^a I^1_{x_1}(\rho,\ \psi)\,d\rho&=\frac{ic}{4\pi k}H_{0z}\cdot\cos\psi,\\ \int_0^a I^1_{y_1}(\rho,\ \psi)\,d\rho&=\frac{ic}{4\pi k}H_{0z}\sin\psi.\end{aligned}\right\} \tag{8.15}$$

Consequently,

$$\left.\begin{aligned}A_x&=\frac{a}{c}\frac{e^{ikR}}{R}\cdot\left[\int_0^{2\pi}\cos\psi\,d\psi\int_0^a I^1_{y_1}(\rho,\ \psi)\,d\rho+\right.\\&\left.+\int_0^{2\pi}\sin\psi\,d\psi\int_0^a I^1_{x_1}(\rho,\ \psi)\,d\rho\right]=0,\\ A_y&=\frac{a}{c}\frac{e^{ikR}}{R}\cdot\left[-\int_0^{2\pi}\cos\psi d\psi\int_0^a I^1_{x_1}(\rho,\ \psi)\,d\rho+\right.\\&\left.+\int_0^{2\pi}\sin\psi d\psi\int_0^a I^1_{y_1}(\rho,\ \psi)\,d\rho\right]=0,\end{aligned}\right\} \tag{8.16}$$

that is, in the direction of the main fringe ($\vartheta=0$) the field from the nonuniform part of the current equals zero.

By using the Bessel functions J_1 and J_2 for the field from the nonuniform part of the current, one may write the equations

$$\left.\begin{aligned}E_\varphi=-H_\vartheta&=\frac{iaE_{0z}}{2}\{[f^1(2)-f^1(1)]J_1(ka\sin\vartheta)+\\&+i[f^1(2)+f^1(1)]J_2(ka\sin\vartheta)\}\frac{e^{ikR}}{R},\\ E_\vartheta=H_\varphi&=\frac{iaH_{0z}}{2}\{[g^1(2)-g^1(1)]J_1(ka\sin\vartheta)+\\&+i[g^1(2)+g^1(1)]J_2(ka\sin\vartheta)\}\frac{e^{ikR}}{R},\end{aligned}\right\} \tag{8.17}$$

which with $ka\sin\vartheta\gg 1$ change to Expressions (8.12), which were already found. In the direction $\vartheta=0$, these equations give a field which equals, in accordance with (8.16), zero, and with intermediate value

they are interpolated. Since the transition from Equations (8.12) to Equations (8.17) is not completely unique, in the angular interval $0 \leq \theta \leq \frac{1}{ka}$ Equations (8.17) may give a certain error. This error is not very significant, since in this interval the field from the uniform part of the current is large.

§ 9. The Total Field Being Scattered by a Disk with Normal Irradiation

Turning to Equations (8.07), (8.08) and (8.17), let us represent the field from the nonuniform part of the current in the following form:

$$\left.\begin{aligned} E_\varphi = -H_\theta = -iaH_{0x}\frac{\cos\varphi}{\sin\theta}J_1(ka\sin\theta)\frac{e^{ikR}}{R} - \\ -\frac{iaH_{0x}}{2}\{[f(2)-f(1)]J_1(ka\sin\theta) + \\ + i[f(2)+f(1)]J_2(ka\sin\theta)\}\cos\varphi\frac{e^{ikR}}{R}, \\ E_\theta = H_\varphi = iaH_{0x}\frac{\sin\varphi}{\sin\theta}\cos\theta J_1(ka\sin\theta)\frac{e^{ikR}}{R} - \\ -\frac{iaH_{0x}}{2}\{[g(2)-g(1)]J_1(ka\sin\theta) + \\ + i[g(2)+g(1)]J_2(ka\sin\theta)\}\sin\varphi\frac{e^{ikR}}{R}. \end{aligned}\right\} \quad (9.01)$$

Here the first terms, as is readily apparent, represent the field from the uniform part of the current taken with the opposite sign. As a result, the total field scattered by the disk (that is, the sum of the fields radiated by the uniform and nonuniform parts of the current) will be expressed only in terms of the functions f and g which determine in the rigorous solution the cylindrical wave from the half-plane's edge

$$\left.\begin{aligned} E_\varphi = -H_\theta = -\frac{iaH_{0x}}{2}\cos\varphi\{[f(2) - \\ -f(1)]J_1(ka\sin\theta) + i[f(2) + \\ + f(1)]J_2(ka\sin\theta)\}\frac{e^{ikR}}{R}, \\ E_\theta = H_\varphi = -\frac{iaH_{0x}}{2}\sin\varphi\{[g(2) - \\ -g(1)]J_1(ka\sin\theta) + i[g(2) + \\ + g(1)]J_2(ka\sin\theta)\}\frac{e^{ikR}}{R}. \end{aligned}\right\} \quad (9.02)$$

Substituting here the explicit expressions for the functions f and g, we arrive at the final expressions for the fringing field

$$\left.\begin{aligned} E_\varphi = -H_\theta = -\frac{ikH_{0x}}{2}\left[\frac{J_1(ka\sin\theta)}{\sin\frac{\theta}{2}} - \right.\\ \left. - i\frac{J_0(ka\sin\theta)}{\cos\frac{\theta}{2}}\right]\frac{e^{ikR}}{R}\cos\varphi,\\ E_\theta = H_\varphi = -\frac{ikH_{0x}}{2}\left[\frac{J_1(ka\sin\theta)}{\sin\frac{\theta}{2}} + \right.\\ \left. + i\frac{J_0(ka\sin\theta)}{\cos\frac{\theta}{2}}\right]\frac{e^{ikR}}{R}\sin\varphi. \end{aligned}\right\} \qquad (9.03)$$

These equations are valid in the right half-space $\left(0<\theta<\frac{\pi}{2}\right)$. In the left half-space $\left(\frac{\pi}{2}<\theta<\pi\right)$, the fringing field is easily found by assuming that its electric field is an even function, and its magnetic field an odd function of the z coordinate:

$$\left.\begin{aligned} E_\varphi(z) = E_\varphi(-z),\\ H_\varphi(z) = -H_\varphi(-z). \end{aligned}\right\} \qquad (9.04)$$

Consequently, in the region $z < 0$ (that is, when $\frac{\pi}{2}<\theta<\pi$)

$$\left.\begin{aligned} E_\varphi = -H_\theta = -\frac{ikH_{0x}}{2}\left[\frac{J_1(ka\sin\theta)}{\cos\frac{\theta}{2}} - \right.\\ \left. - i\frac{J_0(ka\sin\theta)}{\sin\frac{\theta}{2}}\right]\frac{e^{ikR}}{R}\cos\varphi,\\ E_\theta = H_\varphi = \frac{ikH_{0x}}{2}\left[\frac{J_1(ka\sin\theta)}{\cos\frac{\theta}{2}} + \right.\\ \left. + i\frac{J_0(ka\sin\theta)}{\sin\frac{\theta}{2}}\right]\frac{e^{ikR}}{R}\sin\varphi. \end{aligned}\right\} \qquad (9.05)$$

Assuming that in Equations (9.03) and (9.05) $\theta = 0$ and $\theta = \pi$, respectively, we obtain

$$E_y = -\frac{ika^2}{2}\cdot H_{0x}\cdot\frac{e^{ikR}}{R},\quad E_x = 0, \qquad (9.06)$$

which is equivalent to the physical optics approach [see Equation (7.20)].

Expressions (9.03) and (9.05) agree with the result obtained by Braunbek [29] for the scalar fringing field in the far zone. It is also interesting to compare these expressions with the precise numerical results obtained by Belkina [34] by the separation of variables method in the spheroidal coordinate system. It turns out that even with ka = 5 a satisfactory agreement is observed between our approximation method and the rigorous theory. In Figures 20 and 21, graphs of the functions $V^{(1)}(\theta)$ and $V^{(2)}(\theta)$, are presented which allow one to calculate the fringing field on the basis of the equations

$$\left.\begin{aligned} E_\varphi = -H_\theta = \frac{ika^2}{2} E_{0y} \cdot V^{(1)}(\theta) \frac{e^{ikR}}{R} \cos\varphi, \\ E_\theta = H_\varphi = \frac{ika^2}{2} E_{0y} \cdot V^{(2)}(\theta) \frac{e^{ikR}}{R} \sin\varphi. \end{aligned}\right\} \qquad (9.07)$$

The continuous curve corresponds to the rigorous theory [34]. The dash-dot curve corresponds to the field from the uniform part of the current, and the dashed curve corresponds to the field calculated according to Equation (9.03) and (9.05).

Oblique Irradiation

§ 10. The Physical Optics Approach

Let us investigate the general case when the plane wave

$$\mathbf{E} = \mathbf{E}_0 e^{ik(x\sin\gamma + z\cos\gamma)} \qquad (10.01)$$

falls on the disk at an arbitrary angle to its axis. Let us take the spherical coordinate system in such a way that the normal to the incident wave front, n, would lie in the half-plane $\varphi = \frac{\pi}{2}$ and form an angle γ $\left(0 < \gamma < \frac{\pi}{2}\right)$ with the z axis (Figure 22). Adhering to the investigation procedure used in the previous sections, let us first calculate the fringing field in the physical optics approach.

The uniform part of the current excited on the disk by wave (10.01) is determined by Equation (3.01) and has the components

$$j_x^0 = \frac{c}{2\pi} H_{0y} \cdot e^{iky\sin\gamma}, \quad j_y^0 = -\frac{c}{2\pi} H_{0x} e^{iky\sin\gamma}, \quad j_z^0 = 0. \qquad (10.02)$$

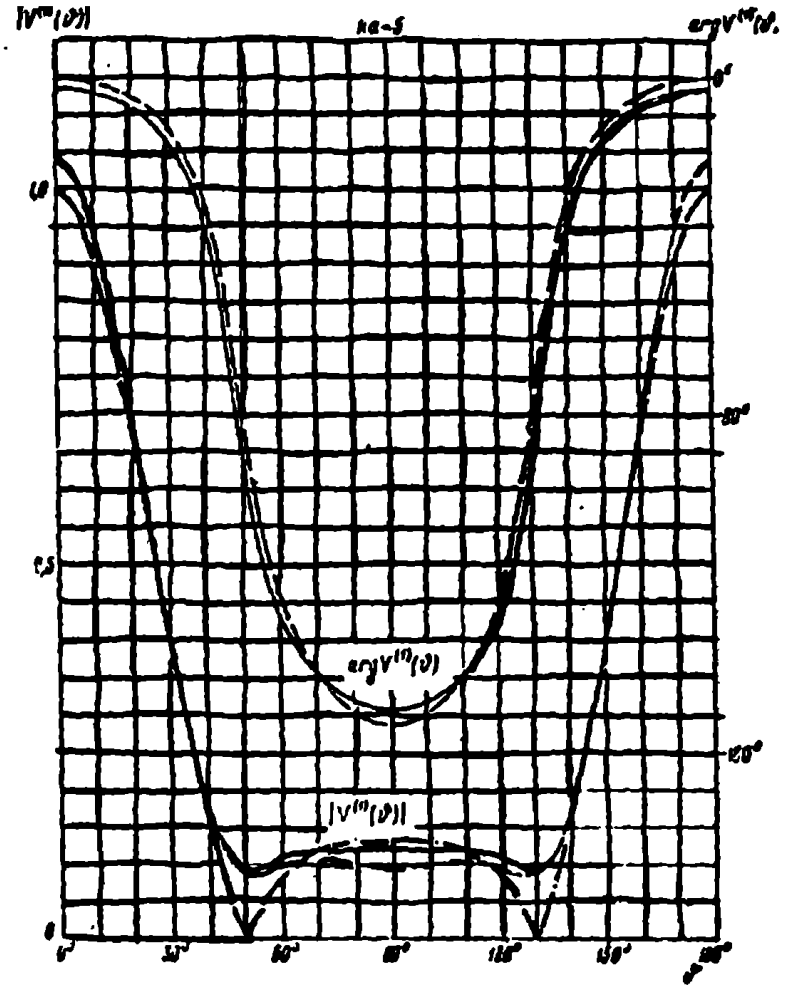

Figure 20. The function $V^{(1)}(\nu)$ for a disk with a normal incidence of the wave. The various curves correspond to different approximations.

The field radiated by it is found, as was done in § 7, by integrating (with the condition $R >> ka^2$). In the case of E-polarization of the incident wave ($\mathbf{E}_0 \perp yoz$), this field equals

$$\left.\begin{aligned} E_\theta = H_\varphi &= -iaE_{0x}\cdot\cos\gamma\cos\theta\cos\varphi\,\frac{J_1(ka\sqrt{\lambda^2+\mu^2})}{\sqrt{\lambda^2+\mu^2}}\,\frac{e^{ikR}}{R}, \\ E_\varphi = -H_\theta &= -iaE_{0x}\cdot\cos\gamma\sin\varphi\,\frac{J_1(ka\sqrt{\lambda^2+\mu^2})}{\sqrt{\lambda^2+\mu^2}}\,\frac{e^{ikR}}{R}, \end{aligned}\right\} \qquad (10.03)$$

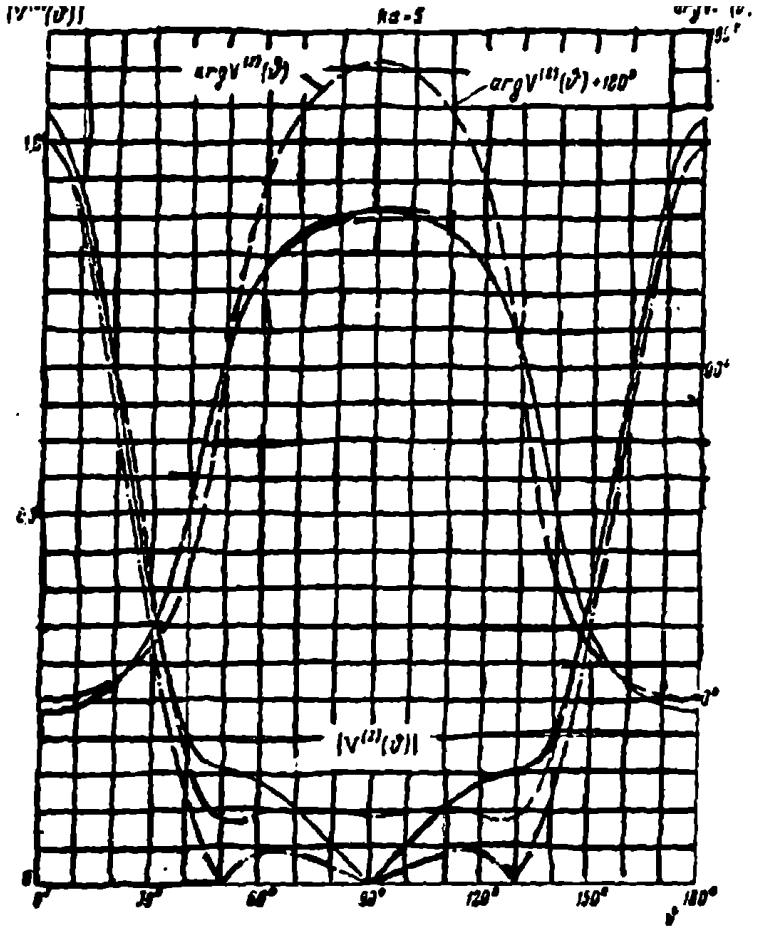

Figure 21. The function $V^{(1)}(\vartheta)$ for a disk with normal incidence of a plane wave. The various curves correspond to different approximations.

and in the case of H-polarization ($\mathbf{H}_0 \perp yoz$)

$$\left.\begin{aligned} E_\vartheta = H_\varphi = -iaH_{0x}\cos\vartheta\sin\varphi\,\frac{J_1(ka\sqrt{\lambda^2+\mu^2})}{\sqrt{\lambda^2+\mu^2}}\,\frac{e^{ikR}}{R}, \\ E_\varphi = -H_\vartheta = -iaH_{0x}\cos\varphi\,\frac{J_1(ka\sqrt{\lambda^2+\mu^2})}{\sqrt{\lambda^2+\mu^2}}\,\frac{e^{ikR}}{R}. \end{aligned}\right\} \qquad (10.04)$$

The quantities λ and μ in Equations (10.03) and (10.04) are determined in the following way:

$$\left.\begin{aligned} \lambda &= \sin\vartheta\cos\varphi, \\ \mu &= \sin\vartheta\sin\varphi - \sin\gamma, \\ \sqrt{\lambda^2+\mu^2} &\geq 0. \end{aligned}\right\} \qquad (10.05)$$

Assuming $\varphi = -\frac{\pi}{2}$ and $\theta = \pi - \gamma \left(\frac{\pi}{2} < \theta < \pi\right)$, in the resulting expressions, let us find the field scattered by the disk in the direction toward its source. With E-polarization of the incident wave, it equals

$$\left.\begin{aligned} E_\varphi &= -H_\theta = -\frac{ikaE_{0x}}{2}\frac{\cos\theta}{\sin\theta}J_1(2ka\sin\theta)\frac{e^{ikR}}{R}, \\ E_\theta &= H_\varphi = 0. \end{aligned}\right\} \qquad (10.06)$$

and with H-polarization

$$\left.\begin{aligned} E_\theta &= H_\varphi = \frac{ikaH_{0x}}{2}\frac{\cos\theta}{\sin\theta}J_1(2ka\sin\theta)\frac{e^{ikR}}{R}, \\ E_\varphi &= H_\theta = 0. \end{aligned}\right\} \qquad (10.07)$$

Using the asymptotic expressions for the Bessel functions, one is able to show that when $R \gg ka^2$ and $ka\sqrt{\lambda^2+\mu^2} \geqslant 1$ the fringing field is radiated from a luminous region on the disk. In the case when $\sqrt{\lambda^2+\mu^2} \to 0$, the luminous region is increased and in the limit (when $\lambda = \mu = 0$) the entire surface of the disk starts to "shine".

§ 11. The Field Radiated by the Nonuniform Part of the Current

Let us calculate the field in the nonuniform part of the current

$$j^s(\rho, \psi) = J(\rho, \psi)e^{ik\rho\sin\gamma\sin\psi}. \qquad (11.01)$$

Its corresponding vector potential

$$A = \frac{a}{c}\frac{e^{ikR}}{R}\int_0^a d\rho\int_0^{2\pi} J(\rho, \psi')e^{-ik\rho\sqrt{\lambda^2+\mu^2}\cos(\psi'-b)}d\psi' \qquad (11.02)$$

by means of the stationary phase method is transformed with $ka\sqrt{\lambda^2+\mu^2} \geqslant 1$ to the form

$$A = \frac{a}{c}\sqrt{\frac{2\pi}{ka\sqrt{\lambda^2+\mu^2}}}e^{i\frac{\pi}{4}}\left[\int_0^a J(\rho, \psi_1)e^{-ik\rho\sqrt{\lambda^2+\mu^2}}d\rho - i\int_0^a J(\rho, \psi_2)e^{ik\rho\sqrt{\lambda^2+\mu^2}}d\rho\right]\frac{e^{ikR}}{R}. \qquad (11.03)$$

Here

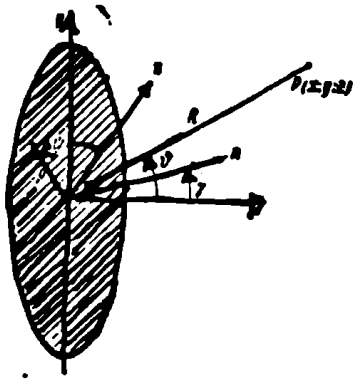

Figure 22. The oblique incidence of a plane wave on a disk. n is the normal to the incident wave front.

$$\psi_1 = \delta, \quad \psi_2 = \pi + \delta \qquad (11.04)$$

are the stationary phase points and the quantity δ is determined by the equalities

$$\sin\delta = \frac{\mu}{\sqrt{\lambda^2+\mu^2}}, \quad \cos\delta = \frac{\lambda}{\sqrt{\lambda^2+\mu^2}}. \qquad (11.05)$$

From Equation (11.03) it follows that with $R \gg ka^2$ and $ka\sqrt{\lambda^2+\mu^2} \gg 1$ the main contribution to the fringing field is given by the luminous region adjacent to the line $\psi = \psi_1$, $\psi = \psi_2$. Thus, the stationary phase points ψ_1, ψ_2 physically correspond to the luminous line on the disk surface.

In order to calculate the vector potential (11.03), it is necessary for us to first express the nonuniform part of the current on the half-plane in terms of its field in the far zone. For this purpose, let us introduce the auxiliary coordinate systems x_1, y_1 and x_2, y_2 (see Figure 23), and let us take the following designations:

α_1, $\beta_1(\alpha_2, \beta_2)$ are the angles between the normal to the incident wave front and the coordinate axes x_1, y_1 (x_2, y_2);

$\phi_1^0(\phi_1^0 = -\phi_2^0)$ is the angle between the z axis and the projection of the indicated normal on the plane $x_1 = 0$;

$\phi_1(\phi_1 = -\phi_2)$ is the angle between the z axis and the direction from the coordinate origin to the point $p(y_1, z)$ which lies in the plane $x_1 = 0$ and is the projection of the observation point $P(x, y, z)$;

r_1 is the distance from the origin to the point $p(y_1, z)$.

The quantities introduced here are determined by the equations:

$$\left.\begin{aligned}
&\cos\alpha_1 = -\sin\gamma\cos\psi_1, \quad \cos\beta_1 = \sin\gamma\sin\psi_1,\\
&\alpha_2 = \pi - \alpha_1, \qquad \beta_2 = \pi - \beta_1,\\
&\sin\varphi_1^0 = \frac{\cos\beta_1}{\sin\alpha_1}, \quad \cos\varphi_1^0 = \frac{\cos\gamma}{\sin\alpha_1},\\
&\sin\varphi_1 = \frac{\sin b\cos(\psi_1-\varphi)}{\sqrt{1-\sin^2 b\sin^2(\psi_1-\varphi)}},\\
&\cos\varphi_1 = \frac{\cos b}{\sqrt{1-\sin^2 b\sin^2(\psi_1-\varphi)}},\\
&\varphi_2 = -\varphi_1, \quad \varphi_2^0 = -\varphi_1^0,\\
&r_1 = R\sqrt{1-\sin^2 b\sin^2(\psi_1-\varphi)}.
\end{aligned}\right\} \tag{11.06}$$

Furthermore, let us write the expressions for the field from the nonuniform part of the current excited by wave (10.01) on an ideally conducting half-plane $-\infty < y_1 < a$. In accordance with § 5, they have the form

$$\left.\begin{aligned}
E_{z_1} &= e^{ikx_1\cos\alpha_1} E_{0z} f^1(\varphi_1, \varphi_1^0)\frac{e^{i\left(k\rho_1+\frac{\pi}{4}\right)}}{\sqrt{2\pi k\rho_1}} e^{ikx_1(\sin\varphi_1^0-\sin\varphi_1)},\\
H_{z_1} &= e^{ikx_1\cos\alpha_1} H_{0z} g^1(\varphi_1, \varphi_1^0)\frac{e^{i\left(k\rho_1+\frac{\pi}{4}\right)}}{\sqrt{2\pi k\rho_1}} e^{ikx_1(\sin\varphi_1^0-\sin\varphi_1)},
\end{aligned}\right\} \tag{11.07}$$

where

$$\left.\begin{aligned}
k_1 &= k\sin\alpha_1,\\
k_1(\sin\varphi_1 - \sin\varphi_1^0) &= k\sqrt{\lambda^2+\mu^2},
\end{aligned}\right\} \tag{11.08}$$

$$\left.\begin{aligned}
f^1(\varphi_1, \varphi_1^0) &= \frac{\sin\frac{\varphi_1-\varphi_1^0}{2}+\cos\frac{\varphi_1+\varphi_1^0}{2}}{\sin\varphi_1^0-\sin\varphi_1} - \frac{\cos\varphi_1^0}{\sin\varphi_1^0-\sin\varphi_1},\\
g^1(\varphi_1, \varphi_1^0) &= \frac{-\sin\frac{\varphi_1-\varphi_1^0}{2}+\cos\frac{\varphi_1+\varphi_1^0}{2}}{\sin\varphi_1^0-\sin\varphi_1} - \frac{\cos\varphi_1}{\sin\varphi_1^0-\sin\varphi_1},
\end{aligned}\right\} \tag{11.09}$$

$$\left(-\frac{\pi}{2} < \varphi_1 < \frac{3\pi}{2}\right).$$

On the other hand, this field may be expressed in terms of the vector potential

$$A = \frac{1}{c}\int_{-\infty}^{a} J(\eta)\, e^{ik\eta\cos\beta_1} d\eta \int_{-\infty}^{\infty} e^{ikl\cos\alpha_1}\frac{e^{ik\sqrt{z^2+(y_1-\eta)^2+(x_1-\xi)^2}}}{\sqrt{z^2+(y_1-\eta)^2+(x_1-\xi)^2}}\, d\xi. \tag{11.10}$$

By means of equation

$$H_0^{(1)}(qD)=\frac{1}{i\pi}\int_{-\infty}^{\infty}\frac{e^{ip\sqrt{D^2+\zeta^2}}}{\sqrt{D^2+\zeta^2}}e^{-i\pi\zeta}d\zeta,$$
$$q=\sqrt{p^2-\ell^2},\quad \operatorname{Im}q>0,\quad D>0, \tag{11.11}$$

which follows from Equation (3.10), if one substitutes z = t, w = ζ, d = -ip, k = -iD, in it we find that

$$A=\frac{i\pi}{e}e^{ikx_1\cos\alpha_1}\int_{-a}^{a}J(\eta)H_0^{(1)}[k\sqrt{z^2+(y_1-\eta)^2}]e^{ik\eta\cos\beta_1}d\eta. \tag{11.12}$$

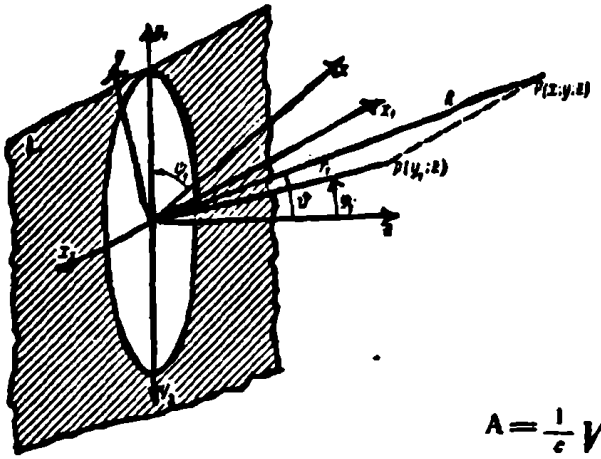

Figure 23. Diffraction by a disk with oblique incidence of a plane wave. The half-plane L lies in the plane of the disk. Its edge is tangent to the circumference of the disk at the point $x_1 = 0$, $y_1 = a$ (a is the radius of the disk).

Taking the fact into account that the nonuniform part of the current is concentrated mainly in the vicinity of the half-plane edge and using the asymptotic representation of the Hankel function, we obtain

$$A=\frac{1}{e}\sqrt{\frac{2\pi}{k_1r_1}}e^{ik(x_1\cos\alpha_1+r_1\sin\alpha_1)+i\frac{\pi}{4}}\int_{-a}^{a}J(\eta)e^{ik\eta\Phi_1}d\eta, \tag{11.13}$$

where

$$\Phi_1=\cos\psi_1-\sin\alpha_1\sin\varphi_1=$$
$$=\sin\gamma\sin\psi_1-\sin\vartheta\cos(\psi_1-\varphi)$$
$$\sqrt{\frac{1-\sin^2\gamma\cos^2\psi_1}{1-\sin^2\vartheta\sin^2(\psi_1-\varphi)}}. \tag{11.14}$$

In the case when $\psi_1 = \delta$ [see Equations (11.04) and (11.05)] the function Φ_1 takes the value

$$\Phi_1=-\sqrt{\lambda^2+\mu^2}. \tag{11.15}$$

Starting from expression (11.13), it is not difficult to show that the fringing field in the far zone is described by the following equations:

$$\left.\begin{aligned} E_{z_0} &= -ik\sin\alpha_1\cos\alpha_1\sin\varphi_1 A_{y_0} + ik\sin^2\alpha_1 A_{z_0}, \\ H_{z_0} &= -ik\sin\alpha_1\cos\varphi_1 A_{y_0}, \end{aligned}\right\} \tag{11.16}$$

where

$$\left.\begin{aligned} A_{y_0} &= \theta_1 I_{y_0}(\psi_1), \quad A_{z_0} = \theta_1 I_{z_0}(\psi_1), \\ \theta_1 &= \frac{1}{c}\sqrt{\frac{2\pi}{k_1 r_1}}\, e^{ik(x_1\cos\alpha_1 + r_1\sin\alpha_1) + i\frac{\pi}{4}}, \end{aligned}\right\} \tag{11.17}$$

$$\left.\begin{aligned} I_{y_0}(\psi_1) &= \int_{-\infty}^{a} J_{y_0}(\eta)\, e^{-ik_1\eta\sqrt{1+\mu^2}}\, d\eta, \\ I_{z_0}(\psi_1) &= \int_{-\infty}^{a} J_{z_0}(\eta)\, e^{-ik_1\eta\sqrt{1+\mu^2}}\, d\eta. \end{aligned}\right\} \tag{11.18}$$

Then by equating expressions (11.07) and (11.16), we find the desired connection between the nonuniform part of the current on the half-plane $-\infty \leq y_1 \leq a$ and its field in the far zone

$$\left.\begin{aligned} I_{y_0}(\psi_1) &= -\frac{e}{ik2\pi}\frac{H_{0z_1}}{\sin\alpha_1\cos\varphi_1} g^1(\varphi_1, \varphi_1^0)\, e^{-ika\sqrt{1+\mu^2}}, \\ I_{z_0}(\psi_1) &= \frac{e}{ik2\pi}\frac{1}{\sin^2\alpha_1}\left[E_{0z_1} f^1(\varphi_1, \varphi_1^0) - \right. \\ &\quad \left. - \cos\alpha_1 \operatorname{tg}\varphi_1 H_{0z_1} g^1(\varphi_1, \varphi_1^0)\right] e^{-ika\sqrt{1+\mu^2}}. \end{aligned}\right\} \tag{11.19}$$

One may show in a completely similar way that the nonuniform part of the current excited by wave (10.01) on the half-plane $-\infty \leq y_2 \leq a$ creates, in the far zone, the fringing field

$$\left.\begin{aligned} E_{x_0} &= -ik\sin\alpha_2\cos\alpha_2\sin\varphi_2 A_{y_0} + ik\sin^2\alpha_2 A_{x_0}, \\ H_{x_0} &= -ik\sin\alpha_2\cos\varphi_2 A_{y_0}, \end{aligned}\right\} \tag{11.20}$$

where

$$\left.\begin{aligned} A_{y_0} &= \theta_2 I_{y_0}(\psi_2), \quad A_{x_0} = \theta_2 I_{x_0}(\psi_2), \\ \theta_2 &= \frac{1}{c}\sqrt{\frac{2\pi}{k_1 r_2}}\, e^{ik(r_2 + x_2\cos\alpha_2) + i\frac{\pi}{4}}, \end{aligned}\right\} \tag{11.21}$$

$$\left.\begin{aligned} I_{\mu_0}(\psi_2) &= \int_{-\infty}^{a} J_{\mu_0}(\eta)\, e^{ikr_1\sqrt{\lambda^2+\mu^2}}\, d\eta, \\ I_{x_0}(\psi_2) &= \int_{-\infty}^{a} J_{x_0}(\eta)\, e^{ikr_1\sqrt{\lambda^2+\mu^2}}\, d\eta. \end{aligned}\right\} \tag{11.22}$$

On the other hand, in accordance with § 5 this field equals

$$\left.\begin{aligned} E_{x_0} &= e^{-ikx_0\cos\alpha_1} E_{0x_0} f^1(\varphi_2, \varphi_2^0)\, \frac{e^{i\left(kr_1+\frac{\pi}{4}\right)}}{\sqrt{2\pi k r_1}}\, e^{ika(\sin\varphi_2^0-\sin\varphi_2)}, \\ H_{x_0} &= e^{-ikx_0\cos\alpha_1} H_{0x_0} g^1(\varphi_2, \varphi_2^0)\, \frac{e^{i\left(kr_1+\frac{\pi}{4}\right)}}{\sqrt{2\pi k r_1}}\, e^{ika(\sin\varphi_2^0-\sin\varphi_2)}. \end{aligned}\right\} \tag{11.23}$$

Here

$$k_1(\sin\varphi_2 - \sin\varphi_2^0) = -\sqrt{\lambda^2+\mu^2}, \tag{11.24}$$

and the functions $f^1(\varphi_2, \varphi_2^0)$ and $g^1(\varphi_2, \varphi_2^0)$ are determined by the equations:

$$\left.\begin{aligned} f^1(\varphi_2, \varphi_2^0) &= \frac{\sin\frac{\varphi_2-\varphi_1^0}{2} - \cos\frac{\varphi_2+\varphi_1^0}{2}}{\sin\varphi_1^0 - \sin\varphi_2} + \frac{\cos\varphi_1^0}{\sin\varphi_1^0 - \sin\varphi_2}, \\ g^1(\varphi_2, \varphi_2^0) &= -\frac{\sin\frac{\varphi_2-\varphi_1^0}{2} + \cos\frac{\varphi_2+\varphi_1^0}{2}}{\sin\varphi_1^0 - \sin\varphi_2} + \frac{\cos\varphi_2}{\sin\varphi_1^0 - \sin\varphi_2} \\ &\left(-\frac{3\pi}{2} < \varphi_2 < \frac{\pi}{2}\right). \end{aligned}\right\} \tag{11.25}$$

Equating the quantities (11.20) and (11.23), we find

$$\left.\begin{aligned} I_{\mu_0}(\psi_2) &= -\frac{c}{ik2\pi}\, \frac{e^{ika\sqrt{\lambda^2+\mu^2}}}{\sin\alpha_1\cos\varphi_1}\, H_{0x_0} g^1(\varphi_2, \varphi_2^0), \\ I_{x_0}(\psi_2) &= \frac{c}{ik2\pi}\, \frac{e^{ika\sqrt{\lambda^2+\mu^2}}}{\sin^2\alpha_1} [E_{0x_0} f^1(\varphi_2, \varphi_2^0) - \\ &\quad - \cos\alpha_1 \operatorname{tg}\varphi_1 H_{0x_0} g^1(\varphi_2, \varphi_2^0)]. \end{aligned}\right\} \tag{11.26}$$

In this way we established the relationship between the nonuniform part of the current on the half-plane and its field in the far zone. Now let us return to a calculation of the field from the nonuniform part of the current flowing on the disk.

Since the disk is assumed to be large in comparison with the wavelength, the nonuniform part of the current in the vicinity of its edge may be approximately considered the same as on a corresponding half-plane. Consequently, the integrals in Equation (11.03) will approximately equal the corresponding integrals from the current on the half-plane:

$$\left.\begin{aligned}
&\int_0^a J_{x_1}(\rho,\ \psi_1)\, e^{-ik\rho\sqrt{\lambda^2+\mu^2}}\, d\rho = I_{x_1}(\psi_1),\\
&\int_0^a J_{y_1}(\rho,\ \psi_1)\, e^{-ik\rho\sqrt{\lambda^2+\mu^2}}\, d\rho = I_{y_1}(\psi_1),\\
&\int_0^a J_{x_2}(\rho,\ \psi_2)\, e^{ik\rho\sqrt{\lambda^2+\mu^2}}\, d\rho = I_{x_2}(\psi_2),\\
&\int_0^a J_{y_2}(\rho,\ \psi_2)\, e^{ik\rho\sqrt{\lambda^2+\mu^2}}\, d\rho = I_{y_2}(\psi_2).
\end{aligned}\right\} \qquad (11.27)$$

As a result, the vector components of (11.03) may be represented in the following form:

$$\left.\begin{aligned}
A_{y_1} &= \frac{1}{c}\sqrt{\frac{2\pi a}{k\sqrt{\lambda^2+\mu^2}}}\,\frac{e^{ikR}}{R}\, e^{i\frac{\pi}{4}}\left[I_{y_1}(\psi_1)+iI_{y_2}(\psi_2)\right],\\
A_{x_1} &= \frac{1}{c}\sqrt{\frac{2\pi a}{k\sqrt{\lambda^2+\mu^2}}}\,\frac{e^{ikR}}{R}\, e^{i\frac{\pi}{4}}\left[I_{x_1}(\psi_1)+iI_{x_2}(\psi_2)\right].
\end{aligned}\right\} \qquad (11.28)$$

Then substituting these values into the equations

$$\left.\begin{aligned}
E_\varphi &= ikA_\varphi = ik\left[A_{y_1}\sin(\psi_1-\varphi) - A_{x_1}\cos(\psi_1-\varphi)\right],\\
E_\theta &= ikA_\theta = ik\left[A_{y_1}\cos(\psi_1-\varphi) + A_{x_1}\sin(\psi_1-\varphi)\right]\cos\theta,
\end{aligned}\right\} \qquad (11.29)$$

we find the field from the nonuniform part of the current flowing on the disk

$$\begin{aligned}
E_\varphi = -H_\theta = \frac{ae^{i\frac{\pi}{4}}}{\sqrt{2\pi ka\sqrt{\lambda^2+\mu^2}}}\,\frac{e^{ikR}}{R}\Bigg\{ & -H_{ox_1}\left[\frac{\sin(\psi_1-\varphi)}{\sin\alpha_1\cos\varphi_1} - \right.\\
& \left. -\frac{\cos(\psi_1-\varphi)}{\sin^2\alpha_1}\cos\alpha_1\operatorname{tg}\varphi_1\right]\times\\
& \times\left[g^1(\varphi_1,\ \varphi_1'')\, e^{-ika\sqrt{\lambda^2+\mu^2}} - ig^1(\varphi_2,\ \varphi_2'')\, e^{ika\sqrt{\lambda^2+\mu^2}}\right] -\\
& -E_{ox_1}\frac{\cos(\psi_1-\varphi)}{\sin^2\alpha_1}\left[f^1(\varphi_1,\ \varphi_1^0)\, e^{-ika\sqrt{\lambda^2+\mu^2}} - \right.\\
& \left. -if^1(\varphi_2,\ \varphi_2^0)\, e^{ika\sqrt{\lambda^2+\mu^2}}\right]\Bigg\}.
\end{aligned} \qquad (11.30)$$

$$E_\theta = H_\varphi = \frac{ae^{i\frac{\pi}{4}}\cos\vartheta}{\sqrt{2\pi ka\sqrt{\lambda^2+\mu^2}}}\frac{e^{ikR}}{R}\left\{-H_{0x_1}\left[\frac{\cos(\psi_1-\varphi)}{\sin\alpha_1\cos\varphi_1}+\right.\right.$$
$$\left.+\frac{\sin(\psi_1-\varphi)}{\sin^2\alpha_1}\cos\gamma_1\operatorname{tg}\varphi_1\right]\left[g^1(\varphi_1,\ \varphi_1^0)\,e^{-ika\sqrt{\lambda^2+\mu^2}}-\right.$$
$$\left.-ig^1(\varphi_2,\ \varphi_2^0)\,e^{ika\sqrt{\lambda^2+\mu^2}}\right]+E_{0x_1}\frac{\sin(\psi_1-\varphi)}{\sin^2\alpha_1}\times \tag{11.31}$$
$$\left.\times\left[f^1(\varphi_1,\ \varphi_1^0)\,e^{-ika\sqrt{\lambda^2+\mu^2}}-if^1(\varphi_2,\ \varphi_2^0)\,e^{ika\sqrt{\lambda^2+\mu^2}}\right]\right\}.$$

The resulting expressions are valid when $ka\sqrt{\lambda^2+\mu^2}\gg 1$. They may be slightly simplified to

$$E_\varphi = -H_\theta = \frac{ae^{i\frac{\pi}{4}}}{\sqrt{2\pi ka\sqrt{\lambda^2+\mu^2}}}\frac{e^{ikR}}{R}\times$$
$$\times\left\{-H_{0x_1}\cos\vartheta\frac{\sin(\psi_1-\varphi)}{\sin^2\alpha_1}\left[g^1(\varphi_1,\ \varphi_1^0)\,e^{-ika\sqrt{\lambda^2+\mu^2}}-\right.\right.$$
$$\left.-ig^1(\varphi_2,\ \varphi_2^0)\,e^{ika\sqrt{\lambda^2+\mu^2}}\right]-E_{0x_1}\frac{\cos(\psi_1-\varphi)}{\sin^2\alpha_1}\times$$
$$\left.\times\left[f^1(\varphi_1,\ \varphi_1^0)\,e^{-ika\sqrt{\lambda^2+\mu^2}}-if^1(\varphi_2,\ \varphi_2^0)\,e^{ika\sqrt{\lambda^2+\mu^2}}\right]\right\}, \tag{11.32}$$
$$E_\theta = H_\varphi = \frac{ae^{i\frac{\pi}{4}}}{\sqrt{2\pi ka\sqrt{\lambda^2+\mu^2}}}\frac{e^{ikR}}{R}\times$$
$$\times\left\{-H_{0x_1}\frac{\cos(\psi_1-\varphi)}{\sin^2\alpha_1}\left[g^1(\varphi_1,\ \varphi_1^0)\,e^{-ika\sqrt{\lambda^2+\mu^2}}-\right.\right.$$
$$\left.-ig^1(\varphi_2,\ \varphi_2^0)\,e^{ika\sqrt{\lambda^2+\mu^2}}\right]+E_{0x_1}\cos\vartheta\frac{\sin(\psi_1-\varphi)}{\sin^2\alpha_1}\times$$
$$\left.\times\left[f^1(\varphi_1,\ \varphi_1^0)\,e^{-ika\sqrt{\lambda^2+\mu^2}}-if^1(\varphi_2,\ \varphi_2^0)\,e^{ika\sqrt{\lambda^2+\mu^2}}\right]\right\},$$

if we use the identities

$$\left.\begin{aligned}\frac{\sin(\psi_1-\varphi)}{\sin\alpha_1\cos\varphi_1}-\frac{\cos(\psi_1-\varphi)}{\sin^2\alpha_1}\cos\alpha_1\operatorname{tg}\varphi_1 &\equiv \frac{\cos\vartheta\sin(\psi_1-\varphi)}{\sin^2\alpha_1},\\ \frac{\cos(\psi_1-\varphi)}{\sin\alpha_1\cos\varphi_1}+\frac{\sin(\psi_1-\varphi)}{\sin^2\alpha_1}\cos\alpha_1\operatorname{tg}\varphi_1 &\equiv \frac{\cos(\psi_1-\varphi)}{\sin^2\alpha_1\cos\vartheta}.\end{aligned}\right\} \tag{11.33}$$

The operations carried out above may be briefly summarized in the following way. The field from the nonuniform part of the current on the disk

$$A = \frac{a}{c}\frac{e^{ikR}}{R}\int_0^{2\pi}d\psi\int_0^a J(\rho,\ \psi)\,e^{ik\rho\Theta}\,d\rho$$

is found (without direct calculation of the current) in terms of the known field of an auxiliary half-plane

$$A=\frac{1}{c}\sqrt{\frac{2\pi}{k_1\rho_1}}\,e^{ik(x_1\cos\alpha_1+y_1\sin\alpha_1)+i\frac{\pi}{4}}\int_{-\infty}^{\infty}J(\eta)\,e^{ik\eta\Phi_1}d\eta$$

by a replacement of

$$\int_0^{\infty}J(\rho,\psi)\,e^{ik\rho\Phi}d\rho \text{ by } \int_{-\infty}^{\infty}J(\eta)\,e^{ik\eta\Phi_1}d\eta$$

in those cases when $\Phi = \Phi_1$. The functions Φ and Φ_1 are determined by the equations

$$\left.\begin{aligned}\Phi&=\sin\gamma\sin\psi-\sin\theta\cos(\psi-\varphi),\\ \Phi_1&=\sin\gamma\sin\psi-\sin\theta\cos(\psi-\varphi)\sqrt{\frac{1-\sin^2\gamma\cos^2\psi}{1-\sin^2\theta\sin^2(\psi-\varphi)}}.\end{aligned}\right\}\qquad(11.34)$$

Solution (11.32) was determined exactly in this way with $ka\sqrt{\lambda^2+\mu^2}\gg 1$, when, for auxiliary half-plane whose edge touches the rim of the disk at the points $\psi = \delta$, $\psi = \pi + \delta$, the phase Φ_1 was equal to Φ.

A solution to the problem using this method also is possible in the case

$$\theta=\gamma,\ \varphi=\frac{\pi}{2}.\qquad(11.35)$$

when $\Phi_1 = \Phi = 0$. The direction $\theta=\gamma,\ \varphi=\frac{\pi}{2}$ corresponds to the principal maximum of the scattering diagram, and therefore is of special interest. Substituting the relationships

$$\left.\begin{aligned}I_{y_1}&=\frac{c}{ik4\pi}\frac{H_{0x_1}}{\sin\gamma_1}\frac{\sin\varphi_1^0-1}{\cos^2\varphi_1^0},\\ I_{x_1}&=\frac{c}{ik4\pi}\frac{1}{\sin^2\alpha_1}(E_{0x_1}+\cos\alpha_1\operatorname{tg}\varphi_1^0 H_{0x_1})\frac{\sin\varphi_1^0-1}{\cos\varphi_1^0}\end{aligned}\right\}\qquad(11.36)$$

which follow in this case from (11.19) into the equations

$$\left.\begin{aligned}A_x&=\frac{a}{c}\frac{e^{ikR}}{R}\int_0^{2\pi}(I_{y_1}\cos\psi+I_{x_1}\sin\psi)\,d\psi,\\ A_y&=\frac{a}{c}\frac{e^{ikR}}{R}\int_0^{2\pi}(I_{y_1}\sin\psi-I_{x_1}\cos\psi)\,d\psi.\end{aligned}\right\}\qquad(11.37)$$

we find the field radiated by the nonuniform part of the current in the direction of the principal maximum. With the E-polarization of the incident wave ($\mathbf{E}_0 \perp yoz$), it equals

$$\left.\begin{aligned} E_\vartheta = H_\varphi = E_{0x}\frac{a}{\pi\sin^2\gamma}\left(2K\cos\gamma - \frac{1+\cos^2\gamma}{\cos\gamma}E\right)\frac{e^{ikR}}{R}, \\ E_\varphi = H_\vartheta = 0, \end{aligned}\right\} \quad (11.38)$$

and with the H-polarization ($\mathbf{H}_0 \perp yoz$) of the incident wave, it equals

$$\left.\begin{aligned} E_\varphi = -H_\vartheta = -E_{0\varphi}\frac{a}{\pi\sin^2\gamma}\times \\ \times\left(2K\cos\gamma - \frac{1+\cos^2\gamma}{\cos\gamma}E\right)\frac{e^{ikR}}{R}, \\ E_\vartheta = H_\varphi = 0, \end{aligned}\right\} \quad (11.39)$$

where

$$K = \int_0^{\frac{\pi}{2}}\frac{d\psi}{\sqrt{1-\sin^2\gamma\sin^2\psi}}, \quad E = \int_0^{\frac{\pi}{2}}\sqrt{1-\sin^2\gamma\sin^2\psi}\,d\psi \quad (11.40)$$

which are complete elliptic integrals. From the resulting expressions, it follows that with the rotation of the incident wave polarization by 90° the phase of the field from the nonuniform part of the current is changed by 180°, as it was in the case of a half-plane. If $\gamma \to 0$, then the difference between the polarizations disappears, and in the limit (when $\gamma = 0$) we arrive at the previous result (8.16).

Numerical calculations were carried out using Equations (11.38) and (11.39). They showed that for values of γ not exceeding 60° the field from the uniform part of the current is at a minimum [illegible] times larger than the field from the nonuniform part of the current.

Scattering Characteristics [illegible]

[illegible]

[illegible] scattered by the disk [illegible] of the field [illegible] and nonuniform part [illegible]

detail the fringing field in the incident plane $\left(x=0,\ \varphi=\pm\frac{\pi}{2}\right)$ where the expressions (11.32) take the form

$$\left.\begin{aligned}
E_\varphi=-H_\theta&=\frac{ae^{i\frac{\pi}{4}}}{\sqrt{2\pi ka|\mu|}}E_{0z}[-f^1(1)e^{-ikap}+if^1(2)e^{ikap}]\frac{e^{ikR}}{R}\\
&\text{with } \varphi=\frac{\pi}{2},\ \theta>\gamma.\\
E_\varphi=-H_\theta&=\frac{ae^{i\frac{\pi}{4}}}{\sqrt{2\pi ka|\mu|}}E_{0z}[-f^1(2)e^{ikap}+if^1(1)e^{-ikap}]\frac{e^{ikR}}{R}\\
&\text{with } \varphi=\frac{\pi}{2},\ \theta<\gamma.\\
E_\varphi=-H_\theta&=\frac{ae^{i\frac{\pi}{4}}}{\sqrt{2\pi ka|\mu|}}E_{0z}[f^1(2)e^{ikap}-if^1(1)e^{-ikap}]\frac{e^{ikR}}{R}\\
&\text{with } \varphi=-\frac{\pi}{2};
\end{aligned}\right\}\qquad(12.01)$$

$$\left.\begin{aligned}
E_\theta=H_\varphi&=\frac{ae^{i\frac{\pi}{4}}H_{0y}}{\sqrt{2\pi ka|\mu|}}[-g^1(1)e^{-ikap}+ig^1(2)e^{ikap}]\frac{e^{ikR}}{R}\\
&\text{with } \varphi=\frac{\pi}{2},\ \theta>\gamma.\\
E_\theta=H_\varphi&=\frac{ae^{i\frac{\pi}{4}}H_{0y}}{\sqrt{2\pi ka|\mu|}}[-g^1(2)e^{ikap}+ig^1(1)e^{-ikap}]\frac{e^{ikR}}{R}\\
&\text{with } \varphi=\frac{\pi}{2},\ \theta<\gamma.\\
E_\theta=H_\varphi&=\frac{ae^{i\frac{\pi}{4}}H_{0y}}{\sqrt{2\pi ka|\mu|}}[g^1(2)e^{ikap}-ig^1(1)e^{-ikap}]\frac{e^{ikR}}{R}\\
&\text{with } \varphi=-\frac{\pi}{2}.
\end{aligned}\right\}\qquad(12.02)$$

The functions $f^1(1)$ and $g^1(1)$ correspond to the field of the auxiliary half-plane $-\infty\leqslant y\leqslant a$, and the functions $f^1(2)$ and $g^1(2)$ correspond to the field of the half-plane $-a\leqslant y\leqslant\infty$. In accordance with Equations (11.00) and (11.25), they are determined by the expressions

$$\left.\begin{aligned}
f^1(1)&=f(1)-\frac{\cos\gamma}{\sin\gamma-\sin\theta},\quad f(1)=\frac{\sin\frac{\theta-\gamma}{2}+\cos\frac{\theta+\gamma}{2}}{\sin\gamma-\sin\theta},\\
g^1(1)&=g(1)-\frac{\cos\theta}{\sin\gamma-\sin\theta},\quad g(1)=\frac{-\sin\frac{\theta-\gamma}{2}+\cos\frac{\theta+\gamma}{2}}{\sin\gamma-\sin\theta}.
\end{aligned}\right\}\qquad(12.03)$$

(Equation continued on next page.)

$$f^1(2)=f(2)+\frac{\cos\gamma}{\sin\gamma-\sin\theta},\quad f(2)=\frac{\sin\frac{\theta-\gamma}{2}-\cos\frac{\theta+\gamma}{2}}{\sin\gamma-\sin\theta},$$
$$g^1(2)=g(2)+\frac{\cos\theta}{\sin\gamma-\sin\theta},\ g(2)=-\frac{\sin\frac{\theta-\gamma}{2}+\cos\frac{\theta+\gamma}{2}}{\sin\gamma-\sin\theta},\qquad(12.03)$$

if $\varphi=\frac{\pi}{2}$ and $\theta<\frac{\pi}{2}$; and

$$f^1(1)=f(1)-\frac{\cos\gamma}{\sin\gamma+\sin\theta},\ f(1)=-\frac{\sin\frac{\theta+\gamma}{2}-\cos\frac{\theta-\gamma}{2}}{\sin\gamma+\sin\theta},$$
$$g^1(1)=g(1)-\frac{\cos\theta}{\sin\gamma+\sin\theta},\quad g(1)=\frac{\sin\frac{\theta+\gamma}{2}+\cos\frac{\theta-\gamma}{2}}{\sin\gamma+\sin\theta},$$
$$f^1(2)=f(2)+\frac{\cos\gamma}{\sin\gamma+\sin\theta},\ f(2)=\frac{\sin\frac{\theta+\gamma}{2}+\cos\frac{\theta-\gamma}{2}}{\sin\gamma+\sin\theta},\qquad(12.04)$$
$$g^1(2)=g(2)+\frac{\cos\theta}{\sin\gamma+\sin\theta},\quad g(2)=\frac{\sin\frac{\theta+\gamma}{2}-\cos\frac{\theta-\gamma}{2}}{\sin\gamma+\sin\theta},$$

if $\varphi=-\frac{\pi}{2}$ and $\theta<\frac{\pi}{2}$.

It was mentioned above that when ka >> 1 in the direction $\theta=\gamma$ ($0^\circ<\gamma\leq 55^\circ$), $\varphi=\frac{\pi}{2}$ the field from the nonuniform part of the current is negligibly small in comparison with the field from the uniform part. Therefore, for the field from the nonuniform part of the current one may write, with the help of Bessel functions, the following interpolation formulas: with $\varphi=\frac{\pi}{2}$

$$E_\varphi=-H_\theta=\frac{ikaE_{0x}}{2}\{[f^1(1)-f^1(2)]J_1(\xi)-$$
$$-i[f^1(1)+f^1(2)]J_2(\xi)\}\frac{e^{ikR}}{R},$$
$$E_\theta=H_\varphi=\frac{ikaH_{0x}}{2}\{[g^1(1)-g^1(2)]J_1(\xi)-$$
$$-i[g^1(1)+g^1(2)]J_2(\xi)\}\frac{e^{ikR}}{R},\qquad(12.05)$$

and with $\varphi=-\frac{\pi}{2}$

$$E_\varphi=-H_\theta=\frac{ikaE_{0x}}{2}\{[f^1(1)-f^1(2)]J_1(\xi)+$$
$$+i[f^1(1)+f^1(2)]J_2(\xi)\}\frac{e^{ikR}}{R},\qquad(12.06)$$

(Equation continued on next page).

$$E_\theta = H_\varphi = \frac{iaH_{0x}}{2}\{[g^1(1) - g^1(2)]J_1(\xi) + \\ + i[g^1(1) + g^1(2)]J_0(\xi)\}\frac{e^{ikR}}{R}. \quad (12.06)$$

where

$$\xi = ka(\sin\theta - \sin\gamma), \\ \zeta = ka(\sin\theta + \sin\gamma). \quad (12.07)$$

These expressions are valid in the region $0 < \theta < \frac{\pi}{2}$; when $|\xi| \gg 1$ and $|\zeta| \gg 1$ they change to Equations (12.01) and (12.02), and in the direction $\theta = \gamma$, $\varphi = \frac{\pi}{2}$ they give a field equal to zero.

Using specific expressions for the functions f^1 and g^1, it is not difficult to establish that the total field scattered by the disk in view of Equations (10.03) and (10.04) may be represented in the following form:

with $\varphi = \frac{\pi}{2}$

$$E_\varphi = -H_\theta = \frac{ikE_{0x}}{2}\{[f(1) - f(2)]J_1(\zeta) - \\ - i[f(1) + f(2)]J_0(\zeta)\}\frac{e^{ikR}}{R}. \\ E_\theta = H_\varphi = \frac{ikH_{0x}}{2}\{[g(1) - g(2)]J_1(\zeta) - \\ - i[g(1) + g(2)]J_0(\zeta)\}\frac{e^{ikR}}{R}. \quad (12.08)$$

and with $\varphi = -\frac{\pi}{2}$

$$E_\varphi = -H_\theta = \frac{ikE_{0x}}{2}\{[f(1) - f(2)]J_1(\xi) + \\ + i[f(1) + f(2)]J_0(\xi)\}\frac{e^{ikR}}{R}. \\ E_\theta = H_\varphi = \frac{ikH_{0x}}{2}\{[g(1) - g(2)]J_1(\xi) + \\ + i[g(1) + g(2)]J_0(\xi)\}\frac{e^{ikR}}{R}. \quad (12.09)$$

It is convenient to write these expressions as follows

$$E_\varphi = -H_\theta = \frac{ikE_{0x}}{2}\Sigma(\theta, \gamma)\frac{e^{ikR}}{R}. \\ E_\theta = H_\varphi = \frac{ikH_{0x}}{2}\Sigma(\theta, \gamma)\frac{e^{ikR}}{R}. \quad (12.10)$$

where the functions $\bar{\Sigma}$ and Σ are determined in the region $0<\vartheta<\frac{\pi}{2}$ by the equations:

$$\left.\begin{aligned}\bar{\Sigma}(\vartheta,\gamma)\\ \Sigma(\vartheta,\gamma)\end{aligned}\right\}=-\frac{J_1(\xi)}{\sin\frac{\vartheta-\gamma}{2}}\pm i\frac{J_2(\xi)}{\cos\frac{\vartheta+\gamma}{2}}\text{ with }\varphi=\frac{\pi}{2},$$
$$\left.\begin{aligned}\bar{\Sigma}(\vartheta,\gamma)\\ \Sigma(\vartheta,\gamma)\end{aligned}\right\}=\frac{J_1(\xi)}{\sin\frac{\vartheta+\gamma}{2}}\mp i\frac{J_2(\xi)}{\cos\frac{\vartheta-\gamma}{2}}\text{ with }\varphi=-\frac{\pi}{2}.\qquad(12.11)$$

and in the region $\frac{\pi}{2}<\vartheta<\pi$

$$\left.\begin{aligned}\bar{\Sigma}(\vartheta,\gamma)\\ \Sigma(\vartheta,\gamma)\end{aligned}\right\}=\mp\frac{J_1(\xi)}{\cos\frac{\vartheta+\gamma}{2}}+i\frac{J_2(\xi)}{\sin\frac{\vartheta-\gamma}{2}}\text{ with }\varphi=\frac{\pi}{2},$$
$$\left.\begin{aligned}\bar{\Sigma}(\vartheta,\gamma)\\ \Sigma(\vartheta,\gamma)\end{aligned}\right\}=\pm\frac{J_1(\xi)}{\cos\frac{\vartheta-\gamma}{2}}-i\frac{J_2(\xi)}{\sin\frac{\vartheta+\gamma}{2}}\text{ with }\varphi=-\frac{\pi}{2}.\qquad(12.12)$$

Here assuming $\gamma = 0$, we obtain the previous relationships (9.03) and (9.05).

In the directions $\vartheta=\gamma$ and $\vartheta=\pi-\gamma$ (with $\varphi=\frac{\pi}{2}$), where the scattering diagram has a principal maximum, it follows from Equations (12.11) and (12.12) that

$$\bar{\Sigma}(\gamma)=\Sigma(\gamma)=-ka\cos\gamma\qquad(12.13)$$

and

$$\bar{\Sigma}(\pi-\gamma)=-\Sigma(\pi-\gamma)=-ka\cos\gamma.\qquad(12.14)$$

In the direction toward the source $\left(\vartheta=\pi-\gamma,\ \varphi=-\frac{\pi}{2}\right)$, the functions $\bar{\Sigma}(\vartheta)$ and $\Sigma(\vartheta)$ take the values

$$\left.\begin{aligned}\bar{\Sigma}(\vartheta)\\ \Sigma(\vartheta)\end{aligned}\right\}=\pm\frac{1}{\sin\vartheta}J_1(\xi)-iJ_2(\xi).\qquad(12.15)$$

Here considering $\vartheta=\pi$, we obtain

$$\bar{\Sigma}(\pi)=-\Sigma(\pi)=ka.\qquad(12.16)$$

which corresponds to the physical optics approach [Equation (7.20)].

The functions $\bar{\Sigma}$ and Σ allow one to calculate

$$\sigma_E = \pi a^2 |\bar{\Sigma}|^2, \quad \sigma_H = \pi a^2 |\Sigma|^2 \tag{12.17}$$

which are the effective scattering surfaces with the E- and H-polarizations of the incident wave. Let us recall that, by definition, the effective scattering surface is a quantity equal to

$$\sigma = 4\pi R^2 \frac{|S|}{|S_0|}, \tag{12.18}$$

where

$$S = \frac{c}{8\pi} \mathrm{Re}[E H^*] \tag{12.19}$$

which is the energy flux density averaged over one oscillation cycle (the Poynting vector) in the scattered wave, and S_0 is a similar quantity for the incident wave.

In this way, we obtained the expressions for the fringing field which approximately take into account the nonuniform part of the current. In the incident plane $\left(\varphi = \pm\frac{\pi}{2}\right)$, they have a form which is rather simple and convenient for calculations. It is also interesting that in this case they satisfy the reciprocity principle as distinct from expressions (10.03) and (10.04) which correspond to the uniform part of the current. It is not difficult to prove this by verifying that Equations (12.11) are not changed with the simultaneous replacement of γ by ϑ and of ϑ by γ, and Equations (12.12) are not changed with the replacement of ϑ by $\pi - \gamma$ and of γ by $\pi - \vartheta$ [in the case $\varphi = -\frac{\pi}{2}$].

However, Equations (12.11) and (12.12) lead to a discontinuity of the magnetic field tangential component H_ϕ on the plane $z = 0$ in which the disk lies. As in the case of diffraction by a strip, the

reason for this is that we did not consider the interaction of the edges. It is also necessary to take into account this interaction in the case of glancing incidence of the plane wave $\left(\gamma=\frac{\pi}{2}\right)$, when the fringing field components E_θ and H_ϕ must be equal to zero.

Let us point out once again in conclusion to this section that expressions (12.11) and (12.12) near directions $\theta=\gamma$, $\theta=\pi-\gamma$ (with $\gamma\neq\frac{\pi}{2}$) have an interpolation character, but in return they allow one to represent the fringing field in the incident plane $x = 0$ in a convenient (uniform) form which frequently is of greatest importance (compare § 24).

CHAPTER III

DIFFRACTION BY A FINITE LENGTH CYLINDER

The distinctive feature of this problem is that, in addition to the nonuniform part of the current on the cylinder's surface which is caused by the discontinuity, there also exists a nonuniform part of the current arising as a consequence of the smooth curve of the surface. This part of the current has the character of waves travelling over the cylindrical surface along geodesic lines [36] — that is, along spirals on the cylinder. These waves, which as they move strike the edge of the cylinder, undergo diffraction and excite secondary surface currents. In turn, the nonuniform part of the current resulting from the discontinuity undergoes diffraction while being propagated over the cylindrical surface. It is clear that specific consideration of all these effects is a very complicated problem.

However, if all the linear dimensions of the cylinder are sufficiently large in comparison with the wavelength, these effects may be neglected when calculating the fringing field in many cases which are of practical interest. In particular, they may be neglected when calculating the field scattered in the direction toward the

source [5, 37]. In this case it is sufficient to consider only the nonuniform part of the current which is caused by the discontinuity of the surface, and we will do this in this Chapter. The equations obtained in this way are generalized to the case when the observation direction does not coincide with the direction of the source.

§ 13. The Physical Optics Approach

Let us investigate the diffraction of plane electromagnetic wave

$$\mathbf{E} = \mathbf{E}_0 e^{ik(y\sin\gamma + z\cos\gamma)} \tag{13.01}$$

on a finite, ideally conducting cylinder of radius a and length l. Let us position the spherical coordinate system in such a way that its origin is at the center of the cylinder, and the normal n to the incident wave front lies in the half-plane $\varphi = \frac{\pi}{2}$ and forms an angle γ $\left(0 \leq \gamma \leq \frac{\pi}{2}\right)$ with the z axis (Figure 24).

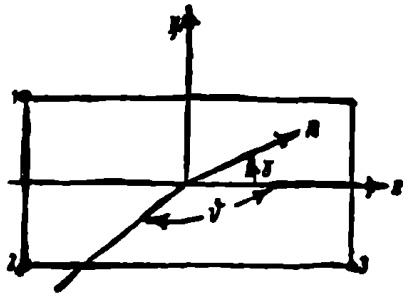

Figure 24. Diffraction of a plane wave by a finite cylinder. n is the normal to the incident wave front.

An incident wave having an arbitrary linear polarizaton always may be represented as the sum of two waves with mutually perpendicular polarizations. Therefore, for a complete solution of the problem, it is sufficient to investigate two particular cases of incident wave polarization:

(1) E-polarization, when the incident wave electric vector is perpendicular to the plane ($\mathbf{E}_0 \perp yoz$) and

(2) H-polarization, when $\mathbf{H}_0 \perp yoz$.

The uniform part of the current excited on the cylindrical surface by wave (13.01) has, with the E-polarization, the components

$$\left.\begin{aligned} f_x^0 &= -\frac{c}{2\pi} E_{0x} \cdot \sin\gamma \sin\psi e^{ikp}, \\ f_y^0 &= \frac{c}{2\pi} E_{0x} \sin\gamma \cos\psi e^{ikp}, \\ f_z^0 &= \frac{c}{2\pi} E_{0x} \cdot \cos\gamma \cos\psi e^{ikp}, \end{aligned}\right\} \tag{13.02}$$

and with the H-polarization it has the components

$$\left.\begin{aligned} f_x^0 &= f_y^0 = 0, \\ f_z^0 &= -\frac{c}{2\pi} H_{0x} \sin\psi e^{ikp}. \end{aligned}\right\} \tag{13.03}$$

where

$$p = a\sin\gamma\sin\psi + \zeta\cos\gamma. \tag{13.04}$$

Let us calculate the field created by these currents in the region $\gamma = -\frac{\pi}{2}$.

The vector potential of the fringing field is determined by the equations

$$A = \frac{a}{c}\int_0^{2\pi} d\psi \int_{-\frac{l}{2}}^{\frac{l}{2}} j^0(\zeta, \psi)\frac{e^{ikr}}{r} d\zeta \text{ with } \gamma = 0 \tag{13.05}$$

and

$$A = \frac{a}{c}\int_{-\pi}^{0} d\psi \int_{-\frac{l}{2}}^{\frac{l}{2}} j^0(\zeta, \psi)\frac{e^{ikr}}{r} d\zeta \text{ with } \gamma > 0, \tag{13.06}$$

where

$$r = \sqrt{\xi^2 + (y-\eta)^2 + (z-\zeta)^2}. \tag{13.07}$$

Since the field in the far zone ($R \gg ka^2, R \gg kl^2$) is of interest to us, these expressions may be simplified by using the relationship

$$r \approx R + a\sin\vartheta\sin\psi - \zeta\cos\vartheta. \tag{13.08}$$

As a result, we obtain a simpler equation

$$A=\frac{a}{c}\frac{e^{ikR}}{R}\int e^{ika\sin\theta\sin\psi}d\psi\int\limits_{-\frac{l}{2}}^{\frac{l}{2}}J^{e}(\zeta,\ \psi)\,e^{-ik\zeta\cos\theta}d\zeta. \tag{13.09}$$

Since the current components are described by the functions $I(\psi)e^{ik\zeta}$, then the problem of finding the field reduces essentially to a calculation of integrals of the type

$$\int\limits_{-\frac{l}{2}}^{\frac{l}{2}}e^{ik\zeta(\cos\gamma-\cos\theta)}d\zeta\int\limits_{-\pi}^{0}I(\psi)\,e^{ip\sin\psi}d\psi=$$
$$=\frac{1}{ik(\cos\gamma-\cos\theta)}\left[e^{i\frac{kl}{2}(\cos\gamma-\cos\theta)}-\right. \tag{13.10}$$
$$\left.-e^{-i\frac{kl}{2}(\cos\gamma-\cos\theta)}\right]\int\limits_{-\pi}^{0}I(\psi)\,e^{ip\sin\psi}\,d\psi.$$

The integral

$$\int\limits_{-\pi}^{0}I(\gamma)\,e^{ip\sin\psi}d\psi,\quad p=ka(\sin\gamma+\sin\theta) \tag{13.11}$$

when p >> 1 is easily calculated by the stationary phase method. The stationary phase point is determined from the condition $\frac{d}{d\psi}\sin\psi=0$ and equals

$$\psi_0=-\frac{\pi}{2}. \tag{13.12}$$

Then assuming $\psi=-\frac{\pi}{2}+\delta$, we find

$$\int\limits_{-\pi}^{0}I(\psi)\,e^{ip\sin\psi}d\psi\approx I(\psi_0)\,e^{-ip}\int\limits_{-\frac{\pi}{2}}^{\frac{\pi}{2}}e^{ip\frac{\delta^2}{2}}d\delta\approx$$
$$\approx\sqrt{\frac{2}{p}}I(\psi_0)\,e^{-ip}\int\limits_{-\infty}^{\infty}e^{it^2}dt=\sqrt{\frac{2\pi}{p}}I(\psi_0)\,e^{-ip+i\frac{\pi}{4}}. \tag{13.13}$$

As a result, we obtain the following expressions for the vector potential:

with E-polarization

$$A_x = \frac{a}{2\pi} E_{0x} \sin\gamma \frac{e^{ikR}}{R} \cdot I, \quad A_y = A_z = 0 \tag{13.14}$$

and with H-polarization

$$A_z = \frac{a}{2\pi} H_{0x} \cdot \frac{e^{ikR}}{R} \cdot I, \quad A_x = A_y = 0, \tag{13.15}$$

where

$$I = \frac{e^{i\frac{kl}{2}(\cos\gamma - \cos\vartheta)} - e^{-i\frac{kl}{2}(\cos\gamma - \cos\vartheta)}}{ik(\cos\gamma - \cos\vartheta)} \times$$
$$\times \sqrt{\frac{2\pi}{ka(\sin\gamma + \sin\vartheta)}} e^{-ika(\sin\gamma + \sin\vartheta) + i\frac{\pi}{4}}. \tag{13.16}$$

The fringing field in the region $\varphi = -\frac{\pi}{2}$ is determined by the relationships

$$\left.\begin{aligned} E_\varphi &= -H_\vartheta = ikA_x, \\ E_\vartheta &= H_\varphi = -ikA_z \sin\vartheta. \end{aligned}\right\} \tag{13.17}$$

Therefore, with the E-polarization it equals

$$\left.\begin{aligned} E_\varphi = -H_\vartheta &= \frac{ika}{2\pi} E_{0x} \sin\gamma \frac{e^{ikR}}{R} \cdot I, \\ E_\vartheta = H_\varphi &= 0, \end{aligned}\right\} \tag{13.18}$$

and with H-polarization

$$\left.\begin{aligned} E_\vartheta = H_\varphi &= -\frac{ika}{2\pi} H_{0x} \cdot \sin\vartheta \frac{e^{ikR}}{R} \cdot I, \\ E_\varphi = H_\vartheta &= 0. \end{aligned}\right\} \tag{13.19}$$

The resulting equations show that the field scattered by the cylindrical surface is created mainly by a luminous band adjacent to the cylinder's generatrix with $\psi = \psi_0 = -\frac{\pi}{2}$. The radiation from this band may be represented [see Equation (13.16)] in the form of spherical waves diverging from its ends (points 2 and 3 in Figure 24).

Now let us write Expressions (13.18) and (13.19) in a form which is most convenient for calculating the effective scattering area

$$\left.\begin{aligned} E_\varphi = -H_\theta &= \frac{ia}{2} E_{0x} \cdot \frac{e^{ikR}}{R} \cdot \overline{\sum}_{\text{ц}}^{0}(\theta, \gamma), \\ E_\theta = H_\varphi &= \frac{ia}{2} H_{0x} \cdot \frac{e^{ikR}}{R} \cdot \sum_{\text{ц}}^{0}(\theta, \gamma). \end{aligned}\right\} \tag{13.20}$$

Here

$$\overline{\sum}_{\text{ц}}^{0} = G \sin\gamma, \quad \sum_{\text{ц}}^{0} = -G \sin\theta, \tag{13.21}$$

and

$$G = 2\sqrt{\frac{2}{\pi ka(\sin\gamma + \sin\theta)}} \times \times \frac{\sin\left[\frac{kl}{2}(\cos\gamma - \cos\theta)\right]}{\cos\gamma - \cos\theta} e^{-ika(\sin\gamma + \sin\theta) + i\frac{\pi}{4}}. \tag{13.22}$$

The index "0" on $\overline{\sum}_{\text{ц}}^{0}$ and $\sum_{\text{ц}}^{0}$ means that the field was calculated in the physical optics approach (based on the uniform part of the current), and the index "c" shows that this fringing field is created by a cylindrical surface. The effective scattering area, in accordance with (12.17), is determined for a cylindrical surface by the relationships

$$\left.\begin{aligned} \sigma_{\text{ц}.E}^{0} &= \pi a^2 \left|\overline{\sum}_{\text{ц}}^{0}\right|^2 = \pi a^2 \sin^2\gamma\, |G|^2, \\ \sigma_{\text{ц}.H}^{0} &= \pi a^2 \left|\sum_{\text{ц}}\right|^2 = \pi a^2 \sin^2\theta\, |G|^2. \end{aligned}\right\} \tag{13.23}$$

In the direction of the mirror-reflected ray $(\theta = \gamma)$, we have

$$\sigma_{\text{ц}.E}^{0} = \sigma_{\text{ц}.H}^{0} = kal^2 \sin\theta = \frac{2\pi a}{\lambda} l^2 \sin\theta. \tag{13.24}$$

In the direction toward the source $(\theta = \pi - \gamma)$, the functions $\overline{\sum}_{\text{c}}^{0}$ and $\sum_{\text{c}}^{0}$ equal

$$\overline{\sum}_{\text{ц}}^{0} = -\sum_{\text{ц}}^{0} = \sqrt{\frac{\sin\theta}{\pi ka}} \cdot \frac{\sin(kl\cos\theta)}{\cos\theta} \cdot e^{-2ika\sin\theta + i\frac{\pi}{4}}. \tag{13.25}$$

These expressions are valid if $ka \sin\theta \gg 1$. It is not difficult to see, by means of equations (13.02) - (13.05), that the fringing field equals zero if $\gamma = 0$ and $\theta = \pi$. Thus in the case of radar (that

is, in the direction toward the source) we find an expression for the fringing field in the region ka sin $\theta \gg 1$ and in the direction $\theta = \pi$. Naturally the desire arises to write interpolation equations — that is, equations which would provide a continuous transition from the region ka sin $\theta \gg 1$ to the direction $\theta = \pi$. Now let us note that the field scattered by a cylinder is comprised of the fields scattered by the lateral (cylindrical) surface and the base (end) of the cylinder. In the physical optics approach, the field scattered by the end of the cylinder is equivalent to the field scattered by a disk. But the field scattered by a disk is described by Bessel functions. Therefore, it is also advisable to express the field scattered by the cylindrical surface in terms of Bessel functions. As s result, the desired interpolation equations for the field scattered by the cylindrical surface may be represented in the form

$$\overline{\sum}_{\pi}^{0} = -\sum_{\pi}^{0} = -\frac{\sin\theta}{2\cos\theta}\left(e^{ikl\cos\theta} - e^{-ikl\cos\theta}\right)\left[J_1(\zeta) - iJ_1(\zeta)\right], \tag{13.26}$$

$$\zeta = 2ka\sin\theta.$$

From this it follows that $\overline{\sum}_{q}^{0} = \sum_{q}^{0} = 0$ in the direction $\theta = \pi$, and with the conditions ka sin $\theta \gg 1$ we obtain Equations (13.25).

The field being scattered by the cylinder's end (by the disk), in accordance with equalities (10.06) and (10.07), is described in the physical optics approach by the equations

$$\left.\begin{matrix}\overline{\sum}_{\lambda}^{0} \\ \sum_{\lambda}^{0}\end{matrix}\right\} = \mp\frac{\cos\theta}{\sin\theta} J_1(\zeta)\, e^{ikl\cos\theta}. \tag{13.27}$$

Consequently, the field scattered by the entire surface of the cylinder will be determined in the plane $\varphi = -\frac{\pi}{2}$ by the equations:

$$\left.\begin{aligned} E_{\varphi} &= -H_{\theta} = \frac{ia}{2} E_{0z} \cdot \frac{e^{ikR}}{R} \overline{\sum}^{0}(\theta), \\ E_{\theta} &= H_{\varphi} = \frac{ia}{2} H_{0r} \cdot \frac{e^{ikR}}{R} \sum^{0}(\theta), \end{aligned}\right\} \tag{13.28}$$

where

$$\left.\begin{matrix}\bar{\Sigma}^{\bullet}(\theta)\\ \Sigma^{\bullet}(\theta)\end{matrix}\right\} = \mp\frac{\sin\theta}{2\cos\theta}\left(e^{ikl\cos\theta} - e^{-ikl\cos\theta}\right)\left[J_1(\zeta) - iJ_2(\zeta)\right] \mp$$
$$\mp\frac{\cos\theta}{\sin\theta}J_1(\zeta)\,e^{ikl\cos\theta} \qquad (\zeta = 2ka\sin\theta). \tag{13.29}$$

These equations allow one to determine in the physical optics approach the effective scattering area of a finite cylinder.

§ 14. The Field Created by the Nonuniform Part of the Current

Let us find the field from the nonuniform part of the current caused by the surface's discontinuity. Figuratively speaking, the field scattered by the cylinder is created by the "luminous" regions on its end and lateral surface. Mathematically this field is described by the sum of spherical waves from the "luminous" points 1, 2 and 3 (see Figure 24). Obviously the field from the nonuniform part of the current also will have the form of spherical waves diverging from these same points.

In the case when the length and diameter of the cylinder are sufficiently large in comparison with the wavelength, one may approximately consider that the nonuniform part of the current near the discontinuity is the same as that on a corresponding wedge. The field radiated by this part of the current in principle may be found in the same way as in the case of the disk. However, such a method is rather complicated. We will find the desired field by a simpler and more graphic method, starting from a physical analysis of the solution obtained for the disk.

For this purpose, let us investigate the structure of waves (12.01) and (12.02) which are radiated by the disk. These equations include the factor

$$\frac{ia}{\sqrt{2\pi ka(\sin\gamma+\sin\nu)}}\frac{e^{ikR}}{R} = i\frac{e^{ikR}}{\sqrt{2\pi kR}}\sqrt{\frac{a}{R}}\frac{1}{\sqrt{\sin\gamma+\sin\theta}}. \tag{14.01}$$

Here $\sqrt{\frac{a}{R}}$ is the unfolding coefficient of the wave. It shows how the field is formed with increasing distance from the disk: the diffracted wave which is cylindrical near the disk unfolds into a spherical wave as the distance from it increases. The coefficient $(\sin\gamma + \sin\theta)^{-1/2}$ is proportional to the width of the luminous region on the disk or, in other words, to the width of the first Fresnel zone. Thus, in Equations (12.01) and (12.12) the functions f^1 and g^1 depend only on the body's geometry — more precisely, on the character of the discontinuity.

Therefore, it is entirely natural to assume that the similar waves which are being scattered by a cylinder have the same structure and differ only in the functions f^1 and g^1 which correspond in this case to a rectangular wedge. Consequently, in the direction toward the source, the field from a nonuniform part of the current flowing on the cylinder may be represented when $ka \sin\theta \gg 1$ in the following way:

$$\left.\begin{aligned} E_\varphi = -H_\theta &= \frac{ia}{\sqrt{2\pi\zeta}} E_{0z}\left\{f^1(1)\, e^{i\left(\zeta-\frac{3\pi}{4}\right)+ika\cos\theta} - \right. \\ &\left. - \left[f^1(2)\, e^{ika\cos\theta} + f^1(3)\, e^{-ika\cos\theta}\right] e^{-i\left(\zeta-\frac{3\pi}{4}\right)}\right\} \frac{e^{ikR}}{R}, \\ E_\theta = H_\varphi &= \frac{ia}{\sqrt{2\pi\zeta}} H_{0z}\cdot\left\{g^1(1)\, e^{i\left(\zeta-\frac{3\pi}{4}\right)+ika\cos\theta} - \right. \\ &\left. - \left[g^1(2)\, e^{ika\cos\theta} + g^1(3)\, e^{-ika\cos\theta}\right] e^{-i\left(\zeta-\frac{3\pi}{4}\right)}\right\} \frac{e^{ikR}}{R}. \end{aligned}\right\} \qquad (14.02)$$

In accordance with § 4, the functions f^1 and g^1 are determined by the equations

$$\left.\begin{aligned} \left.\begin{matrix} f^1(1) \\ g^1(1) \end{matrix}\right\} &= \frac{\sin\frac{\pi}{n}}{n}\left(\frac{1}{\cos\frac{\pi}{n}-1} \mp \right. \\ &\left. \mp \frac{1}{\cos\frac{\pi}{n}-\cos\frac{\pi-2\theta}{n}}\right) \pm \frac{\cos\theta}{2\sin\theta}, \\ \left.\begin{matrix} f^1(2) \\ g^1(2) \end{matrix}\right\} &= \frac{\sin\frac{\pi}{n}}{n}\left(\frac{1}{\cos\frac{\pi}{n}-1} \mp \frac{1}{\cos\frac{\pi}{n}-\cos\frac{2\theta}{n}}\right) \mp \end{aligned}\right\} \qquad (14.03)$$

(Equation continued on next page.)

$$\mp\frac{\cos\theta}{2\sin\theta}\mp\frac{\sin\theta}{2\cos\theta},$$

$$\left.\begin{matrix}f^1(3)\\ g^1(3)\end{matrix}\right\}=\frac{\sin\frac{\pi}{n}}{n}\left(\frac{1}{\cos\frac{\pi}{n}-1}+\right.$$

$$\left.+\frac{1}{\cos\frac{\pi}{n}-\cos\frac{\pi+2\theta}{n}}\right)\mp\frac{\sin\theta}{2\cos\theta}. \qquad (14.03)$$

where

$$n=\frac{3}{2}. \qquad (14.04)$$

In Chapter IV, we will show [see Equation (17.25)] that in the direction $\theta=\pi-\gamma=\pi$ one may neglect the field from the nonuniform part of the current flowing on the cylinder in comparison with the field from the uniform part, if $ka\gg 1$. Therefore, for the field from the nonuniform part of the current, one may write with the help of Bessel functions the following interpolation equations:

$$\left.\begin{aligned}E_\varphi=-H_\theta&=\frac{ka}{2}E_{0z}\cdot\frac{e^{ikR}}{R}\overline{\sum}^1(\theta),\\ E_\theta=H_\varphi&=\frac{ka}{2}H_{0z}\cdot\frac{e^{ikR}}{R}\sum^1(\theta).\end{aligned}\right\} \qquad (14.05)$$

Here

$$\left.\begin{aligned}\overline{\sum}^1(\theta)&=[\overline{M}^1J_1(\zeta)+i\overline{N}^1J_2(\zeta)]\,e^{ikl\cos\theta}-\\ &\quad-f^1(3)[J_1(\zeta)-iJ_2(\zeta)]\,e^{-ikl\cos\theta},\\ \sum^1(\theta)&=[M^1J_1(\zeta)+iN^1J_2(\zeta)]\,e^{ikl\cos\theta}-\\ &\quad-g^1(3)[J_1(\zeta)-iJ_2(\zeta)]\,e^{-ikl\cos\theta},\end{aligned}\right\} \qquad (14.06)$$

and the functions $\overline{M}^1$, $\overline{N}^1$ and M^1, N^1 respectively equal

$$\left.\begin{matrix}\overline{M}^1\\ \overline{N}^1\end{matrix}\right\}=f^1(1)\mp f^1(2),\quad \left.\begin{matrix}M^1\\ N^1\end{matrix}\right\}=g^1(1)\mp g^1(2), \qquad (14.07)$$

or

$$\left.\begin{aligned}
\left.\begin{matrix}\overline{M}^1\\ M^1\end{matrix}\right\} &= \frac{\sin\frac{\pi}{n}}{n}\left(\mp\frac{1}{\cos\frac{\pi}{n}-\cos\frac{\pi-2\theta}{n}}\pm\right.\\
&\left.\pm\frac{1}{\cos\frac{\pi}{n}-\cos\frac{2\theta}{n}}\right)=\frac{\cos\theta'}{\sin\theta}\pm\frac{\sin\theta}{2\cos\theta},\\
\left.\begin{matrix}\overline{N}^1\\ N^1\end{matrix}\right\} &= \frac{\sin\frac{\pi}{n}}{n}\left(\frac{2}{\cos\frac{\pi}{n}-1}\mp\right.\\
&\mp\frac{1}{\cos\frac{\pi}{n}-\cos\frac{\pi-2\theta}{n}}\mp\\
&\left.\mp\frac{1}{\cos\frac{\pi}{n}-\cos\frac{2\theta}{n}}\right)\mp\frac{\sin\theta}{2\cos\theta}.
\end{aligned}\right\} \qquad (14.08)$$

The resulting Equations (14.05) change when $ka\sin\theta \gg 1$ into Equations (14.02), and in the direction $\theta = \pi$ they give a value equal to zero for the field.

§ 15. The Total Fringing Field

Summing Expressions (13.28) and (14.05), it is not difficult to see that the total field scattered by a cylinder will equal

$$\left.\begin{aligned}
E_z &= -H_\theta = \frac{ia}{2}E_{0z}\cdot\frac{e^{ikR}}{R}\cdot\sum(\theta),\\
E_\theta &= H_z = \frac{ka}{2}H_{0z}\cdot\frac{e^{ikR}}{R}\cdot\sum(\theta).
\end{aligned}\right\} \qquad (15.01)$$

where

$$\left.\begin{aligned}
\sum(\theta) &= [\overline{M}J_1(\zeta)+i\overline{N}J_2(\zeta)]\,e^{ikl\cos\theta}-\\
&\quad -f(3)[J_1(\zeta)-iJ_2(\zeta)]\,e^{-ikl\cos\theta},\\
\sum(\theta) &= [MJ_1(\zeta)+iNJ_2(\zeta)]\,e^{ikl\cos\theta}-\\
&\quad -g(3)[J_1(\zeta)-iJ_2(\zeta)]\,e^{-ikl\cos\theta},\\
&\zeta = 2ka\sin\theta.
\end{aligned}\right\} \qquad (15.02)$$

and the functions $\overline{M}$, $\overline{N}$ and M, N are expressed only in terms of the functions f and g which correspond to the asymptotic solution for a rectangular wedge

$$\left.\begin{matrix}\bar{M}\\ \bar{N}\end{matrix}\right\}=f(1)\mp f(2),\quad \left.\begin{matrix}M\\ N\end{matrix}\right\}=g(1)\mp g(2). \tag{15.03}$$

or

$$\left.\begin{aligned}\left.\begin{matrix}\bar{M}\\ M\end{matrix}\right\}&=\frac{\sin\frac{\pi}{n}}{n}\left(\mp\frac{1}{\cos\frac{\pi}{n}-\cos\frac{\pi-2\vartheta}{n}}\mp\frac{1}{\cos\frac{\pi}{n}-\cos\frac{2\vartheta}{n}}\right),\\ \left.\begin{matrix}\bar{N}\\ N\end{matrix}\right\}&=\frac{\sin\frac{\pi}{n}}{n}\left(\frac{2}{\cos\frac{\pi}{n}-1}\mp\frac{1}{\cos\frac{\pi}{n}-\cos\frac{\pi-2\vartheta}{n}}\mp\frac{1}{\cos\frac{\pi}{n}-\cos\frac{2\vartheta}{n}}\right).\end{aligned}\right| \tag{15.04}$$

The functions f(3) and g(3) in turn are determined by the equation

$$\left.\begin{matrix}f(3)\\ g(3)\end{matrix}\right\}=\frac{\sin\frac{\pi}{n}}{n}\left(\frac{1}{\cos\frac{\pi}{n}-1}\mp\frac{1}{\cos\frac{\pi}{n}-\cos\frac{\pi+2\vartheta}{n}}\right). \tag{15.05}$$

Thus only the functions f and g are included in the final expressions for the scattering characteristic of a plane wave by a cylinder.

In the direction $\vartheta=\pi$, the functions $\bar{\Sigma}(\vartheta)$ and $\Sigma(\vartheta)$ take, as in the case of a disk, the values

$$\bar{\Sigma}(\pi)=-\Sigma(\pi)=ka e^{-ikl}, \tag{15.06}$$

and with $\vartheta=\frac{\pi}{2}$ they respectively equal

$$\left.\begin{aligned}\bar{\Sigma}\left(\frac{\pi}{2}\right)&=-\left(\frac{\frac{2}{n}\sin\frac{\pi}{n}}{\cos\frac{\pi}{n}-1}+\frac{1}{n}\operatorname{ctg}\frac{\pi}{n}+ikl\right)[J_1(\zeta)-iJ_2(\zeta)],\\ \Sigma\left(\frac{\pi}{2}\right)&=i\left(\frac{\frac{4}{n}\sin\frac{\pi}{n}}{\cos\frac{\pi}{n}-1}-\frac{1}{n}\operatorname{ctg}\frac{\pi}{n}-ikl\right)J_2(\zeta)+\\ &\quad+\left(\frac{1}{n}\operatorname{ctg}\frac{\pi}{n}+ikl\right)J_1(\zeta),\end{aligned}\right| \tag{15.07}$$

where $\zeta = 2ka$. The terms in this equation which contain the factor kl refer to the field from the uniform part of the current, and the remaining terms refer to the field from the nonuniform part of the current.

In accordance with (12.17), the effective scattering area of the cylinder is determined with the E-polarization of the incident wave by the function

$$\sigma_E = \pi a^2 |\bar{\Sigma}(\theta)|^2, \tag{15.08}$$

and with the H-polarization of the incident wave by the function

$$\sigma_H = \pi a^2 |\Sigma(\theta)|^2. \tag{15.09}$$

Let us note that Expressions (15.02) for the scattering field may be obtained directly on the basis of an analogy with the Equations (12.06), omitting the calculation of the fields from the uniform and nonuniform parts of the current. In the same way, one may obtain the expressions

$$\begin{aligned}
\bar{\Sigma}(\theta, \theta_0) &= [\bar{M}J_1(\xi) + i\bar{N}J_2(\xi)]\, e^{i\frac{M}{2}(\cos\theta + \cos\theta_0)} - \\
&\quad - f(3)[J_1(\xi) - iJ_2(\xi)]\, e^{-i\frac{M}{2}(\cos\theta + \cos\theta_0)}, \\
\Sigma(\theta, \theta_0) &= [MJ_1(\xi) + iNJ_2(\xi)]\, e^{i\frac{M}{2}(\cos\theta + \cos\theta_0)} - \\
&\quad - g(3)[J_1(\xi) - iJ_2(\xi)]\, e^{-i\frac{M}{2}(\cos\theta + \cos\theta_0)},
\end{aligned} \tag{15.10}$$

which are suitable for calculating the fringing field in the region $\varphi = -\frac{\pi}{2}$, $\frac{\pi}{2} < \theta$; $\theta_0 < \pi$ ($\theta_0 = \pi - \gamma$). The quantities here equal

$$\xi = ka(\sin\theta + \sin\theta_0) \tag{15.11}$$

$$\left.\begin{aligned}
\left.\begin{matrix}\bar{M}\\ M\end{matrix}\right\} &= \frac{\sin\frac{\pi}{n}}{n} \times \\
&\times \left(\mp \frac{1}{\cos\frac{\pi}{n} - \cos\frac{\pi - \theta - \theta_0}{n}} + \frac{1}{\cos\frac{\pi}{n} - \cos\frac{\theta + \theta_0}{n}} \right), \\
\left.\begin{matrix}\bar{N}\\ N\end{matrix}\right\} &= \frac{\sin\frac{\pi}{n}}{n} \left(\frac{2}{\cos\frac{\pi}{n} - \cos\frac{\theta - \theta_0}{n}} \mp \right. \\
&\left. \mp \frac{1}{\cos\frac{\pi}{n} - \cos\frac{\pi - \theta - \theta_0}{n}} + \frac{1}{\cos\frac{\pi}{n} - \cos\frac{\theta + \theta_0}{n}} \right).
\end{aligned}\right\} \tag{15.12}$$

$$\left.\begin{matrix} f(3) \\ g(3) \end{matrix}\right\} = \frac{\sin\frac{\pi}{n}}{n}\left(\frac{1}{\cos\frac{\pi}{n}-\cos\frac{\vartheta-\vartheta_0}{n}} \mp \frac{1}{\cos\frac{\pi}{n}-\cos\frac{\pi+\vartheta+\vartheta_0}{n}}\right). \qquad (15.13)$$

Expressions (15.10) satisfy the reciprocity principle — that is, they do not change their values if one interchanges ϑ and ϑ_0. When $\vartheta=\vartheta_0$, they change into the previous Expressions (15.02).

Equations (15.02) and (15.10) describe the radiation from the currents flowing only on part of the cylinder's surface: on the one end (when $z = \frac{l}{2}$) and on half of the lateral surface ($-\pi \leq \psi \leq 0$). Moreover, these expressions do not take into account the nonuniform part of the current caused by the curvature of the cylindrical surface. Therefore, they must be refined with values of ϑ and ϑ_0 which are close to $\frac{\pi}{2}$ and π. However, in the case $\vartheta=\vartheta_0$ — that is, in the direction towards the source — these corrections may be neglected if the parameters ka and kl are sufficiently large. Numerical calculations performed by us on the basis of Equations (15.02) show that this evidently may be done already when $ka = \pi$ and $kl = 10\pi$. The graphs of the functions $\frac{\sigma_E}{\pi a^2} = |\Sigma(\vartheta)|^2$ and $\frac{\sigma_H}{\pi a^2} = |\Sigma(\vartheta)|^2$ constructed for this case in Figures 25 and 26 agree with the experimental curve[1] (the dashed line): the position of the maxima and minima basically agree, and the number of diffraction fringes is the same. For the purpose of illustrating the effect of the ends, we constructed a graph of the effective scattering area for those same values of ka and kl, taking into account only the uniform part of the current on the cylindrical surface (Figure 27). A comparison of Figures 25, 26 and 27 shows that the effect of the ends begins to appear when $\vartheta = 120°$.

Footnote (1) appears on page 89.

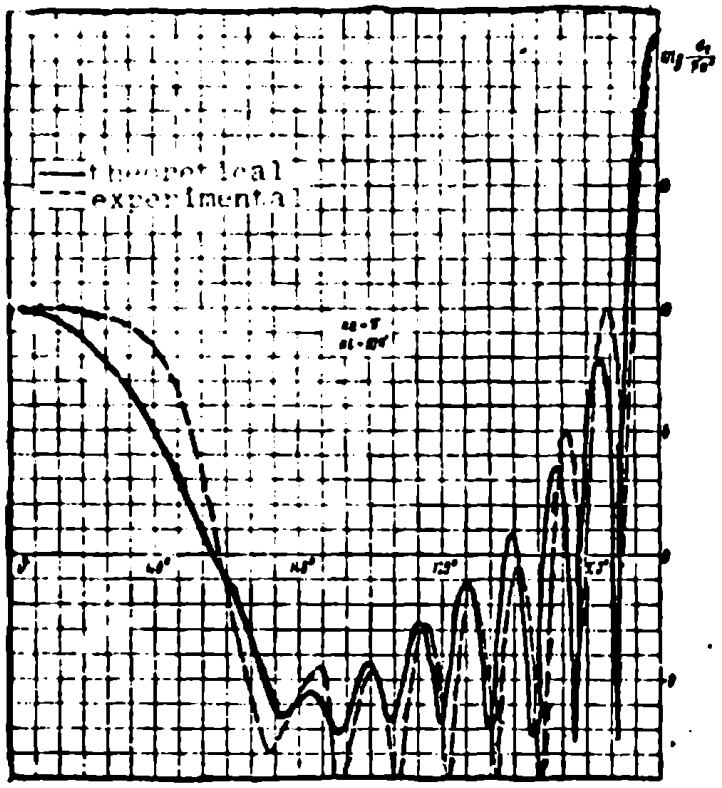

Figure 25. Diagram of the effective scattering surface for a finite cylinder. The case of E-polarization.

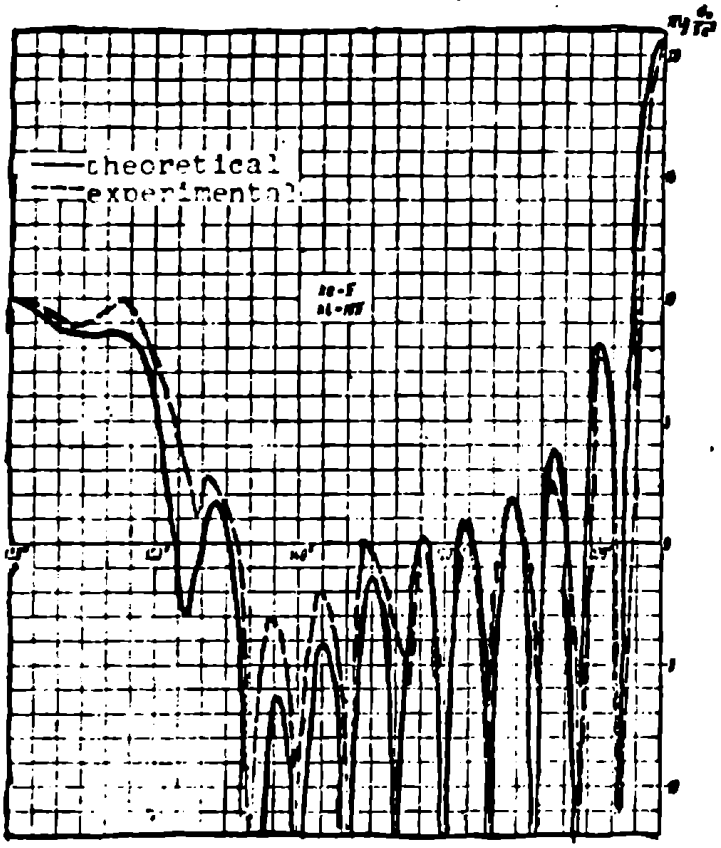

Figure 26. Diagram of the effective scattering surface for a finite cylinder. The case of H-polarization

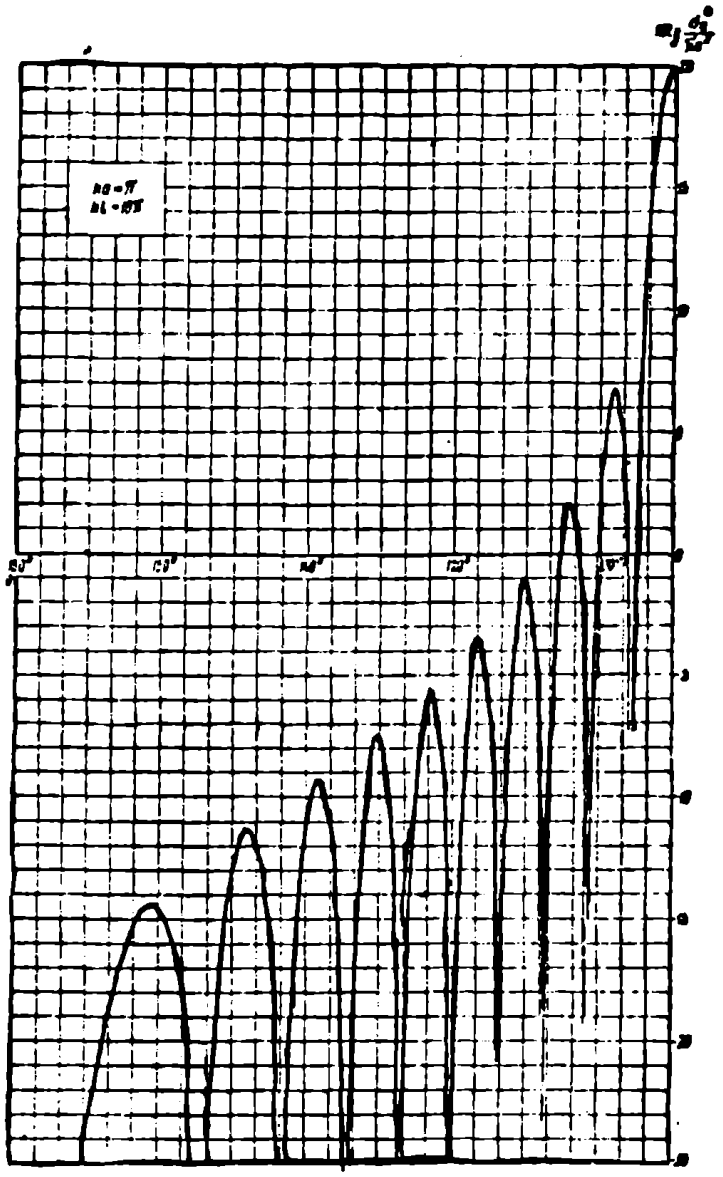

Figure 27. The effective scattering area of the lateral surface of a cylinder in the physical optics approach [see (13.26)].

FOOTNOTES

1. on page 86. The experimental curves shown in Figures 25 and 26 and also those in Figures 31, 32, 65 and 71 were obtained by Ye. N. Mayzels and L. S. Chugunova.

CHAPTER IV

DIFFRACTION OF A PLANE WAVE INCIDENT ALONG THE SYMMETRY AXIS OF FINITE BODIES OF ROTATION

In this Chapter we will refine the physical optics approach for certain other bodies of rotation, whose surfaces have circular discontinuities. We will limit ourselves to the case when a plane electromagnetic wave falls on the bodies along their symmetry axis.

As before, we will assume that the linear dimensions of the bodies are large in comparison with the wavelength. In this case the currents in the vicinity of a circular discontinuity of any convex surface of rotation may be approximately considered to be the same as that on a corresponding conical body. Consequently, it is sufficient to study the field from the nonuniform part of the current which is caused by the circular discontinuity of the surface, using such a body as an example.

§ 16. The Field Created by the Nonuniform Part of the Current

Let a plane electromagnetic wave fall on a conical body in the positive direction of the z axis (Figure 28). From the relationships

$$\left.\begin{aligned}\mathbf{E} &= -\frac{1}{ik}(\operatorname{grad}\operatorname{div}\mathbf{A} + k^2\mathbf{A}),\\ \mathbf{H} &= \operatorname{rot}\mathbf{A}\end{aligned}\right| \qquad (16.01)$$

we find the following expressions for the fringing field in the wave zone:

$$\left.\begin{aligned}E_x &= H_y = ikA_x,\\ E_y &= -H_x = ikA_y\end{aligned}\right\} \text{ with } \theta = 0 \qquad (16.02)$$

and

$$\left.\begin{aligned}E_x &= -H_y = ikA_x,\\ E_y &= H_x = ikA_y\end{aligned}\right\} \text{with } \theta = \pi. \qquad (16.03)$$

The vector potential is determined by the equation

$$\mathbf{A} = \frac{1}{c}\frac{e^{ikr}}{r}\int_0^{2\pi}\left[\int_0^{l_1} J_1(\zeta)\, e^{\pm ik\zeta\cos\psi}(a - \zeta\sin\alpha)\,d\zeta + \right.$$
$$\left. + \int_0^{l_2} J_2(\zeta)\, e^{\pm ik\zeta\cos\psi}(a - \zeta\sin\alpha)\,d\zeta\right]d\psi. \qquad (16.04)$$

Here r is the distance from the discontinuity to the observation point, $J_1(\zeta)$ is the surface current density flowing on the irradiated side of the body, and $J_2(\zeta)$ is the current density on the shadowed side. The upper sign in the exponents refers to the case $\theta = \pi$, and the lower sign refers to the case $\theta = 0$. Since the nonuniform part of the current is concentrated mainly in the vicinity of the discontinuity, the vector potential corresponding to it may be represented in the form

$$\mathbf{A} = \frac{a}{c}\frac{e^{ikr}}{r}\int_0^{2\pi}\left(\int_0^{\infty} J_1'(\zeta)\, e^{\pm ik\zeta\cos\psi}d\zeta + \right.$$
$$\left. + \int_0^{\infty} J_2'(\zeta)\, e^{\mp ik\zeta\cos\psi}d\zeta\right)d\psi. \qquad (16.05)$$

Obviously the nonuniform part of the current near the discontinuity of a conical surface may be considered to be approximately the same as on a corresponding wedge (Figure 29). In the local cylindrical coordinate system r_1, ϕ_1, z_1, the field from the nonuniform part

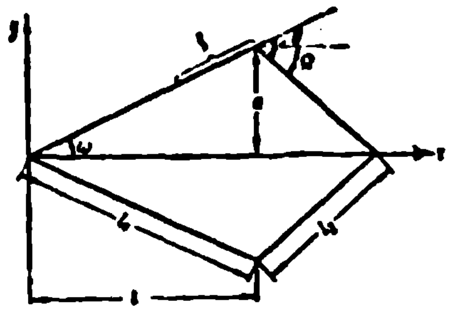

Figure 28. Diffraction of a plane wave by a conical body. The plane wave is propagated along the z axis.

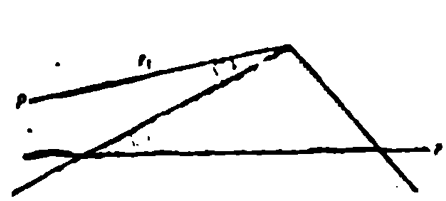

Figure 29. The dihedral angle corresponding to the discontinuity of a conical surface.

of the current flowing on such a wedge is determined in the far zone ($kr_1 >> 1$) by the following equations:

$$\left.\begin{array}{l} E_{z_1}(\psi) = -H_{\varphi_1}(\psi) = ikA_{z_1}(\psi), \\ H_{z_1}(\psi) = E_{\varphi_1}(\psi) = -ikA_{\varphi_1}(\psi), \end{array}\right\} \quad (16.06)$$

where

$$A = \frac{1}{c}\sqrt{\frac{2\pi}{kr_1}}\left[\int_0^\infty j_1^1(\zeta)e^{ik\zeta\cos\psi}d\zeta + \int_0^\infty j_1^1(\zeta)e^{[illegible]}d\zeta\right]e^{i\left(kr_1 \mp \frac{\pi}{4}\right)}. \quad (16.07)$$

Here the upper sign in the exponents refers to the case $\phi_1 = \pi + \omega$, and the lower sign — to the case $\phi_1 = \omega$. On the other hand, in § 4 it was shown that this field equals

$$\left.\begin{array}{l} E_{z_1}(\psi) = E_{0z_1}(\psi) f^1 \dfrac{e^{i\left(kr_1 + \frac{\pi}{4}\right)}}{\sqrt{2\pi kr_1}}, \\ H_{z_1}(\psi) = H_{0z_1}(\psi) g^1 \dfrac{e^{i\left(kr_1 + \frac{\pi}{4}\right)}}{\sqrt{2\pi kr_1}}, \end{array}\right\} \quad (16.08)$$

where $E_{0z_1}(\psi)$, $H_{0z_1}(\psi)$ are the values of the incident wave amplitude at the wedge edge, and f^1 and g^1 are angular functions characterizing the scattering diagram.

Let us introduce the designation

$$J=\int_0^\infty J_1^1(\zeta)e^{\pm ik\zeta\cos\vartheta}d\zeta+\int_0^\infty J_2^1(\zeta)e^{\mp ik\zeta\cos\vartheta}d\zeta. \tag{16.09}$$

Equating Expressions (16.06) and (16.08), we find

$$J_{z_1}=\frac{cE_{0z_1}(\psi)}{ik2\pi}f^1,\quad J_{\varphi_1}=\frac{cH_{0z_1}(\psi)}{ik2\pi}g^1. \tag{16.10}$$

The components J_{z_1} and J_{ϕ_1} are mutually perpendicular, and when $\vartheta=0$ and $\vartheta=\pi$ they are parallel to the plane x0y (Figure 30). The different orientation of the unit vector e_{ϕ_1} when $\vartheta=0$ and $\vartheta=\pi$ is connected with the fact that the angle ϕ_1 is measured from the irradiated face of the wedge. In the original x, y, z coordinate system the vector J has the components

$$\left.\begin{aligned}J_x&=J_{z_1}\sin\psi-J_{\varphi_1}\cos\psi,\\J_y&=-J_{z_1}\cos\psi-J_{\varphi_1}\sin\psi\end{aligned}\right\}\text{with }\vartheta=0 \tag{16.11}$$

and

$$\left.\begin{aligned}J_x&=J_{z_1}\sin\psi+J_{\varphi_1}\cos\psi,\\J_y&=-J_{z_1}\cos\psi+J_{\varphi_1}\sin\psi\end{aligned}\right\}\text{with }\vartheta=\pi. \tag{16.12}$$

Substituting Expressions (16.10) here, we obtain

$$\left.\begin{aligned}J_x&=\frac{c}{ik2\pi}[f^1E_{0z_1}(\psi)\sin\psi-g^1H_{0z_1}(\psi)\cos\psi],\\J_y&=\frac{-c}{ik2\pi}[f^1E_{0z_1}(\psi)\cos\psi+g^1H_{0z_1}(\psi)\sin\psi]\end{aligned}\right\}\text{with }\vartheta=0 \tag{16.13}$$

and

$$\left.\begin{aligned}J_x&=\frac{c}{ik2\pi}[f^1E_{0z_1}(\psi)\sin\psi+g^1H_{0z_1}(\psi)\cos\psi],\\J_y&=-\frac{c}{ik2\pi}[f^1E_{0z_1}(\psi)\cos\psi-g^1H_{0z_1}(\psi)\sin\psi]\end{aligned}\right\}\text{with }\vartheta=\pi. \tag{16.14}$$

Now identifying the current near the conical surface discontinuity with the current on the wedge, we find the components of vector potential (16.05)

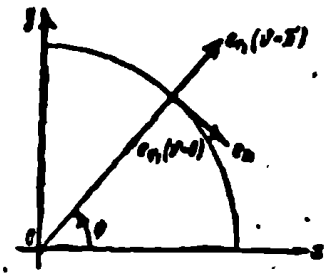

Figure 30. The relative orientation of the unit vectors e_{φ_1} and e_{z_1} in the cases $\theta = 0$ and $\theta = \pi$.

$$\left.\begin{aligned} A_x &= \frac{a}{ik2\pi}\frac{e^{ikr}}{r}\int_0^{2\pi} [f' E_{0z_1}(\psi)\sin\psi - \\ &\quad - g' H_{0z_1}(\psi)\cos\psi]\,d\psi, \\ A_y &= -\frac{a}{ik2\pi}\frac{e^{ikr}}{r}\int_0^{2\pi} [f' E_{0z_1}(\psi)\cos\psi + \\ &\quad + g' H_{0z_1}(\psi)\sin\psi]\,d\psi \end{aligned}\right\} \text{with } \theta = 0 \quad (16.15)$$

and

$$\left.\begin{aligned} A_x &= \frac{a}{ik2\pi}\frac{e^{ikr}}{r}\int_0^{2\pi} [f' E_{0z_1}(\psi)\sin\psi + \\ &\quad + g' H_{0z_1}(\psi)\cos\psi]\,d\psi, \\ A_y &= -\frac{a}{ik2\pi}\frac{e^{ikr}}{r}\int_0^{2\pi} [f' E_{0z_1}(\psi)\cos\psi - \\ &\quad - g' H_{0z_1}(\psi)\sin\psi]\,d\psi. \end{aligned}\right\} \text{with } \theta = \pi. \quad (16.16)$$

Furthermore, let the plane wave be polarized in such a way that $E_0 \| 0x$. Then

$$E_{0z_1}(\psi) = E_{0x}\sin\psi, \quad H_{0z_1}(\psi) = -E_{0x}\cos\psi. \quad (16.17)$$

Considering these relationships and substituting Expressions (16.15) and (16.16) into Equations (16.02) and (16.03), we find the field from the nonuniform part of the current which is caused by the circular discontinuity of the conical surface

$$\left.\begin{aligned} E_x &= H_y = \frac{aE_{0x}}{2}(f' + g')\frac{e^{ikr}}{r} \\ E_y &= H_x = 0 \end{aligned}\right| \text{with } \theta = 0 \quad (16.18)$$

and

$$\left.\begin{aligned} E_x &= -H_y = \frac{aE_{0x}}{2}(f' - g')\frac{e^{ikr}}{r} \\ E_y &= H_x = 0 \end{aligned}\right| \text{with } \theta = \pi. \quad (16.19)$$

Equation (16.18) is applicable for the values $0 \leq \omega < \frac{\pi}{2}$, $\omega < \theta \leq \pi$, and Equation (16.19) for the values $0 \leq \omega < \frac{\pi}{2}$, $0 \leq \theta < \pi$. In the case of a

disk $\left(\theta = \frac{\pi}{2}, \Phi = \pi\right)$, the field from the nonuniform part of the current equals zero on the z axis, since $f^1 = -f^{-1} = -1/2$ when $\theta = 0$, and $f^1 = g^1 = -1/2$ when $\theta = \pi$ [compare (5.10)].

Using the results obtained in the following sections, we will calculate the effective scattering area (in the direction $\theta = \pi$) for specific bodies, assuming that they are irradiated by the plane wave

$$E_0 = H_0 = E_{0x} e^{ikz}. \tag{16.20}$$

and their linear dimensions are large in comparison with the wavelength.

§ 17. A Cone

Let a cone (Figure 28) be irradiated by plane electromagnetic wave (16.20). The uniform part of the current which is excited on the cone's surface has the components

$$\left.\begin{aligned} f_r^0 &= \frac{c}{2\pi} E_{0x} \sin\alpha\, e^{ikz}, \\ f_\varphi^0 &= 0, \\ f_z^0 &= \frac{c}{2\pi} E_{0x} \cos\alpha \cos\varphi\, e^{ikz} \end{aligned}\right\} \tag{17.01}$$

and creates in the direction $\theta = \pi$ (with $R \gg ka^2$, $R \gg kl^2$) the field

$$\left.\begin{aligned} E_x = -H_y &= -E_{0x} \frac{i}{4k} \operatorname{tg}^2\alpha \frac{e^{ikR}}{R} + \\ &+ E_{0x}\left(\frac{i}{4k}\operatorname{tg}^2\alpha + \frac{a}{2}\operatorname{tg}\alpha\right)\frac{e^{ikR}}{R} e^{2ikl}, \\ E_y = H_x &= 0. \end{aligned}\right\} \tag{17.02}$$

Here the first term describes the spherical wave diverging from the vertex of the cone, and the remaining terms describe the spherical wave from its base.

The field caused by the discontinuity of the surface at the cone base is a spherical wave, and is determined in accordance with

(16.19) by the expression

$$\left.\begin{aligned} E_z = -H_y = -\frac{a}{2}E_{0z}\left(\operatorname{tg}\omega + \frac{\frac{2}{n}\sin\frac{\pi}{n}}{\cos\frac{\pi}{n}-\cos\frac{2\omega}{n}}\right)\frac{e^{ikR}}{R}e^{2ikl}, \\ E_y = H_z = 0. \end{aligned}\right\} \qquad (17.03)$$

where

$$n = 1 + \frac{\omega+\Omega}{\pi}. \qquad (17.04)$$

An asymptotic calculation of the rigorous diffraction series for a semi-infinite cone [38-40] shows that in the direction $\theta = \pi$ one may neglect the effect of the nonuniform part of the current caused by the conical point. Therefore, summing (17.02) and (17.03), we obtain the following expression for the fringing field:

$$\left.\begin{aligned} E_z = -H_y = -E_{0z}\left[\frac{i}{2}\operatorname{tg}^2\omega\left(1-e^{2ikl}\right)+\right. \\ \left.+ ka\frac{\frac{2}{n}\sin\frac{\pi}{n}}{\cos\frac{\pi}{n}-\cos\frac{2\omega}{n}}e^{2ikl}\right]\frac{e^{ikR}}{2kR}, \\ E_y = H_z = 0. \end{aligned}\right\} \qquad (17.05)$$

Let us point out the following important feature of the resulting equation. In the problems which were investigated in the previous chapters, the edge waves of the fringing field were expressed only in terms of the functions f and g. But now in the equation for the spherical wave from the cone's base, in addition to the term which depends on f and g [the last term in the bracket of Equation (17.05)], there is an additional term [term $-i/2\operatorname{tg}^2\omega e^{2ikl}$ in Equation (17.05)] which does not depend on these functions and is determined by the uniform part of the current. Therefore, it is impossible to represent the resulting spherical wave from the cone's base only in terms of the functions f and g which characterize the total edge wave diagram from the corresponding wedge edge. This important fact was not considered in [41, 44], as a consequence of which their authors did

not succeed in obtaining correct results for a cone with an arbitrary aperture angle $\omega(0 \leq \omega \leq \pi/2)$.

The effective scattering area in accordance with (12.18) is determined by the equation

$$\sigma = \pi a |\Sigma|^2. \tag{17.06}$$

where the function Σ is connected with the fringing field by the relationship

$$E_\theta = -H_\varphi = -\frac{a}{2} E_{0x} \frac{e^{ikR}}{R} \Sigma \tag{17.07}$$

and equals

$$\Sigma = \frac{1}{ka} \operatorname{tg}^2 \omega \sin kl\, e^{ikl} + \frac{\frac{2}{n} \sin \frac{\pi}{n}}{\cos \frac{\pi}{n} - \cos \frac{2\omega}{n}} e^{2ikl}. \tag{17.08}$$

The analogous function in the physical optics approach may be written in accordance with (17.02) in the form

$$\Sigma^0 = \frac{1}{ka} \operatorname{tg}^2 \omega \sin kl\, e^{ikl} - \operatorname{tg} \omega\, e^{2ikl}. \tag{17.09}$$

With the deforming of the top part of the cone into a disk $\left(\omega \to \frac{\pi}{2},\ l \to 0\right)$, Equations (17.08) and (17.09) are transformed, respectively, to the form

$$\left.\begin{aligned} \Sigma &= -ika - \frac{1}{n} \operatorname{ctg} \frac{\pi}{n}, \\ \Sigma^0 &= -ika. \end{aligned}\right\} \tag{17.10}$$

Furthermore, it follows from (17.08) and (17.09) that for large values of the parameter $ka(ka \gg \operatorname{tg}^2 \omega)$ the functions Σ and Σ^0 may be represented in the form

$$\Sigma = \frac{\frac{2}{n} \sin \frac{\pi}{n}}{\cos \frac{\pi}{n} - \cos \frac{2\omega}{n}} e^{2ikl}. \tag{17.11}$$

$$\Sigma^0 = \operatorname{tg}\omega\, e^{2ika}. \tag{17.12}$$

Thus even in the case of short waves (ka >> $\operatorname{tg}^2\omega$, but R >> kl^2), our Expression (17.08) does not change into the physical optics equation, but substantially differs from it because

$$\sigma = \pi a^2 \left| \frac{\frac{2}{n}\sin\frac{\pi}{n}}{\cos\frac{\pi}{n} - \cos\frac{2\omega}{n}} \right|^2 \tag{17.13}$$

and

$$\sigma^0 = \pi a^2 \operatorname{tg}^2\omega. \tag{17.14}$$

With this

$$\sigma = \sigma^0 \left| \frac{\frac{2}{n}\sin\frac{\pi}{n}}{\left(\cos\frac{\pi}{n} - \cos\frac{2\omega}{n}\right)\operatorname{tg}\omega} \right|^2, \tag{17.15}$$

that is, for sufficiently short waves (or for sufficiently large dimensions of the cone) the function σ is proportional to σ^0. The coefficient of proportionality here does not depend on the cone dimensions, but is determined only by its shape.

This result is graphically illustrated by the curves giving the effective scattering area of a cone (ω = 10°25', k = π, Ω = 90°) as a function of its length (Figure 31). Whereas our equation (the continuous line) is in satisfactory agreement with the results of measurements (the small crosses)[1], the physical optics approach (the dashed line) gives values which are smaller than the experimental values by 13-15 dB. For sharply pointed cones, the nonuniform part of the current has an especially large values. In Figure 32, a curve is constructed for the effective surface of a cone (ka = 2.75 π, Ω = 90°)

Footnote (1) appears on page 113.

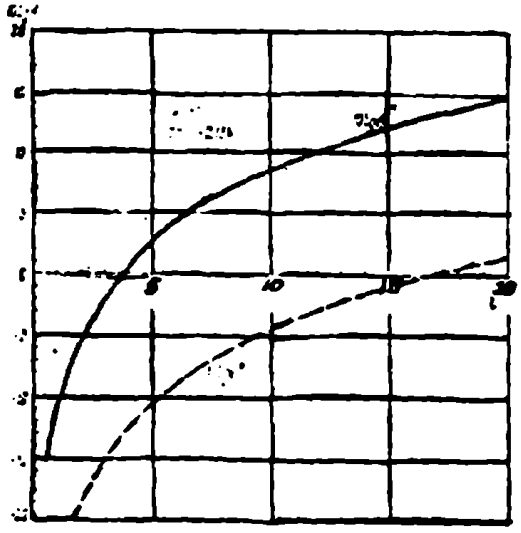

Figure 31. The effective scattering area of a finite cone as a function of its length. The function σ (the continuous line) was calculated on the basis of equation (17.06) which considers the nonuniform part of the current in the vicinity of the circular discontinuity. The function σ^0 (the dashed line) corresponds to the physical optics approach.

with its deformation into a disk ($\omega \to 90°$). The discrepancy between our curve and the physical optics approach here reaches almost 30 dB when $\omega = 2°$.

Expression (17.08) obtained by us also allows one, in contrast to the physical optics approach (17.09), to evaluate the role of the shape of the shadowed part of the body and shows that the reflected signal will be larger, the closer this shape is to a funnel-shaped form ($\Omega \approx \pi - \omega$). Thus, for example, in the case $\omega = 10°$, $kl = 10\pi$ ($k = \pi$) the signal reflected by the cone may exceed by 15 dB the value corresponding to physical optics (see Figure 33) if $\Omega \approx 170°$.

Let us note that our Expression (17.13) is equivalent to the expression presented in the above-mentioned papers [41, 44]. However, the latter expression is applicable only for sharply pointed cones, whereas we have, in addition to (17.13), Equation (17.08) which is suitable for cones with any aperture angle ω $\left(0 \leq \omega \leq \frac{\pi}{2}\right)$.

The calculation method discussed may be generalized in the case of asymmetric irradiation of the cone. However, with asymmetric irradiation, generally speaking, it is necessary to take into account the nonuniform part of the current caused by the point of the cone.

In concluding this section, let us calculate the effective scattering area for a body which is formed by rotation around the

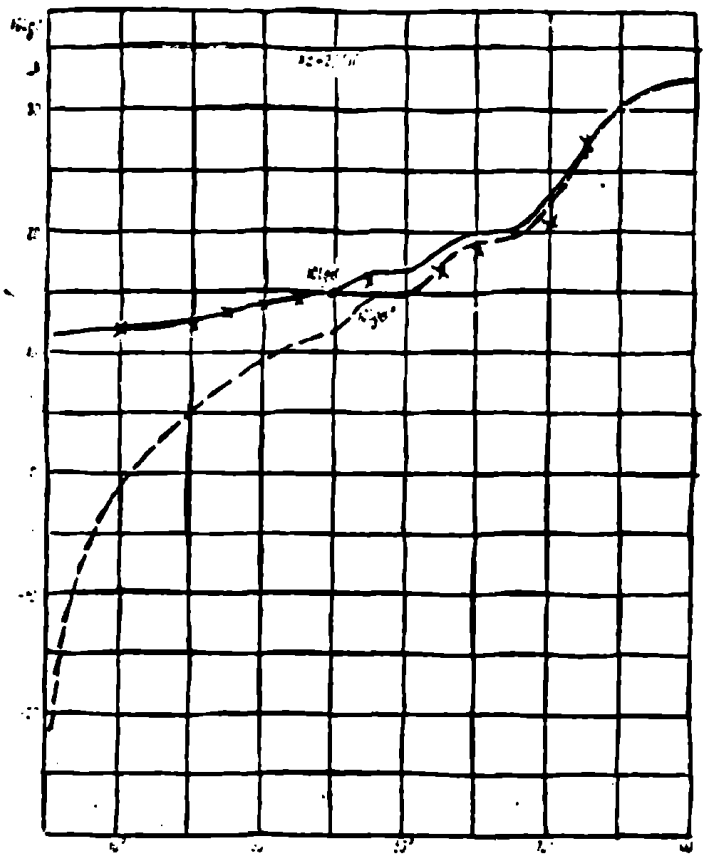

Figure 32. The effective scattering area of a finite cone as a function of the vertex angle.

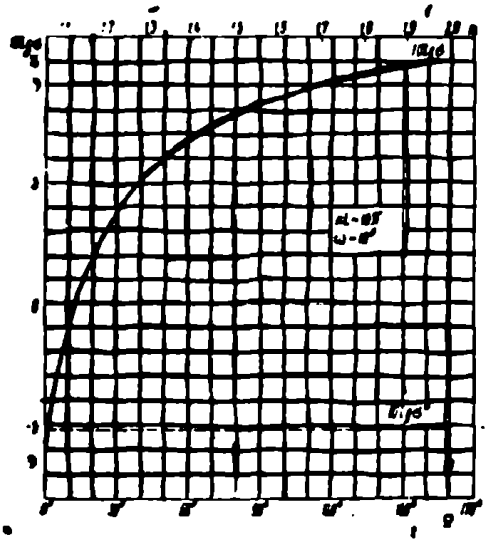

Figure 33. The effective scattering area of a finite cone as a function of the shape of the shaded part.

z axis of the plane figure shown in Figure 34. Integrating the uniform part of the current, it is not difficult to show that the field scattered in the direction $\vartheta=\pi$ by the lateral surface of the truncated cone (Figure 35) is determined by the equation

$$E_{\varphi} = -H_{\psi} = E_{0x}\cdot\left[-\left(\frac{i}{4k}\operatorname{tg}^2\omega_1+\frac{a_1}{2}\operatorname{tg}\omega_1\right)e^{2ikl_1}+\right.$$

$$\left.+\left(\frac{i}{4k}\operatorname{tg}^2\omega_1+\frac{a_2}{2}\operatorname{tg}\omega_1\right)e^{2ik(l_1+l_2)}\right]\frac{e^{ikR}}{R}. \qquad (17.16)$$

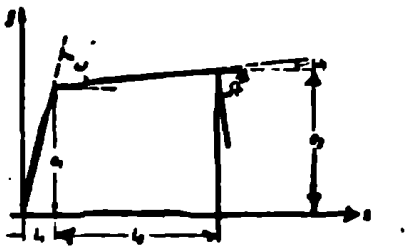

Figure 34. The generatrix of the surface of rotation.

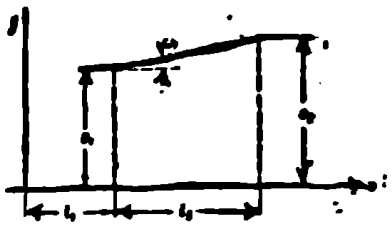

Figure 35. The generatrix of of a truncated conical surface.

Summing this expressing with (17.02), where the quantities l and a must be replaced by l_1 and a_1, we find the field from the uniform part of the current flowing on the entire illuminated side of the body

$$E_z = -H_y = -\frac{a_1 E_{0x}}{2}\sqrt{\frac{1}{ka_1}}\operatorname{tg}^2\omega\sin kl_1\, e^{ikl_1} - \operatorname{tg}\omega\, e^{2ikl_1} + \\ + \left[\frac{1}{ka_1}\operatorname{tg}^2\omega_1\sin kl_2\, e^{ikl_2} + \left(1 - \frac{a_2}{a_1}e^{2ikl_2}\right)\operatorname{tg}\omega_1\right] e^{2ikl_1}\sqrt{\frac{1}{j}}\frac{e^{ikR}}{R}. \qquad (17.17)$$

The field radiated by the nonuniform part of the current is determined in accordance with § 16 by the equation

$$E_z = -H_y = -\frac{a_1 E_{0x}}{2}\left[\left(\frac{\frac{2}{n_1}\sin\frac{\pi}{n_1}}{\cos\frac{\pi}{n_1} - \cos\frac{2\omega}{n_1}} + \operatorname{tg}\omega - \operatorname{tg}\omega_1\right)e^{2ikl_1} + \right. \\ \left. + \frac{a_2}{a_1}\left(\frac{\frac{2}{n_2}\sin\frac{\pi}{n_2}}{\cos\frac{\pi}{n_2} - \cos\frac{2\omega_1}{n_2}} + \operatorname{tg}\omega_1\right)e^{2ik(l_1+l_2)}\right]\frac{e^{ikR}}{R}, \qquad (17.18)$$

where

$$n_1 = 1 + \frac{\omega - \omega_1}{\pi},\quad n_2 = 1 + \frac{\omega_1 + \Omega}{\pi}. \qquad (17.19)$$

Now summing (17.17) and (17.18), we obtain a refined expression for the field scattered in the direction $\theta = \pi$

$$E_z = -H_y = -\frac{a_1 E_{0x}}{2}\left(\frac{1}{ka_1}\operatorname{tg}^2\omega\sin kl_1 e^{ikl_1} + \right. \qquad (17.20)$$

(Equation continued on next page.)

$$+\frac{\frac{2}{n_2}\sin\frac{\pi}{n_2}}{\cos\frac{\pi}{n_2}-\cos\frac{2\omega}{n_2}}e^{2ikl_1}+\frac{1}{ka_1}\operatorname{tg}^2\omega_2\sin kl_2e^{ik(l_1+2l_2)}+$$

$$+\frac{a_2}{a_1}\frac{\frac{2}{n_2}\sin\frac{\pi}{n_2}}{\cos\frac{\pi}{n_2}-\cos\frac{2\omega_1}{n_2}}e^{2ik(l_1+l_2)}\Bigg)\frac{e^{ikR}}{R}. \qquad (17.20)$$

Consequently, the effective scattering area will equal

$$\sigma=\pi a_1^2\left|\frac{1}{ka_1}\operatorname{tg}^2\omega\sin kl_1e^{ikl_1}+\frac{\frac{2}{n_1}\sin\frac{\pi}{n_1}}{\cos\frac{\pi}{n_1}-\cos\frac{2\omega}{n_1}}e^{2ikl_1}+\right.$$

$$\left.+\frac{1}{ka_1}\operatorname{tg}^2\omega_1\sin kl_2e^{ik(l_1+2l_2)}+\frac{a_2}{a_1}\frac{\frac{2}{n_2}\sin\frac{\pi}{n_2}}{\cos\frac{\pi}{n_2}-\cos\frac{2\omega_1}{n_2}}e^{2ik(l_1+l_2)}\right|^2. \qquad (17.21)$$

In the physical optics approach, the analogous quantity equals

$$\sigma^0=\pi a_1^2\left|\frac{1}{ka_1}\operatorname{tg}^2\omega\sin kl_1e^{ikl_1}-\operatorname{tg}\omega e^{2ikl_1}+\right.$$

$$\left.+\left[\frac{1}{ka_2}\operatorname{tg}^2\omega_1\sin kl_2e^{ikl_2}+\left(1-\frac{a_2}{a_1}e^{2ikl_2}\right)\operatorname{tg}\omega_1\right]e^{2ikl_1}\right|^2. \qquad (17.22)$$

When the top part of the cone is deformed into a disk $\left(\omega\to\frac{\pi}{2},\ l_1\to 0\right)$, Equations (17.21) and (17.22) take the form

$$\sigma=\pi a_1^2\left|-ika_1-\frac{1}{n_1}\operatorname{ctg}\frac{\pi}{n_1}+\frac{1}{ka_1}\operatorname{tg}^2\omega_1\sin kl_2e^{ikl_2}+\right.$$

$$\left.+\frac{a_2}{a_1}\frac{\frac{2}{n_2}\sin\frac{\pi}{n_2}}{\cos\frac{\pi}{n_2}-\cos\frac{2\omega_1}{n_2}}e^{2ikl_2}\right|^2, \qquad (17.23)$$

$$\sigma^0=\pi a_1^2\left|-ika_1+\frac{1}{ka_1}\operatorname{tg}^2\omega_1\sin kl_2e^{ikl_2}+\right.$$

$$\left.+\left(1-\frac{a_2}{a_1}e^{2ikl_2}\right)\operatorname{tg}\omega_1\right|^2. \qquad (17.24)$$

In these expressions assuming $\omega_1 = 0$, we find the effective scattering area for a finite cylinder

$$\sigma = \pi a_1^2 \left| -ika_1 - \frac{1}{n_1} \operatorname{ctg} \frac{\pi}{n_1} + \frac{\frac{2}{n_2} \sin \frac{\pi}{n_2}}{\cos \frac{\pi}{n_2} - 1} e^{2ikl_1} \right|^2, \tag{17.25}$$

$$\sigma^0 = \pi a_1^2 (ka_1)^2, \tag{17.26}$$

in connection with which

$$n_1 = \frac{3}{2}, \quad n_2 = 1 + \frac{\Omega}{\pi}. \tag{17.27}$$

Equation (17.25) is more precise than Equation (15.06) which was derived in § 15, where the value of the field in the direction $\theta = \pi$ was taken in the physical optics approach.

§ 18. A Paraboloid of Rotation

Let us calculate the effective scattering area of a paraboloid of rotation $r^2 = 2pz$ (Figure 36) which is irradiated by plane wave (16.20). The uniform part of the current excited on the paraboloid's surface has the components

$$\left.\begin{aligned} j_x^0 &= \frac{c}{2\pi} E_{0x} \sin \alpha e^{ikz}, \\ j_y^0 &= 0, \\ j_z^0 &= \frac{c}{2\pi} E_{0x} \cos \alpha \cos \frac{\varphi}{2} e^{ikz}. \end{aligned}\right\} \tag{18.01}$$

Integrating this current, it is not difficult to show that in the direction $\vartheta = \pi$ it radiates the field

$$\left.\begin{aligned} E_x &= -H_y = -E_{0x} \cdot \frac{a}{2} (1 - e^{2ikl}) \operatorname{tg} \omega \frac{e^{ikR}}{R}, \\ E_y &= H_x = 0. \end{aligned}\right\} \tag{18.02}$$

Here a is the radius of the base of the paraboloid; $l = \frac{a^2}{2p} = \frac{a}{2} \operatorname{ctg} \omega$ is its length; α is the angle between the z axis and the tangent to the generatrix of the paraboloid ($r^2 = 2pz$). At the point $z = l$, the angle α takes the value $\alpha = \omega \left(\operatorname{tg} \omega = \frac{p}{a} \right)$.

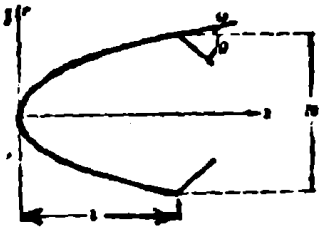

Figure 36. Diffraction of a plane wave by a paraboloid of rotation.

The field from the nonuniform part of the current caused by the discontinuity of the paraboloid's surface is determined by Equation (17.03). The field from the nonuniform part of the current which is caused by the smooth curve of the paraboloid's surface equals zero in the case of symmetric radiation [45]. Therefore, summing (18.02) and (17.03) we find the expression for the resulting fringing field.

$$\left.\begin{aligned} E_x = -H_y = -\frac{aE_{0x}}{2}\left(\operatorname{tg}\omega + \frac{\frac{2}{n}\sin\frac{\pi}{n}}{\cos\frac{\pi}{n}-\cos\frac{2\omega}{n}}e^{2ikl}\right)\frac{e^{ikR}}{R}, \\ E_y = H_x = 0 \end{aligned}\right| \qquad \left(n = 1+\frac{\omega+\Omega}{\pi}\right). \tag{18.03}$$

Consequently, the effective scattering area of the paraboloid will be determined by the relationship

$$\sigma = \pi a^2\left|\operatorname{tg}\omega + \frac{\frac{2}{n}\sin\frac{\pi}{n}}{\cos\frac{\pi}{n}-\cos\frac{2\omega}{n}}e^{2ikl}\right|^2, \tag{18.04}$$

which, when the paraboloid is deformed into a disk $\left(\omega\to\frac{\pi}{2},\ l\to 0,\ \Omega = \text{const}\right)$, is transformed to the form

$$\sigma = \pi a^2\left|ika + \frac{1}{n}\operatorname{ctg}\frac{\pi}{n}\right|^2. \tag{18.05}$$

Comparing Expression (18.04) with the equation

$$\sigma^0 = \pi a^2\operatorname{tg}^2\omega\,|1-e^{2ikl}|^2, \tag{18.06}$$

which physical optics gives for the effective scattering area, we see that they differ significantly from one another. First of all, the oscillating character of the function σ^0 draws our attention:

the reflected signal equals zero if a whole number of half-waves $\left(l = \frac{\lambda}{2} n,\ n = 1, 2, 3 \ldots\right)$ is fitted into the length of the paraboloid, and it takes a maximum value if a half-integral number of half-waves $\left(l = \frac{\lambda}{2}\left(n + \frac{1}{2}\right),\ n = 1, 2, 3 \ldots\right)$ is contained in this length.

A calculation performed by us on the basis of Equation (18.04) for paraboloids with the parameters $\Omega = 90°$, $\mathrm{tg}\omega = 0.1$ ($k = \pi$) shows (Figure 37) that, although the oscillating character of the effective scattering area is preserved, the amplitude of the oscillations is only 2 dB, and the maximum values of the function σ exceed the corresponding values in the physical optics approach by almost 13 dB. A still stronger divergence between the results of our theory and physical optics is detected when the paraboloid is deformed into a disk (Figure 38, $ka = 3\pi$, $k = \pi$, $\Omega = 90°$, $\omega \to 90°$).

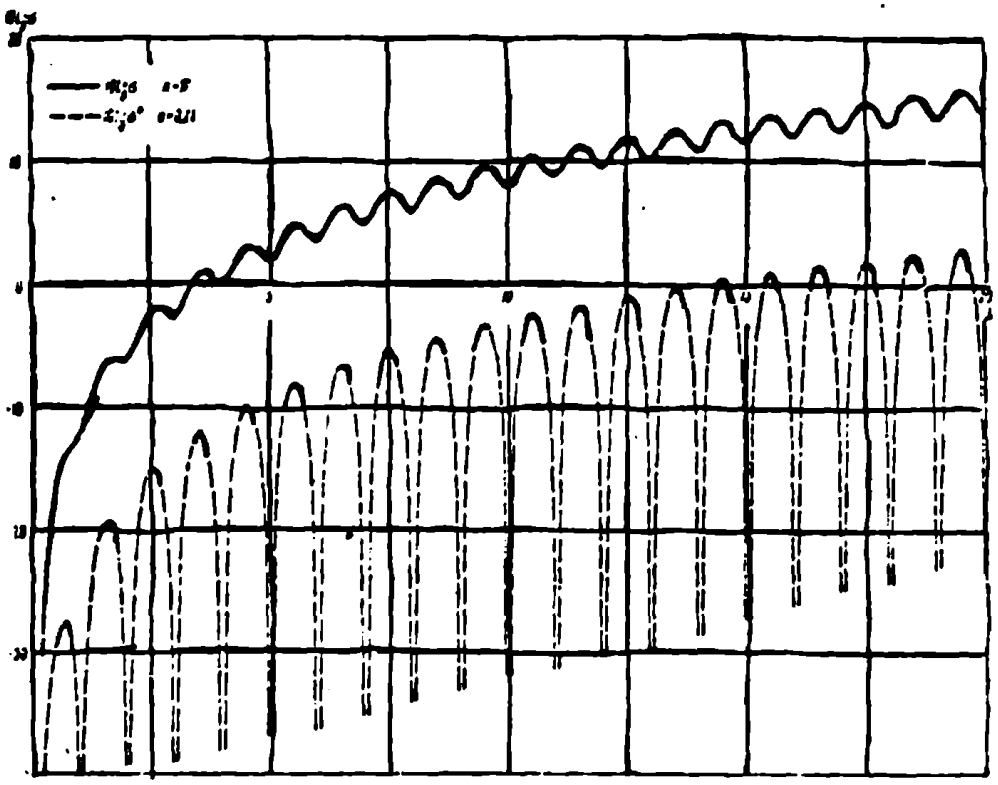

Figure 37. The effective scattering area of a finite paraboloid as a function of its length with a constant value of the angle ω ($\mathrm{tg}\omega = 0.1$). The diameter of the base varies.

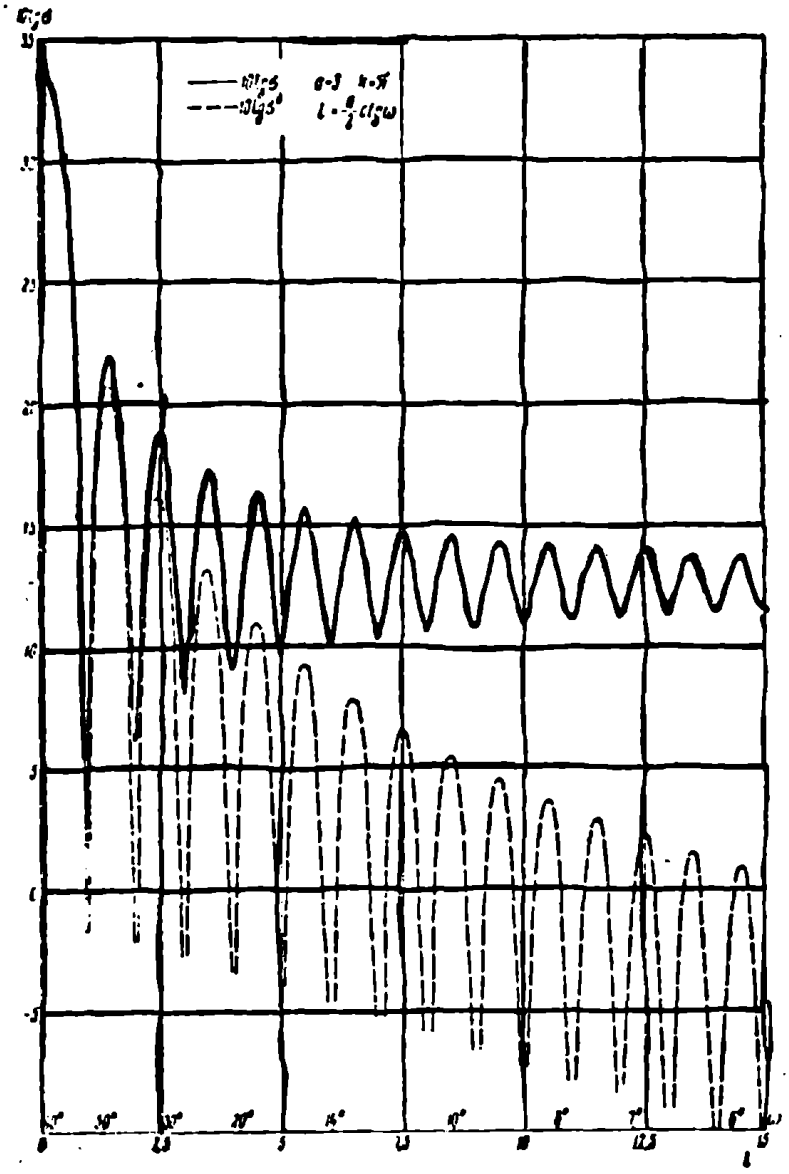

Figure 38. The effective scattering area of a finite paraboloid as a function of its length with a constant radius of the base.

As in the case of a cone, the shape of the shadowed part turns out to have a substantial influence on the reflected signal. For example, for a paraboloid with the parameters ka = 2π, kl = 10 π, $t_{r}\omega$ = 0.1 (k = π), the reflected signal increases by 44 dB with an increase of Ω($\omega < \Omega < \pi - \omega$) (Figure 39).

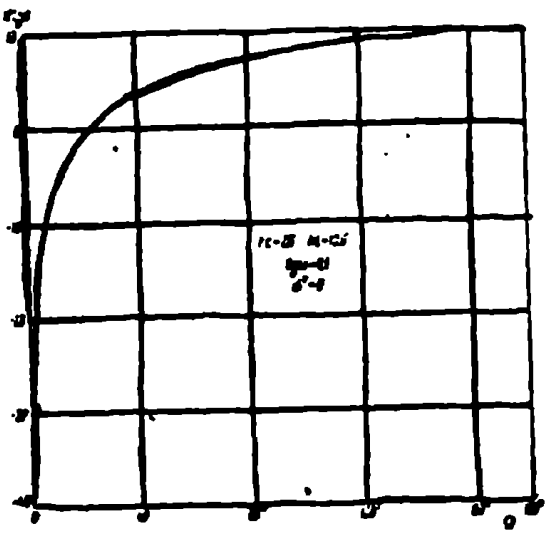

Figure 39. The effective scattering area of a finite paraboloid as a function of the shape of the shaded part.

In concluding this section, let us dwell for a moment on the question of calculating the effective scattering area for bodies of rotation of a complex shape, whose elements are the lateral surfaces of truncated paraboloids. The field from the nonuniform part of the current arising in the vicinity of circular discontinuities may be determined without difficulty from Equation (17.03). The field from the uniform part of the current is found by quadratures. Thus, the field being created in the direction $\theta = \pi$ by the uniform part of the current which flows on the lateral surface of the truncated paraboloid $r^2 = 2pz (p = a_1 tg\omega_1 = a_2 tg\omega_2$; see Figure 40) is determined by the equation

$$\left.\begin{aligned} E_\theta = -H_\varphi = -\frac{1}{2} E_{0\theta} (a_1 tg\,\omega_1 - a_2 tg\,\omega_2 e^{2ikl_0}) e^{ikl_0} \frac{e^{ikR}}{R}, \\ E_\varphi = H_\theta = 0. \end{aligned}\right\} \qquad (18.07)$$

Here

$$l_0 = \frac{1}{2}(a_2 ctg\,\omega_2 - a_1 ctg\,\omega_1) \qquad (18.08)$$

is the height of the truncated paraboloid (the distance between its bases). Let us note that Equation (18.07) is a simple algebraic corollary of Expression (18.02): it is the difference of the fields scattered, respectively, by the paraboloid of height $l_1 + l_0 = \frac{a_2^2}{2p}$ and by the paraboloid of height $l_1 = \frac{a_1^2}{2p}$.

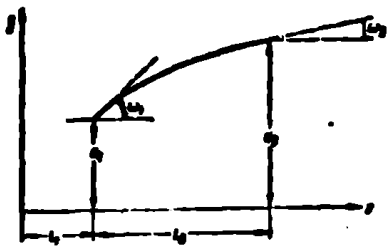

Figure 40. The generatrix of the lateral surface of a truncated paraboloid of rotation.

§ 19. A Spherical Surface

Incident wave (16.20) excites a surface current on the surface of an ideally conducting sphere (a radius of ρ and a center on the z axis at the point $z = \rho$). The uniform part of this current has the components

$$\left.\begin{aligned} j_x^0 &= -\frac{c}{2\pi} E_{0x} \cos\theta e^{ikz}, \\ j_y^0 &= 0, \\ j_z^0 &= \frac{c}{2\pi} E_{0x} \sin\theta \cos\varphi e^{ikz}. \end{aligned}\right\} \qquad (19.01)$$

The currents flowing on a spherical ring cut from the sphere's surface by the planes $z = l_1$ and $z = l_1 + l_2$ (Figure 41) create, in the direction $\vartheta = \pi$, the field

$$\left.\begin{aligned} E_x &= -H_\varphi = E_{0x}\left[-\left(\frac{a_1}{2}\operatorname{tg}\omega_1 - \frac{i}{4k}\right)e^{2ikl_1} + \right. \\ &\qquad \left. + \left(\frac{a_2}{2}\operatorname{tg}\omega_2 - \frac{i}{4k}\right)e^{2ik(l_1+l_2)}\right]\frac{e^{ikR}}{R}, \\ E_y &= H_x = 0, \end{aligned}\right\} \qquad (19.02)$$

where

$$\left.\begin{aligned} l_1 &= \rho(1 - \sin\omega_1), \\ l_2 &= \rho(\sin\omega_1 - \sin\omega_2); \end{aligned}\right\} \qquad (19.03)$$

$$\rho = \frac{a_1}{\cos\omega_1} = \frac{a_2}{\cos\omega_2}. \qquad (19.04)$$

Here a_1 is the radius of the first cross section; a_2 is the radius of the second cross section; $\omega_1(\omega_2)$ is the angle between the z axis and the tangent to the meridian at the point $z = l_1(z_2 = l_1 + l_2)$.

Furthermore, assuming in Equation (19.02) $\omega_1 = \frac{\pi}{2}$ ($\omega_2 = \text{const}$), we obtain in the physical optics approach an expression for the field scattered by the spherical segment (Figure 42)

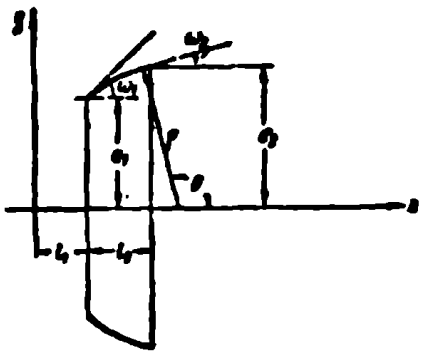

Figure 41. A ring cut from the surface of its sphere by the planes $z = l_1$ and $z = l_1 + l_2$.

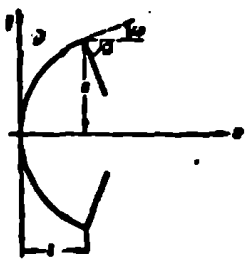

Figure 42. A spherical segment with a conically shaped base.

$$E_x = -H_y = E_{0x}\left[-\frac{a}{2\cos\omega}+\frac{1}{4k}+\right.$$
$$\left.+\left(\frac{a}{2}\operatorname{tg}\omega-\frac{1}{4k}\right)e^{2ikl}\right]\frac{e^{ikR}}{R}. \qquad (19.05)$$

Here we used the new designations

$$\left.\begin{aligned} a &= a_2, \quad \omega = \omega_2, \\ l &= l_2 = \rho(1-\sin\omega). \end{aligned}\right\} \qquad (19.06)$$

Equations (19.02) and (19.05) are simplified if $ka_1 \gg 1$ and $ka_2 \gg 1$. Thus, the field from the spherical ring will equal

$$E_x = -H_y = -E_{0x}\left(\frac{a_1}{2}\operatorname{tg}\omega_1-\frac{a_2}{2}\operatorname{tg}\omega_2 e^{2ikl_2}\right)e^{2ikl_1}\frac{e^{ikR}}{R}, \qquad (19.07)$$

and the field from the spherical segment will equal

$$E_x = -H_y = -\frac{aE_{0x}}{2}(\sec\omega-\operatorname{tg}\omega\, e^{2ikl})\frac{e^{ikR}}{R}. \qquad (19.08)$$

If here one assumes $\omega = 0$, then equation

$$E_x = -H_y = -\frac{aE_{0x}}{2}\frac{e^{ikR}}{R} \qquad (19.09)$$

gives us the field scattered by a hemisphere. The value of the effective scattering area corresponding to it will equal, in accordance with (17.06),

$$\sigma^* = \pi a^2. \qquad (19.10)$$

Now let us find the field scattered by the spherical segment considering the discontinuity of the surface; one may neglect the perturbation of the current as a consequence of the smooth curve of the surface if ka >> 1 [74]. The nonuniform part of the current which is caused by the discontinuity creates in the direction $\vartheta=\pi$ the field (17.03). Summing the latter with the field (19.08), we find the desired field

$$E_x=-H_y=-\frac{aE_{0x}}{2}\left(\frac{1}{\cos\omega}+\frac{\frac{2}{n}\sin\frac{\pi}{n}}{\cos\frac{\pi}{n}-\cos\frac{2\omega}{n}}e^{2ikl}\right)\frac{e^{ikR}}{R}. \tag{19.11}$$

Consequently, the effective scattering area of a spherical segment will equal

$$\sigma=\pi a^2\left|\frac{1}{\cos\omega}+\frac{\frac{2}{n}\sin\frac{\pi}{n}}{\cos\frac{\pi}{n}-\cos\frac{2\omega}{n}}e^{2ikl}\right|^2, \qquad n=1+\frac{\omega+\Omega}{\pi}. \tag{19.12}$$

In the physical optics approach, a similar quantity is determined by field (19.08) and equals

$$\sigma^0=\pi a^2\left|\frac{1}{\cos\omega}-\operatorname{tg}\omega\,e^{2ikl}\right|^2. \tag{19.13}$$

With the deforming of the spherical surface into a disk $\left(\omega\to\frac{\pi}{2},\ l\to 0,\ \Omega=\text{const}\right)$, Equations (19.12) and (19.13) are transformed, respectively, to the form

$$\left.\begin{aligned}\sigma&=\pi a^2\left|ika+\frac{1}{n}\operatorname{ctg}\frac{\pi}{n}\right|^2,\\ \sigma^0&=\pi a^2(ka)^2.\end{aligned}\right\} \tag{19.14}$$

It follows from Equations (19.12) and (19.13) that the effective scattering area of a spherical segment is an oscillating function of its length. The oscillation period equals $\frac{\lambda}{2}$. Numerical calculations performed on the basis of these equations showed (Figure 43) that, with small angles of the discontinuity (Ω = 15°), one may still neglect the field from the nonuniform part of the current. In Figure 44, graphs are constructed for the effective scattering area of a

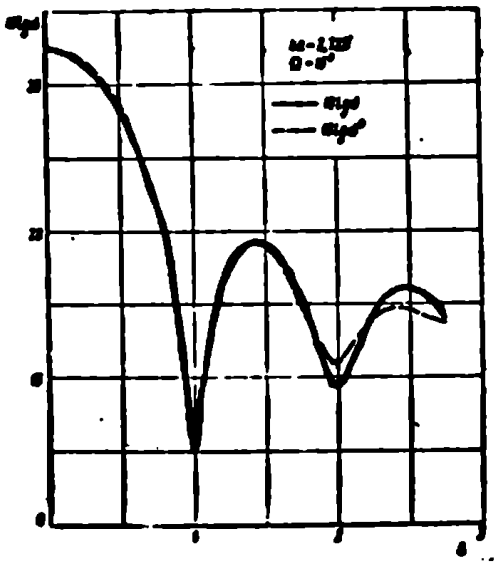

Figure 43. The effective scattering area of a spherical segment as a function of its length with a constant radius of the base. The function σ (the continuous line) is calculated on the basis of Equation (19.12) which considers the nonuniform part of the current near the discontinuity. The function σ^0 (the dashed line) is calculated from Equation (19.13), and corresponds to the physical optics approach.

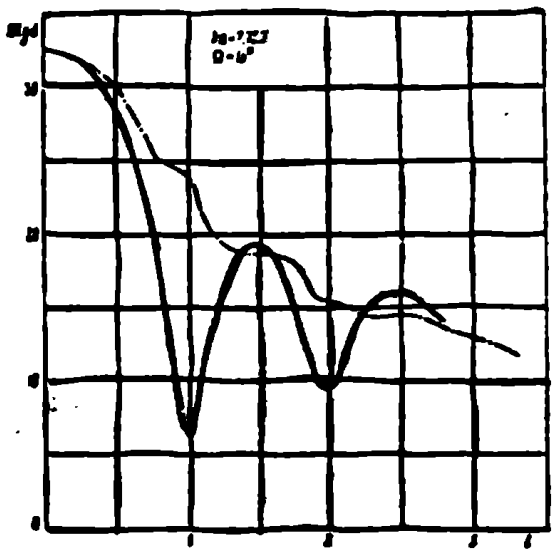

Figure 44. A comparison of the effective scattering area of a spherical segment (continuous line) and a finite cone (dashed line) which have the same bases.

spherical segment and a finite cone (the dashed curve) which have the same diameter and base shape.

* * * * * *

The results obtained in this Chapter show that the reflected signal depends substantially on the shape of the shaded part of the body, and increases with an increase of the concavity. However, since the nonuniform part of the current is concentrated mainly near the discontinuity, that part of the shaded surface which is several wavelengths away from the discontinuity evidently will not have a noticeable effect on the reflected signal and may be an arbitrary shape.

It is interesting that our expressions, which agree satisfactorily with experiments, even with large (in comparison with the wavelengths) dimensions of the bodies, do not change into the physical optics equations, but differ from them substantially. At the same time, physical optics, contrary to the widely held opinion concerning its reliability in such cases, leads to a significant discrepancy with experiments.

The method used in this Chapter allows one to calculate the effective scattering area associated with the symmetric irradiation of any convex body of rotation, the surface of which has circular discontinuities. It may also be generalized to the case of asymmetric irradiation. However, when doing this it is necessary to take into account the nonuniform part of the current caused by the point and the smooth curve of the surface.

FOOTNOTES

1. on page 98. See footnote on page 86.

CHAPTER V

SECONDARY DIFFRACTION

In the previous chapters, an approximate solution of diffraction problems was carried out which was based on the representation of the fringing field in the form of the sum of the fields from the uniform and nonuniform parts of the surface current. The first field was found by quadratures, and the second field by approximation; it was assumed that the nonuniform part of the current near the discontinuity (edge) of a surface is the same as on a corresponding wedge.

However, the fields found by such a method are actually the fields from the currents flowing, not only on the flat and curved parts of the body's surface, but also to some extent on the geometric extension of these sections. The error in the expressions for the fringing field which is thus introduced is most significant with a glancing incident wave, when the edge zone occupied by the nonuniform part of the current is noticeably broadened, and also with a glancing radiation, when the direction to the observation point forms a small angle with the given section of the surface. In these cases, the results obtained earlier are in need of substantial corrections. We already talked about this briefly in § 6 and § 12.

For the purpose of refining the solutions which were found previously, it is necessary to assume that in actuality the currents flow only on the body's surface, and that a wave travelling from one edge to the other will undergo a perturbation at the latter. The process of forming the fringing field when this occurs may be investigated in the following way. The edge wave propagated from one of the edges is diffracted by the other edges; the waves arising with this in turn are diffracted by adjacent edges, etc. In this chapter, we will investigate the case when the dimensions of the surface faces are so large in comparison with the wavelength that it is sufficient to limit oneself to considering the diffraction of only the primary edge waves. This phenomenon we shall call secondary diffraction.

In this chapter, secondary diffraction by an infinitely long strip (§ 20 - § 23) and by a circular disk (§ 24) is studied. The solution of these problems may be obtained by means of the principle of duality from the solution of the diffraction problems for an infinite slit and a circular hole in a flat, ideally conducting screen. In the latter case, the physical treatment of diffraction of edge waves is significantly simpler; it is exactly for this reason, therefore, that almost all diffraction studies of edge waves are related to holes in a plane screen. However, we will not take such a path, but we shall investigate a strip and a disk directly. This approach has the advantage that it is easily generalized to the case of three-dimensional bodies.

§ 20. Secondary Diffraction by a Strip. Formulation of the Problem.

Let an infinitely thin, ideally conducting strip of width 2a and unlimited length be orientated in space as shown in Figure 45. A plane electromagnetic wave incident normal to the strip's edges is directed at an angle α to the plane xoz and has the following form:

$$\mathbf{E}=\mathbf{E}_0 e^{ik(x\cos\alpha+y\sin\alpha)},\quad \mathbf{H}=\mathbf{H}_0 e^{ik(x\cos\alpha+y\sin\alpha)}. \tag{20.01}$$

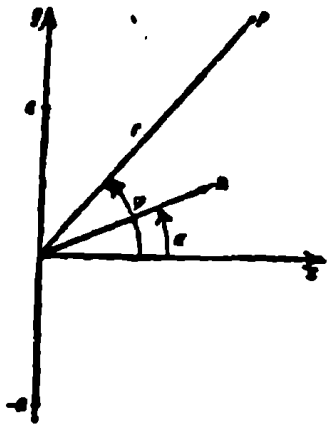

Figure 45. The transverse cross section of a strip with the plane xoy, x = 0, y = a and x = 0, y = -a are the coordinates of the strip's edge; n is the normal to the incident plane wave front.

In § 6 approximation expressions were found for the fringing field in the far zone which did not consider the interaction of the edges. In the case of E-polarization of the incident wave $(E_0 \| 0z)$, these expressions may be represented in the form

$$\left.\begin{aligned} E_z = -H_\varphi = E_{0z}\left[f(1)e^{ika(\sin\alpha-\sin\varphi)} + \right. \\ \left. + f(2)e^{-ika(\sin\alpha-\sin\varphi)}\right]\frac{e^{i\left(kr+\frac{\pi}{4}\right)}}{\sqrt{2\pi kr}}, \\ E_\varphi = H_z = 0, \end{aligned}\right\} \tag{20.02}$$

and in the case of H-polarization $(H_0 \| 0z)$

$$\left.\begin{aligned} H_z = E_\varphi = H_{0z}\left[g(1)e^{ika(\sin\alpha-\sin\varphi)} + \right. \\ \left. + g(2)e^{-ika(\sin\alpha-\sin\varphi)}\right]\frac{e^{i\left(kr+\frac{\pi}{4}\right)}}{\sqrt{2\pi kr}}, \\ H_\varphi = E_z = 0. \end{aligned}\right\} \tag{20.03}$$

Let us recall that the functions f and g included here are determined in the region $|\varphi| < \frac{\pi}{2}$ (when $|\alpha| < \frac{\pi}{2}$) by the following relationships:

$$f(1) = \frac{\cos\frac{\alpha+\varphi}{2} - \sin\frac{\alpha-\varphi}{2}}{\sin\alpha - \sin\varphi}, \quad f(2) = -\frac{\cos\frac{\alpha+\varphi}{2} + \sin\frac{\alpha-\varphi}{2}}{\sin\alpha - \sin\varphi}, \tag{20.04}$$

$$g(1) = -f(2), \quad g(2) = -f(1). \tag{20.05}$$

The first terms in Equations (20.02) and (20.03) describe cylindrical waves diverging from edge 1 (y = a), and the second terms describe the cylindrical waves diverging from edge 2 (y = -a). The

nonuniform part of the current on each side of the strip also has the form of waves which diverge from edges 1 and 2, and are an "analytical extension" of the corresponding terms in Equations (20.02) and (20.03). The current wave encountering the opposite edge is reflected from it. Or else one may say that each of the cylindrical waves propagated from edge 1 or 2 undergoes diffraction by the opposite edge (secondary diffraction).

If the strip's width is sufficiently large in comparison with the wavelength, then one may approximately assume that the oncoming current wave near the strip's edge will be the same as on a corresponding half-plane excited by a linear source, the moment of which is selected in a definite way. It is also obvious that the current waves reflected from the edge will also coincide. Consequently, the problem of secondary diffraction by a strip may be reduced to the problem of the diffraction of a cylindrical wave by a half-plane.

The field created at the point P by a current filament parallel to the half-plane's edge and passing through the point Q (Figure 46) may be found by means of the reciprocity principle. In the case of E-polarization, it is determined by the relationship

$$E_z = \frac{p_z}{p_{oz}} E_z(Q). \tag{20.06}$$

and in the case of H-polarization

$$H_z = \frac{m_z}{m_{oz}} H_z(Q). \tag{20.07}$$

Here p_z (m_z) is the electric (magnetic) moment of the current filament passing through the Q; p_{oz} (m_{oz}) is the moment of the auxiliary current filament passing through the point P with the coordinates (ϕ", R), and H_z (Q) or E_z (Q) is the field created by the auxiliary filament at the point Q.

Now let us remove the auxiliary current filament to such a distance that the cylindrical wave arriving from it may be considered

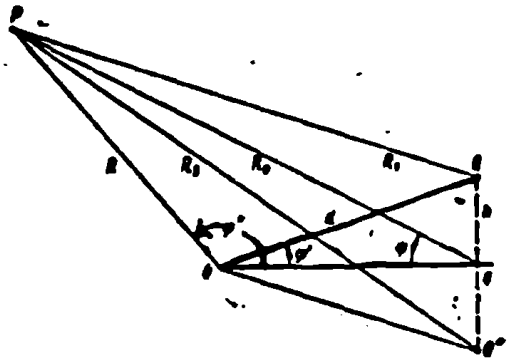

Figure 46. Diffraction of a cylindrical wave by a half-plane. Q is the source, Q^* is the mirror image of the source, and P is the observation point.

to be a plane wave on the section from the edge of the half-plane to the point Q. In this case, in accordance with § 1 and § 2 the field created by it at the point Q will equal

$$\left.\begin{aligned} E_z(Q) &= E_{0z}(0)\,[u(d, \varphi' - \varphi'') - u(d, \varphi' + \varphi'')], \\ H_z(Q) &= H_{0z}(0)\,[u(d, \varphi' - \varphi'') + u(d, \varphi' + \varphi'')]. \end{aligned}\right\} \tag{20.08}$$

The functions u introduced here are determined (for the values $0 < \varphi'' < \pi$) by the equations

$$\left.\begin{aligned} u(d, \varphi' - \varphi'') &= e^{-ikd\cos(\varphi' - \varphi'')}\frac{e^{-i\frac{\pi}{4}}}{\sqrt{\pi}} \times \int_{\infty \cos\frac{\varphi' - \varphi''}{2}}^{\sqrt{2kd}\cos\frac{\varphi' - \varphi''}{2}} e^{iq^2}dq + \\ &+ \begin{cases} e^{-ikd\cos(\varphi' - \varphi'')} & \text{with } 0 < \varphi' < \pi + \varphi'' \\ 0 & \text{with } \pi + \varphi'' < \varphi' < 2\pi, \end{cases} \\ u(d, \varphi' + \varphi'') &= e^{-ikd\cos(\varphi' + \varphi'')}\frac{e^{-i\frac{\pi}{4}}}{\sqrt{\pi}} \times \int_{\infty \cos\frac{\varphi' + \varphi''}{2}}^{\sqrt{2kd}\cos\frac{\varphi' + \varphi''}{2}} e^{iq^2}dq + \\ &+ \begin{cases} e^{-ikd\cos(\varphi' + \varphi'')} & \text{with } 0 < \varphi' < \pi - \varphi'' \\ 0 & \text{with } \pi - \varphi'' < \varphi' < 2\pi, \end{cases} \end{aligned}\right\} \tag{20.09}$$

and the quantities E_z (0) and H_z (0) are the values of the primary field created by the auxiliary filament at points corresponding to the half-plane's edge. In accordance with Equations (1.21) and (1.22), this field may be represented when kR >> 1 in the form

$$\left.\begin{aligned} E_{0z}(0) &= ik^2 p_{0z}\sqrt{\frac{2\pi}{kR}}\,e^{i\left(kR - \frac{\pi}{4}\right)}, \\ H_{0z}(0) &= ik^2 m_{0z}\sqrt{\frac{2\pi}{kR}}\,e^{i\left(kR - \frac{\pi}{4}\right)}. \end{aligned}\right\} \tag{20.10}$$

Consequently, an electric current filament located above an ideally conducting half-plane excites, at the point P, the field

$$E_z = ik^2 p_z [u(d, \varphi' - \varphi'') - u(d, \varphi' + \varphi'')] \sqrt{\frac{2\pi}{kR}} e^{i\left(kR - \frac{\pi}{4}\right)}, \qquad (20.11)$$

and a magnetic current filament excites, at the point P, the field

$$H_z = ik^2 m_z [u(d, \varphi' - \varphi'') + u(d, \varphi' + \varphi'')] \sqrt{\frac{2\pi}{kR}} e^{i\left(kR - \frac{\pi}{4}\right)}. \qquad (20.12)$$

It is easy to see that the exponent $e^{ik[R - d\cos(\varphi' - \varphi'')]}$ in these expressions corresponds to the primary cylindrical wave arriving at the observation point P, and the exponent $e^{ik[R - d\cos(\varphi' + \varphi'')]}$ corresponds to the reflected cylindrical wave.

The moments m_z and p_z must be selected in such a way that in the direction $\phi'' = \pi$ (Figure 46) the filament would create a field equal to the field of the primary edge wave above an infinite, ideally conducting plane. We will conclude these calculations in the following sections, but for now let us make still one other comment on the formulation of the problem.

In the previous chapters it was shown that the scattering object may be approximated by a series of sources — "luminous" lines and points. Therefore, the problem of secondary diffraction may be formulated as a problem of searching for functions which describe the continuous change of the field of each such source during the passage through the boundary of the light and shadow corresponding to the source.

§ 21. Secondary Diffraction by a Strip (H-Polarization)

A current filament with the moment m_z which is positioned above an ideally conducting plane (h = 0, Figure 46) creates in space the field

$$H_z = ik^2 m_z 2\pi H_0^{(1)}(kR_1). \qquad (21.01)$$

Far from the filament (when $kR_1 >> 1$), this field is described by the asymptotic expression

$$H_z = 4\pi k^2 m_z \frac{e^{i\left(kR_1 + \frac{\pi}{4}\right)}}{\sqrt{2\pi kR_1}}. \qquad (21.02)$$

But the primary edge wave in the direction $\phi'' = \pi$ takes the value

$$H_z = H_{0z}(Q)\, g(Q) \frac{e^{i\left(kR_1 + \frac{\pi}{4}\right)}}{\sqrt{2\pi kR_0}}, \qquad (21.03)$$

where $H_{0z}(Q)$ is the field of the incident plane wave at the point Q; $g(Q)$ is the value of the angular function of the primary cylindrical wave in the direction towards the opposite edge of the strip. Equating Expressions (21.02) and (21.03), we find the filament's moment, the field of which we use to approximate the primary edge wave, in the form

$$m_z = \frac{1}{4\pi k^2} H_{0z}(Q)\, g(Q). \qquad (21.04)$$

As a result, the field created by the filaments located above the half-plane $-a \leq x \leq \infty$ and corresponding to edge 1 (Figure 21) may be represented for region $|\varphi_1| \leq \frac{\pi}{2}$ in the form

$$H_z(1) = H_z^+(1) + H_z^-(1). \qquad (21.05)$$

The function

$$H_z^+(1) = \frac{1}{\pi} H_{0z} g(1) \int_{\pi}^{2\sqrt{ka}\cos\left(\frac{\pi}{4} - \frac{\varphi}{2}\right)} e^{iq^2} dq \frac{e^{ikr}}{\sqrt{2kr}} e^{ika(\sin\alpha - \sin\varphi)} \qquad (21.06)$$

describes the wave radiated by the sources m_{1z}^+, and the function

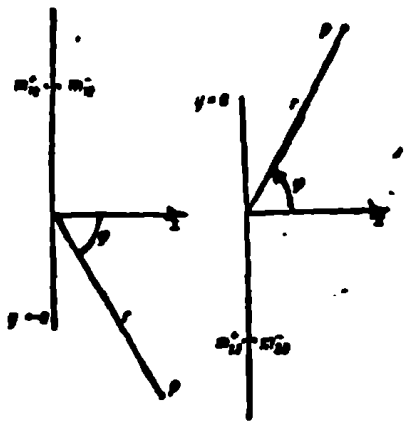

Figure 47. The problem of secondary diffraction by a strip.
m_{1z}^{+} and m_{1z}^{-} are the sources, the fields of which are used when approximating the primary edge wave being propagated from edge 1 (y = a);
m_{2z}^{+} and m_{2z}^{-} are the sources, the fields from which are used when approximating the primary wave from edge 2 (y = -a).

$$H_z^-(1)=\frac{1}{\pi}H_{0z}\bar{g}(1)\times\int_{\infty}^{\sqrt{ka}\cos\left(\frac{\varphi}{2}-\frac{\varphi_0}{2}\right)}e^{iq^2}dq\,\frac{e^{ikr}}{\sqrt{2kr}}e^{ika(\sin\varphi-\sin\varphi_0)}+$$
$$+H_{0z}\bar{g}(1)\frac{e^{i\left(kr+\frac{\pi}{4}\right)}}{\sqrt{2\pi kr}}e^{ika(\sin\varphi-\sin\varphi_0)} \qquad (21.07)$$

describes the wave radiated by the source m_{1z}^{-}. The sum of these waves equals

$$H_z(1)=\frac{2}{\pi}H_{0z}\bar{g}(1)\times\int_{\infty}^{\sqrt{ka}\cos\left(\frac{\varphi}{2}-\frac{\varphi_0}{2}\right)}e^{iq^2}dq\,\frac{e^{ikr}}{\sqrt{2kr}}e^{ika(\sin\varphi-\sin\varphi_0)}+$$
$$+H_{0z}\bar{g}(1)\frac{e^{i\left(kr+\frac{\pi}{4}\right)}}{\sqrt{2\pi kr}}e^{ika(\sin\varphi-\sin\varphi_0)} \qquad (21.08)$$

The first term in this expression is the desired secondary wave from edge 2, and the second term is the field radiated by the filament which is loacted above the ideally conducting plane x = 0 and has the moment

$$m_{0z}^{-}=\frac{1}{4\pi k^2}H_{0z}\bar{g}(1)e^{ika\sin\varphi_0}. \qquad (21.09)$$

where

$$\bar{g}(1)=g(1)\Big|_{\varphi=-\frac{\varphi_0}{2}+\pi}. \qquad (21.10)$$

Summing the secondary wave which has been found with the unperturbed primary wave from edge 1; we obtain

$$H_z(1-2)=$$

$$=H_{0z}\frac{2}{\pi}\bar{g}(1)\times\int_{-\infty}^{2\sqrt{ka}\cos\left(\frac{\pi}{4}-\frac{\varphi}{2}\right)}e^{iq^2}dq\,\frac{e^{ikr}}{\sqrt{2kr}}e^{ika(\sin\alpha-\sin\varphi)}+$$

$$+H_{0z}\bar{g}(1)\frac{e^{i\left(kr+\frac{\pi}{4}\right)}}{\sqrt{2\pi kr}}e^{ika(\sin\alpha-\sin\varphi)}. \qquad (21.11)$$

This expression reduces to zero if one assumes $\phi = -\pi/2$; consequently, the secondary diffraction eliminates the field discontinuities which occurred in the previous approximation when $\phi = -\pi/2$. However, in the direction $\phi = \pi/2$ the field (21.11) is different from zero. Since H_z is an odd function of the x coordinate, the relationship $H_z|_{\varphi=\frac{\pi}{2}-0}\neq 0$ means that the fringing field components H_z and E_ϕ will undergo a discontinuity with a transition through the direction $\phi = \pi/2$. The reason for such a jump, as before, is that in our calculations the plane x = 0 is a plane of currents. By finding the secondary wave from edge 2, we actually considered that the diffraction takes place not on the edge of a finite width strip, but on the edge of an ideally conducting half-plane $-a<y<\infty$.

Again the resulting discontinuity has an order of magnitude of $\frac{1}{\sqrt{ka}\sqrt{kr}}$. It is clear that one may completely eliminate the field discontinuities only with consideration of multiple diffraction. However, the calculation of fields arising with multiple diffraction requires specific consideration of the following terms in order of smallness in the expansion of the primary edge in inverse powers of $\sqrt{kr}$ (see, for example, [46]). All this greatly complicates the calculations. Therefore, we, using the condition ka >> 1, will limit ourselves to an investigation of secondary diffraction, and in order to eliminate the discontinuities in the plane x = 0, we will proceed in the following way.

Let us consider the quantity $\tilde{g}(1)$ in the Expression (21.11) to be a function of the angle ϕ [see Equation (20.05)], that is, let us replace $\tilde{g}(1)$ by the function $g(1)$. In this case the equation

$$H_z(1-2)=$$
$$=H_{01}\cdot\frac{2}{\pi}g(1)\times\int_{-\infty}^{\sqrt{ka}\cos\left(\frac{\pi}{4}-\frac{\varphi}{2}\right)}e^{jq^2}dq\,\frac{e^{jkr}}{\sqrt{2kr}}e^{jka(\sin\theta-\sin\varphi)}+$$
$$+H_{01}g(1)\frac{e^{j\left(kr+\frac{\pi}{4}\right)}}{\sqrt{2\pi kr}}e^{jka(\sin\theta-\sin\varphi)}. \qquad (21.12)$$

will give qualitatively correct results not only when $\varphi\approx-\frac{\pi}{2}$, but also with all other values of ϕ. Actually, the Fresnel integral is close to zero if $\sqrt{ka}\cos\left(\frac{\pi}{4}-\frac{\varphi}{2}\right)\gg1$, and in Equation (21.12) only the second term remains, as must be the case. Therefore, Equation (21.12) may be investigated as an interpolation equation, and it may be applied with any values of $\varphi\left(|\varphi|<\frac{\pi}{2}\right)$. It is easy to establish that now the fringing field does not undergo a discontinuity with the passage through plane x = 0, since Expression (21.12) becomes zero when $\varphi=\pm\frac{\pi}{2}$.

It is interesting to note that Equation (21.12) automatically follows from Equation (21.08) if in the latter equation one replaces $\tilde{g}(1)$ by $g(1)$. Essentially, this substitution is equivalent to the assumption that the moments of the filaments, the fields of which are used for approximating the primary edge waves, depend on the radiation direction (that is, on the azimuth ϕ of the observation point)

$$m_{10}^{-}=-m_{10}^{+}=\frac{1}{4\pi kb^2}H_{01}g(1)e^{jka\sin\theta}. \qquad (21.13)$$

Such a determination of the moments of the auxiliary linear sources is used, for example, in the work of Millar [47].

Precisely in the same way that Equations (21.06) and (21.07) were obtained, we find (when x > 0)

$$H_z^+(2) = \frac{1}{\pi} H_{oz}\bar{g}(2) \int_{\infty}^{2\sqrt{ka}\cos\left(\frac{\varphi}{4}+\frac{\varphi}{2}\right)} e^{iq^2}dq \frac{e^{ikr}}{\sqrt{2kr}} e^{-ika(\sin\alpha-\sin\varphi)}. \tag{21.14}$$

$$H_z^-(2) = \frac{1}{\pi} H_{oz}\bar{g}(2) \int_{\infty}^{2\sqrt{ka}\cos\left(\frac{\varphi}{4}+\frac{\varphi}{2}\right)} e^{iq^2}dq \frac{e^{ikr}}{\sqrt{2kr}} e^{-ika(\sin\alpha-\sin\varphi)} +$$

$$+ H_{oz}\bar{g}(2) \frac{e^{i\left(kr+\frac{\pi}{4}\right)}}{\sqrt{2\pi kr}} e^{-ika(\sin\alpha-\sin\varphi)}. \tag{21.15}$$

These expressions give the field created by the filaments which are located above the ideally conducting half-plane $-\infty \leq y \leq a$ and have the moments

$$m_{oz}^- = -m_{oz}^+ = \frac{1}{4\pi k^2} H_{oz}\bar{g}(2) e^{-ika\sin\alpha}. \tag{21.16}$$

In accordance with Equation (21.04), here

$$\bar{g}(2) = g(2)\Big|_{\varphi=\frac{\pi}{2}-\alpha}. \tag{21.17}$$

Furthermore, summing (21.14) and (21.15), we obtain

$$H_z(2) = H_{oz}\frac{2}{\pi}\bar{g}(2) \int_{\infty}^{2\sqrt{ka}\cos\left(\frac{\varphi}{4}+\frac{\varphi}{2}\right)} e^{iq^2}dq \frac{e^{ikr}}{\sqrt{2kr}} e^{-ika(\sin\alpha-\sin\varphi)} +$$

$$+ H_{oz}\bar{g}(2) \frac{e^{i\left(kr+\frac{\pi}{4}\right)}}{\sqrt{2\pi kr}} e^{-ika(\sin\alpha-\sin\varphi)}. \tag{21.18}$$

Here the first term is the desired secondary wave from edge 1, and the second term is the field radiated by the filament which is located above the ideally conducting plane x = 0 and has the moment m_{2z}^-. Summing the secondary wave which has been found with the unperturbed primary wave from edge 2, we have

$$H_s(2-1)=H_{os}\frac{2}{\pi}\bar{g}(2)\int_{\infty}^{2\sqrt{ka}\cos\left(\frac{\alpha}{4}+\frac{\varphi}{2}\right)}e^{iq^2}dq\,\frac{e^{ikr}}{\sqrt{2kr}}e^{-ika(\sin\alpha-\sin\varphi)}+$$

$$+H_{os}g(2)\frac{e^{i\left(kr+\frac{\pi}{4}\right)}}{\sqrt{2\pi kr}}e^{-ika(\sin\alpha-\sin\varphi)}. \qquad (21.19)$$

It is not difficult to see that the resulting expression becomes zero if one assumes $\varphi=\frac{\pi}{2}$ in it. Consequently, the secondary diffraction eliminates the field discontinuity which we had earlier (§ 6) when $\varphi=\frac{\pi}{2}$, but at the same time it leads to a field discontinuity when $\varphi=-\frac{\pi}{2}$. Again the resulting field discontinuity may be eliminated by the above indicated method, replacing the quantity $\tilde{g}(2)$ by $g(2)$ — that is, by assuming the moments m_{2z}^{-} and m_{2z}^{+} depend on the observation angle ϕ. Actually as a result of such a substitution, we obtain from (21.19) the expression

$$H_s(2-1)=H_{os}\frac{2}{\pi}g(2)\int_{\infty}^{2\sqrt{ka}\cos\left(\frac{\alpha}{4}+\frac{\varphi}{2}\right)}e^{iq^2}dq\,\frac{e^{ikr}}{\sqrt{2kr}}e^{-ika(\sin\alpha-\sin\varphi)}+$$

$$+H_{os}g(2)\frac{e^{i\left(kr+\frac{\pi}{4}\right)}}{\sqrt{2\pi kr}}e^{-ika(\sin\alpha-\sin\varphi)}, \qquad (21.20)$$

which vanishes when $\varphi=\pm\frac{\pi}{2}$. This expression may be investigated as an interpolation equation which describes the field created in the region $|\varphi|<\frac{\pi}{2}$ by the primary wave of edge 2 with consideration of its diffraction at edge 1.

Now summing (21.12) and (21.20), we obtain the following expression for the total field scattered by the strip:

$$H_s=H_{os}\left[G(1,\varphi)g(1)e^{ika(\sin\alpha-\sin\varphi)}+\right.$$

$$\left.+G(2,\varphi)g(2)e^{-ika(\sin\alpha-\sin\varphi)}\right]\frac{e^{i\left(kr+\frac{\pi}{4}\right)}}{\sqrt{2\pi kr}}. \qquad (21.21)$$

Here

$$G(1,\varphi)=\frac{2}{\sqrt{\pi}}e^{-i\frac{\pi}{4}}\times\int_{0}^{2\sqrt{ka}\cos\left(\frac{\pi}{4}-\frac{\varphi}{2}\right)}e^{iq^2}dq \tag{21.22}$$

is the shading function of the primary wave travelling from edge 1, and

$$G(2,\varphi)=\frac{2}{\sqrt{\pi}}e^{-i\frac{\pi}{4}}\times\int_{0}^{2\sqrt{ka}\cos\left(\frac{\pi}{4}+\frac{\varphi}{2}\right)}e^{iq^2}dq \tag{21.23}$$

is the shading function of the primary wave travelling from edge 2. These functions show that the primary wave from edge 1 undergoes the greatest perturbation when $\varphi\approx-\frac{\pi}{2}$, and the wave from edge 2 undergoes the greatest perturbation when $\varphi\approx\frac{\pi}{2}$.

An important property of Equation (21.21) is that it becomes zero when $\varphi=\pm\frac{\pi}{2}$ — that is, the field discontinuity which we had earlier at the plane x = 0 is completely eliminated.

In concluding this section, let us return to Expressions (21.11) and (21.19) which lead to discontinuities of the fringing field in the plane of the strip (x = 0). One may show that the sum of these expressions

$$H_z=H_{oz}\frac{2}{\pi}\frac{e^{ikr}}{\sqrt{2kr}}\left[\bar{g}(1)\int_{\infty}^{2\sqrt{ka}\cos\left(\frac{\pi}{4}-\frac{\varphi}{2}\right)}e^{iq^2}dq\,e^{ika(\sin\alpha-\sin\varphi)}+\right.$$
$$\left.+\bar{g}(2)\int_{\infty}^{2\sqrt{ka}\cos\left(\frac{\pi}{4}+\frac{\varphi}{2}\right)}e^{iq^2}dq\,e^{-ika(\sin\alpha-\sin\varphi)}\right]+$$
$$+H_{oz}\left[g(1)e^{ika(\sin\alpha-\sin\varphi)}+g(2)e^{-ika(\sin\alpha-\sin\varphi)}\right]\frac{e^{i\left(kr+\frac{\pi}{4}\right)}}{\sqrt{2\pi kr}} \tag{21.24}$$

agrees, when $\sqrt{ka}\cos\left(\frac{\pi}{4}\pm\frac{\varphi}{2}\right)>1$, with the asymptotic solution obtained in the book [50] by means of integral equations. The solution found in [50] has the greatest precision when $\alpha\approx 0, \varphi\approx 0$, and it is completely useless if $\alpha\approx\pm\frac{\pi}{2}$ or $\varphi\approx\pm\frac{\pi}{2}$.

§ 22. Secondary Diffraction by a Strip (E-Polarization)

It is known that a current filament with an electric moment p_z which is found at a distance h from an infinite, ideally conducting plane (see Figure 46) creates in space the field

$$E_z = ik^2 p_z \pi [H_0^{(1)}(kR_1) - H_0^{(1)}(kR_2)]. \qquad (22.01)$$

With small values of h (and $R_{1,2} >> kh^2$), this expression is transformed to the form

$$E_z = -i2p_z k^2 h \sin\psi \sqrt{\frac{2\pi}{kR_0}} e^{i\left(kR_0+\frac{\pi}{4}\right)}. \qquad (22.02)$$

The primary edge wave is determined by the relationship

$$E_z = E_{0z}(q) f(q) \frac{e^{i\left(kR_0+\frac{\pi}{4}\right)}}{\sqrt{2\pi kR_0}}, \qquad (22.03)$$

where $E_{0z}(q)$ is the value of the incident plane wave field at the point q ($R_0 = 0$). Consequently, the primary edge wave in the direction $\psi = 0$ may be investigated as the wave from a current filament located above an ideally conducting plane if one assumes the filament moment to be equal to

$$p_z = \frac{i}{4\pi k^2 h} E_{0z}(q) \frac{f(q)}{\sin\psi}\Big|_{\psi=0}. \qquad (22.04)$$

The field, created at the point P by the current filament with a moment p_z which is parallel to the half-plane's edge and passes through the point Q, is determined by Expression (20.11). Expanding

the right-hand member of this expression into a series in terms of the small quantity h($h \to 0$) and limiting ourselves to the first term which is different from zero, we obtain

$$E_0 = ik^2 p_0 \frac{\partial}{\partial h} \left| u(d, \varphi' - \varphi'') - u(d, \varphi' + \varphi'') \right|_{h=0} \sqrt{\frac{2\pi}{kR}} e^{i\left(kR - \frac{\pi}{4}\right)}. \quad (22.05)$$

By means of relationships (22.04) and (22.05), one may show that current filaments with moments p_{1z}^- and p_{1z}^+ which are located on the ideally conducting half-plane $-\infty < y < a$ and correspond to edge 1 (see Figure 47) create in the region $|\varphi| < \frac{\pi}{2}$ the field

$$E_0 = E_{0z} \frac{2}{\pi} \frac{e^{ikr}}{\sqrt{2kr}} \left[\cos\varphi \int_{-\infty}^{2\sqrt{ka}\cos\left(\frac{\pi}{4} - \frac{\varphi}{2}\right)} e^{iq^2} dq + \right.$$
$$\left. + \frac{i}{2\sqrt{ka}} \sin\left(\frac{\pi}{4} - \frac{\varphi}{2}\right) e^{2ika(1+\sin\varphi)} \right] \bar{I}(1) e^{ika(\sin\alpha - \sin\varphi)} +$$
$$+ E_{0z} \bar{I}(1) \cos\varphi \frac{e^{i\left(kr + \frac{\pi}{4}\right)}}{\sqrt{2\pi kr}} e^{ika(\sin\alpha - \sin\varphi)}. \quad (22.06)$$

The current filaments with the moments p_{2z}^- and p_{2z}^+ which are located above the ideally conducting half-plane $-\infty < y < a$ and correspond to edge 2 create in the same region the field

$$E_0 = E_{0z} \frac{1}{\pi} \frac{e^{ikr}}{\sqrt{2kr}} \left[\cos\varphi \int_{-\infty}^{2\sqrt{ka}\cos\left(\frac{\pi}{4} + \frac{\varphi}{2}\right)} e^{iq^2} dq + \right.$$
$$\left. + \frac{i}{2\sqrt{ka}} \sin\left(\frac{\pi}{4} + \frac{\varphi}{2}\right) e^{2ika(1-\sin\varphi)} \right] \bar{I}(2) e^{-ika(\sin\alpha - \sin\varphi)} +$$
$$+ E_{0z} \bar{I}(2) \cos\varphi \frac{e^{i\left(kr + \frac{\pi}{4}\right)}}{\sqrt{2\pi kr}} e^{-ika(\sin\alpha - \sin\varphi)}. \quad (22.07)$$

The first terms in Expressions (22.06) and (22.07) are the desired secondary waves, and the last terms in the expressions are the fields from the current filaments located above the ideally conducting plane x = 0 and having the moments

$$p_{1z}^{-} = \frac{I}{4\pi k^2 b} E_{0z} \cdot \bar{I}(1) e^{-ikb\sin\varphi}, \quad p_{2z}^{-} = \frac{I}{4\pi k^2 b} E_{0z} \cdot \bar{I}(2) e^{-ikb\sin\varphi}, \tag{22.08}$$

where

$$\bar{I}(1) = \frac{I(1)}{\cos\varphi}\Big|_{\varphi=-\frac{\pi}{2}+\varphi}; \quad \bar{I}(2) = \frac{I(2)}{\cos\varphi}\Big|_{\varphi=\frac{\pi}{2}-\varphi}. \tag{22.09}$$

Summing the secondary waves which have been found with the unperturbed primary waves, we obtain the total field scattered by the strip

$$E_z = -H_\varphi = E_{0z}\frac{2}{\pi}\sqrt{\frac{e^{ikr}}{2kr}}\left\{\bar{I}(1)\left[\cos\varphi \times \int_{\infty}^{2\sqrt{kb}\cos\left(\frac{\pi}{4}-\frac{\varphi}{2}\right)} e^{iq^2}dq + \right.\right.$$
$$\left.+\frac{I}{2\sqrt{kb}}\sin\left(\frac{\pi}{4}-\frac{\varphi}{2}\right)e^{2ikb(1+\sin\varphi)}\right] e^{ikb(\sin\theta-\sin\varphi)} +$$
$$+\bar{I}(2)\left[\cos\varphi \times \int_{\infty}^{2\sqrt{kb}\cos\left(\frac{\pi}{4}+\frac{\varphi}{2}\right)} e^{iq^2}dq + \right.$$
$$\left.\left.+\frac{I}{2\sqrt{kb}}\sin\left(\frac{\pi}{4}+\frac{\varphi}{2}\right)e^{2ikb(1-\sin\varphi)}\right] e^{-ikb(\sin\theta-\sin\varphi)}\right\} +$$
$$+E_{0z}\left[I(1)e^{ikb(1+\sin\theta-\sin\varphi)} + I(2)e^{-ikb(\sin\theta-\sin\varphi)}\right]\times$$
$$\times\frac{e^{i\left(kr+\frac{\pi}{4}\right)}}{\sqrt{2\pi kr}}. \tag{22.10}$$

Now assuming, as in the case of the H-polarization, that the moments $p_{1z}^{\pm}$ and $p_{2z}^{\pm}$ depend on the angle ϕ, by replacing

$$\bar{I}(1) \text{ by } \frac{I(1)}{\cos\varphi} \quad \text{and} \quad \bar{I}(2) \text{ by } \frac{I(2)}{\cos\varphi}, \tag{22.11}$$

we obtain

$$E_z = -H_\varphi = E_{0z}\left[F(1,\varphi)I(1)e^{ikb(\sin\theta-\sin\varphi)} + \right.$$
$$\left.+F(2,\varphi)I(2)e^{-ikb(\sin\theta-\sin\varphi)}\right]\frac{e^{i\left(kr+\frac{\pi}{4}\right)}}{\sqrt{2\pi kr}}. \tag{22.12}$$

where

$$\left.\begin{aligned} F(1,\varphi) &= \frac{2}{\varphi+\frac{\pi}{2}} e^{-i\frac{\pi}{4}}\left[\int_0^{2\sqrt{ka}\cos\left(\frac{\pi}{4}-\frac{\varphi}{2}\right)} e^{iq^2}dq + \right. \\ &\left. + \frac{i}{4\sqrt{ka}} \frac{e^{2ika(1+\sin\varphi)}}{\cos\left(\frac{\pi}{4}-\frac{\varphi}{2}\right)}\right], \\ F(2,\varphi) &= \frac{2}{\varphi-\frac{\pi}{2}} e^{-i\frac{\pi}{4}}\left[\int_0^{2\sqrt{ka}\cos\left(\frac{\pi}{4}+\frac{\varphi}{2}\right)} e^{iq^2}dq + \right. \\ &\left. + \frac{i}{4\sqrt{ka}} \frac{e^{2ika(1-\sin\varphi)}}{\cos\left(\frac{\pi}{4}+\frac{\varphi}{2}\right)}\right]. \end{aligned}\right\} \quad (22.13)$$

are the shading functions. They show that the primary wave from edge 1 undergoes the greatest perturbation near $\varphi_* = -\frac{\pi}{2}$, and the wave from edge 2 undergoes the greatest perturbation in the vicinity of $\varphi_* = \frac{\pi}{2}$.

§ 23. The Scattering Characteristics of a Plane Wave by a Strip

Expressions (21.21) and (22.12) which were obtained above for the field scattered by a strip approximately take into account the interaction of the edges and are valid when $|\varphi| < \frac{\pi}{2}$. However, they are not applicable with a glancing incidence of a plane wave on a strip (when $\alpha = \pm\frac{\pi}{2}$).

In order to find equations which are applicable in this case, let us proceed in the following way. Let us write the expressions for the field radiated by the strip in the direction α with the incidence of a plane wave in the direction ϕ (Figure 45)

$$\left.\begin{aligned} E_z &= -H_z = E_{0z}\left[F(2,\alpha) j(1) e^{ika(\sin\alpha-\sin\varphi)} + \right. \\ &\left. + F(1,\alpha) j(2) e^{-ika(\sin\alpha-\sin\varphi)}\right] \frac{e^{i\left(kr+\frac{\pi}{4}\right)}}{\sqrt{2\pi kr}}, \\ H_z &= E_{0z} = H_{0z}\left[G(2,\alpha) g(1) e^{ika(\sin\alpha-\sin\varphi)} + \right. \\ &\left. + G(1,\alpha) g(2) e^{-ika(\sin\alpha-\sin\varphi)}\right] \frac{e^{i\left(kr+\frac{\pi}{4}\right)}}{\sqrt{2\pi kr}}. \end{aligned}\right\} \quad (23.01)$$

Here $|\alpha| < \frac{\pi}{2}$, but ϕ cannot approximate $\pm\pi/2$. Now let us note that the expressions for the fringing field must satisfy the reciprocity principle — that is, they must not change with the simultaneous replacement of α by ϕ and ϕ by α. Comparing Equations (21.21), (20.12) and (23.01), it is not difficult to obtain the expressions

$$\left.\begin{aligned} E_z = -H_\varphi = E_{0z}[F(1,\varphi)F(2,\alpha)f(1)e^{ika(\sin\alpha-\sin\alpha)} + \\ + F(2,\varphi)F(1,\alpha)f(2)e^{-ika(\sin\alpha-\sin\varphi)}]\frac{e^{i\left(kr+\frac{\pi}{4}\right)}}{\sqrt{2\pi kr}}, \\ H_z = E_\varphi = H_{0z}[G(1,\varphi)G(2,\alpha)g(1)e^{ika(\sin\alpha-\sin\varphi)} + \\ + G(2,\varphi)G(1,\alpha)g(2)e^{-ika(\sin\alpha-\sin\varphi)}]\frac{e^{i\left(kr+\frac{\pi}{4}\right)}}{\sqrt{2\pi kr}}, \end{aligned}\right\} \quad (23.02)$$

which satisfy the reciprocity principle, have no discontinuities anywhere, and are suitable for making calculations with any values of α and φ $\left(|\alpha| \leq \frac{\pi}{2},\ |\varphi| < \frac{\pi}{2}\right)$. From the second equation of (23.02), it follows that $H_z = E_\phi = 0$ when $\varphi = \pm\frac{\pi}{2}$ — that is, the fringing field does not experience discontinuities in the plane $x = 0$. Moreover, $H_z = E_\phi = 0$ with any values of ϕ if $\alpha = \pm\frac{\pi}{2}$ — that is, a plane wave polarized perpendicularly to the strip does not undergo diffraction with a glancing incidence.

The resulting Equations (23.02) may be investigated as interpolation equations. Actually, with $|\alpha| < \frac{\pi}{2}$ when $\sqrt{ka}\cos\left(\frac{\alpha}{4} \pm \frac{\alpha}{2}\right) \gg 1$ the functions $F(1, \alpha)$, $F(2, \alpha)$, $G(1, \alpha)$ and G (2, α) are close to one, and Equations (23.02) change into the previous Expressions (21.21) and (22.12). But if $|\varphi| \ll \frac{\pi}{2}$ and $\sqrt{ka}\cos\left(\frac{\varphi}{4} \pm \frac{\varphi}{2}\right) \gg 1$, then the functions $F(1, \varphi)$, $F(2, \varphi)$, G (1, ϕ) and G (2, ϕ) are close to one, and Equations (23.02) change into Equations (23.01). Let us recall that the functions F and G are determined by relationships (21.22), (21.23) and (22.13).

In the direction of the principal maximum of the scattering diagram ($\phi = \alpha$), Equations (23.02) take the following form:

$$\left.\begin{aligned} H_z &= H_{0z}\left[\left(2ika\cos\alpha+\frac{1}{\cos\alpha}\right)G(1,\alpha)\,G(2,\alpha)+\right.\\ &\left.+G(1,\alpha)\frac{\partial G(2,\alpha)}{\partial\alpha}-G(2,\alpha)\frac{\partial G(1,\alpha)}{\partial\alpha}\right]\frac{e^{i\left(kr+\frac{\pi}{4}\right)}}{\sqrt{2\pi kr}},\\ E_z &= E_{0z}\left[\left(2ika\cos\alpha+\frac{1}{\cos\alpha}\right)F(1,\alpha)F(2,\alpha)+\right.\\ &\left.+F(1,\alpha)\frac{\partial F(2,\alpha)}{\partial\alpha}-F(2,\alpha)\frac{\partial F(1,\alpha)}{\partial\alpha}\right]\frac{e^{i\left(kr+\frac{\pi}{4}\right)}}{\sqrt{2\pi kr}}. \end{aligned}\right\} \qquad (23.03)$$

Hence when $\alpha=\pm\frac{\pi}{2}$ we have

$$H_z=0,$$

$$E_z=E_{0z}\left(\frac{2}{\pi}\right)^{\frac{3}{2}}e^{i\frac{3\pi}{4}}\left[\pi\sqrt{ka}\left(\int_0^{2\sqrt{ka}}e^{iq^2}dq+\frac{i}{4\sqrt{ka}}e^{ika}\right)+\right.$$

$$\left.+\frac{i^2}{3\sqrt{ka}}\int_0^{2\sqrt{ka}}e^{iq^2}dq\right]\frac{e^{ikr}}{\sqrt{kr}}. \qquad (23.04)$$

It is interesting to observe that Expressions (23.02) to some extent take into account, in addition to secondary diffraction, also tertiary diffraction. Actually, for the values $|\alpha|\leqslant\frac{\pi}{2}$ and $|\varphi|\leqslant\frac{\pi}{2}$, we have

$$G(1,\varphi)\,G(2,\alpha)\,e^{ika(\sin\alpha-\sin\varphi)}\approx e^{ika(\sin\alpha-\sin\varphi)}-$$

$$-\frac{e^{ika(2+\sin\alpha+\sin\varphi)}}{2\sqrt{\pi ka}\cos\left(\frac{\pi}{4}-\frac{\varphi}{2}\right)}e^{i\frac{\pi}{4}}-\frac{e^{ika(2-\sin\alpha-\sin\varphi)}}{2\sqrt{\pi ka}\cos\left(\frac{\pi}{4}+\frac{\alpha}{2}\right)}e^{i\frac{\pi}{4}}+$$

$$+\frac{i}{4\pi ka}\frac{e^{ika(4-\sin\alpha+\sin\varphi)}}{\cos\left(\frac{\pi}{4}-\frac{\varphi}{2}\right)\cos\left(\frac{\pi}{4}+\frac{\alpha}{2}\right)}. \qquad (23.05)$$

The physical meaning of the four terms in the right-hand member of this equation is illustrated in Figure 48 (Figure 48a corresponds to the first term; Figure 48b corresponds to the second term, etc.).

Taking into account condition (6.15), one may write the equations for the fringing field in the left half-space ($\frac{\pi}{2}\leqslant|\varphi|\leqslant\pi$ but $|\alpha|\leqslant\frac{\pi}{2}$) in the same form as (23.02). Thus, the functions $G(1,\alpha)$, $G(2,\alpha)$ and

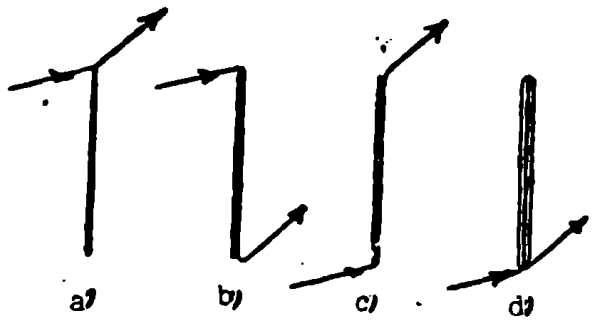

Figure 48. The schematic diagram of the waves corresponding to the various terms in Equation (22.05).

$F(1, a)$, $F(2, a)$ will, as before, be described by the relationships (21.22), (21.23) and (22.13). The remaining functions in Equations (22.02) will be determined when $\frac{\pi}{2} < |\varphi| < \pi$ by the following equations:

$$\left.\begin{aligned} G(1, \varphi) &= \frac{2}{\sqrt{\pi}} e^{-i\frac{\pi}{4}} \cdot \int_0^{\pm 2\sqrt{ka}\sin\left(\frac{\pi}{4}+\frac{\varphi}{2}\right)} e^{iq^2} dq, \\ G(2, \varphi) &= \frac{2}{\sqrt{\pi}} e^{-i\frac{\pi}{4}} \cdot \int_0^{-2\sqrt{ka}\sin\left(\frac{\pi}{4}-\frac{\varphi}{2}\right)} e^{iq^2} dq, \end{aligned}\right\} \qquad (23.06)$$

$$\left.\begin{aligned} F(1, \varphi) &= \frac{2}{\sqrt{\pi}} e^{-i\frac{\pi}{4}} \left[\int_0^{\pm 2\sqrt{ka}\sin\left(\frac{\pi}{4}+\frac{\varphi}{2}\right)} e^{iq^2} dq \mp \right. \\ &\quad \left. \mp \frac{i}{4\sqrt{ka}} \frac{e^{2ika(1+\sin\varphi)}}{\sin\left(\frac{\pi}{4}+\frac{\varphi}{2}\right)} \right], \\ F(2, \varphi) &= \frac{2}{\sqrt{\pi}} e^{-i\frac{\pi}{4}} \left[\int_0^{-2\sqrt{ka}\sin\left(\frac{\pi}{4}-\frac{\varphi}{2}\right)} e^{iq^2} dq \mp \right. \\ &\quad \left. \mp \frac{i}{4\sqrt{ka}} \frac{e^{2ika(1-\sin\varphi)}}{\sin\left(\frac{\pi}{4}-\frac{\varphi}{2}\right)} \right], \end{aligned}\right\} \qquad (23.07)$$

$$g(1) = \frac{\cos^2\frac{\varphi}{2} + \sin^2\frac{\varphi}{2}}{\sin\alpha - \sin\varphi}, \quad g(2) = \frac{\cos^2\frac{\varphi}{2} - \sin^2\frac{\varphi}{2}}{\sin\alpha - \sin\varphi}. \tag{7.08}$$

$$f(1) = g(2), \quad f(2) = g(1). \tag{7.09}$$

The upper sign in Expressions (7.06) – (7.09) must be taken when $\frac{\pi}{2} < \varphi < \pi$, and the lower sign must be taken when $-\pi < \varphi < -\frac{\pi}{2}$.

Assuming $\varphi = -\pi + \alpha$ (with $0 < \alpha < \frac{\pi}{2}$) in Equations (7.07) and (7.06) – (7.09), let us find the field radiated by the strip in the direction toward the source

$$\left.\begin{aligned} H_\theta &= H_{0\theta}[G^0(2, \alpha)g(1)e^{i2ka\sin\alpha} + \\ &+ G^0(1, \alpha)g(2)e^{-i2ka\sin\alpha}]e^{i\left(kr+\frac{\pi}{4}\right)}\sqrt{2\pi kr}, \\ E_\theta &= E_{0\theta}[F^0(2, \alpha)f(1)e^{i2ka\sin\alpha} + \\ &+ F^0(1, \alpha)f(2)e^{-i2ka\sin\alpha}]e^{i\left(kr+\frac{\pi}{4}\right)}\sqrt{2\pi kr}. \end{aligned}\right| \tag{7.10}$$

where

$$g(1) = f(2) = -\frac{1+\sin\alpha}{2\sin\alpha}, \quad g(2) = f(1) = -\frac{1}{2\sin\alpha}. \tag{7.11}$$

When $\alpha = 0$, we have

$$\left.\begin{aligned} H_\theta &= -H_{0\theta}\left[(2ka+1)G(1, 0) - 2\sqrt{\frac{2ka}{\pi}}e^{i\left(2ka+\frac{\pi}{4}\right)}\right]\times \\ &\times G(1, 0)e^{i\left(kr+\frac{\pi}{4}\right)}\sqrt{2\pi kr}, \\ E_\theta &= E_{0\theta}\left[(2ka+1)F(1, 0) + \sqrt{\frac{1}{2\pi ka}}e^{i\left(2ka+\frac{\pi}{4}\right)}\right]\times \\ &\times F(1, 0)e^{i\left(kr+\frac{\pi}{4}\right)}\sqrt{2\pi kr}. \end{aligned}\right| \tag{7.12}$$

Calculations of the scattering characteristics were carried out based on the equations derived above. These scattering characteristics are the functions $h(\alpha, \phi)$ and $e(\alpha, \phi)$ determining the fringing field by means of the relationships

$$\left.\begin{aligned} E_s &= E_{0s} ka e(\alpha, \varphi) \sqrt{\frac{2}{\pi kr}} e^{i\left(kr+\frac{3\pi}{4}\right)}, \\ H_s &= H_{0s} ka h(\alpha, \varphi) \sqrt{\frac{2}{\pi kr}} e^{i\left(kr+\frac{3\pi}{4}\right)}. \end{aligned}\right\} \qquad (23.13)$$

The calculations were performed for the values $ka=\sqrt{28}$ and $ka=\sqrt{80}$. In Figures 49 - 62, the following designations were used: 1) the functions h and e correspond to the rigorous theory; 2) the functions h_0 and e_0 correspond to the field from the uniform part of the current (the physical optics approach); 3) the functions h_1 and e_1 correspond to the field from the uniform and nonuniform parts of the current, but without consideration of the interaction of the edges; 4) the functions h_2 and e_2 correspond to the fringing field with consideration of secondary diffraction calculated on the basis of equations (23.13), (23.02) and (23.10). Thus, in accordance with § 6,

$$\left.\begin{aligned} e_0 &= \cos\alpha \frac{\sin[ka(\sin\alpha-\sin\varphi)]}{ka(\sin\alpha-\sin\varphi)}, \\ h_0 &= \cos\varphi \frac{\sin[ka(\sin\alpha-\sin\varphi)]}{ka(\sin\alpha-\sin\varphi)} \end{aligned}\right\} \qquad (23.14)$$

and

$$\left.\begin{matrix} e_1 \\ h_1 \end{matrix}\right\} = \frac{1}{2ka}\left\{\frac{\sin[ka(\sin\alpha-\sin\varphi)]}{\sin\frac{\alpha-\varphi}{2}} \mp i\frac{\cos[ka(\sin\alpha-\sin\varphi)]}{\cos\frac{\alpha+\varphi}{2}}\right\}. \qquad (23.15)$$

where $|\alpha|<\frac{\pi}{2}$, $|\varphi|<\frac{\pi}{2}$.

The results obtained show that our approximation equations agree satisfactorily with the rigorous theory already when $ka=\sqrt{28}$, although in the given case approximately one and one-half wavelengths are fitted into the width of the strip. In the direction toward the source $\left(\varphi=-\pi+\alpha,\ 0<\alpha<\frac{\pi}{2}\right)$, and also with glancing irradiation of the

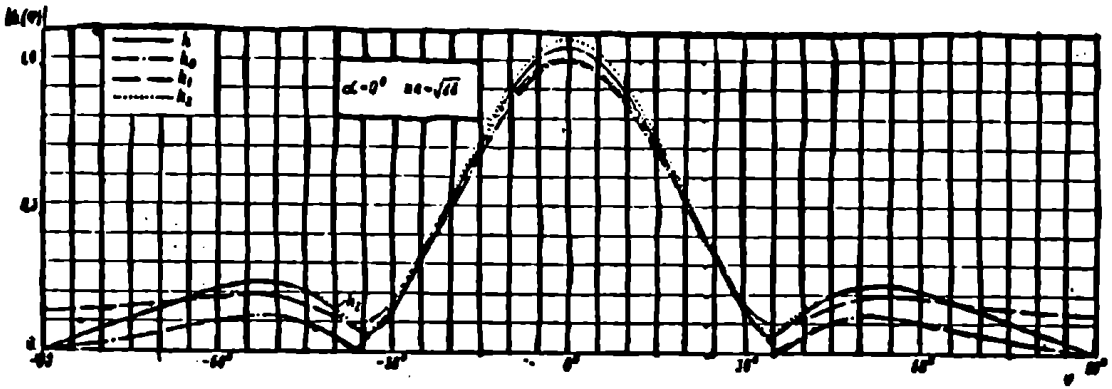

Figure 49. The scattering diagram of a field by a strip as a function of the incident angle of a plane wave (a) and the parameter $\sqrt{ka}$. The various curves correspond to various approximations.

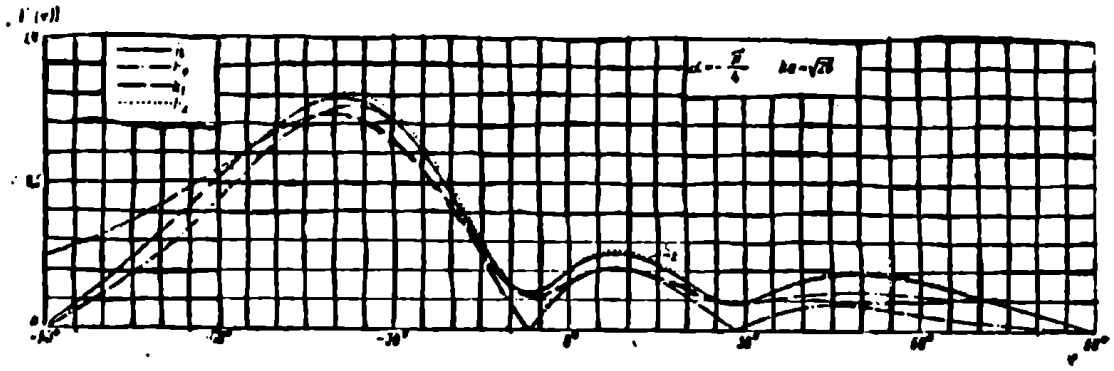

Figure 50. The same as Figure 49 with $\alpha = -\frac{\pi}{4}$.

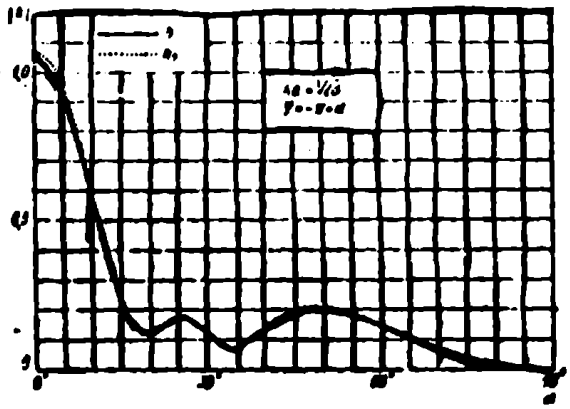

Figure 51. The same as Figure 49 when $\phi = -\pi + \alpha$.

strip ($\alpha = -\pi/2$), when the functions e_0 and h_0, and e_1 and h_1 lead to qualitatively incorrect results, the functions e_2 and h_2 give, as in the remaining cases, fully satisfactory results. Actually, the curve $|h_2|$ coincides almost everywhere with the curve $|h|$ (Figure 49-54) within the limits of graphical precision. But the calculated values of the function $|e_2|$ differ from the corresponding values of the function $|e|$ only by hundredths of a percent (Figure 55 - 62). The better agreement with the rigorous theory associated with the E-polarization is explained by the weaker interaction of the edges in this case. A certain discrepancy of the curves $|h_2|$ and $|h|$ in the vicinity of the principal scattering maximum is explained by the interpolation character of our equations.

As a consequence of the interpolation character of Equations (23.02), the integral scattering diameter obtained from Expressions (23.03) when $\alpha = 0$ does not coincide with the integral diameter found by Clemmow [46] in the form of the first terms of an asymptotic expansion in inverse powers of $\sqrt{ka}$. However, our equations, as distinct from the similar equations obtained by other authors, allow one to calculate the scattering characteristics with any incident angles of the plane wave.

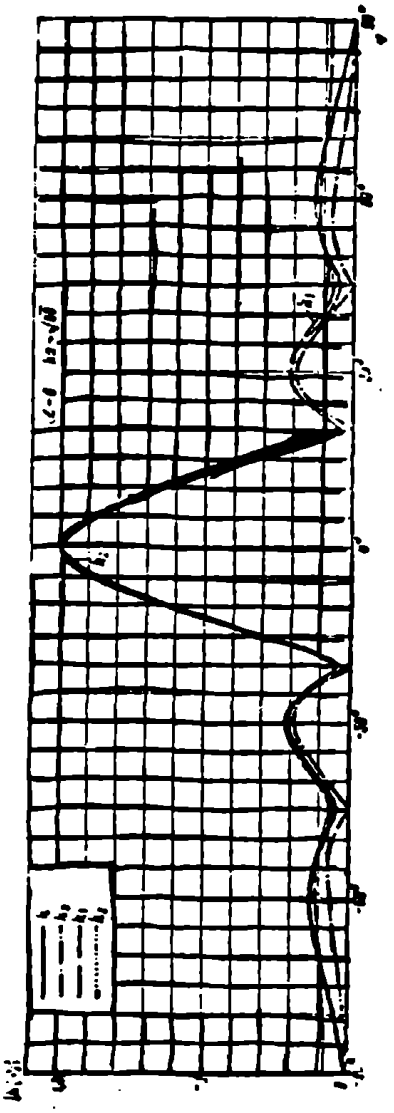

Figure 52. The function h (α, φ) for a strip (α = 0, ka = $\sqrt{80}$).

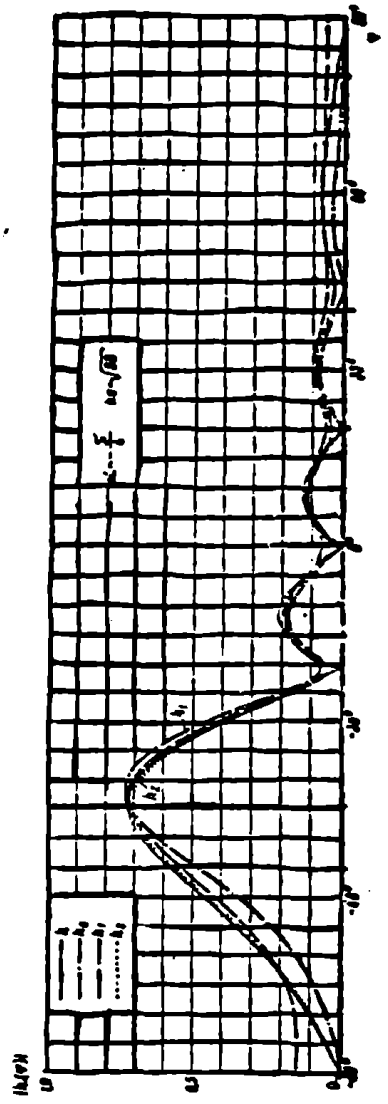

Figure 53. The same as Figure 52 when $\alpha = -\frac{\pi}{4}$.

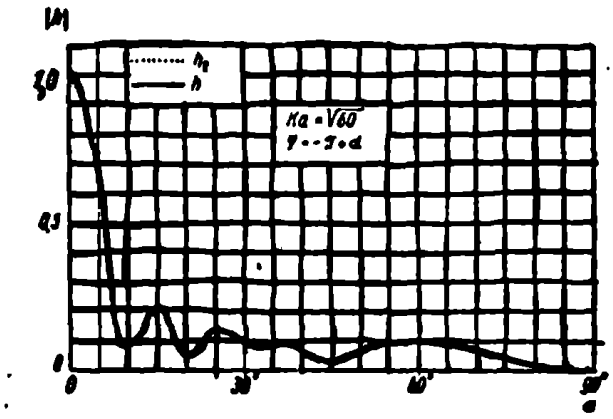

Figure 54. The same as Figure 52 when $\phi = -\pi + \alpha$.

Let us note that the functions $e(\alpha, \phi)$ and $h(\alpha, \phi)$ for Figures 49 - 52 were calculated on the basis of rigorous series which were obtained by the separation of variables in the elliptic coordinate system (compare [23])(1).

§ 24. Secondary Diffraction by a Disk

Let us refine the approximate solution of the diffraction problem for a disk which was found in Chapter II.

Let an infinitely thin, ideally conducting disk of radius a be found in free space. Let us orientate the spherical coordinate system in such a way that the normal n to the incident wave front would lie in the half-plane $\phi = \pi/2$, and form an angle $\gamma \left(0 \leq \gamma \leq \frac{\pi}{2}\right)$ with the z axis (Figure 63). Let us prescribe the incident plane wave field in

$$\mathbf{E} = \mathbf{E}_0 e^{ik(y \sin\gamma + z\cos\gamma)}, \quad \mathbf{H} = \mathbf{H}_0 e^{ik(y\sin\gamma + z\cos\gamma)}. \tag{24.01}$$

(1)Footnote appears on page 162.

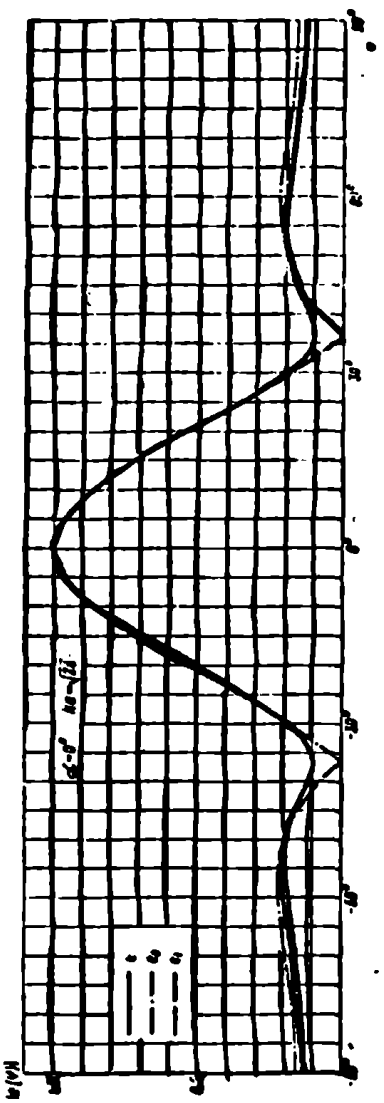

Figure 55. The function $e(\alpha, \phi)$ for a strip ($\alpha = 0$, $ka = \sqrt{28}$).

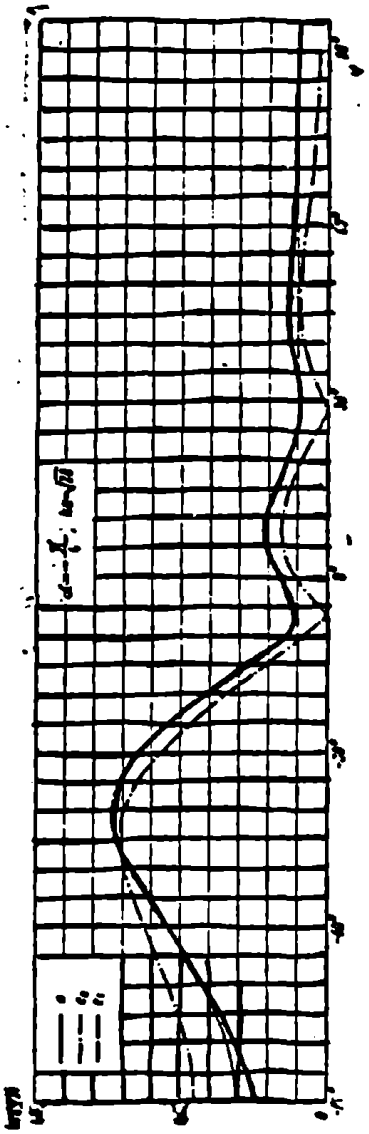

Figure 56. The same as Figure 55 when $\alpha = -\frac{\pi}{4}$.

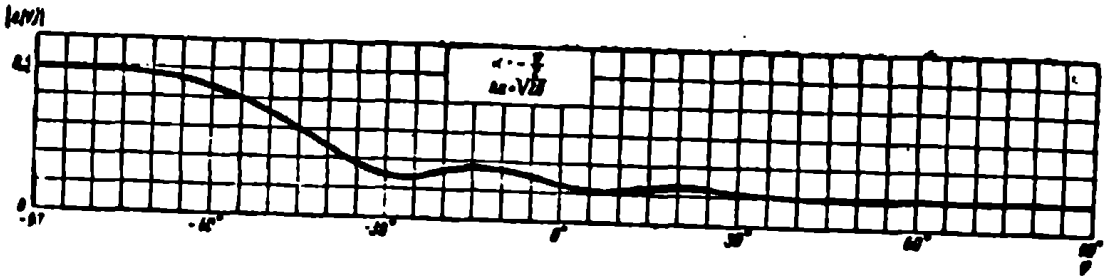

Figure 57. The same as Figure 55 when $\alpha = -\frac{\pi}{2}$.

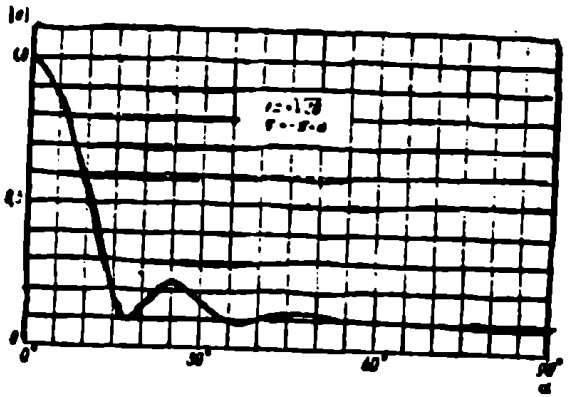

Figure 58. The same as Figure 55 when $\phi = -\pi + \alpha$.

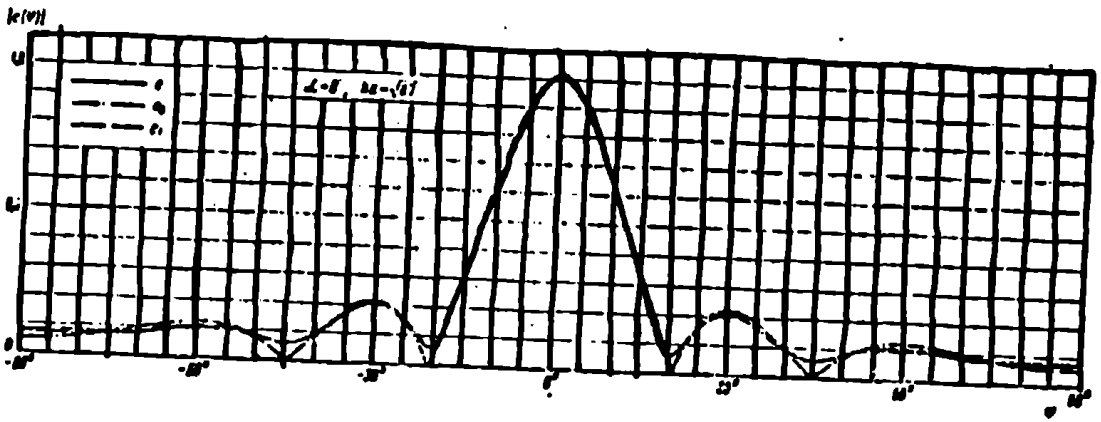

Figure 59. The function $e(\alpha, \phi)$ for a strip ($\alpha + 0$, $ka = \sqrt{80}$). The electric vector is parallel to the strip's edge.

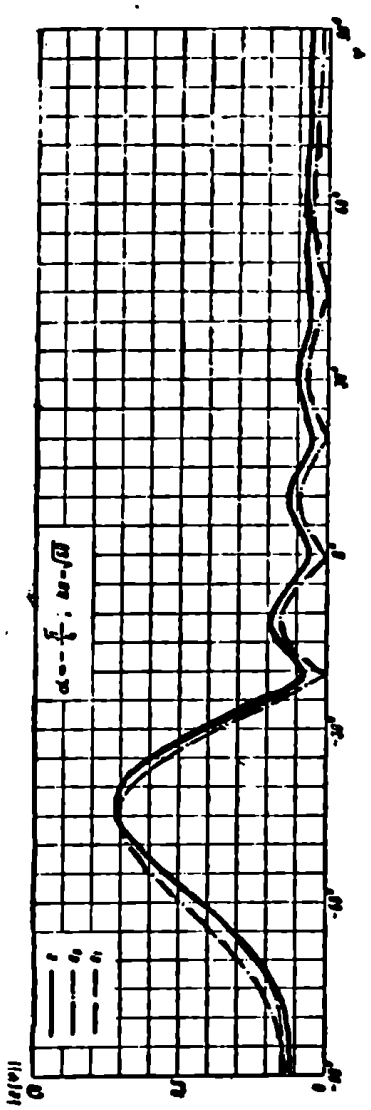

Figure 60. The same as Figure 59 when $\alpha = -\frac{\pi}{4}$.

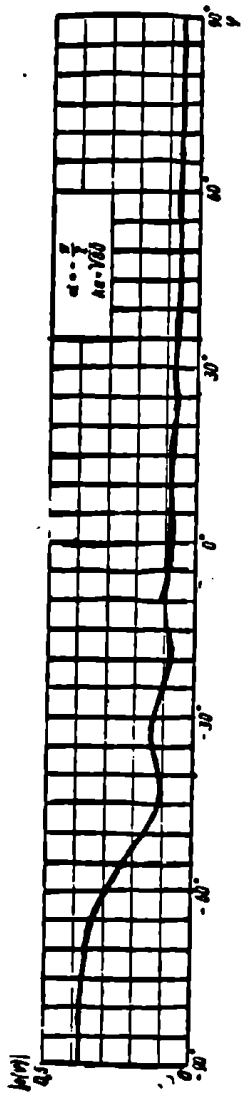

Figure 61. The same as Figure 59 when $\alpha = -\frac{\pi}{2}$.

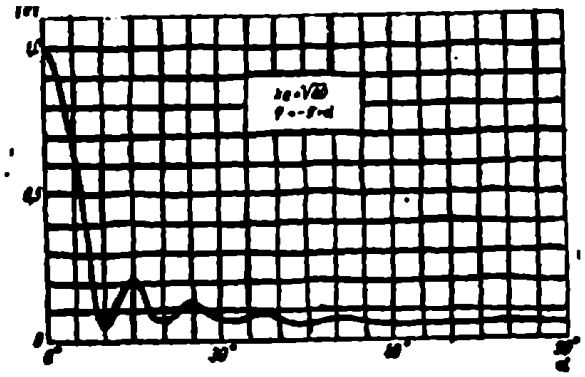

Figure 62. The same as Figure 59 when $\phi = -\pi + \alpha$.

In accordance with § 12, the fringing field in the plane $\phi = \pm\pi/2$ is described (when $R >> ka^2$) by the equations

$$\left.\begin{aligned} E_\gamma = -H_\theta &= \frac{iaE_{0z}}{2}\left\{[f(2,\delta) - f(1,\delta)]J_1(\zeta) + \right. \\ &\left. + i[f(2,\delta) + f(1,\delta)]J_0(\zeta)\right\}\frac{e^{ikR}}{R}, \\ H_\gamma = E_\theta &= \frac{iaH_{0z}}{2}\left\{[g(2,\delta) - g(1,\delta)]J_1(\zeta) + \right. \\ &\left. + i[g(2,\delta) + g(1,\delta)]J_0(\zeta)\right\}\frac{e^{ikR}}{R}. \end{aligned}\right\} \qquad (24.02)$$

These expressions are valid when $\theta < \frac{\pi}{2}$ and $\gamma < \frac{\pi}{2}$. The quantities included in them are determined by the relationships:

$$\left.\begin{aligned} f(1,\delta) &= \frac{\cos\frac{\delta+\theta}{2} - \sin\frac{\delta-\theta}{2}}{\sin\delta - \sin\theta}, \\ f(2,\delta) &= -\frac{\cos\frac{\delta+\theta}{2} + \sin\frac{\delta-\theta}{2}}{\sin\delta - \sin\theta}, \\ g(1,\delta) &= -f(2,\delta), \quad g(2,\delta) = -f(1,\delta), \end{aligned}\right\} \qquad (24.03)$$

$$\zeta = ka(\sin\theta - \sin\delta), \qquad (24.04)$$

$$\delta=\begin{cases}\gamma \text{ with } \varphi=\frac{\pi}{2}\\ -\gamma \text{ with } \varphi=-\frac{\pi}{2}.\end{cases} \tag{24.05}$$

Let us note that here

$$\left.\begin{aligned} f(1,\delta)&=\begin{cases}f(1) \text{ with } \varphi=\frac{\pi}{2}\\ f(2) \text{ with } \varphi=-\frac{\pi}{2},\end{cases}\\ f(2,\delta)&=\begin{cases}f(2) \text{ with } \varphi=\frac{\pi}{2}\\ f(1) \text{ with } \varphi=-\frac{\pi}{2},\end{cases}\\ g(1,\delta)&=\begin{cases}g(1) \text{ with } \varphi=\frac{\pi}{2}\\ g(2) \text{ with } \varphi=-\frac{\pi}{2},\end{cases}\\ g(2,\delta)&=\begin{cases}g(2) \text{ with } \varphi=\frac{\pi}{2}\\ g(1) \text{ with } \varphi=-\frac{\pi}{2},\end{cases}\end{aligned}\right\} \tag{24.06}$$

and the functions f(1), f(2), g(1) and g(2) are determined by the Equations (12.03) and (12.04).

When $\zeta \gg 1$, Expressions (24.02) take the form

$$\left.\begin{aligned} E_\varphi=-H_\theta&=\frac{ia E_{0\varphi}}{\sqrt{2\pi\zeta}}\left[f(2,\delta)e^{i\left(\zeta-\frac{3\pi}{4}\right)}-\right.\\ &\left.-f(1,\delta)e^{-i\left(\zeta-\frac{3\pi}{4}\right)}\right]\frac{e^{ikR}}{R},\\ H_\varphi=E_\theta&=\frac{ia H_{0\varphi}}{\sqrt{2\pi\zeta}}\left[g(2,\delta)e^{i\left(\zeta-\frac{3\pi}{4}\right)}-\right.\\ &\left.-g(1,\delta)e^{-i\left(\zeta-\frac{3\pi}{4}\right)}\right]\frac{e^{ikR}}{R}.\end{aligned}\right\} \tag{24.07}$$

They show that the fringing field in this region may be investigated as the sum of spherical waves from two luminous points on the rim of the disk with the polar angle $\psi = \pm\pi/2$. The diffraction by a disk of each of these waves may be studied as was done in the case of a strip, but we shall proceed differently.

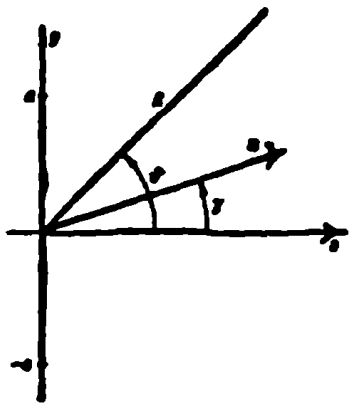

Figure 63. The cross section of a disk with the plane yOz; n is the normal to the incident wave front.

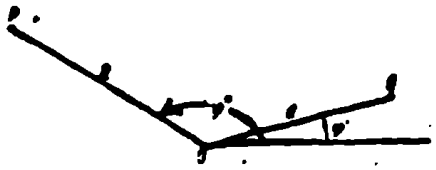

Figure 64. Excitation of a half-plane by an elementary dipole which is located at the point Q.

Let us compare the shading of spherical and cylindrical waves by a half-plane. Let an ideally conducting half-plane be found in free space, and let there be an elementary dipole at the point Q (Figure 64). Let us find the field in the plane perpendicular to the half-plane's edge and passing through the point Q.

In accordance with the reciprocity principle, it is determined for the electric dipole by the relationship

$$E_z = \frac{p_z}{p_{0z}} E_z(Q), \tag{24.08}$$

and for the magnetic dipole by the relationship

$$H_z = \frac{m_z}{m_{0z}} H_z(Q). \tag{24.09}$$

Here $p_z(m_z)$ is the electric (magnetic) dipole moment found at the point Q; p_{oz} and m_{oz} are the moments of the auxiliary dipoles which are placed at the point P; $E_z(Q)$ and $H_z(Q)$ are the fields created by the auxiliary dipoles at the point Q.

Now let us remove the auxiliary dipoles to such a distance that the spherical wave arriving from them may be considered to be a plane wave on the section from the half-plane's edge to the point Q. In this case, in accordance with Equation (20.08), the field created by the wave at the point Q will equal

$$\left.\begin{aligned} E_z(Q) &= E_{0z}(0)[u(d, \varphi' - \varphi'') - u(d, \varphi' + \varphi'')], \\ H_z(Q) &= H_{0z}(0)[u(d, \varphi' - \varphi'') + u(d, \varphi' + \varphi'')]. \end{aligned}\right\} \tag{24.10}$$

The expressions

$$E_{0z}(0) = k^2 p_{0z} \frac{e^{ikR}}{R}, \quad H_{0z}(0) = k^2 m_{0z} \frac{e^{ikR}}{R} \tag{24.11}$$

determine the fields created by the auxiliary dipoles in free space (with the absence of the half-plane) at the point 0.

Consequently, the fields excited at the point P by the electric and magnetic dipoles which are found at the point Q above the half-plane equal respectively

$$\left.\begin{aligned} E_z &= k^2 p_z [u(d, \varphi' - \varphi'') - u(d, \varphi' + \varphi'')] \frac{e^{ikR}}{R}, \\ H_z &= k^2 m_z [u(d, \varphi' - \varphi'') + u(d, \varphi' + \varphi'')] \frac{e^{ikR}}{R}. \end{aligned}\right\} \tag{24.12}$$

With the absence of the half-plane, these dipoles create at the point P the field

$$\left.\begin{aligned} E_z &= k^2 p_z \frac{e^{ikR}}{R} e^{-ikd\cos(\varphi' - \varphi'')}, \\ H_z &= k^2 m_z \frac{e^{ikR}}{R} e^{-ikd\cos(\varphi' - \varphi'')}. \end{aligned}\right\} \tag{24.13}$$

Comparing Expressions (24.12) and (24.13) we find the shading functions

$$\left.\begin{aligned} \bar{F} &= [u(d, \varphi' - \varphi'') - u(d, \varphi' + \varphi'')] e^{ikd\cos(\varphi' - \varphi'')}, \\ \bar{G} &= [u(d, \varphi' - \varphi'') + u(d, \varphi' + \varphi'')] e^{ikd\cos(\varphi' - \varphi'')}. \end{aligned}\right\} \tag{24.14}$$

In the case when the current filament passes through the point Q parallel to the half-plane's edge, the field at the point P is determined — in accordance with (20.11) and (20.12) — by the equations

$$\left.\begin{aligned} E_z &= ik^2 p_z [u(d, \varphi' - \varphi'') - u(d, \varphi' + \varphi'')] \sqrt{\frac{2\pi}{kR}} e^{i\left(kR - \frac{\pi}{4}\right)}, \\ H_z &= ik^2 m_z [u(d, \varphi' - \varphi'') + u(d, \varphi' + \varphi'')] \sqrt{\frac{2\pi}{kR}} e^{i\left(kR - \frac{\pi}{4}\right)}. \end{aligned}\right\} \qquad (24.15)$$

With the absence of a half-plane, these sources create at the point P the field

$$\left.\begin{aligned} E_z &= ik^2 p_z \sqrt{\frac{2\pi}{kR}} e^{i\left(kR - \frac{\pi}{4}\right)} e^{-ikd\cos(\varphi' - \varphi'')}, \\ H_z &= ik^2 m_z \sqrt{\frac{2\pi}{kR}} e^{i\left(kR - \frac{\pi}{4}\right)} e^{-ikd\cos(\varphi' - \varphi'')}. \end{aligned}\right\} \qquad (24.16)$$

Comparing Equations (24.15) and (24.16), we obtain the same Expressions (24.14) for the shading functions. Consequently, a spherical wave in the direction perpendicular to an ideally conducting half-plane is shaded by it the same as a cylindrical wave.

Let us note, however, that Expressions (24.14) are not equivalent to Expressions (21.22), (21.23) and (22.13), since the first represent the shading function by a half-plane of a wave from a single source, and the latter represent the shading function of an edge wave which we approximate by waves from two sources located on both sides of the corresponding half-plane. Since the shading functions of spherical and cylindrical waves are the same, the edge wave shading functions of a strip and a disk also will coincide.

Therefore, the approximation expressions for a field scattered by a disk which take account of secondary diffraction may be represented in the region $\varphi = \pm\frac{\pi}{2}$, $0 < \vartheta < \frac{\pi}{2}$ (with $\zeta >> 1$) in the following form:

$$
\left.
\begin{aligned}
E_\varphi = -H_\theta &= \frac{i\omega F_\infty}{4\pi s}\left[F(2,\theta)f(2,\delta)e^{i\left(\zeta-\frac{3\pi}{4}\right)}-\right.\\
&\left.-F(1,\theta)f(1,\delta)e^{-i\left(\zeta-\frac{3\pi}{4}\right)}\right]\frac{e^{i\omega R}}{R},\\
H_\varphi = E_\theta &= \frac{i\omega H_\infty}{4\pi s}\left[G(2,\theta)g(2,\delta)e^{i\left(\zeta-\frac{3\pi}{4}\right)}-\right.\\
&\left.-G(1,\theta)g(1,\delta)e^{-i\left(\zeta-\frac{3\pi}{4}\right)}\right]\frac{e^{i\omega R}}{R}.
\end{aligned}
\right\} \qquad (24,17)
$$

where the functions F and G are obtained from Equations (21,23), (21,28) and (22,13) by the replacement of φ by θ. Equations (24,17) may be investigated as the asymptotic representation (with $\zeta \gg 1$) of the following expressions:

$$
\begin{aligned}
E_\varphi = -H_\theta &= \frac{i\omega F_\infty}{2}\left\{[F(2,\theta)f(2,\delta) - F(1,\theta)f(1,\delta)]J_0(\zeta)+\right.\\
&\left.+i[F(2,\theta)f(2,\delta)+F(1,\theta)f(1,\delta)]J_1(\zeta)\right\}\frac{e^{i\omega R}}{R},\\
H_\varphi = E_\theta &= \frac{i\omega H_\infty}{2}\left\{[G(2,\theta)g(2,\delta) - G(1,\theta)g(1,\delta)]J_0(\zeta)+\right.\\
&\left.+i[G(2,\theta)g(2,\delta)+G(1,\theta)g(1,\delta)]J_1(\zeta)\right\}\frac{e^{i\omega R}}{R}.
\end{aligned}
\qquad (24,18)
$$

These expressions hold in the region $\theta \leq \frac{\pi}{2}$ for the values $\delta = \frac{\pi}{2}$ and $\gamma \leq \frac{\pi}{2}$. Using Equation (24,18), let us write the expressions for the field radiated by a disk in the direction γ when a plane wave is incident on it (from left to right) at an angle δ

$$
\left.
\begin{aligned}
E_\varphi = -H_\theta &= \frac{i\omega F_\infty}{2}\left\{[F(2,\delta)f(1,\delta)\right.\\
&\left.-F(1,\delta)f(2,\delta)]J_0(\zeta)+i[F(2,\delta)f(1,\delta)+\right.\\
&\left.+F(1,\delta)f(2,\delta)]J_1(\zeta)\right\}\frac{e^{i\omega R}}{R},\\
H_\varphi = E_\theta &= \frac{i\omega H_\infty}{2}\left\{[G(2,\delta)g(1,\delta)\right.\\
&\left.-G(1,\delta)g(2,\delta)]J_0(\zeta)+i[G(2,\delta)g(1,\delta)+\right.\\
&\left.+G(1,\delta)g(2,\delta)]J_1(\zeta)\right\}\frac{e^{i\omega R}}{R}.
\end{aligned}
\right\} \qquad (24,19)
$$

Here $\gamma \geq \frac{\pi}{2}\left(\gamma \leq \frac{\pi}{2}\right)$ and $\delta \leq \frac{\pi}{2}$.

Starting from Expressions (24.18) and (24.19), it is not difficult to write interpolation equations for the fringing field which are suitable for any values of γ and ϑ in the interval $(0; \pi/2)$, but when $\phi = \pm/2$;

$$E_\varphi = -H_\vartheta = \frac{ikaE_{0\varphi}}{2}\left\{[F(2,\vartheta)F(1,\delta)f(2,\delta) - \right.$$
$$- F(1,\vartheta)F(2,\delta)f(1,\delta)]J_1(\zeta) + i[F(2,\vartheta)F(1,\delta)f(2,\delta) +$$
$$\left. + F(1,\vartheta)F(2,\delta)f(1,\delta)]J_2(\zeta)\right\}\frac{e^{ikR}}{R}, \qquad (24.20)$$

$$E_\vartheta = H_\varphi = \frac{ikH_{0\varphi}}{2}\left\{[G(2,\vartheta)G(1,\delta)g(2,\delta) - \right.$$
$$- G(1,\vartheta)G(2,\delta)g(1,\delta)]J_1(\zeta) + i[G(2,\vartheta)G(1,\delta)g(2,\delta) +$$
$$\left. + G(1,\vartheta)G(2,\delta)g(1,\delta)]J_2(\zeta)\right\}\frac{e^{ikR}}{R}. \qquad (24.21)$$

Let us note that when $\gamma = 0$ these expressions will be valid for any values of the azimuth ϕ, since then any point of space may be considered to be located in the incident plane.

In the direction of the scattering diagram's principal maximum — that is, when $\vartheta = \gamma, \varphi = \frac{\pi}{2}$ — the fringing field (24.20) and (24.21) takes the form

$$\left.\begin{aligned} E_\varphi &= -H_\vartheta = \frac{ika^2}{2}E_{0\varphi}\cdot F(2,\gamma)F(1,\gamma)\frac{e^{ikR}}{R}\cos\gamma, \\ E_\vartheta &= H_\varphi = \frac{ika^2}{2}H_{0\varphi}\cdot G(2,\gamma)G(1,\gamma)\frac{e^{ikR}}{R}\cos\gamma. \end{aligned}\right\} \qquad (24.22)$$

However, these expressions have an interpolation character, and with small values of the angle γ it is impossible to consider them to be more precise than the simple equations of § 9 and § 12. In particular, with $\gamma = 0$, when the fringing field must not depend on the incident wave polarization, they give values which are different for the E-polarization and H-polarization by small quantities of the order of $\frac{1}{\sqrt{ka}}$. Therefore, in this case (when $\gamma = 0$) it makes sense to use Expressions (24.20) and (24.21) only far from the z axis, switching to Equations (24.02) near the z axis.

Equations (24.20) and (24.21) have the following important properties, They do not have discontinuities, they include the case of glancing incidence of a plane wave, and they satisfy the reciprocity principle. From them it follows that $E_z = H_\varphi = 0$ when $\vartheta = \frac{\pi}{2}$ — that is, the fringing field does not experience a discontinuity on the plane z = 0. Moreover, $E_\vartheta = H_\varphi = 0$ with any values of ϑ, if $\gamma = \frac{\pi}{2}$, — that is, a plane wave polarized perpendicular to the disk's plane does not experience diffraction with glancing irradiation of the disk.

As in the case of diffraction by a strip, the new approximation expressions consider to some extent tertiary diffraction [see Equations (23.05) and Figure 48].

Using Condition (9.04), it is not difficult to write equations for the fringing field in the left half-space $\left(\frac{\pi}{2} < \vartheta < \pi;\ \varphi = \pm\frac{\pi}{2}\right)$

$$\begin{aligned} E_\varphi = -H_\vartheta = \frac{ikaE_{0z}}{2}\Big\{&[F(2,\pi-\vartheta)F(1,\delta)f(2,\delta) - \\ &- F(1,\pi-\vartheta)F(2,\delta)f(1,\delta)]J_1(\zeta) + \\ &+ i[F(2,\pi-\vartheta)F(1,\delta)f(2,\delta) + \\ &+ F(1,\pi-\vartheta)F(2,\delta)f(1,\delta)]J_2(\zeta)\Big\}\frac{e^{ikR}}{R}, \end{aligned} \tag{24.23}$$

$$\begin{aligned} E_\vartheta = H_\varphi = \frac{ikaH_{0z}}{2}\Big\{&[G(2,\pi-\vartheta)G(1,\delta)g(2,\delta) - \\ &- G(1,\pi-\vartheta)G(2,\delta)g(1,\delta)]J_1(\zeta) + \\ &+ i[G(2,\pi-\vartheta)G(1,\delta)g(2,\delta) + \\ &+ G(1,\pi-\vartheta)G(2,\delta)g(1,\delta)]J_2(\zeta)\Big\}\frac{e^{ikR}}{R}, \end{aligned} \tag{24.23}$$

where the functions f and g are determined by the equations

$$\left.\begin{aligned} g(1,\delta) = f(2,\delta) &= \frac{\cos\frac{\delta+\vartheta}{2} + \sin\frac{\delta-\vartheta}{2}}{\sin\delta - \sin\vartheta}, \\ f(1,\delta) = g(2,\delta) &= \frac{\cos\frac{\delta+\vartheta}{2} - \sin\frac{\delta-\vartheta}{2}}{\sin\delta - \sin\vartheta}. \end{aligned}\right\} \tag{24.24}$$

In the direction towards the source $\left(\vartheta = \pi - \gamma,\ \varphi = -\frac{\pi}{2}\right)$, the fringing field equals

$$\left.\begin{aligned}
E_\varphi = -H_\theta = \frac{ikE_0}{2}\int\{[F^2(1,\delta)f(2,\delta) - \\
- F^2(2,\delta)f(1,\delta)]J_1(\zeta) + i[F^2(1,\delta)f(2,\delta) + \\
+ F^2(2,\delta)f(1,\delta)]J_2(\zeta)\}\frac{e^{ikR}}{R}, \\
E_\theta = H_\varphi = \frac{ikH_0}{2}\int\{[G^2(1,\delta)g(2,\delta) - \\
- G^2(2,\delta)g(1,\delta)]J_1(\zeta) + i[G^2(1,\delta)g(2,\delta) + \\
+ G^2(2,\delta)g(1,\delta)]J_2(\zeta)\}\frac{e^{ikR}}{R},
\end{aligned}\right\} \qquad (24.25)$$

where

$$\left.\begin{aligned}
\delta = -\gamma; \\
f(1,\delta) = g(2,\delta) = -\frac{1+\sin\gamma}{2\sin\gamma}; \\
f(2,\delta) = g(1,\delta) = \frac{1-\sin\gamma}{2\sin\gamma}.
\end{aligned}\right\} \qquad (24.26)$$

As was already noted, it makes sense to use Equations (24.25) only far from the z axis, changing to Expression (12.15) of the previous approximation in the vicinity of the z axis. A calculation of functions $\Sigma(\pi-\gamma)$ and $\bar{\Sigma}(\pi-\gamma)$ (Figures 65 and 66) which determine the effective scattering surface [see Expressions (12.17)] was performed on the basis of these equations when ka = 5. A comparison was carried out of this calculation with the results of measurements. The two experimental diagrams (the dashed lines)[2] depicted in Figure 65 characterize the experimental precision. As distinct from the previous approximations, which lead in this case to qualitatively incorrect results [see Equations (10.06), (10.07) and (12.15)], we observe a satisfactory agreement of theory with experiment.

For verifying the results obtained, a calculation was also carried out of the functions $V^{(1)}(\theta)$ and $V^{(2)}(\theta)$ [see Equations (9.07)] when ka = 5 (Figure 67 and 68) with normal irradiation of a disk by a plane wave. Curve 1 corresponds to the field calculated from the rigorous theory [34]; curve 2 corresponds to the field from

---

[2] Footnote appears on page 162.

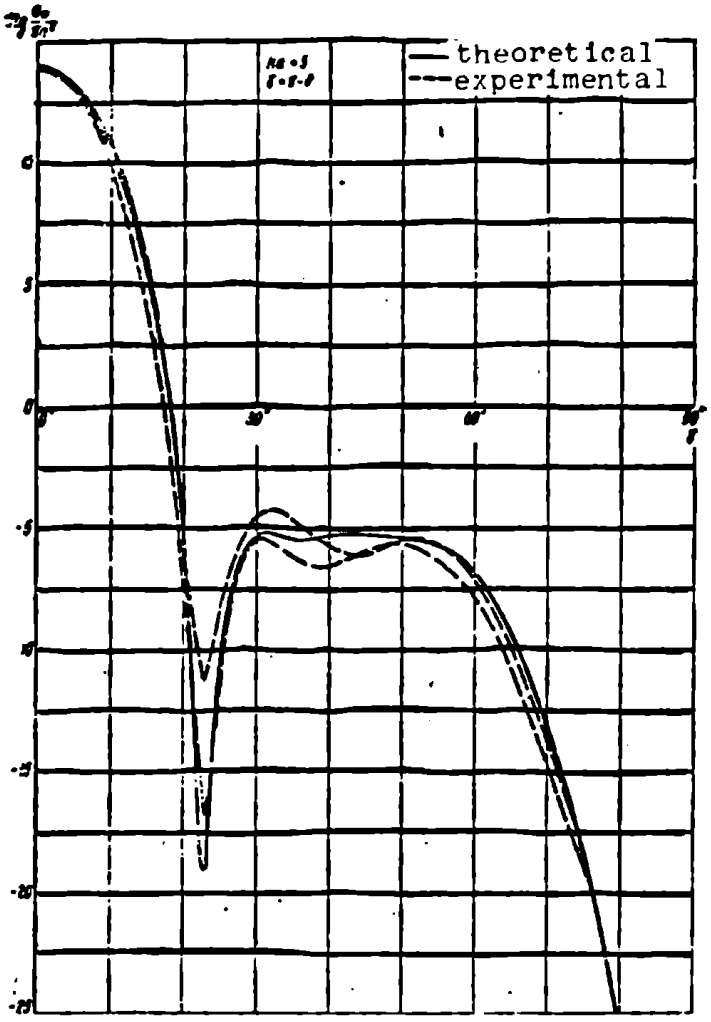

Figure 65. The diagram of a disk's effective scattering surface when the plane wave's magnetic vector is perpendicular to the incident plane.

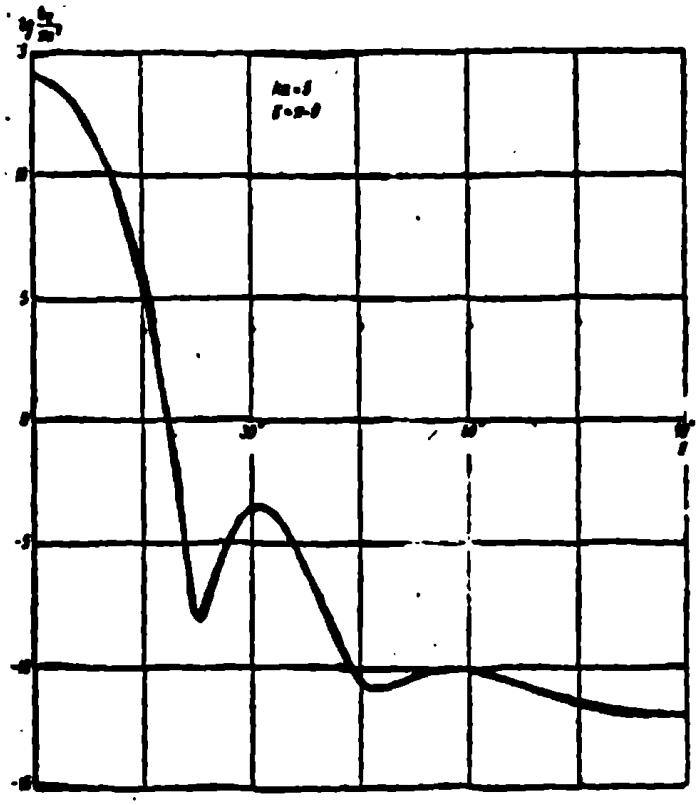

Figure 66. The calculated diagram of a disk's effective scattering surface when the plane wave's electric vector is perpendicular to the incident plane.

the uniform part of the current (the physical optics approach). Curve 3 corresponds to the field from the uniform and nonuniform parts of the current, but without the interaction of the edges. Curve 4 corresponds to the field with consideration of secondary diffraction. As is seen from these graphs, consideration of the edge interaction refines the previous approximation and ensures better agreement with the rigorous theory results.

The problem of secondary diffraction by a cylinder may be solved by a similar method. However, considering that the corrections which

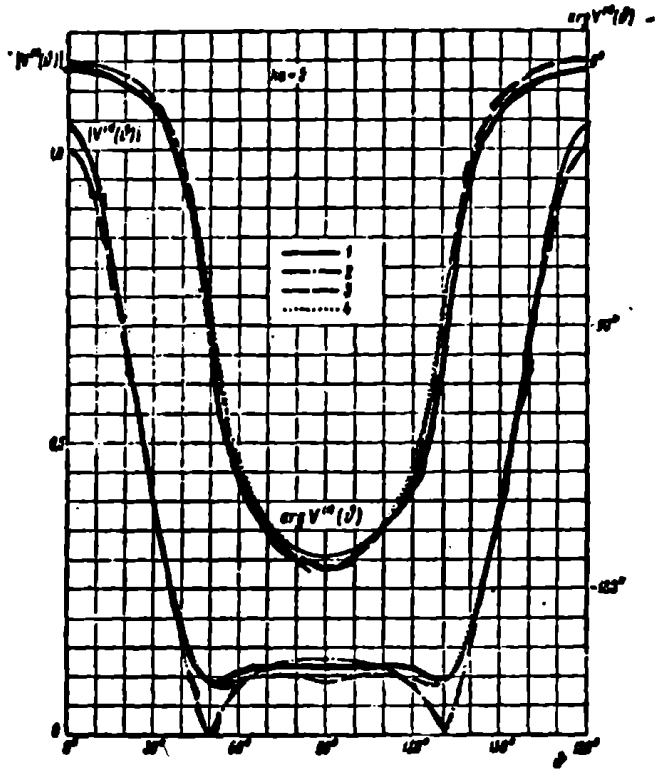

Figure 67. The function $V^{(1)}(\vartheta)$ for a disk with normal incidence of a plane wave (curve 4). Curves 1, 2 and 3 from Figure 20 are drawn for comparison.

depend on the secondary diffraction here are small (on the order of 1 dB) when $ka = \pi$, $kl = 10\pi$, and the equations are substantially more complicated, we shall not cite them here.

In the problems investigated above, the edge waves have the character of cylindrical or spherical waves — that is, they decrease rather rapidly with the distance from the edge. Therefore, in the case when the linear dimensions of the faces are approximately two wavelengths, it is sufficient to limit ourselves to a consideration

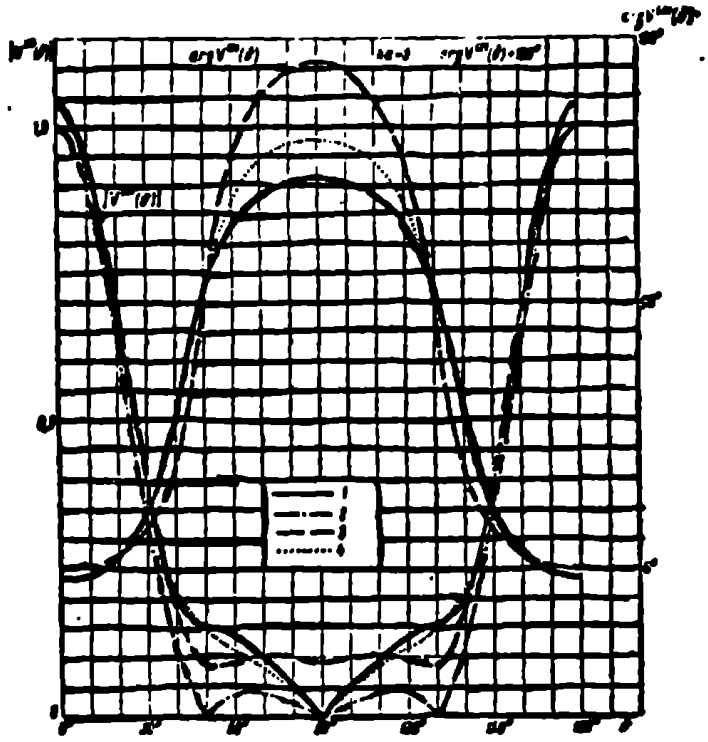

Figure 68. The function $V^{(2)}(\vartheta)$ for a disk with the normal incidence of a plane wave (curve 4). Curves 1, 2 and 3 from Figure 21 are drawn for comparison

of only secondary waves. In Chapter VII we will investigate the problem of a dipole in which the edge waves decrease so slowly that it is necessary to consider multiple diffraction.

§ 25. A Brief Review of the Literature

In this and previous chapters, approximation expressions were obtained for the scattering characteristics of a plane wave by various bodies. These expressions were derived with the help of physical considerations which do not pretend to be mathematically rigorous, and they are adequate for sufficiently short waves. In the literature,

there are a number of works in which similar results were obtained. A majority of these works also are not characterized by mathematical rigor, and they are based on certain physical assumptions. Therefore, one may relate them to the physical theory of diffraction. Only in a few works (related to the simpler diffraction problems) did they succeed in obtaining specific results at a higher level of mathematical rigor — more precisely, while developing asymptotic methods of mathematical diffraction theory.

We will briefly list the most important results obtained in a number of papers and books, grouping the material in the following sequence:

1. Diffraction by plane, infinitely thin plates (an infinite strip, a circular disk) and diffraction by auxiliary apertures in a flat screen (an infinite slit, a circular hole).

2. Diffraction by three-dimensional bodies with edges (a finite cylinder, a finite cone, etc.).

3. Other diffraction problems.

When investigating the first group of diffraction problems, it is necessary to keep in mind the principle of duality [4] which enables one to easily change from a strip to a slit, from a disk to a circular hole, etc. In the literature as a rule, they preferred to investigate apertures in an infinite flat screen, whereas in our book, diffraction by a strip and a disk was studied. This approach facilitates the transition to three-dimensional bodies (see the remarks at the beginning of this chapter).

Based on the time of appearance (if we do not consider the works of Schwarzschild [25] which we talked about in the Introduction), one should first of all mention the works of Braunbek [28 - 30] which were devoted to the diffraction of a scalar wave by a circular hole in a flat screen. Assuming that the plane wave is incident normal to

the screen, the author obtained an approximation solution in the form of a surface integral. The boundary values of the integrand were taken from the rigorous solution to the problem of diffraction by a half-plane which was found by Sommerfeld. The field was calculated in the far zone on the axis of the hole and far from it, and also on the axis near the screen. Using this approach, Braunbek recently solved the problem of scalar wave diffraction by an aperture in a concially shaped screen [31].

In the papers of Frahn [32, 33], this method was used for the diffraction of electromagnetic waves. Diffraction of a plane wave incident normal to an ideally conducting screen with a circular hole was investigated. The field was calculated in the hole and on the axis, and also the field in the far zone and the transmission coefficient (the ratio of the energy passing through the hole to the energy falling on it) were calculated.

In these works of Braunbek and Frahn, secondary diffraction was not considered. The expressions obtained by them for the fringing field intensity in the far zone agree with similar expressions following from our equations (§ 9).

Karp and Russek [51] studied diffraction by a slit in the case when the incident wave's electric vector is parallel to the slit edge. They investigated each semi-infinite part of the screen as a half-plane excited by the incident wave field and a "virtual" source localized on the edge of the opposite half-plane. The moments of these sources were determined from a system of two algebraic equations which were obtained by using the asymptotic expressions resulting from the rigorous solution for the half-plane. Secondary diffraction was considered, and partially the general interaction. Special attention was allotted to calculating the transmission coefficient, but equations for the scattering characteristics which would be suitable with all directions of incident wave propagation were absent.

Clemmow [46] and Millar [47 - 49] in their works calculated the transmission coefficients with normal irradiation of a slit and a hole, and also the field in the hole. The solution was sought by means of curvilinear integrals of the fictitious linear currents on the aperture edges. The interaction of the edges was considered. The case of inclined irradiation was not investigated, since it turned out to be too complicated for investigation by this method.

The "geometric theory of diffraction" of Keller [42 - 44] which deals with diffraction rays is of special interest. The phase and amplitutude corresponding to each diffraction ray are determined at each ray point on the basis of geometric considerations and the law of the conservation of energy. The initial diffraction ray amplitude is assumed to be proportional to the incident ray amplitude at the point of its diffraction. The unknown proportionality constant between the amplitudes and the initial phase difference is determined from a comparison with the results of well-known solutions of diffraction problems. In this way, the fields scattered with the normal incidence of a plane wave on a slit and hole in a flat screen are found. These fields are obtained with consideration of multiple diffractions, but they are not precise wave equation solutions, since their calculation was started from approximation relations. Moreover, geometric diffraction theory is not applicable near caustics, and also in the vicinity of the scattering diagram principal maximum.

In a recently published paper of Buchal and Keller [52], a new method for the solution of diffraction problems for holes in a flat screen was proposed. The caustics and shadow boundaries here are investigated as thin boundary layers, inside of which a rapid field change takes place. This method supplements geometric diffraction theory, and in particular enables one to find the field at caustics and on the shadow boundary.

Recently, the method of integral equations has been applied to the solution of diffraction problems of holes in a flat screen. In particular, Greenberg [53, 54] reduced the solution of this problem

to an integral equation for a "shadow" current which is, in our terminology, half the nonuniform part of the current. The resulting integral equations may be solved (with any ratio between the dimensions of the hole and the wavelength) by the method of successive approximations. Moreover, they allow one to obtain asymptotic expressions which are suitable for short waves. In Reference [55] Greenberg found an asymptotic expression for the current on a strip with ka >> 1 (2a is the strip's width). Greenberg and Pimenov [56] obtained a similar solution in the case of normal incidence of a plane wave on a circular hole. Using the same method, an asymptotic expression was found for the current on a flat ring [57], the width and inner diameter of which are a great deal larger than the wavelength.

The above listed works [53 - 57] already relate to the mathematical theory of diffraction: in them the first terms of the asymptotic expansions for the current were obtained with the desire evidently to also be able to calculate the following terms. Unfortunately, the asymptotic expressions which have been found up to now refer only to currents, and one is obliged to calculate the scattering characteristics by means of numerical quadratures [56]. As a consequence of the rapid oscillation of the integrands, such a method leads to rather unwieldy calculations and does not enable one to formulate a clear representation of the fringing field formation, and also does not allow one to study this field properly.

Millar [58] investigated the problems of electromagnetic wave diffraction by slits in a flat screen. The system of integral equations obtained by him for the current is solved by the method of successive approximations. The field in the hole is calculated from the currents which are found, and then on the basis of the field in the hole the field in the far zone and the transmission coefficient are calculated. All the indicated quantities are represented in the form of an asymptotic expansion in reciprocal powers of the parameter $\sqrt{ka}$. A solution also is obtained in the case of glancing incidence of a plane wave.

Let us note that the asymptotic expressions obtained by the method of integral equations are distinguished by their considerable complexity, and frequently require tabulation of the new special functions appearing in the expressions.

In the recently issued volume of Handbuch der Physik [50], which is devoted to diffraction theory, the complex characteristic of plane wave scattering by a strip was studied directly, omitting the calculation of the currents. For this characteristic, a singular integral equation was formulated, the solution of which was sought in the form of an asymptotic series in reciprocal powers of $\sqrt{ka}$. The first term of the series corresponds to Equations (6.14) and (6.16). The following term takes into account the interaction of the edges, and becomes infinite with the glancing incidence of a plane wave and also for observation points lying in the strip's plane. Therefore, the simple expressions obtained in [50] do not allow one to construct the complete scattering characteristic. In [50] diffraction by a disk, a sphere, and an infinite circular cylinder was investigated, and also a review of the general methods of diffraction theory and a bibliography encompassing a large number of works (mainly German and American) were given.

The book of King and Yu [59] presented (as a rule without derivation) a series of asymptotic expressions relating to a slit and a circular hole and also to other diffraction objects. Here, however, equations from which one would be able to construct the scattering characteristics of a strip and a disk with any incidence of a plane wave also are missing.

Works on diffraction by three-dimensional bodies having edges are comparatively scarce. In the paper of Siegel et al. [41], the effective scattering surface for a finite cone with the incidence of a plane wave on it along the symmetry axis is calculated from elementary arguments. The expressions obtained here do not fully characterize the fringing field, and are suitable only for sharp cones to which we already referred in § 17. In the papers of Keller [44], the

diffraction ray concept is used for calculating the scattering of scalar and electromagnetic plane waves by a finite circular cone with a flat base and also by a cone having a spherical rounding off instead of a flat base. The resulting expressions are not applicable in the vicinity of certain irradiation and observation directions. In § 17 we showed that the field scattered by a cone and by certain bodies of rotation is not expressed only in terms of the functions f and g, which refer to diffraction rays diverging from a wedge edge. This result evidently attests to the impossibility of complete calculation of the scattering characteristic with the diffraction ray concept.

Diffraction problems arising in antenna theory are usually distinguished by their great complexity, since the corresponding metal bodies (mirror, horn, etc.) have a complicated shape. Since the dimensions of these bodies and the dimensions of the radiating apertures are considerably larger than the wavelength, the application of physical diffraction theory to antenna problems is very promising. only the first steps have been taken in this direction. Thus, Kinber [60, 61] performed a calculation of the decoupling and lateral radiation of mirror antennas. The feature specific to mirror antennas is that diffraction rays arising at the mirror's edge undergo multiple reflection on its concave surface. This multiple reflection was studied by Kinber in more detail as applied to the concave surface of a cylinder and sphere [62, 63].

Diffraction problems relating to an antenna dipole — a thin cylindrical conductor — are investigated in Chapter VII, and references to the literature are also given there.

In conclusion, let us say a few words about diffraction of short waves by smooth bodies. The basic principles relating to such problems were set forth in the fundamental works of Fok and Leontovich. These principles were established by the following methods of mathematical diffraction theory:

1. By the method of an integral equation for the current on the surface of a good conducting body (the local character of the field in the half-shade region, see [17]);

2. By the method of asymptomtic summing of diffraction series (the current on a paraboloid [64, 65]; the propagation of radio waves above the spherical Earth [18, 66]);

3. By the parabolic equation method (the propagation of radio waves above the flat [67] and spherical [68, 69] Earth; the field of a plane electromagnetic wave in the half-shade region for any convex body [70]).

Keller [47], basing his work on the diffraction ray concept, obtained an expression for the field in a deep shadow with diffraction by a convex cylinder with a variable curvature. In the particular cases of an elliptic and a parabolic cylinder, as was shown in the works of Vaynshteyn and Fedorov [71] and of Ivanov [35], Keller's equations agree with the results of the more rigorous mathematic investigation. This allows one to more precisely study (see [71]) the conversion of diffraction rays to ordinary rays and vice versa.

The parabolic equation method described in so-called ray coordinates is a more general approach to diffraction by convex bodies. This method allows one to obtain a general expression for the Green function in the case of a circular cylinder [72, 73]. Evidently this method can subsequently be successfully applied also to other cases, among them three-dimensional diffraction problems.

FOOTNOTES

Footnote (1) on page 138.

These calculations were performed under the guidance of P. S. Mikazan.

Footnote (2) on page 150.

See the footnote on page 86.

CHAPTER VI

CERTAIN PHENOMENA CONNECTED WITH THE NONUNIFORM PART OF THE SURFACE CURRENT

In the previous chapters, a theoretical investigation was conducted of the field radiated by the nonuniform part of the current. In this chapter we will discuss a method for measuring this field (§ 26) and we will investigate the phenomenon of the reflected signal's depolarization (§ 27).

An experimental method for measuring the field from the nonuniform part of the current was first proposed for bodies of rotation in the paper of Ye. N. Mayzel's and the author [12]. Later it was shown that this method has a universal character, and is suitable for measuring the field from the nonuniform part of the current excited by a plane wave on any metal body [13].

§ 26. Measurement of the Field Radiated by the Nonuniform Part of the Current

Let an ideally conducting body of arbitrary shape be found in free space. A surface element of this body is shown in Figure 60.

The coordinate system was selected in such a way that its origin would lie near the body, and the source Q would be located in the plane x = 0. If the distance between the body and the source is a great deal larger than the body's dimensions, then the incident wave in the vicinity of the body may be investigated as a plane wave. Let us represent it in the form

$$E_x = E_{0x} e^{ikr(\sin\gamma + z\cos\gamma)}, \quad E_y = 0. \tag{26.01}$$

Here γ is the angle between the normal N to the wave front and the z axis.

Now let us place in front of the source, parallel to the radiated wave front, a polarizer P which transformed linear polarized radiation into a circularly polarized wave. Let the wave passing through the polarizer with an electric vector E_n lag in phase by 90° behind the wave with an electric vector E_τ (Figure 70). In this case, the polarizer achieves a clockwise rotation(1). As a result, the incident wave field at the coordinate origin will equal

$$E_x = \frac{e^{i\frac{\pi}{4}}}{\sqrt{2}} E_{0x}, \quad H_x = \frac{e^{-i\frac{\pi}{4}}}{\sqrt{2}} E_{0x}. \tag{26.02}$$

The field scattered by the body may be represented in the wave zone in the following way:

$$\left.\begin{aligned} E_\varphi = -H_\theta &= \frac{ikaE_{0x}}{2} \frac{e^{i\frac{\pi}{4}}}{\sqrt{2}} \overline{\Sigma}(\theta, \varphi) \frac{e^{ikR}}{R}, \\ E_\theta = H_\varphi &= \frac{ikaE_{0x}}{2} \frac{e^{-i\frac{\pi}{4}}}{\sqrt{2}} \Sigma(\theta, \varphi) \frac{e^{ikR}}{R}, \end{aligned}\right\} \tag{26.03}$$

where a is a certain length characterizing the body's size and $\overline{\Sigma}(\theta, \varphi)$ and $\Sigma(\theta, \varphi)$ are unknown angular functions. In the general case, the

(1) Footnote appears on page 174.

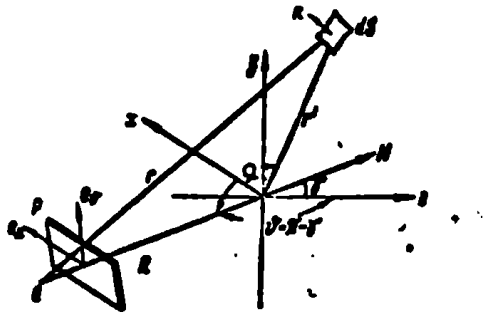

Figure 69. The problem of electromagentic wave diffraction by an arbitrary metal body.

dS - is a surface element of the body.
N - the normal to the incident wave front,
Q - the source,
P - the polarizer converting linearly polarized radiation to a wave with circular polarization.

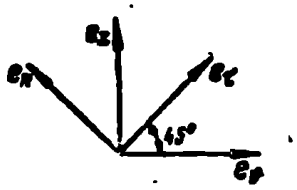

Figure 70.

field (26.03) is an elliptically polarized wave. In the direction toward the source $\left(\theta=\pi-\gamma,\ \varphi=-\frac{\pi}{2}\right)$, this wave passes through the polarizer and creates behind it the field

$$\left.\begin{aligned} E_z=-H_\theta=\frac{iaE_{0x}}{2}\sum_+\frac{e^{ikR}}{R}e^{i\frac{\pi}{2}},\\ E_\theta=H_z=\frac{iaE_{0x}}{2}\sum_-\frac{e^{ikR}}{R}.\end{aligned}\right\} \tag{26.04}$$

where

$$\sum_\pm=\frac{1}{2}\left(\sum\pm\overline{\sum}\right). \tag{26.05}$$

If the source radiates a wave of another polarization ($H_0 \perp$ yoz), then the wave reflected by the body and passing through the polarizer is described at the point Q by similar relationships

$$\left.\begin{aligned} H_z=E_\theta=\frac{iaH_{0x}}{2}\sum_+\frac{e^{ikR}}{R}e^{i\frac{\pi}{2}},\\ H_\theta=-E_z=\frac{iaH_{0x}}{2}\sum_-\frac{e^{ikR}}{R}.\end{aligned}\right\} \tag{26.06}$$

Now let us investigate in the physical optics approach the diffraction of a plane linearly polarized wave by the same body. According to definition (3.01), the uniform part of the current excited on the body's surface by a plane wave with E-polarization of the incident wave ($E_0 \perp$ yoz) equals

$$\left.\begin{aligned} f_x^0 &= -\frac{c}{2\pi} E_{0x}(n_y \sin\gamma + n_z \cos\gamma)\, e^{i\psi}, \\ f_y^0 &= \frac{c}{2\pi} E_{0x} \cdot n_x \cdot \sin\gamma \cdot e^{i\psi}, \\ f_z^0 &= \frac{c}{2\pi} E_{0x} \cdot n_x \cos\gamma e^{i\psi}, \end{aligned}\right\} \qquad (26.07)$$

and with H-polarization ($H_0 \perp yOz$)

$$\left.\begin{aligned} f_x^0 &= 0, \\ f_y^0 &= \frac{c}{2\pi} H_{0x} \cdot n_z e^{i\psi}, \\ f_z^0 &= -\frac{c}{2\pi} H_{0x} \cdot n_y \cdot e^{i\psi}. \end{aligned}\right\} \qquad (26.08)$$

Here E_{ox} and H_{ox} are the electric and magnetic field amplitudes of the incident wave with E-polarization and H-polarization, respectively; $\psi = k(y' \sin\gamma + z' \cos\gamma)$ is the incident wave phase at the point (x', y', z') on the body's surface; n_x, n_y, n_z, are the components of the normal to the surface at the same point.

Furthermore, calculating the vector potential in the far zone on the basis of this current and substituting its values into the equations

$$\left.\begin{aligned} E_\varphi &= -H_\theta = ikA_\varphi, \\ E_\theta &= H_\varphi = ikA_\theta, \end{aligned}\right\} \qquad (26.09)$$

we find the fringing field. With E-polarization, it equals

$$E_\varphi = -H_\theta = \frac{ik}{2\pi} E_{0x} \cdot \frac{e^{ikR}}{R} \cdot \int [n_x \sin\gamma \cos\varphi + \\ + (n_y \sin\gamma + n_z \cos\gamma) \sin\varphi]\, e^{i\Phi} dS, \qquad (26.10)$$

$$E_\theta = H_\varphi = \frac{ik}{2\pi} E_{0x} \cdot \frac{e^{ikR}}{R} \cdot \int [n_x (\sin\gamma \cos\theta \sin\varphi - \cos\gamma \sin\theta) - \\ - (n_y \sin\gamma + n_z \cos\gamma) \cos\varphi \cos\theta]\, e^{i\Phi} dS, \qquad (26.10)$$

and with H-polarization

$$E_\varphi = -H_\theta = \frac{ik}{2\pi} H_{0x} \cos\varphi \frac{e^{ikR}}{R} \int n_z e^{i\Phi} dS,$$

$$E_\theta = H_\varphi = \frac{ik}{2\pi} H_{0x} \frac{e^{ikR}}{R} \int_S (n_y \sin\theta + n_z \sin\varphi \cos\theta) e^{i\Phi} dS. \qquad (26.11)$$

Here R, θ , ϕ are the spherical coordinates of the observation point, $\Phi = \psi - kr' \cos\Omega$, and integration is carried out over the illuminated elements of the body's surface. In the case of radar when the observation and irradiation directions coincide $\left(\theta = \pi - \gamma,\ \varphi = -\frac{\pi}{2}\right)$, Equations (26.10) and (26.11) yield

$$\left.\begin{aligned} E_x = -H_\theta = -\frac{ik}{2\pi} E_{0x} \frac{e^{ikR}}{R} \int (n_y \sin\gamma + \\ + n_z \cos\gamma) e^{i\Phi} dS, \\ E_\theta = H_x = 0 \end{aligned}\right\} \qquad (26.12)$$

and

$$\left.\begin{aligned} E_\theta = H_x = \frac{ik}{2\pi} H_{0x} \frac{e^{ikR}}{R} \int (n_y \sin\gamma + \\ + n_z \cos\gamma) e^{i\Phi} dS, \\ E_x = H_\theta = 0. \end{aligned}\right\} \qquad (26.13)$$

Furthermore, assuming the incident wave amplitudes ar specified by Equation (26.02), let us write Expressions (26.12) and (26.13) in the following way:

$$\left.\begin{aligned} E_x = -H_\theta = \frac{iaE_{0x}}{2} \frac{e^{i\frac{\pi}{4}}}{\sqrt{2}} \frac{e^{ikR}}{R} \bar{\Sigma}^\circ, \\ E_\theta = H_x = \frac{iaE_{0x}}{2} \frac{e^{-i\frac{\pi}{4}}}{\sqrt{2}} \frac{e^{ikR}}{R} \Sigma^\circ, \end{aligned}\right\} \qquad (26.14)$$

where

$$\Sigma^\circ = -\bar{\Sigma}^\circ = \frac{k}{\pi a} \int (n_y \sin\gamma + n_z \cos\gamma) e^{i\Phi} dS. \qquad (26.15)$$

Now let us represent the angular functions of fringing field (26.03) in the form

$$\left.\begin{aligned}\bar{\Sigma} &= \bar{\Sigma}^0 + \bar{\Sigma}^1,\\ \Sigma &= \Sigma^0 + \Sigma^1,\end{aligned}\right\} \tag{26.16}$$

where the functions Σ^0, $\bar{\Sigma}^0$ and Σ^1, $\bar{\Sigma}^1$ refer to the field radiated by the uniform and nonuniform part of the current, respectively. Substituting these expressions into Equations (26.04) and (26.06) and taking into account relationship (26.15), let us find the fringing field passing through the polarizer P toward the source Q. In the case of E-polarization, it equals

$$\left.\begin{aligned}E_z &= -H_\theta = -\frac{ikE_{0z}}{4}(\Sigma^1 + \bar{\Sigma}^1)\frac{e^{ikR}}{R}e^{i\frac{\varphi}{2}},\\ E_\theta &= H_z = \frac{ikE_{0z}}{4}(2\Sigma^0 + \Sigma^1 - \bar{\Sigma}^1)\frac{e^{ikR}}{R},\end{aligned}\right\} \tag{26.17}$$

and in the case of H-polarization

$$\left.\begin{aligned}H_z &= E_\theta = \frac{ikH_{0z}}{4}(\Sigma^1 + \bar{\Sigma}^1)\frac{e^{ikR}}{R}e^{i\frac{\varphi}{2}},\\ H_\theta &= -E_z = \frac{ikH_{0z}}{4}(2\Sigma^0 + \Sigma^1 - \bar{\Sigma}^1)\frac{e^{ikR}}{R}.\end{aligned}\right\} \tag{26.18}$$

The physical meaning of the result obtained is as follows. The field scattered by the body at the point Q is the sum of two waves polarized in mutually perpendicular directions. The reflected wave which is polarized the same as the primary radiation of the source is determined by the function $\Sigma_+ = \frac{1}{2}(\Sigma^1 + \bar{\Sigma}^1)$, and is created only by the nonuniform part of the current. The reflected wave with the perpendicular polarization is described by the function $\Sigma_- = 2\Sigma^0 + \Sigma^1 - \bar{\Sigma}^1$, and is the field radiated by both parts of the current. Let us note that in the general case the functions Σ^1 and $\bar{\Sigma}^1$ do not coincide, and therefore they are not balanced out in the expressions for Σ_-. In other words, the field radiated by the uniform part of the current in this case may not be separated from the fringing field.

Thus, the investigated method allows one to separate from the total field scattered by any metal body of finite dimensions that part of the field which is caused by a distortion of the surface (the

curvature, a sharp bend, a point, a bulge, a hole, etc.). One should note that, in the case of electromagnetic wave scattering by a system of separate bodies, the separable part of the field is due not only to the surface's distortion, but also to the diffraction interaction of the bodies.

It is necessary, however, to keep in mind that it is possible to realize the indicated fringing field distribution not in an arbitrary observation direction, but only in a direction for which the condition $\Sigma^0 = -\bar{\Sigma}^0$ is fulfilled — for example, in the direction towards the source.

Consideration of the nonuniform part of the current also enables one to explain the reflected wave depolarization which we will investigate in the following section.

Figure 71 presents the results of measurements[2] and calculations of the effective scattering surface

$$\sigma^+ = \pi a^2 |\dot{\Sigma}_+|^2 = \frac{1}{4}\pi a^2 |\Sigma^1 + \bar{\Sigma}^1|^2, \qquad (26.19)$$

which is dependent upon the nonuniform part of the current excited by a plane electromagnetic wave on a disk. The disk's diameter equals $2a = \frac{5\lambda}{\pi}$ (λ is the wavelength). The calculations were performed with consideration of the secondary diffraction on the basis of the approximation equations for the functions Σ and $\bar{\Sigma}$ which were derived in § 24. Since it is difficult to prepare a thin disk with a sufficiently flat surface, the measurements were performed with an obtuse cone close to the shape of a disk and having a height approximately equal to one tenth of the diameter.

As is seen from Figure 71, the theoretical and experimental curves are fairly close together. A certain divergence between them, especially in the region of γ values close to 90°, may evidently be explained both by the model's conical shape and also by the

---

[2] Footnote appears on page 174.

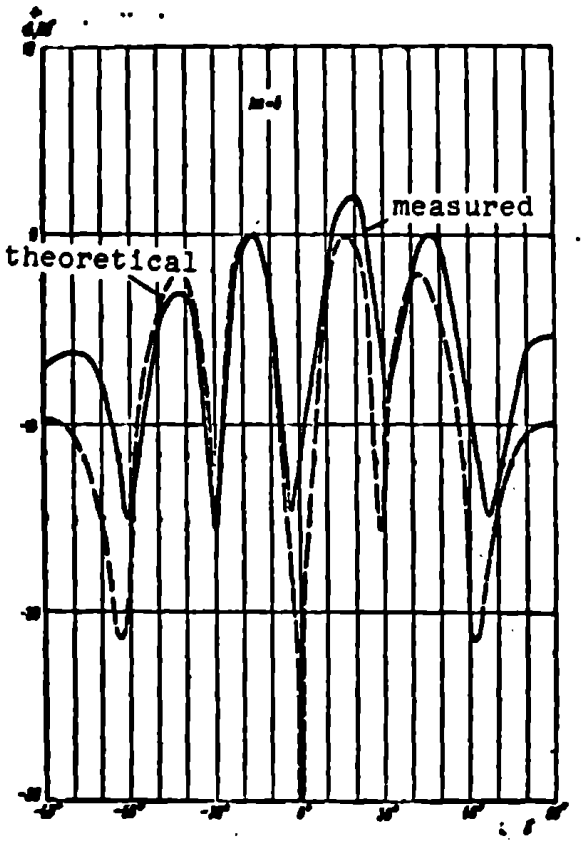

Figure 71. Diagram of the radiation from the nonuniform part of the current flowing on a disk.

approximation character of the computational equations. The value $\gamma = 90°$ corresponds to the direction along the disk's surface, and the value $\gamma = 0°$ — to the direction normal to the disk.

§ 27. Reflected Wave Depolarization

Let us again return to the problem of scattering of an electromagnetic wave by an arbitrary metal body. The relative position of the source Q, of a surface element of the irradiated body, and of the coordinate system is shown in Figure 69. Let us recall that the

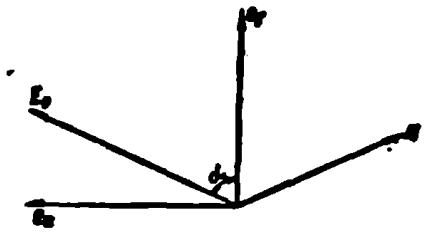

Figure 72.

source Q is in the plane y0z, and radiates a linearly polarized wave. Furthermore, we shall assume that the polarizer P which is shown in Figure 69 is now absent.

Let us designate by α the angle between the plane y0z and the incident wave electric vector $\mathbf{E}_0$ (Figure 72). The field of this wave will be represented in the form

$$E_x = H_{0\gamma} = E_{0x} e^{ik(y\sin\gamma + z\cos\gamma)},$$
$$H_x = -E_{0\gamma} = H_{0x} e^{ik(y\sin\alpha + z\cos\gamma)}, \qquad (27.01)$$

where

$$E_{0x} = E_0 \sin\alpha, \quad H_{0x} = -E_0\cos\alpha, \quad \frac{E_{0x}}{E_{0\gamma}} = \operatorname{tg}\alpha. \qquad (27.02)$$

The field scattered by the body is determined in the wave zone by the equations

$$\left.\begin{aligned} E_\varphi = -H_\vartheta &= \frac{ia}{2}\left[E_{0x}\bar{\Sigma}_1(\gamma,\vartheta,\varphi) + \right. \\ &\left. + H_{0x}\Sigma_1(\gamma,\vartheta,\varphi)\right]\frac{e^{ikR}}{R}. \\ E_\vartheta = H_\varphi &= \frac{ia}{2}\left[E_{0x}\bar{\Sigma}_2(\gamma,\vartheta,\varphi) + \right. \\ &\left. + H_{0x}\Sigma_2(\gamma,\vartheta,\varphi)\right]\frac{e^{ikR}}{R}. \end{aligned}\right\} \qquad (27.03)$$

Here a is a certain length characterizing the body's dimensions, R, ϑ, ϕ are the spherical coordinates of the observation point, $\bar{\Sigma}_{1,2}(\gamma,\vartheta,\varphi)$ and $\Sigma_{1,2}(\gamma,\vartheta,\varphi)$ are unknown angular functions.

It is obvious that the fringing field polarization — that is, the orientation of its electric vector in space — depends in a complex way on the observation and irradiation directions. In the

direction toward the source, it may not coincide with the polarization of the wave radiated by the source. Such a phenomenon is called reflected wave depolarization.

It is easy to establish the reason for depolarization, if one investigates the fringing field as the sum of the fields radiated by the uniform and nonuniform parts of the current. According to § 26, the uniform part of the current radiates the following field in the direction towards the source $\left(\theta=\pi-\gamma,\ \varphi=-\frac{\pi}{2}\right)$

$$\left.\begin{aligned} E_\alpha = -H_\theta &= \frac{ikE_{0x}}{2}\frac{e^{ikR}}{R}\bar{\Sigma}^0, \\ E_\theta = H_\varphi &= \frac{ikH_{0x}}{2}\frac{e^{ikR}}{R}\Sigma^0. \end{aligned}\right\} \qquad (27.04)$$

The functions $\bar{\Sigma}^0$ and Σ^0 satisfy the condition $\Sigma^0 = -\bar{\Sigma}^0$, and are described by Equation (26.15). From Equation (27.04), let us immediately obtain the equality

$$\frac{E_\alpha}{E_\theta} = \operatorname{tg}\alpha, \qquad (27.05)$$

which means that in the physical optics approach the reflected wave does not experience depolarization. Consequently, the reflected wave depolarization is caused only by the nonuniform part of the current or, in other words, by the surface distortion.

Let us derive an equation for the magnitude of angle δ. This is the angle by which the electric field vector of the reflected wave is turned in respect to the electric vector of the wave radiated by the source. For this purpose, let us represent the functions $\bar{\Sigma}_{1(2)}$ and $\Sigma_{1(2)}$ in the form

$$\left.\begin{aligned} \bar{\Sigma}_{1(2)} &= \bar{\Sigma}^0_{1(2)} + \bar{\Sigma}^1_{1(2)}, \\ \Sigma_{1(2)} &= \Sigma^0_{1(2)} + \Sigma^1_{1(2)}, \end{aligned}\right\} \qquad (27.06)$$

where the terms $\bar{\Sigma}^0_{1(2)}$ and $\Sigma^0_{1(2)}$ correspond to the field radiated by the uniform part of the current, and the terms $\bar{\Sigma}^1_{1(2)}$ and $\Sigma^1_{1(2)}$

correspond to the field radiated by the nonuniform part of the current. Comparing Expressions (27.04) and (27.03), we find that

$$\left.\begin{aligned} \bar{\Sigma}_1^0 &= \bar{\Sigma}^0, \quad \Sigma_1^0 = 0, \\ \bar{\Sigma}_2^0 &= 0, \quad \Sigma_2^0 = -\bar{\Sigma}^0. \end{aligned}\right\} \tag{27.07}$$

Therefore, the field scattered in the direction towards the source $\left(\vartheta = \pi - \gamma,\ \varphi = -\frac{\pi}{2}\right)$, will equal

$$\left.\begin{aligned} E_x = -H_\varphi &= \frac{ika}{2}\left[E_{0x}\left(\bar{\Sigma}^0 + \bar{\Sigma}_1^1\right) + H_{0x}\Sigma_1^1\right]\frac{e^{ikR}}{R}, \\ E_\varphi = H_x &= \frac{ika}{2}\left[E_{0x}\bar{\Sigma}_2^1 - H_{0x}\left(\bar{\Sigma}^0 - \Sigma_1^1\right)\right]\frac{e^{ikR}}{R}. \end{aligned}\right\} \tag{27.08}$$

This field's electric vector forms an angle β with the yoz plane. The angle β is determined by the equation

$$\operatorname{tg}\beta = \frac{E_x}{E_\varphi} = \frac{\bar{\Sigma}^0 + \bar{\Sigma}_1^1 - \Sigma_1^1 \operatorname{ctg}\alpha}{\bar{\Sigma}^0 - \Sigma_2^1 + \bar{\Sigma}_2^1 \operatorname{tg}\alpha} \operatorname{tg}\alpha. \tag{27.09}$$

As a result, the desired angle δ which characterizes the depolarization magnitude will equal

$$\delta = \alpha - \beta. \tag{27.10}$$

Thus, the field from the nonuniform part of the current, separable "in a pure form" by means of a polarizer (§ 26), leads to depolarization of the scattered radiation.

Specific results from the depolarization calculation of waves reflected from certain bodies may be found, for example, in the works of Chytil [75 - 77] and Beckmann [78]. In particular, in Reference [77] it was shown that the depolarization effect on the effective scattering surface of convex bodies in practice may be neglected only with the condition $ka \gtrsim 4$.

FOOTNOTES

Footnote (1) on page 164. A system of metal plates parallel to the e_τ vector may serve as the simplest example of such a polarizer.

Footnote (2) on page 169. See the footnote on page 86.

CHAPTER VII

DIFFRACTION BY A THIN CYLINDRICAL CONDUCTOR

In almost all the works devoted to the diffraction of plane electromagnetic waves by a thin cylindrical conductor, the current induced in the conductor was studied, and then, by integrating this current, the fringing field in the far zone was calculated. However, in view of the complexity of this problem, they succeeded in obtaining relatively simple equations only in the particular case when the observation direction and the direction toward the source coincided, and was perpendicular to the conductor axis. In the general case when these directions did not coincide and were arbitrary, the expressions for the fringing field became very complicated and unsuitable for making calculations. Since they were obtained by integrating approximation expressions for the current, it turns out that they have still one other shortcoming — they do not satisfy the principle of duality.

In this chapter, explicit expressions are obtained for the fringing field which are suitable for making calculations with any direction of irradiation and observation. We shall consider both the primary edge waves excited by the incident plane wave and also the secondary, tertiary, etc. edge waves. The total fringing field is found by summing all the diffraction waves.

§ 28. Current Waves in an Ideally Conducting Vibrator

The electrodynamic problem of determining the current in thin cylindrical conductors (vibrator) usually is reduced to an integro-differential equation. The latter is derived by means of boundary conditions on the conductor surface, and is substantially simplified in the case of thin conductors when the inequalities

$$\frac{a}{L} \ll 1 \text{ and } ka \ll 1, \tag{28.01}$$

are fulfilled, where a is the radius and L is the length of the conductor and $k = \frac{2\pi}{\lambda} = \frac{\omega}{c}$.

Its solution may be found, for example, by the method of successive approximations [79, 80] or by the perturbation method [85]. Recently, Vaynshteyn [81, 82] proposed a new solution for this equation. Since we will subsequently base our work on the results of References [81, 82], let us discuss them in more detail.

Let us assume that the vibrator's symmetry axis coincides with the z axis, and its ends have the coordinates $z = z_1$ and $z = z_2$ ($L = z_2 - z_1$). In the case of excitation of the dipole by a concentrated external field

$$E_z^e = \mathcal{E}^0(z) \tag{28.02}$$

the current J(z) in the conductor may obviously be written in the form of the sum of the waves travelling along the conductor with a velocity c from the excitation point $z = 0$ and the ends $z = z_1$ and $z = z_2$. In Reference [81] it was shown that the complex amplitudes of these waves are slowly varying functions of the z coordinate. These functions may be approximately expressed in terms of the function $\psi(z)$, so that we obtain the following expression for the current J(z):

$$J(z) = J_0[\psi(|z|)e^{ik|z|} + A_1\psi(z - z_1)e^{ik(z-z_1)} + A_2\psi(z_2 - z)e^{ik_2(z_2-z)}]. \tag{28.03}$$

Here the quantity

$$J_0 = \frac{cE}{4\ln\frac{i}{\gamma ka}}, \quad \gamma = 1{,}781\ldots \tag{28.04}$$

determines the initial value of the current wave propagated from the excitation point[1]. The function $\psi(z)$ is the solution of the integral equation, and in addition to the variable z it also depends on the parameters k and a. We will not list here all the properties of the function $\psi(z)$, but let us note only that it satisfies the conditions

$$\psi(0) = 1, \quad \psi(\infty) = 0, \tag{28.05}$$

and its absolute value monotonically decreases with an increase of z. This decrease, which is rather slow and does not have an exponential character, is due to radiation.

The constants A_1 and A_2 determine the initial values of the current waves originating at the points $z = z_1$ and $z = z_2$, respectively, and travelling in the direction towards the opposite end of the conductor. These constants wre found from the conditions at the conductor ends

$$J(z_1) = J(z_2) = 0 \tag{28.06}$$

and equal

$$\left.\begin{aligned} A_1 &= -\frac{1}{D}[\psi(-z_1) - \psi(z_2)\psi(L)e^{2ikz_2}]e^{-ikz_1}, \\ A_2 &= -\frac{1}{D}[\psi(z_2) - \psi(-z_1)\psi(L)e^{-2ikz_1}]e^{ikz_2}, \end{aligned}\right\} \tag{28.07}$$

where

$$D = 1 - \psi^2(L)e^{2ikL}. \tag{28.08}$$

---

(1) Footnote appears on page 216.

Considering that the quantity 1/D is equal to the infinite geometric progression,

$$\frac{1}{D} = 1 + \psi^2(L)e^{2ikL} + \psi^4(L)e^{4ikL} + \ldots, \tag{28.09}$$

Expression (28.03) may be written in the expanded form

$$\begin{aligned} J(z) = J_0\{&\psi(|z|)e^{ik|z|} - \psi(-z_1)e^{-ikz_1}[\psi(z-z_1)e^{ik(z-z_1)} - \\ &- \psi(L)e^{ikL}\psi(z_1-z)e^{ik(z_1-z)} + \psi^2(L)e^{2ikL}\psi(z- \\ &- z_1)e^{ik(z-z_1)} - \ldots] - \psi(z_2)e^{ikz_2}[\psi(z_2-z)e^{ik(z_2-z)} - \\ &- \psi(L)e^{ikL}\psi(z-z_2)e^{ik(z-z_2)} + \\ &+ \psi^2(L)e^{2ikL}\psi(z_2-z)e^{ik(z_2-z)} - \ldots]\}. \end{aligned} \tag{28.10}$$

The physical meaning of Expression (28.03) is seen from this. The first term in Equation (28.10) is the primary current wave which coincides with the wave excited by a concentrated emf in an infinitely long conductor. The second term (in all brackets) corresponds to the current resulting from the reflection of the primary current wave from the conductor end $z = z_1$, and as a result of subsequent reflections from the conductor ends which arise from this wave $-J_0\psi(-z_1)e^{-ikz_1}\psi(z-z_1)e^{ik(z-z_1)}$. The third term (in all brackets) corresponds to the current resulting from the reflection of the primary wave from the end $z = z_2$ and as a result of the subsequent reflections from the conductor ends arising from this wave $-J_0\psi(z_2)e^{ikz_2}\psi(z_2-z)e^{ik(z_2-z)}$.

It also follows from Equation (28.03) that external field (28.02) excites in the semi-infinite conductor $(z_1 \leqslant z \leqslant \infty)$ the current

$$J(z) = J_0[\psi(|z|)e^{ik|z|} - \psi(-z_1)e^{-ikz_1}\psi(z-z_1)e^{ik(z-z_1)}], \tag{28.11}$$

and in the semi-infinite conductor $(-\infty \leqslant z \leqslant z_2)$ the current

$$J(z) = J_0[\psi(|z|)e^{ik|z|} - \psi(z_2)e^{ikz_2}\psi(z_2-z)e^{ik(z_2-z)}]. \tag{28.12}$$

Comparing these expressions with the proper terms in (28.10), we see that the reflection of all the current waves at the end of a finite

length vibrator occurs in the same way as at the end of a semi-infinite conductor.

In the case of a passive vibrator $(z_1 < z < z_2)$, excited by the plane wave

$$E_z^e = E_{0z} e^{i\omega z}, \quad \omega = -k\cos\vartheta, \tag{28.13}$$

the current also is represented in the form of the sum of waves (see [82])

$$\begin{aligned} J(z) = S[e^{-ikz} - \psi_-(z - z_1)e^{i\omega z_1 + ik(z - z_1)} - \\ - \psi_+(z_2 - z)e^{i\omega z_1 + ik(z_2 - z)} + \bar{A}_1\psi(z - z_1)e^{-ik(z - z_1)} + \\ + \bar{A}_2\psi(z_2 - z)e^{ik(z_2 - z)}], \end{aligned} \tag{28.14}$$

where the first term corresponds to the current excited by a plane wave in an infinitely long conductor. Its complex amplitude S equals

$$S = \frac{i\omega E_{0z}}{2k^2\sin^2\vartheta \ln\frac{2i}{\gamma ka\sin\vartheta}}. \tag{28.15}$$

The second and third terms are primary edge waves arising as a consequence of the cut-off of the current Se^{-iwz}. They are expressed in terms of the functions ψ + (z) and ψ - (z) which depend, in addition to the variable z and the parameters k and a, on the angle ϑ. These functions satisfy the relationships

$$\left.\begin{aligned} &\psi_\pm(0) = 1, \quad \psi_\pm(\infty) = 0, \\ &\psi_+(z)\big|_{\vartheta=\pi} = \psi_-(z)\big|_{\vartheta=0} = \psi(z), \\ &\psi_+(z)\big|_{\vartheta=0} = \psi_-(z)\big|_{\vartheta=\pi} = 1. \end{aligned}\right\} \tag{28.16}$$

The initial values of the primary edge waves are such that their sum with the wave Se^{-iwz} gives a current equal to zero at the conductor ends.

The last two terms in Equation (28.14) correspond to secondary, tertiary, etc., edge waves, and have the same form as they do for a

transmitting vibrator [compare Equation (26.03)]. The unknown coefficients $\tilde{A}_1$ and $\tilde{A}_2$ are found from Conditions (28.06) and equal

$$\left.\begin{aligned}\tilde{A}_1 &= \frac{1}{D}\,e^{i(k+\omega)z_1}[\psi_+(L) - \\ &- \psi_-(L)\psi(L)e^{i(k-\omega)L}]e^{-ikz_1}, \\ \tilde{A}_2 &= \frac{1}{D}\,e^{-i(k-\omega)z_2}[\psi_-(L) - \\ &- \psi_+(L)\psi(L)e^{i(k+\omega)L}]e^{ikz_2}.\end{aligned}\right\} \tag{28.17}$$

Using equality (28.09), Expression (28.14) may be written in the more graphic form

$$\left.\begin{aligned}J(z) = S\{&e^{i\omega z} - \psi_-(z - z_1)\,e^{i\omega z_1 + ik(z-z_1)} + \\ &+ \psi_-(L)\,e^{i\omega z_1 + i\omega L}[\psi(z_2 - z)\,e^{ik(z_2-z)} - \\ &- \psi(L)e^{ikL}\psi(z - z_1)\,e^{ik(z-z_1)} + \\ &+ \psi^2(L)\,e^{2ikL}\psi(z_2 - z)\,e^{ik(z_2-z)} - \ldots] - \\ &- \psi_+(z_2 - z)\,e^{i\omega z_2 + ik(z_2-z)} + \\ &+ \psi_+(L)\,e^{i\omega z_2 + ikL}[\psi(z - z_1)\,e^{ik(z-z_1)} - \\ &- \psi(L)e^{ikL}\psi(z_2 - z)\,e^{ik(z_2-z)} + \\ &+ \psi^2(L)\,e^{2ikL}\psi(z - z_1)e^{ik(z-z_1)} - \ldots]\}.\end{aligned}\right\} \tag{28.18}$$

Here besides the wave Se^{iwz} and the primary edge waves, which we talked about in connection with Equation (28.14), the secondary, tertiary, etc. waves diverging from the ends $z = z_1$ and $z = z_2$ are explicitly written out; they correspond to the first, second, etc. terms in the graphs.

Passing to the limit in Equation (28.14) when $z_2 \to \infty$, we find the current in the semi-infinite conductor (z_1, ∞)

$$J(z) = S\cdot[e^{i\omega z} - \psi_-(z - z_1)\,e^{i\omega z_1 + ik(z-z_1)}] \tag{28.19}$$

and, similarly, we find the current in the semi-infinite conductor $(-\infty, z_2)$

$$J(z) = S\cdot[e^{i\omega z} - \psi_+(z_2 - z)\,e^{i\omega z_2 + ik(z_2-z)}]. \tag{28.20}$$

It is not difficult to see that in the case of a passive vibrator the reflection of current waves at its ends occurs in the same way as at the end of a semi-infinite conductor.

Thus, the complex amplitudes of current waves in a thin, finite length conductor are proportional to the functions $\psi(z)$ and $\psi_{\pm}(z)$ which monotonically decrease with an increase of z as a consequence of radiation. Let us note several properties of current waves in a vibrator. Each advancing wave in sum with the reflected wave excited by it gives a zero current at the conductor's end. In the case $L = z_1 - z_1 \approx n\frac{\lambda}{2}$ $(n = 1, 2, 3 \ldots)$ and $D \gtrsim 0$, a current resonance begins in the vibrator.

The precision of Expressions (28.03) and (28.14) obtained by the method of slowly varying functions is different in various sections of the conductor. It is comparatively low near the conductor's ends (and in the vicinity of the point z = 0 of a transmitting vibrator) where the current waves arise, and where their complex amplitude varies rather rapidly. As the distance from these vibrator elements increases, the precision of these equations increases without limit.

It should be stated that with a more rigorous approach [79, 90] the amplitudes of all the reflected waves will be determined by different functions; however, the difference between them rapidly decreases with an increase of the reflection number. The functions $\psi(z)$ and $\psi_{\pm}(z)$ only approximately describe these current waves, but on the other hand they allow one to effectively sum them and to obtain closed equations.

Using the variational method for the functions $\psi(z)$ and $\psi_{\pm}(z)$, we obtained the approximate, but on the other hand, simple equations (see [83])

$$\psi(z) = \frac{\ln\frac{-1}{\gamma^2 q}}{\ln\frac{2ix}{\gamma} - E(2qx)e^{-2iqx}}, \qquad (28.21)$$

(Equation continued on next page)

$$\psi_{\pm}(z)=-\frac{\ln\frac{-1}{\gamma^{2}q_{\pm}}}{\ln\frac{2ix}{\gamma}-E(2q_{\pm}x)e^{-2iq_{\pm}x}}\Bigg\} \tag{28.21}$$

where

$$\ln(-1)=i\pi,\ \ln i=i\frac{\pi}{2}. \tag{28.22}$$

$$x=\frac{kz}{q},\ \ q=(ka)^{2},\ \ q_{\pm}=q\frac{1\mp\cos\theta}{2} \tag{28.23}$$

and

$$E(y)=\mathrm{Ci}\,y+i\,\mathrm{si}\,y=-\int_{y}^{\infty}\frac{e^{it}}{t}\,dt. \tag{28.24}$$

The integral cosine Ci y and the integral sine si y are determined by the relationships

$$\mathrm{Ci}\,y=-\int_{y}^{\infty}\frac{\cos t}{t}\,dt,\ \ \mathrm{si}\,y=-\int_{y}^{\infty}\frac{\sin t}{t}\,dt \tag{28.25}$$

and are thoroughly tabulated functions.

The equations written above for the current in a finite conductor are distinguishable by their visualizability, and they enable one to liken the conductor to a section of a transmission line in which, however, the attenuation of the current waves takes place, not according to an exponential law, but according to a more complicated law which is determined by Equations (28.21). In addition, the diffraction character of the problem is reflected in the equations. The conductor's specific features as a diffraction object are included in the very slow attenuation of the current waves. As a consequence of this, it is impossible to limit oneself to considering only secondary and tertiary diffractions, and it is necessary to sum all the reflected waves. As a result of such a summation, a "resonance denominator" D appears which takes into account the resonance properties of a thin, finite length conductor.

§ 29. Radiation of a Transmitting Vibrator

The radiation characteristic of a transmitting vibrator may be calculated from a known equation by integrating the currents in it. However, such an approach is not advisable because, as was indicated above, the precision of Equations (28.03) is different in different parts of the conductor, and is low near its ends ($z = z_1$ and $z = z_2$) and the point $z = 0$. The principle of duality gives more precise results. This principle leads to the following expression for the radiation field in the far zone [82]:

$$\left.\begin{aligned} E_\theta = H_\varphi &= \frac{\mathcal{E}}{2\sin\theta \ln\frac{2i}{\gamma ka\sin\theta}} \frac{e^{ikR}}{R} \cdot f(\theta), \\ E_\varphi = H_\theta &= 0. \end{aligned}\right\} \tag{29.01}$$

The function

$$\begin{aligned} f(\theta) = 1 - \psi_+(z_1)\, e^{ikz_1(1-\cos\theta)} - \psi_-(-z_1)\, e^{-ikz_1(1+\cos\theta)} + \\ + B_1\psi_+(L)\, e^{ikz_1(1-\cos\theta)} + B_2\psi_-(L)\, e^{-ikz_1(1+\cos\theta)} \end{aligned} \tag{29.02}$$

is connected with the current (28.14) excited in a vibrator by plane wave (28.13) by the relationship

$$J(0) = Sf(\theta). \tag{29.03}$$

The coefficients B_1 and B_2 do not depend on the angle θ.

Expression (29.02) enables one to trace the formation of the radiation. The first term (one) is the radiation field of an infinitely long conductor excited by a concentrated emf. Propagating in the direction $\theta = 0$, this field reaches the conductor's end $z = z_2$ and — being diffracted by it — generates a primary edge wave (the second term). In a similar way, the primary edge wave diverging from the conductor's end $z = z_1$ is excited (the third term). The last two terms in Equation (29.02) determine the waves arising as a result of subsequent diffraction (secondary, tertiary, etc.). The amplitudes B_1 and B_2 of these waves may be found from the conditions

$$f(0) = f(\pi) = 0, \tag{29.04}$$

which means that the radiation of a finite conductor in the direction of its geometric extension must be equal to zero. These conditions, together with a consideration of the relationships (28.05) and (28.16), lead to the system of equations.

$$\left.\begin{aligned} B_1 + B_2\psi(L)\,e^{-2ikz_1} &= \psi(-z_1)\,e^{-2ikz_1}, \\ B_1\psi(L)\,e^{2ikz_2} + B_2 &= \psi(z_2)\,e^{2ikz_2}, \end{aligned}\right\} \tag{29.05}$$

from which we find without difficulty

$$\left.\begin{aligned} B_1 &= \frac{1}{D}\left[\psi(-z_1) - \psi(L)\psi(z_2)\,e^{2ikz_2}\right]e^{-2ikz_1}, \\ B_2 &= \frac{1}{D}\left[\psi(z_2) - \psi(L)\psi(-z_1)\,e^{-2ikz_1}\right]e^{2ikz_2}. \end{aligned}\right\} \tag{29.06}$$

Keeping in mind (28.09), let us represent the functions $f(\theta)$ in a more graphic form

$$\begin{aligned} f(\theta) = 1 &- \psi_+(z_2)\,e^{ikz_2(1-\cos\theta)} + \psi(z_1)\,e^{ik(L+z_2)} \times \\ &\times \left[\psi_-(L)\,e^{-ikz_1\cos\theta} - \psi(L)\,e^{ikL}\psi_+(L)\,e^{-ikz_2\cos\theta} + \right. \\ &\left. + \psi^2(L)\,e^{2ikL}\psi_-(L)\,e^{-ikz_1\cos\theta} - \ldots\right] - \\ &- \psi_-(-z_1)\,e^{-ikz_1(1+\cos\theta)} + \psi(-z_1)\,e^{ik(L-z_1)} \times \\ &\times \left[\psi_+(L)\,e^{-ikz_2\cos\theta} - \psi(L)\,e^{ikL}\cdot\psi_-(L)\,e^{-ikz_1\cos\theta} + \right. \\ &\left. + \psi^2(L)\,e^{2ikL}\cdot\psi_+(L)\,e^{-ikz_2\cos\theta} - \ldots\right], \end{aligned} \tag{29.07}$$

where the secondary, tertiary, etc. waves corresponding to the first, second, and following terms in the brackets are explicitly written out.

Thus, the field radiated by a transmitting vibrator arises as a result of multiple diffraction of edge waves at the vibrator's ends. Let us note in connection with this that the edge wave is diffracted by the opposite end of the vibrator in the same way as at the end of

a corresponding semi-infinite conductor. It is not difficult to establish this by investigating the radiation of a semi-infinite conductor excited by a concentrated emf.

§ 30. Primary and Secondary Diffraction by a Passive Vibrator

Let a plane electromagnetic wave fall at an angle ϑ_0 on a thin cylindrical conductor of length $L = z_2 - z_1$ and radius a (Figure 73). For purposes of generality, we will consider that the incident wave's electric field E_0 forms an angle α with the plane of the figure. Then, its tangential component on the conductor surface will equal

$$E_z^e = E_{0z} \cdot e^{i w_0 z}, \tag{30.01}$$

where

$$E_{0z} = E \sin \vartheta_0, \quad E_0' = E_0 \cos \alpha, \quad w_0 = -k \cos \vartheta_0. \tag{30.02}$$

The current induced in the vibrator by this field was investigated by us in § 28. As was already indicated above, Expression (28.14) which was obtained for it has a relatively low precision near the conductor ends. Therefore, it is inadvisable to seek the fringing field by integration of the current. Let us also note that the fringing field found by such a method does not satisfy the principle of duality.

We shall seek the scattering characteristic of a passive vibrator by starting from the following scattering picture which naturally follows from the previous results. An incident plane wave, being diffracted at the conductor ends, excites primary edge waves which are radiated into the surrounding space. Being propagated along the conductor, each of these waves experiences diffraction at the opposite end of the conductor and excites secondary edge waves. The latter, in turn, generate tertiary edge waves, etc. The total fringing field is comprised of the sum of all the edge waves being formed during sequential (multiple) diffraction at the conductor's ends.

In § 28 and 29, we noted that current waves are reflected from the ends of a finite length conductor the same as from the end of a semi-infinite conductor, and that the diffraction of these waves at each end takes place in the same way as at the end of a semi-infinite conductor. Therefore, the primary edge waves may be found from the problem of scattering of a plane wave by the semi-infinite conductor (z_1, ∞) and the conductor $(-\infty, z_2)$. The sum of such waves gives the primary diffraction field

$$E_\theta^{(1)} = H_\varphi^{(1)} = -E \frac{e^{ikR}}{\sqrt{kR}} \cdot F^{(1)}(\vartheta, \vartheta_0), \tag{30.03}$$

where

$$F^{(1)}(\vartheta, \vartheta_0) = \frac{i}{2\sqrt{2}} \frac{\operatorname{ctg}\frac{\vartheta}{2}\operatorname{ctg}\frac{\vartheta_0}{2}}{(\cos\vartheta + \cos\vartheta_0)\Phi(-k\cos\vartheta, -k\cos\vartheta_0)} e^{-ikz_1(\cos\vartheta + \cos\vartheta_0)} - \frac{i}{2\sqrt{2}} \frac{\operatorname{tg}\frac{\vartheta}{2}\operatorname{tg}\frac{\vartheta_0}{2}}{(\cos\vartheta + \cos\vartheta_0)\Phi(k\cos\vartheta, k\cos\vartheta_0)} e^{-ikz_2(\cos\vartheta + \cos\vartheta_0)}. \tag{30.04}$$

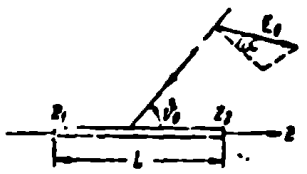

Figure 73. The incidence of a plane wave on a thin cylindrical conductor; ϑ_0 is the incident angle.

The function $\Phi(w, w_0)$ may be calculated by means of the rigorous solution to the problem of a semi-infinite vibrator (see [82] § 3 and [83] § 4), and in this case, it satisfies the relationship

$$\left.\begin{aligned} \Phi(w, w_0)\Phi(-w, -w_0) &= \ln\frac{2i}{\gamma w a} \cdot \ln\frac{2i}{\gamma w_0 a}, \\ w = \sqrt{k^2 - w^2}, \quad w_0 &= \sqrt{k^2 - w_0^2}. \end{aligned}\right\} \tag{30.05}$$

However, henceforth it will not be necessary to have the rigorous expression for the function Φ. Let us note that Equations (30.03) and (30.04) are similar to Expressions (6.13) for a strip. These latter expressions do not take into account secondary diffraction.

The secondary edge wave propagated from the end $z = z_2$ is excited during diffraction at this end of the primary current wave

$$\dots - S\psi_-^0(z - z_1)e^{i\omega_0 t + ik(z-z_1)}, \qquad (30.06)$$

where by $\psi_\pm^0(z)$ we mean the functions obtained from the functions $\psi_\pm(z)$ by replacing θ by θ_0. For the purpose of calculating the desired secondary waves, it is necessary for us, first of all, to find that external field which, when applied to an infinite conductor $(-\infty \leq z \leq \infty)$, would excite the current (30.06) on its section $(z_1 \leq z \leq \infty)$.

For this purpose, let us study the current induced in an infinite conductor by the external field

$$E_z^e = \hat{E}_{0z}e^{i\omega_0 t}\cdot s(z - z_1), \quad s(z - z_1) = \begin{cases} 1 \text{ with } z < z_1 \\ 0 \text{ with } z > z_1. \end{cases} \qquad (30.07)$$

Let us assume that ω_0 has a small negative imaginary part (Im $\omega_0 \leq 0$). We may regard the quantity $\hat{E}_{0z}e^{i\omega_0 t}d\zeta$ as a concentrated emf which, in accordance with equation (28.03), creates in an infinite conductor

$$\frac{c\hat{E}_{0z}}{4\ln\frac{l}{\gamma ka}}\cdot\psi(|z - \zeta|)e^{i\omega_0 t + ik(z-\zeta)}d\zeta. \qquad (30.08)$$

Therefore, in accordance with the principle of superposition, the total current created in the region $z_1 \leq z < \infty$ by the external field (30.07) will equal

$$J(z) = -\frac{c\hat{E}_{0z}}{4\ln\frac{l}{\gamma ka}}\cdot\int_{-\infty}^{z_1}\psi(z - \zeta)e^{i\omega_0 t + ik(z-\zeta)}d\zeta =$$

$$= -\frac{c\hat{E}_{0z}}{4\ln\frac{l}{\gamma ka}}e^{i\omega_0 t}\cdot\int_{z-z_1}^{\infty}\psi(\xi)e^{ik\xi}d\xi. \qquad (30.09)$$

The resulting integral may be expressed in terms of the functions $\psi(z - z_1)$ and $\psi_-^0(z - z_1)$, and the corresponding relationships derived in § 2 of [82]. As a result, we find

$$J(z)=\frac{c\hat{E}_{0\tau}e^{i\varphi_0}}{8ik\sin^2\frac{\theta_0}{2}\ln\frac{i}{\gamma ka}}\psi(z-z_1)e^{ik(z-z_1)}-$$

$$-\frac{c\hat{E}_{0\tau}e^{i\varphi_0}}{2ik\sin^2\theta_0\ln\frac{i}{\gamma ka\cos\frac{\theta_0}{2}}}\psi_-^0(z-z_1)e^{ik(z-z_1)}. \tag{30.10}$$

Thus, it turns out that external field (30.07) excites, in addition to the wave ψ_-^0, also the wave ψ. In order to excite a "pure" ψ_-^0 wave, it is necessary obviously to apply an additional external field

$$E_z^e=\mathcal{E}_1\delta(z-z_1), \tag{30.11}$$

such that

$$\frac{c\hat{E}_{0\tau}e^{i\varphi_0}}{8ik\sin^2\frac{\theta_0}{2}\ln\frac{i}{\gamma ka}}\psi(z-z_1)e^{ik(z-z_1)}+$$

$$+\frac{c\mathcal{E}_1}{4\ln\frac{i}{\gamma ka}}\psi(z-z_1)e^{ik(z-z_1)}=0. \tag{30.12}$$

Hence,

$$\mathcal{E}_1=-\frac{\hat{E}_{0\tau}e^{i\varphi_0}}{2ik\sin^2\frac{\theta_0}{2}}. \tag{30.13}$$

In order that the sum of external fields (30.07) and (30.11) would create the current (30.06), it is still necessary to fulfill the equality

$$\frac{c\hat{E}_{0\tau}}{2ik\sin^2\theta_0\ln\frac{i}{\gamma ka\cos\frac{\theta_0}{2}}}=S=\frac{i\omega E_{0\tau}}{2k^2\sin^2\theta_0\ln\frac{2i}{\gamma ka\sin\theta_0}}, \tag{30.14}$$

which determines the quantity

$$\hat{E}_{0z} = -E_{0z}\frac{\ln\frac{i}{\gamma ka\cos\frac{\vartheta_0}{2}}}{\ln\frac{2i}{\gamma ka\sin\vartheta_0}}. \qquad (30.15)$$

Consequently, for the excitation in an infinite conductor (with $z > z_1$) of current waves (30.06), it is necessary to apply the external field

$$E_z^e = E_{0z}\frac{\ln\frac{i}{\gamma ka\cos\frac{\vartheta_0}{2}}}{\ln\frac{2i}{\gamma ka\sin\vartheta_0}}\left[\frac{e^{iw_0 z_1}}{2ik\sin^2\frac{\vartheta_0}{2}}\delta(z-z_1) - e^{iw_0 z}\varepsilon(z-z_1)\right],$$

$$\varepsilon(z-z_1) = \begin{cases} 1 \text{ with } z<z_1 \\ 0 \text{ with } z>z_1. \end{cases} \qquad (30.16)$$

In a completely similar way, one may show that the external field

$$E_z^e = E_{0z}\frac{\ln\frac{i}{\gamma ka\sin\frac{\vartheta_0}{2}}}{\ln\frac{2i}{\gamma ka\sin\vartheta_0}}\left[\frac{e^{iw_0 z_2}}{2ik\cos^2\frac{\vartheta_0}{2}}\delta(z_2-z) - e^{iw_0 z}\varepsilon(z_2-z)\right],$$

$$\varepsilon(z_2-z) = \begin{cases} 1 \text{ with } z>z_2 \\ 0 \text{ with } z<z_2 \end{cases} \qquad (30.17)$$

excites the following current in an infinite single-wire line (with $z < z_2$)

$$-Se^{iw_0 z_2}\mathcal{J}_4^0(z_2-z)e^{ik(z_2-z)}. \qquad (30.18)$$

Now let us study the diffraction of current waves (30.06) by the semi-infinite conductor $(-\infty, z_2)$. For this purpose, let us use the Lorentz lemma [4]

$$\int (j_1^e E_2 + j_2^m H_1)\,dV = 0. \qquad (30.19)$$

Here $j_1^e = -i\omega p_1\delta(R - R')$ is the current of the auxiliary dipole with the moment p_1 which is located at point 1 with the coordinates (R, ϑ); H_1

is its field on the conductor surface, where the external currents j_2^m are specified; E_2 is the field created by these currents at point 1 (Figure 74).

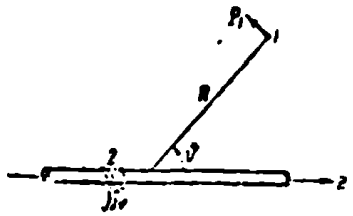

Figure 74.

The external current j_2^m is determined by the well-known equation

$$j_2^m = -\frac{c}{4\pi}[nE] \qquad (30.20)$$

in terms of the electric field E on the conductor's surface. In view of the boundary condition

$$E_z + E_z^e = 0 \qquad (30.21)$$

we have

$$j_{2\varphi}^m = -\frac{c}{4\pi} E_z^e. \qquad (30.22)$$

Furthermore, defining the dipole moment p_1 in terms of its field in free space (at the point x = y = z = 0)

$$E_{0\theta}' = -k^2 p_1 \frac{e^{ikR}}{R} \sin\vartheta \qquad (30.23)$$

and changing from the magnetic intensity $H_{1\phi}$ to the total current

$$J = \frac{ca}{2} H_{1\varphi}, \qquad (30.24)$$

induced by the dipole in the conductor, we obtain from the Lorentz lemma the following relationship:

$$E_{2\vartheta} = H_{2z} = \frac{k^2 \sin\vartheta}{i\omega E_{0\theta}'} \cdot \frac{e^{ikR}}{R} \cdot \int_{-\infty}^{z_0} E_z^e J(z)\, dz. \qquad (30.25)$$

If the dipole p_1 is moved to a distance $R \gg z_2 - z_0$, then the field radiated by it may be investigated on the section $z_2 - z_0$ of

the semi-infinite conductor $(-\infty, z_2)$ as a plane wave. Then the current induced in this section of the conductor will be determined by the equation

$$J(z) = S\left[e^{i\omega z} - e^{i\omega z_1}\psi_+(z_1 - z)\,e^{ik(z_1 - z)}\right], \tag{30.26}$$

where

$$S = \frac{i\omega E'_{0\theta}}{2k^2 \sin^2\vartheta \ln\dfrac{2i}{\gamma ka\sin\vartheta}}, \quad \omega = -k\cos\vartheta. \tag{30.27}$$

We will select the quantity z_0 in such a way that, at a distance $z_2 - z_0$ from the conductor end, the reflected current wave would be practically equal to zero $(\psi_+(z_1 - z_0) \approx 0)$. Substituting the function (30.26) into the right-hand member of Equality (30.25) and taking for the quantity E_z^e the external field (30.16), we obtain

$$E_{2\vartheta} = H_{2\varphi} = \frac{1}{2\sin\vartheta \ln\dfrac{2i}{\gamma ka\sin\vartheta}} \times$$

$$\times \frac{e^{ikR}}{R}\int_{-\infty}^{z_2} E_z^e\left[e^{i\omega z} - \psi_+(z_1 - z)\,e^{i\omega z_1 + ik(z_1 - z)}\right]dz =$$

$$= \frac{1}{2\sin\vartheta \ln\dfrac{2i}{\gamma ka\sin\vartheta}}\frac{e^{ikR}}{R}\left\{\mathcal{E}_1\left[e^{i\omega z_1} - \psi_+(L)\,e^{i\omega z_1 + ikL}\right] + \right.$$

$$\left. + \hat{E}_{0\vartheta}\frac{e^{i(\omega+\omega_0)z_1}}{i(\omega+\omega_0)} - \hat{E}_{0\vartheta}e^{i(k+\omega)z_1}\int_{-\infty}^{z_1} e^{-i(k-\omega_0)z}\psi_+(z_1 - z)\,dz.\right\} \tag{30.28}$$

An important feature of this relationship is that the integration is performed here not along the entire conductor $(-\infty, z_2)$, but only along part of it $(-\infty, z_1)$, where the function $\psi_+(z_1 - z)$ describes the current with good precision. The integrals here are calculated the same as in Equation (30.09). As a result, the field radiated by the semi-infinite conductor $(-\infty, z_2)$ will equal

$$E_{2\vartheta} = H_{2\varphi} = \frac{1}{2\sin\vartheta \ln\dfrac{2i}{\gamma ka\sin\vartheta}}\frac{e^{ikR}}{R} \times$$

(Equation continued on next page)

$$\times\left\{\dot{\mathcal{E}}_0\left[e^{ikz_1}-\psi_+(L)\,e^{ik(z_1+L)}\right]-\frac{\dot{E}_{0\tau}e^{i(\omega t+\varphi_0)}}{ik(\cos\theta+\cos\theta_0)}+\right.$$

$$\left.+\frac{\dot{E}_{0\tau}e^{ikL+i(\omega t+\varphi_0)}}{ik(\cos\theta-\cos\theta_0)}\left[\psi_+(L)\frac{\sin^2\frac{\theta}{2}\ln\frac{i}{\gamma ka\sin\frac{\theta}{2}}}{\cos^2\frac{\theta_0}{2}\ln\frac{i}{\gamma ka\cos\frac{\theta_0}{2}}}-\psi_-^0(L)\right]\right\}. \qquad (30.29)$$

The terms in the braces having the phase factor e^{iwz} correspond to the desired secondary wave diverging from the conductor's end $z = z_2$. Using Equations (30.13) and (30.15), this wave may be represented in the form

$$E_\theta^{(r)}(z_2)=H_\varphi^{(r)}(z_2)=-\frac{\mathcal{E}^{(2)}(z_2)\frac{1}{2i}}{2\sin\theta\ln\frac{1}{\gamma ka\sin\theta}}\frac{e^{ikR}}{R}e^{-ikz_2\cos\theta}, \qquad (30.30)$$

where

$$\mathcal{E}^{(2)}(z_2)=-\frac{4iEe^{i(\omega t+\varphi_0)+ikL}}{k\sin\theta_0(\cos\theta+\cos\theta_0)\ln\frac{2i}{\gamma ka\sin\theta_0}}\times$$

$$\times\left[\cos^2\frac{\theta_0}{2}\cos^2\frac{\theta}{2}\ln\frac{i}{\gamma ka\cos\frac{\theta_0}{2}}\psi_+(L)-\right.$$

$$\left.-\sin^2\frac{\theta_0}{2}\sin^2\frac{\theta}{2}\ln\frac{i}{\gamma ka\sin\frac{\theta}{2}}\psi_-^0(L)\right]. \qquad (30.31)$$

In a similar way, let us find the secondary diffraction wave being propagated from the end $z = z_1$. In order to do this, it is necessary to investigate the diffraction of primary wave (30.18) at the end $z = z_1$ of the semi-infinite conductor $(z_1 \le z < \infty)$. In this case, the principle of duality leads to the following relationship

$$E_{z\theta}=-H_{z\varphi}=-\frac{k^2\sin\theta}{i\omega E_{0\tau}'}\frac{e^{ikR}}{R}\int_{z_1}^{\infty}E_z^e J(z)\,dz, \qquad (30.32)$$

which, after substituting the function (30.17) and the current

$$J(z)=-\frac{i\omega E_{0\tau}'}{2k^2\sin^2\theta\ln\frac{2i}{\gamma ka\sin\theta}}\left[e^{ikz}-\psi_-(z-z_1)\,e^{i\omega z_1+ik(z-z_1)}\right], \qquad (30.33)$$

in it gives us the field radiated by the semi-infinite conductor (z_1, ∞). The wave radiated by the conductor's end is the desired secondary edge wave and may be represented in the form

$$E_{\theta}^{(2)}(z_1) = H_{\varphi}^{(2)}(z_1) = -\frac{\mathcal{B}^{(2)}(z_1)}{2\sin\theta \ln\frac{2i}{\gamma ka\sin\theta}} \frac{e^{ikR}}{R} e^{-ikz_1\cos\theta}, \tag{30.34}$$

where

$$\mathcal{B}^{(2)}(z_1) = -\frac{4iEe^{i\varkappa_0 z_1 + ikL}}{k\sin\vartheta_0(\cos\theta+\cos\vartheta_0)\ln\frac{2i}{\gamma ka\sin\vartheta_0}} \times$$
$$\times\left[\sin^2\frac{\vartheta_0}{2}\sin^2\frac{\theta}{2}\ln\frac{i}{\gamma ka\sin\frac{\vartheta_0}{2}}\psi_-(L) - \right.$$
$$\left. -\cos^2\frac{\vartheta_0}{2}\cos^2\frac{\theta}{2}\ln\frac{i}{\gamma ka\cos\frac{\theta}{2}}\psi_+^0(L)\right]. \tag{30.35}$$

Otherwise, this expression may be written directly by replacing, in Equations (30.30) and (30.31), z_2 by z_1, θ by $\pi-\theta$ and ϑ_0 by $\pi-\vartheta_0$.

§ 31. Multiple Diffraction of Edge Waves

The secondary waves (30.30) and (30.34) which were found are the waves diverging from the ends of the semi-infinite conductors $(-\infty, z_2)$ and (z_1, ∞). If one excites an infinite single-wire line by the external field

$$E_z^e = \mathcal{B}_2^{(2)}\delta(z-z_2), \tag{31.01}$$

where

$$\mathcal{B}_2^{(2)} = \mathcal{B}^{(2)}(z_2)\big|_{\theta=\pi} = E\frac{2i\ln\frac{i}{\gamma ka}\psi_-^{(0)}(L)}{k\sin\vartheta_0\ln\frac{2i}{\gamma ka\sin\vartheta_0}} e^{ikL-ikz_2\cos\vartheta_0}, \tag{31.02}$$

then a spherical wave arises which with $\theta\approx\pi$ coincides with wave (30.30). With the excitation of an infinite line by the concentrated emf

$$E_\theta^e = \mathcal{E}_1^{(2)} \delta(z - z_1). \tag{31.03}$$

where

$$\mathcal{E}_1^{(2)} = \mathcal{E}^{(0)}(z_1)\big|_{\theta=0} = E \frac{2i \ln \frac{l}{\gamma ka}\, \psi_+^0(L)}{k \sin\theta_0 \ln \frac{2l}{\gamma ka \sin\theta_0}} e^{ikL - ikz_1 \cos\theta_0}, \tag{31.04}$$

a wave arises which coincides with wave (30.34) when $\theta \approx 0$. It is not difficult to see that these external fields actually excite in an infinite single-wire line current waves which are equivalent to the secondary current waves in a passive vibrator [that is, equivalent to those waves which are expressed by the first terms in the brackets of Equation (28.18)]. Therefore, the tertiary waves may be investigated as edge waves radiated by the semi-infinite conductors (z_1, ∞) and $(-\infty, z_2)$ with their excitation by the external fields (31.01) and (31.03), respectively. From Equations (30.25) and (30.32), we find without difficulty the total field radiated with the indicated excitation by the conductor (z_1, ∞)

$$E_\theta = H_\varphi = \frac{\mathcal{E}_2^{(2)}}{2 \sin\theta \ln \frac{2l}{\gamma ka \sin\theta}} \frac{e^{ikR}}{R} \left[e^{ikz_1} - \psi_-(L) e^{ikz_1 + ikL} \right] \tag{31.05}$$

and the total field radiated by the conductor $(-\infty, z_2)$

$$E_\theta = H_\varphi = \frac{\mathcal{E}_1^{(2)}}{2 \sin\theta \ln \frac{2l}{\gamma ka \sin\theta}} \frac{e^{ikR}}{R} \left[e^{ikz_2} - \psi_+(L) e^{ikz_2 + ikL} \right]. \tag{31.06}$$

As a result, we obtain for the tertiary waves diverging from the ends z_1 and z_2 the following expressions:

$$E_\theta^{(3)}(z_1) = H_\varphi^{(3)}(z_1) = \frac{\mathcal{E}^{(2)}(z_1)}{2 \sin\theta \ln \frac{2l}{\gamma ka \sin\theta}} \frac{e^{ikR}}{R} e^{-ikz_1 \cos\theta}, \tag{31.07}$$

$$E_\theta^{(3)}(z_2) = H_\varphi^{(3)}(z_2) = \frac{\mathcal{E}^{(2)}(z_2)}{2 \sin\theta \ln \frac{2l}{\gamma ka \sin\theta}} \frac{e^{ikR}}{R} e^{-ikz_2 \cos\theta}, \tag{31.08}$$

where

$$\left.\begin{aligned}\mathcal{E}^{(3)}(z_1) &= -\mathcal{E}_2^{(2)}\cdot\psi_-(L)e^{ikL},\\ \mathcal{E}^{(3)}(z_2) &= -\mathcal{E}_1^{(2)}\cdot\psi_+(L)e^{ikL}.\end{aligned}\right\} \tag{31.09}$$

In the directions toward the opposite end of the conductor, these waves are equivalent to the radiation of an infinite single-wire line excited by the external fields

$$E_z^e = \mathcal{E}_1^{(3)}\cdot\delta(z-z_1),\quad \mathcal{E}_1^{(3)} = \mathcal{E}^{(3)}(z_1)\big|_{\theta=0}, \tag{31.10}$$

$$E_z^e = \mathcal{E}_2^{(3)}\cdot\delta(z_2-z),\quad \mathcal{E}_2^{(3)} = \mathcal{E}^{(3)}(z_2)\big|_{\theta=\pi}. \tag{31.11}$$

Consequently, the quaternary waves again may be investigated as edge waves radiated by the semi-infinite conductors $(-\infty, z_2)$ and (z_1, ∞) with their excitation by the external fields (31.10) and (31.11). Using the reciprocity principle, we easily obtain

$$\left.\begin{aligned}E_\theta^{(4)}(z_1) = H_\varphi^{(4)}(z_1) &= \frac{\mathcal{E}^{(3)}(z_1)}{2\sin\theta\ln\frac{\gamma ka\sin\theta}{2i}}\frac{e^{ikR}}{R}e^{-ikz_1\cos\theta},\\ E_\theta^{(4)}(z_2) = H_\varphi^{(4)}(z_2) &= \frac{\mathcal{E}^{(3)}(z_2)}{2\sin\theta\ln\frac{\gamma ka\sin\theta}{2i}}\frac{e^{ikR}}{R}e^{-ikz_2\cos\theta},\end{aligned}\right\} \tag{31.12}$$

where

$$\left.\begin{aligned}\mathcal{E}^{(4)}(z_1) &= -\mathcal{E}_2^{(3)}\cdot\psi_-(L)e^{ikL},\\ \mathcal{E}^{(4)}(z_2) &= -\mathcal{E}_1^{(3)}\cdot\psi_+(L)e^{ikL},\end{aligned}\right\} \tag{31.13}$$

In a completely similar way, the n^{th} order edge waves

$$\left.\begin{aligned}E_\theta^{(n)}(z_1) = H_\varphi^{(n)}(z_1) &= \frac{\mathcal{E}^{(n)}(z_1)}{2\sin\theta\ln\frac{\gamma ka\sin\theta}{2i}}\frac{e^{ikR}}{R}e^{-ikz_1\cos\theta},\\ E_\theta^{(n)}(z_2) = H_\varphi^{(n)}(z_2) &= \frac{\mathcal{E}^{(n)}(z_2)}{2\sin\theta\ln\frac{\gamma ka\sin\theta}{2i}}\frac{e^{ikR}}{R}e^{-ikz_2\cos\theta},\end{aligned}\right\} \tag{31.14}$$

are found. Here

$$\left.\begin{aligned}\mathcal{B}^{(n)}(z_1)&=-\mathcal{B}_2^{(n-1)}\cdot\psi_-(L)e^{ikL},\\ \mathcal{B}^{(n)}(z_2)&=-\mathcal{B}_1^{(n-1)}\cdot\psi_+(L)e^{ikL}\end{aligned}\right\}\qquad(31.15)$$

and

$$\mathcal{B}_1^{(n)}=\mathcal{B}^{(n)}(z_1)\big|_{b=0},\quad \mathcal{B}_2^{(n)}=\mathcal{B}^{(n)}(z_2)\big|_{b=0}.\qquad(31.16)$$

Thus, the field arising with multiple diffractions (starting with the second) may be represented in the following form:

$$\sum_{n=2}^{\infty}[E_\phi^{(n)}(z_1)+E_\phi^{(n)}(z_2)]=$$
$$=\frac{1}{2\sin\vartheta\ln\frac{2i}{\gamma ka\sin\theta}}\frac{e^{ikR}}{R}\left[\sum_{n=2}^{\infty}\mathcal{B}^{(n)}(z_1)e^{-ikz_1\cos\theta}+\right.$$
$$\left.+\sum_{n=2}^{\infty}\mathcal{B}^{(n)}(z_2)e^{-ikz_2\cos\theta}\right].\qquad(31.17)$$

where

$$\sum_{n=2}^{\infty}\mathcal{B}^{(n)}(z_1)=$$
$$=\mathcal{B}^{(2)}(z_1)+[\mathcal{B}_1^{(2)}\cdot\psi(L)e^{ikL}-\mathcal{B}_2^{(2)}]\frac{\psi_-(L)}{D}e^{ikL},\qquad(31.18)$$

$$\sum_{n=2}^{\infty}\mathcal{B}^{(n)}(z_2)=$$
$$=\mathcal{B}^{(2)}(z_2)+[\mathcal{B}_2^{(2)}\cdot\psi(L)e^{ikL}-\mathcal{B}_1^{(2)}]\frac{\psi_+(L)}{D}e^{ikL},\qquad(31.19)$$

and the functions $\mathcal{B}^{(2)}(z_{1,2})$ and $\mathcal{B}_{1,2}^{(2)}$ are determined by Equations (30.31), (30.35), (31.02) and (31.04). We will not write out here the rather unwieldy final expression for this field, but we will proceed with a calculation of the total field scattered by a vibrator.

§ 32. Total Fringing Field

Before beginning the derivation of the expression for the scattering characteristic, let us make the following observation. The

functions ϕ which enter into Equation (30.04) satisfy relationships (30.05), and may be found by factoring. However, our investigation of the successive waves arising with diffraction at the conductor's ends was approximate. Therefore, it makes no sense to use the precise Expression (30.04) for the primary field. We shall use the approximation expressions for the function Φ

$$\left.\begin{aligned}\Phi(-k\cos\vartheta,\ -k\cos\vartheta_0) &= \ln\frac{i}{\gamma ka\sin\frac{\vartheta}{2}\sin\frac{\vartheta_0}{2}},\\ \Phi(k\cos\vartheta,\ k\cos\vartheta_0) &= \ln\frac{i}{\gamma ka\cos\frac{\vartheta}{2}\cos\frac{\vartheta_0}{2}},\end{aligned}\right\} \tag{32.01}$$

which were obtained by the variational method and have a precision which is sufficient for our purpose (see [83]). More precisely speaking, we will use approximation Equations (32.01) in conjunction with the rigorous Expression (30.05), and we will set

$$\left.\begin{aligned}\frac{1}{\Phi(-k\cos\vartheta,\ -k\cos\vartheta_0)} &= \frac{\ln\frac{i}{\gamma ka\cos\frac{\vartheta}{2}\cos\frac{\vartheta_0}{2}}}{\ln\frac{2i}{\gamma ka\sin\vartheta}\ln\frac{2i}{\gamma ka\sin\vartheta_0}},\\ \frac{1}{\Phi(k\cos\vartheta,\ k\cos\vartheta_0)} &= \frac{\ln\frac{i}{\gamma ka\sin\frac{\vartheta}{2}\sin\frac{\vartheta_0}{2}}}{\ln\frac{2i}{\gamma ka\sin\vartheta}\ln\frac{2i}{\gamma ka\sin\vartheta_0}}.\end{aligned}\right\} \tag{32.02}$$

Then the primary field will equal

$$\begin{aligned}E_\vartheta^{(1)} = H_\varphi^{(1)} = &-\frac{iE}{2(\cos\vartheta+\cos\vartheta_0)\ln\frac{2i}{\gamma ka\sin\vartheta}\ln\frac{2i}{\gamma ka\sin\vartheta_0}}\cdot\frac{e^{ikR}}{kR}\times\\ \times\Bigg[&\operatorname{ctg}\frac{\vartheta_0}{2}\operatorname{ctg}\frac{\vartheta}{2}\ln\frac{i}{\gamma ka\cos\frac{\vartheta}{2}\cos\frac{\vartheta_0}{2}}e^{-ikz_1(\cos\vartheta+\cos\vartheta_0)}\\ &-\operatorname{tg}\frac{\vartheta_0}{2}\operatorname{tg}\frac{\vartheta}{2}\ln\frac{i}{\gamma ka\sin\frac{\vartheta}{2}\sin\frac{\vartheta_0}{2}}e^{-ikz_1(\cos\vartheta+\cos\vartheta_0)}\Bigg].\end{aligned} \tag{32.03}$$

Now summing Expressions (31.17) and (32.03), we find the total field scattered by a passive vibrator in the form

$$E_\theta = H_\varphi = -E \cdot \frac{e^{ikR}}{kR} \cdot F(\theta, \theta_0), \tag{32.04}$$

where

$$F(\theta, \theta_0) = \frac{2i}{(\cos\theta + \cos\theta_0)\sin\theta\sin\theta_0 \ln\frac{2i}{\gamma ka\sin\theta}\ln\frac{2i}{\gamma ka\sin\theta_0}} \times$$

$$\times \left\{ \cos^2\frac{\theta}{2}\cos^2\frac{\theta_0}{2}\ln\frac{i}{\gamma ka\cos\frac{\theta}{2}\cos\frac{\theta_0}{2}} e^{-ikz_1(\cos\theta+\cos\theta_0)} - \right.$$

$$- \sin^2\frac{\theta}{2}\sin^2\frac{\theta_0}{2}\ln\frac{i}{\gamma ka\sin\frac{\theta}{2}\sin\frac{\theta_0}{2}} e^{-ikz_2(\cos\theta+\cos\theta_0)} +$$

$$+ e^{ikL}\left[\sin^2\frac{\theta}{2}\sin^2\frac{\theta_0}{2}\ln\frac{i}{\gamma ka\sin\frac{\theta_0}{2}}\psi_- - \right.$$

$$\left. - \cos^2\frac{\theta}{2}\cos^2\frac{\theta_0}{2}\ln\frac{i}{\gamma ka\cos\frac{\theta}{2}}\psi_+^0\right] e^{-ik(z_1\cos\theta_0 + z_1\cos\theta)} +$$

$$+ e^{ikL}\left[\sin^2\frac{\theta}{2}\sin^2\frac{\theta_0}{2}\ln\frac{i}{\gamma ka\sin\frac{\theta}{2}}\psi_-^0 - \right.$$

$$\left. - \cos^2\frac{\theta}{2}\cos^2\frac{\theta_0}{2}\ln\frac{i}{\gamma ka\cos\frac{\theta_0}{2}}\psi_+\right] e^{-ik(z_2\cos\theta + z_1\cos\theta_0)} -$$

$$- \frac{(\cos\theta_0 + \cos\theta_0)\ln\frac{i}{\gamma ka}}{2D} e^{2ikL}[\psi_+^0\psi e^{ikL - ikz_2\cos\theta_0} -$$

$$- \psi_-^0 e^{-ikz_1\cos\theta_0}]\psi_- e^{-ikz_1\cos\theta} -$$

$$- \frac{(\cos\theta + \cos\theta_0)\ln\frac{i}{\gamma ka}}{2D} e^{2ikL}[\psi_-^0\psi e^{ikL - ikz_1\cos\theta_0} -$$

$$\left. - \psi_+^0 e^{-ikz_2\cos\theta_0}]\psi_+ e^{-ikz_2\cos\theta}\right\}, \tag{32.05}$$

in which all the functions $\psi_\pm$ and $\psi_\pm^0$ have the argument L. The resulting expression, despite its complexity, has a clear physical meaning. Actually, the first term in the braces corresponds to the primary edge wave radiated by the conductor's end $z = z_1$; the second term corresponds to the primary wave radiated by the conductor's end $z = z_2$. The terms included in the first pair of brackets refer to the secondary wave departing from the end $z = z_1$, and the terms in the second set of brackets refer to the secondary wave departing from the end $z = z_2$. The remaining terms describe the sum of all subsequent waves arising with multiple diffraction and have a resonance character. The resonance begins with $L = z_2 - z_1 \approx n\cdot\lambda/2 (n = 1, 2, 3...)$ when $\Omega \approx 0$.

Another important feature of the scattering characteristic is that it satisfies the reciprocity principle — that is, it does not change its value with a mutual interchange of ϑ and ϑ_0. One may also show that the vibrator does not radiate in the directions along its axis, and it does not scatter electromagnetic waves with glancing irradiation, that is,

$$F(0, \vartheta_0) = F(\pi, \vartheta_0) = F(\vartheta, 0) = F(\vartheta, \pi) = 0. \tag{32.06}$$

Furthermore, using representation (28.25) for the functions ψ and $\psi_{\pm}$, we obtain the following expression for scattering characteristic (32.05) in the direction of the mirror-reflected ray ($\vartheta = \pi - \vartheta_0$):

$$\begin{aligned}
F(\pi-\vartheta_0, \vartheta_0) = &-\frac{kL}{2i\ln\frac{2i}{\gamma ka\sin\vartheta_0}} + \\
&+ kL\,\frac{(\psi_+^0)^2 E\left(2kL\sin^2\frac{\vartheta_0}{2}\right) + (\psi_-^0)^2 E\left(2kL\cos^2\frac{\vartheta_0}{2}\right)}{4\left(\ln\frac{2i}{\gamma ka\sin\vartheta_0}\right)^2} + \\
&+ \frac{i}{\left(\sin\vartheta_0 \ln\frac{2i}{\gamma ka\sin\vartheta_0}\right)^2}\left\{\ln\frac{2i}{\gamma ka\sin\vartheta_0} - \frac{1}{2} + \right. \\
&+ \left(\frac{1}{2}\psi_+^0\cos^2\frac{\vartheta_0}{2} - \ln\frac{i}{\gamma ka\sin\frac{\vartheta_0}{2}}\right)\psi_+^0 e^{ikL(1-\cos\vartheta_0)} + \\
&+ \left(\frac{1}{2}\psi_-^0\sin^2\frac{\vartheta_0}{2} - \ln\frac{i}{\gamma ka\cos\frac{\vartheta_0}{2}}\right)\psi_-^0 e^{ikL(1+\cos\vartheta_0)} - \\
&- \frac{\ln\frac{i}{\gamma ka}}{D} e^{2ikL}\left[\psi_+^0\psi_- e^{ikL(1-\cos\vartheta_0)} - \psi_-^0\right]\psi_+^0 - \\
&\left. - \frac{\ln\frac{i}{\gamma ka}}{D} e^{2ikL}\left[\psi_-^0\psi_+ e^{ikL(1+\cos\vartheta_0)} - \psi_+^0\right]\psi_-^0\right\}.
\end{aligned} \tag{32.07}$$

With glancing irradiation of a vibrator, when $\vartheta_0 = 0$ or $\vartheta_0 = \pi$, it follows from this that $F(\pi, 0) = F(0, \pi) = 0$.

Now assuming that $\vartheta_0 = \frac{\pi}{2}$ in Equation (32.07), we obtain the relationship

$$\begin{aligned}
F\left(\frac{\pi}{2}, \frac{\pi}{2}\right) = &-\frac{kL}{2\ln\frac{2i}{\gamma ka}} + kL\,\frac{\psi^2 E(kL)}{2\left(\ln\frac{2i}{\gamma ka}\right)^2} + \\
&+ \frac{i}{\left(\ln\frac{2i}{\gamma ka}\right)^2}\left[\ln\frac{2i}{\gamma ka} - \frac{1}{2} + \left(\frac{1}{2}\psi - 2\ln\frac{\sqrt{2}\,i}{\gamma ka}\right)\psi e^{ikL} + \right.
\end{aligned}$$

Equation continued on next page

$$\left. + 2\psi^2 \cdot \frac{\ln \frac{i}{\gamma ka}}{1 + \psi e^{ikL} e^{2ikL}} \right],$$
$$\bar{\psi} = \psi^0_{\pm}\Big|_{\vartheta_0 = \frac{\pi}{2}}.$$

(32.08)

which characterizes the reflected field magnitude with normal irradiation.

Let us also write the expressions for the function $F(\vartheta, \vartheta_0)$ which corresponds to the radar case when the observation and irradiation directions coincide $(\vartheta = \vartheta_0)$

$$F(\vartheta, \vartheta) =$$
$$= \frac{i}{\left(\sin\vartheta \ln \frac{2i}{\gamma ka \sin\vartheta}\right)^2 \cos\vartheta} \left\{ \cos^4 \frac{\vartheta}{2} \ln \frac{i}{\gamma ka \cos^2 \frac{\vartheta}{2}} e^{-2ikz_0 \cos\vartheta} - \right.$$
$$- \sin^4 \frac{\vartheta}{2} \ln \frac{i}{\gamma ka \sin^2 \frac{\vartheta}{2}} e^{-2ikz_0 \cos\vartheta} +$$
$$+ 2 \left[\sin^4 \frac{\vartheta}{2} \ln \frac{i}{\gamma ka \sin \frac{\vartheta}{2}} \psi_-(L) - \right.$$
$$\left. - \cos^4 \frac{\vartheta}{2} \ln \frac{i}{\gamma ka \cos \frac{\vartheta}{2}} \psi_+(L) \right] e^{-ik(z_0 + z_0)\cos\vartheta + ikL} -$$
$$- 2 \frac{\cos\vartheta}{D} \ln \frac{i}{\gamma ka} \psi(L) \psi_+(L) \psi_-(L) e^{-ik(z_0 + z_0)\cos\vartheta + 2ikL} +$$
$$+ \frac{\cos\vartheta}{D} \ln \frac{i}{\gamma ka} \cdot [\psi_-^2(L) e^{-2ikz_0 \cos\vartheta} +$$
$$\left. + \psi_+^2(L) e^{-2ikz_0 \cos\vartheta}] e^{2ikL} \right\}. \qquad (32.09)$$

We may show that when $\vartheta = \frac{\pi}{2}$ Equation (32.09) leads to Expression (32.08).

The scattering characteristic (32.05) which was found above was obtained by summing all the waves formed with multiple diffraction. Such a method is very graphic, but somewhat lengthy. One may arrive at the same result more quickly if it is assumed that the edge wave diffraction process at the passive vibrator's ends takes place, starting with tertiary action, the same as at the end of a transmitting

vibrator. Therefore, the passive vibrator's scattering diagram may be directly sought in the form

$$F(\theta, \theta_0) = \frac{2l}{\sin\theta \sin\theta_0 \ln \frac{2l}{\gamma ka \sin\theta}} \ln \frac{2l}{\gamma ka \sin\theta_0} \cdot f(\theta, \theta_0), \tag{3.7.10}$$

where

$$f(\theta, \theta_0) = \frac{1}{\cos\theta + \cos\theta_0} \times$$
$$\times \left\{ \cos^2\frac{\theta}{2} \cos^2\frac{\theta_0}{2} \ln \frac{l}{\gamma ka \cos\frac{\theta}{2} \cos\frac{\theta_0}{2}} e^{-ikz_1(\cos\theta + \cos\theta_0)} - \right.$$
$$- \sin^2\frac{\theta}{2} \sin^2\frac{\theta_0}{2} \ln \frac{l}{\gamma ka \sin\frac{\theta}{2} \sin\frac{\theta_0}{2}} e^{-ikz_2(\cos\theta + \cos\theta_0)} +$$
$$+ e^{ikl} \left[\sin^2\frac{\theta}{2} \sin^2\frac{\theta_0}{2} \ln \frac{l}{\gamma ka \sin\frac{\theta_0}{2}} \psi_-(L) - \right.$$
$$- \cos^2\frac{\theta}{2} \cos^2\frac{\theta_0}{2} \ln \frac{l}{\gamma ka \cos\frac{\theta}{2}} \left. \psi_+^*(L) \right] e^{-ikz_1\cos\theta_0 + z_2\cos\theta)} +$$
$$+ e^{ikl} \left[\sin^2\frac{\theta}{2} \sin^2\frac{\theta_0}{2} \ln \frac{l}{\gamma ka \sin\frac{\theta}{2}} \psi_-^*(L) \right.$$
$$\left. \left. - \cos^2\frac{\theta}{2} \cos^2\frac{\theta_0}{2} \ln \frac{l}{\gamma ka \cos\frac{\theta_0}{2}} \psi_+(L) \right] e^{-ik(z_2\cos\theta + z_1\cos\theta_0)} \right\} +$$
$$+ C_1\psi_-(L) e^{-ikz_1\cos\theta} + C_2\psi_+(L) e^{-ikz_2\cos\theta}. \tag{3.7.11}$$

The last two terms in Equation (3.7.11) are the sum of all edge waves starting with the tertiary waves which are propagated from the conductor's ends $z = z_1$ and $z = z_2$, respectively. The constants C_1 and C_2 are determined from the condition

$$f(0, \theta_0) = f(\pi, \theta_0) = 0, \tag{3.7.12}$$

which leads to the system of equations:

$$\left. \begin{aligned} C_1\psi_+(L)e^{ikl} + C_2 &= \frac{1}{2} \ln \frac{l}{\gamma ka} \psi_+^*(L) e^{ikl - ikz_2\cos\theta_0}, \\ C_1 + C_2\psi_+(L)e^{ikl} &= \frac{1}{2} \ln \frac{l}{\gamma ka} \psi_-^*(L) e^{ikl - ikz_1\cos\theta_0}, \end{aligned} \right\} \tag{3.7.13}$$

from which

$$\left.\begin{aligned} C_1 &= -\frac{1}{2D}e^{ikL}\cdot\ln\frac{l}{\gamma ka}\cdot\left[\psi_+^0\psi e^{ikL-ikz_0\cos\theta_0}-\right.\\ &\qquad\left.-\psi_-^0 e^{-ikz_0\cos\theta_0}\right],\\ C_2 &= -\frac{1}{2D}e^{ikL}\cdot\ln\frac{l}{\gamma ka}\cdot\left[\psi_-^0\psi e^{ikL-ikz_0\cos\theta_0}-\right.\\ &\qquad\left.-\psi_+^0 e^{-ikz_0\cos\theta_0}\right]. \end{aligned}\right\} \qquad (32.14)$$

§ 33. A Vibrator Which is Short in Comparison With the Wavelength (a Passive Dipole)

The theory of plane wave scattering by a thin cylindrical vibrator which is discussed in this chapter is based on a number of physical considerations. One good aspect of this theory is the fact that its precision increases with the length of the vibrator, since the current waves whose diffraction we are investigating are expressed more clearly, the longer the vibrator. However, one may also show that for short vibrators, the length of which is small in comparison with the wavelength, the equations derived by us have good precision.

It is clear that a vibrator which is short in comparison with the wavelength acts as a dipole, creating a fringing field

$$E_\theta = H_\varphi = -k^2 p_z \frac{e^{ikR}}{kR}\sin\theta, \qquad (33.01)$$

where the dipole moment p_z may be calculated by solving the electrostatic problem. This dipole moment depends on the dimensions and shape of the vibrator. In accordance with [93], the dipole moment of a cylinder in a uniform electrostatic field E_z equals

$$p_z = D(l)\left(\frac{L}{2}\right)^3\cdot E_z, \qquad (33.02)$$

where $D(l)$ is a dimensionless function $l = L/2a$ which is shown in Figure 75 by the continuous curve. With $l >> 1$, one may calculate the function $D(l)$ by means of the asymptotic expansion

$$D(l) = \frac{2}{3}\left(\frac{1}{\Omega_2}+\frac{0{,}977}{\Omega_2^2}+\ldots\right),\ \Omega_2 = 2\left(\ln 4l - \frac{7}{3}\right). \qquad (33.03)$$

If in this expansion one limits oneself to the first term, then

$$D(l)=\frac{1}{3\left(\ln\frac{4l}{a}-\frac{7}{3}\right)}. \tag{33.04}$$

The results of numerical calculations based on Equations (33.04) are shown in Figure 75 by the dashed curve: we see that the latter equation gives a good precision already with $l \gtrsim 9$.

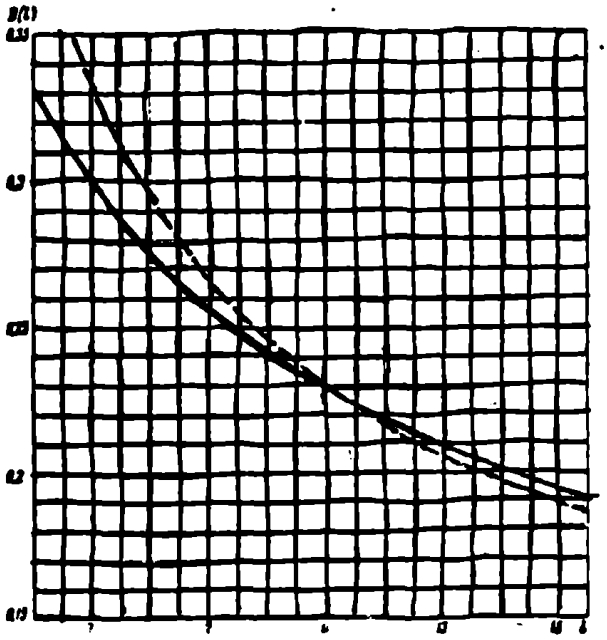

Figure 75. Graph of the function D(l) which determines the cylinder's dipole moment.

Thus, the dipole moment of a vibrator which is short in comparison with the wavelength equals

$$p_z=E\frac{L^3}{24}\frac{\sin\vartheta_0}{\ln\frac{2L}{a}-\frac{7}{3}}\left\{1+O\left[\left(\ln\frac{L}{a}\right)^{-2}\right]\right\}, \tag{33.05}$$

and its scattering characteristic must have the form

$$F(\vartheta, \vartheta_0) = \frac{k^2 L^2}{24} \frac{\sin\vartheta \sin\vartheta_0}{\ln\frac{2L}{a} - \frac{7}{3}} \left\{1 + O\left[\left(\ln\frac{L}{a}\right)^{-2}\right]\right\}. \qquad (33.06)$$

In this section we find the first two terms of the expansion of the vibrator's scattering characteristic F in reciprocal powers of the large parameter L/a (with $\lambda \to \infty$), and we compare them with Expression (33.06). We shall limit ourselves to the case $\vartheta = \vartheta_0 = \frac{\pi}{2}$, when the function F is described by the simpler Equation (32.08).

With small values of the argument z, the functions $\psi(z)$ and $\bar{\psi}(z) = \psi_+|_{\vartheta=\frac{\pi}{2}} = \psi_-|_{\vartheta=\frac{\pi}{2}}$ [see Equations (28.21)] may be represented in the form

$$\left.\begin{aligned} \psi(z) &= 1 - \frac{g(z) - g(0)}{2g(0)} + O\left(\frac{1}{g^2(0)}\right), \\ \bar{\psi}(z) &= 1 - \frac{\bar{g}(z) - \bar{g}(0)}{2\bar{g}(0)} + O\left(\frac{1}{\bar{g}^2(0)}\right). \end{aligned}\right\} \qquad (33.07)$$

The functions g and $\bar{g}$ included here are determined by the equations:

$$g(z) - g(0) = \ln\frac{2\gamma kz}{i} + e^{-2ikz}\int_z^\infty \frac{e^{2ikv}}{v}\,dv, \quad g(0) = \ln\frac{i}{\gamma ka} \qquad (33.08)$$

and

$$\bar{g}(z) - \bar{g}(0) = \ln\frac{\gamma kz}{i} + e^{-ikz}\int_z^\infty \frac{e^{ikv}}{v}\,dv, \quad \bar{g}(0) = \ln\frac{2i}{\gamma ka}. \qquad (33.09)$$

Let us note that Expressions (33.07) completely agree with the corresponding terms of the aysmptotic expansion for the functions ψ and $\bar{\psi}$, which may be obtained from the initial integral equations which determine these functions (see, for example, [81], § 4).

Limiting ourselves in the expansion for the functions $\psi(z)$ and $\bar{\psi}(z)$ to terms of the order of $(kz)^3$, we have

$$\psi(z)=1-\frac{1}{\ln\frac{i}{\gamma ka}}\left[ikz\left(\ln\frac{2\gamma kz}{i}-1\right)+\right.$$
$$\left.+k^2z^2\left(\ln\frac{2\gamma kz}{i}-\frac{3}{2}\right)-i\frac{2}{3}k^3z^3\left(\ln\frac{2\gamma kz}{i}-\frac{11}{6}\right)\right] \tag{33.10}$$

and

$$\bar{\psi}(z)=1-\frac{1}{2\ln\frac{i}{\gamma ka}}\left[ikz\left(\ln\frac{\gamma kz}{i}-1\right)+\right.$$
$$\left.+\frac{k^2z^2}{2}\left(\ln\frac{\gamma kz}{i}-\frac{3}{2}\right)-i\frac{k^3z^3}{6}\left(\ln\frac{\gamma kz}{i}-\frac{11}{6}\right)\right]. \tag{33.11}$$

In addition, terms of the order $\left(\ln\frac{i}{\gamma ka}\right)^{-2}$ are omitted in Expressions (33.10) and (33.11). Now if we substitute these expressions into Equation (32.08), then one should omit terms of the order $\left(\ln\frac{i}{\gamma ka}\right)^{-3}$ in it. Therefore, the function $F\left(\frac{\pi}{2},\frac{\pi}{2}\right)$ may be represented in the form

$$F\left(\frac{\pi}{2},\frac{\pi}{2}\right)=\frac{i}{\left(\ln\frac{2i}{\gamma ka}\right)^2}\left\{\frac{ikL}{2}\left[\ln\frac{2i}{\gamma ka}-E(kL)\right]+\right.$$
$$+\ln\frac{2i}{\gamma ka}-\frac{1}{2}+\frac{1}{2}e^{ikL}-2\bar{\psi}(L)\ln\frac{\sqrt{2}\,i}{\gamma ka}e^{ikL}+$$
$$\left.+\frac{2\ln\frac{i}{\gamma ka}}{1+\psi(L)e^{ikL}}\bar{\psi}^2(L)e^{2ikL}\right\}. \tag{33.12}$$

Furthermore, taking into account Equations (33.10) and (33.11), we find

$$\frac{ikL}{2}\left[\ln\frac{2i}{\gamma ka}-E(kL)\right]=$$
$$=\frac{ikL}{2}\left(\ln\frac{2i}{\gamma ka}-\ln\frac{\gamma kL}{i}-ikL+\frac{k^2L^2}{4}\right), \tag{33.13}$$

$$\ln\frac{2i}{\gamma ka}-\frac{1}{2}+\frac{1}{2}e^{ikL}=$$
$$=\ln\frac{2i}{\gamma ka}+\frac{ikL}{2}-\frac{k^2L^2}{4}-i\frac{k^3L^3}{12}, \tag{33.14}$$

$$2\bar{\psi}(L)\ln\frac{\sqrt{2}\,i}{\gamma ka}e^{ikL}=2\left(1+ikL-\frac{k^2L^2}{2}-i\frac{k^3L^3}{6}\right)\ln\frac{\sqrt{2}\,i}{\gamma ka}-$$
$$-ikL\left(\ln\frac{\gamma kL}{i}-1\right)+k^2L^2\left(\frac{1}{2}\ln\frac{\gamma kL}{i}-\frac{1}{4}\right)+$$
$$+ik^3L^3\left(\frac{1}{6}\ln\frac{\gamma kL}{i}-\frac{1}{18}\right). \tag{33.15}$$

and finally

$$\frac{2\ln\frac{l}{\gamma ka}}{1+\psi(L)e^{ikL}}\bar{\psi}^0(L)e^{2ikL}=$$

$$=-\left(1+i\frac{3}{2}kL-k^2L^2-i\frac{9}{24}k^3L^3\right)\ln\frac{l}{\gamma ka}-$$

$$-\frac{ikL}{2}\ln\frac{\gamma kL}{l}+\frac{ikL}{2}(1+\ln 2)+\frac{k^2L^2}{2}\ln\frac{\gamma kL}{l}-\frac{k^2L^2}{2}(1+\ln 2)+$$

$$+i\frac{5}{24}k^3L^3\ln\frac{\gamma kL}{l}-ik^3L^3\left(\frac{14}{72}+\frac{5\ln 2}{24}\right). \quad (33.16)$$

(33.16)

Using these relationships, it is not difficult to show that

$$F\left(\frac{\pi}{2},\ \frac{\pi}{2}\right)=\frac{k^2L^2}{24}\left\{\frac{1}{\ln\frac{L}{a}}+\frac{\frac{7}{3}-\ln 2}{\left(\ln\frac{L}{a}\right)^2}+O\left[\left(\ln\frac{L}{a}\right)^{-3}\right]\right\}. \quad (33.17)$$

The equation which has been found may be rewritten in the form

$$F\left(\frac{\pi}{2};\ \frac{\pi}{2}\right)=\frac{k^2L^2}{24\left(\ln\frac{2L}{a}-\frac{7}{3}\right)}\left\{1+O\left[\left(\ln\frac{L}{a}\right)^{-2}\right]\right\}. \quad (33.18)$$

It completely agrees with Equation (33.06) which follows from [92].

This result confirms the correctness of scattering characteristic (32.05) calculated by us, and shows that it is applicable for vibrators of any length.

§ 34. The Results of Numerical Calculations

The function $F(0, \theta_0)$ enables one to calculate the integral scattering thickness S and the effective scattering area σ of a passive vibrator. The integral scattering thickness is determined by the relationship

$$S=\frac{P}{p}, \quad (34.01)$$

where

$$p=\frac{c}{8\pi^2}E_0^2 \quad (34.02)$$

is the energy flux density in the incident wave averaged over an oscillation period, and

$$P = \frac{c}{8\pi} \operatorname{Re} \int \mathbf{n} [\mathbf{E}\mathbf{H}^*] dS = \frac{1}{2} E \sin \vartheta_0 \operatorname{Re} \int_{z_1}^{z_2} J(z) e^{ikz \cos \vartheta_0} dz \qquad (34.03)$$

is the value of the energy scattered by the vibrator into the surrounding space averaged over a period. Since one may represent the fringing field in the far zone in the direction $\vartheta = \pi - \vartheta_0$ by the equations

$$E_\vartheta = H_\varphi = -\frac{ik}{c} \sin \vartheta_0 \frac{e^{ikR}}{R} \cdot \int_{z_1}^{z_2} J(z) e^{ikz \cos \vartheta_0} dz \qquad (34.04)$$

and

$$E_\vartheta = H_\varphi = -E \frac{e^{ikR}}{kR} \cdot F(\pi - \vartheta_0, \vartheta_0), \qquad (34.05)$$

then, having determined from this the integral

$$\int_{z_1}^{z_2} J(z) e^{ikz \cos \vartheta_0} dz = \frac{cE}{ik^2 \sin \vartheta_0} \cdot F(\pi - \vartheta_0, \vartheta_0) \qquad (34.06)$$

we obtain

$$S = \frac{\lambda^2}{\pi} \cos^2 \alpha \cdot \ln F(\pi - \vartheta_0, \vartheta_0). \qquad (34.07)$$

Calculations of the quantity S/L^2 (with $\alpha = 0$, $\vartheta_0 = \frac{\pi}{2}$), performed by us for vibrators with the parameter $\chi = \frac{1}{2 \ln ka}$ taking the values $\chi = -0.05$ and $\chi = -0.1$, are found to be in agreement with the results of Leontovich and Levin [85]. With $\chi = -0.1$, our curve (the dotted line in Figure 76) is only slightly displaced in the direction of longer wavelengths and gives slightly higher resonance peaks.

The effective scattering area σ according to the definition equals

$$\sigma(\vartheta, \vartheta_0) = \frac{P_r \cdot 4\pi R^2}{p}, \qquad (34.08)$$

where p is the known quantity (34.02) and

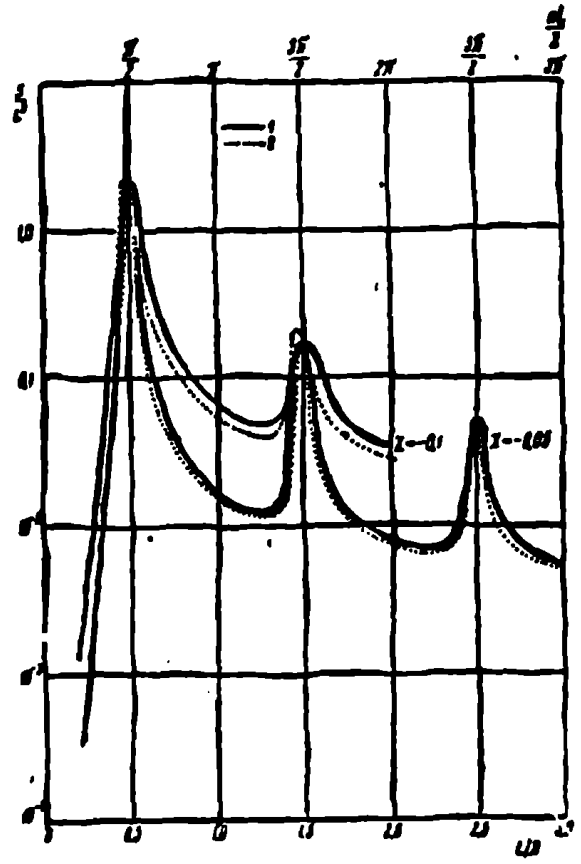

Figure 76. The integral scattering thickness of a vibrator as a functior. of its length (with normal incidence of a plane wave). Curves 1 were calculated by Leontovich and Levin [85]. Curves 2 were calculated on the basis of Equation (34.07).

$$P_r = \frac{c}{8\pi}|E_\theta|^2 = \frac{c}{8\pi}\frac{|F(\theta,\theta_0)|^2}{k^2R^2}E^2 \qquad (34.09)$$

represents the average value of the energy flux density scattered by the vibrator in the direction θ . Consequently

$$\sigma(\theta,\theta_0) = \frac{\lambda^2}{\pi}\cos^2\alpha\cdot|F(\theta,\theta_0)|^2. \qquad (34.10)$$

If the receiving antenna operates with the same polarization as the transmitting antenna, then the corresponding value of the effective area will equal

$$\sigma_a(\vartheta, \vartheta_0) = \frac{\lambda^2}{\pi}\cos^2\alpha \cdot |F(\vartheta, \vartheta_0)|^2 \qquad (34.11)$$

In the case of radar when the transmitting and receiving antennas are combined and the polarization is arbitrary, the vibrator's scattering properties are characterized by the average value

$$\bar{\sigma}(\vartheta) = \frac{1}{2\pi}\int_0^{2\pi} \sigma_a(\vartheta, \vartheta_0)\, d\alpha = \frac{3\lambda^2}{8\pi}|F(\vartheta, \vartheta_0)|^2. \qquad (34.12)$$

In Figures 77 and 78, the results of calculations performed on the basis of Equations (34.12) and (32.08) for the case of normal irradiation $\left(\vartheta = \frac{\pi}{2}\right)$ are represented by the dotted lines. Figure 77 illustrates the dependence of the function $\bar{\sigma}$ on the quantity kL with a given value of $\Omega_p = 2\ln\frac{2L}{a} = 15$. — that is, when the ratio of the vibrator's length to its diameter equals L/2a = 452. In Figure 78 the graph of the function $\bar{\sigma}$ is constructed as a function of the frequency $f = c/\lambda \cdot 10^{-6}$ (in megahertz) for the prescribed parameters L = 5 cm and Ω_p = 15. Here the curves plotted by Lindroth [79] are drawn with a continuous line, and the curve in Figure 77 calculated by Van Vleck et al. [86] is traced by the dash-dot-curve.

The curves of Lindroth and Van Vleck were calculated by integrating the current which is found as a result of the approximate solution of the integral equation. However, this procedure was performed in [79] and [86] in a different way. Lindroth obtained an expression for the fringing field in the form of an expansion in reciprocal powers of the parameter Ω_p. The expression includes terms of the order of Ω_p^{-3}. In [86] a different kind of approximation was used which led, as can be seen from Figure 77, to rather rough result especially in the resonance region. Our curve (the dotted area) agrees almost everywhere within the limits of graphical precision wit the curve of Lindroth. A noticeable divergence is observed only in the magnitude of the first resonance peak.

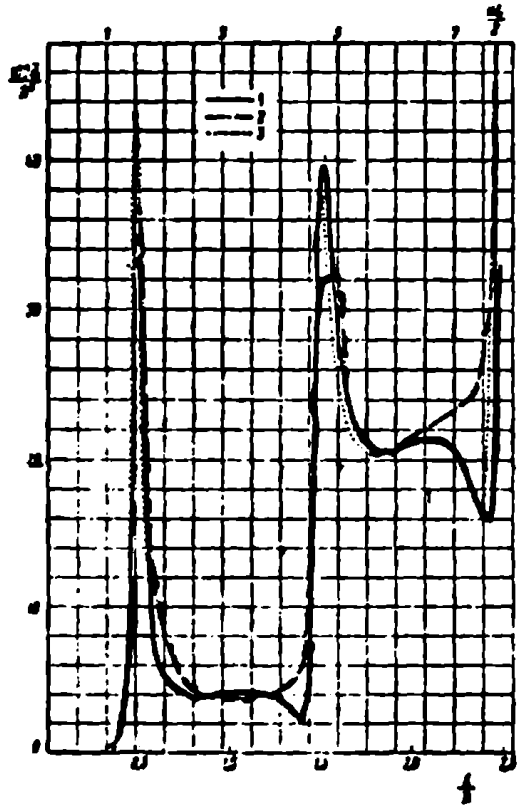

Figure 77. The effective scattering area of a vibrator as a function of its length with normal incidence of a plane wave. Curve 1 was calculated by Lindroth [79]; curve 2 was calculated by Van Vleck [86] by means of the method of integral equations; curve 3 was calculated on the basis of Equation (34.12).

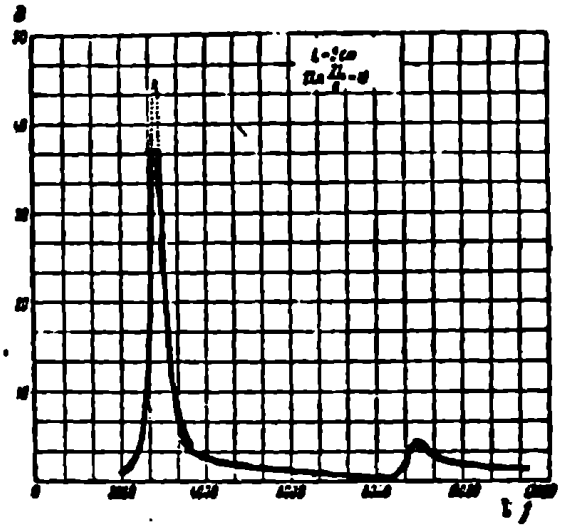

Figure 78. The effective scattering area of a vibrator as a function of the frequency $f = c/\lambda \cdot 10^{-6}$ (in megahertz) with normal incidence of a plane wave. The designations are the same as those in Figure 77.

In Figure 79 and 80 radar diagrams are constructed for vibrators of a length $L = 0.5\lambda$ and $L = 2\lambda$ with the specified value $L/a = 900$. Curves 1 were calculated by Tai using the variational method [87]. Curves 3 were obtained by the method of induced emf [86]; curves 4 were obtained by the above-indicated method of Van Vleck. The results of calculations based on our Equations (34.12), (32.08) and (32.09) are shown by curves 2.

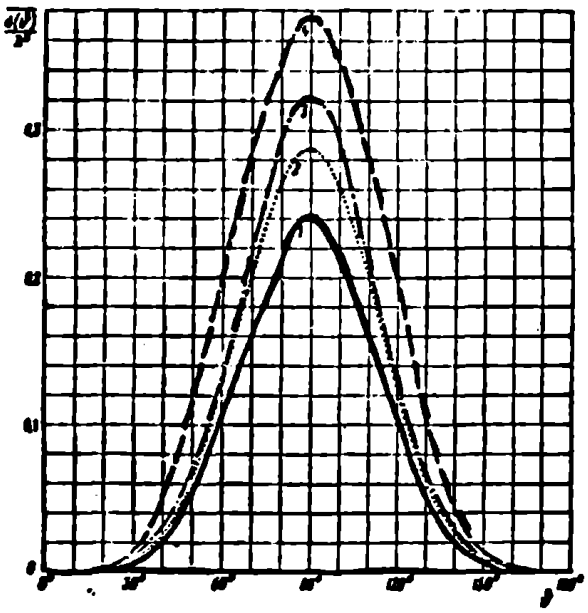

Figure 79. A comparison of the diagrams for the effective scattering area of a half-wave vibrator calculated by various methods.

Curve 1 was calculated by Tai [87] by the variational method;

Curve 2 was calculated on the basis of Equation (34.12);

Curve 3 was calculated by the method of induced emf (in the work of Van Vleck [86]);

Curve 4 was calculated by Van Vleck [86] by the method of integral equations.

In the cited references, the fringing field was calculated by the direct integration of the current. In order to determine the current, various approximation methods were used. In the variational method [87] a functional was constructed for this purpose which was stationary in respect to small current variations. Then the current was sought in the form of some function containing undetermined constants. These constants were found from the condition of the functional's stationarity. This method enables one to rather easily

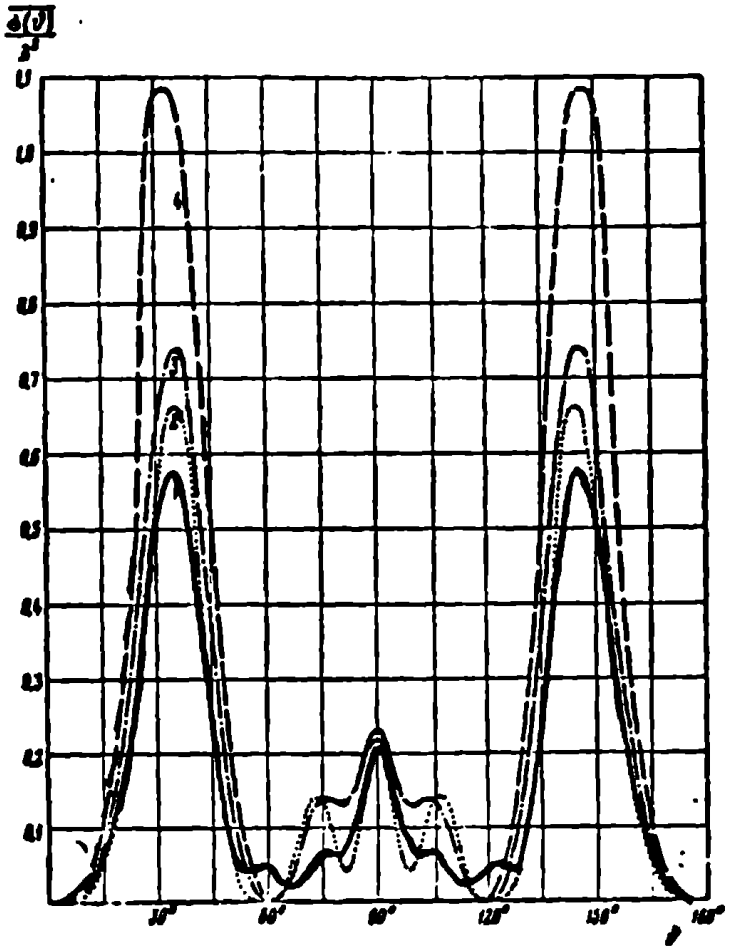

Figure 80. Diagrams for the effective scattering area of a vibrator calculated by various methods. The designations are the same as those in Figure 79:

$L = 2\lambda$

obtain the first approximation; however, its results, especially for long conductors, may depend in a substantial way on the form of the trial function. In the induced emf method [86], the current is sought in the form of a combination of trigonometric functions with unknown coefficients. These coefficients are determined by using the law of conservation of energy. This is the simplest method, but it has a number of serious defects. Thus, as a consequence of incorrectly accounting for the current component having the incident field phase,

it leads to inaccurate results in the case of odd resonances (especially for long conductors), and it does not give the displacement of the resonance peaks from the values $\lambda = 2L/n$ ($n = 1, 3, 5....$) in the direction of longer wavelengths.

The results obtained by us are also approximate. However, our Equation (32.05) satisfies the reciprocity principle, and is applicable for any length vibrator. For very short vibrators $L << \lambda$, it changes into the asymptotic expression for the scattering characteristic of a dipole (see § 33). For vibrators with a length of several wavelengths ($L \approx n\lambda$, $n = 1, 2, 3, 4$), Equation (32.05) gives satisfactory results. Calculations performed on its basis for radar reflection with normal irradiation agree with the results of Lindroth. Good agreement is also observed with the results of Leontovich and Levin for the integral scattering characteristic. With an increase of the vibrator's length, the precision of this equation increases, and in this way it is favorably distinguished from the equations proposed for the scattering characteristics by other authors.

Moreover, the divergence between the various approximation methods indicates the necessity of performing rather detailed calculations based on precise methods, for the purpose of evaluating the actual error of the approximation methods. Such calculations may be performed, for example, by means of the method discussed in References [88, 89] or [91].

FOOTNOTE

Footnote (1) on page 177.

Let us note that one may refine Equation (28.04) by multiplying its righthand member by the factor θ_0 (usually $\theta_0 \tilde{\approx} 1$) calculated in Reference [84].

CONCLUSION

In this book, the solution of a number of diffraction problems was obtained based on the approximate consideration of the field perturbation in the vicinity of a sharp bend of the surface or a sharp edge. Equations were derived for the scattering characteristics, or in certain cases (chapter IV), for the radar reflection thicknesses with a specified irradiation direction. The expressions which have been found have a clear physical meaning. They satisfy the reciprocity principle, and they are convenient for making calculations.

The results obtained enable us to form a more complete concept of the applicability limits of the physical optics approach. It is usually customary to assume that this approach gives reliable results only if the body's dimensions are large in comparison with the wavelength. Such an opinion is based on the following argument. The physical optics approach considers only the radiation from the uniform part of the current, and does not include in the calculations the nonuniform part of the current which is concentrated in the vicinity of the bends and the sharp edges. Therefore, when the body's dimensions are considerably larger than the wavelength, the nonuniform part of the current occupies a relatively small part of the body's surface. Therefore, one would think that its influence would be small.

But in actuality it turns out that the reliability of physical optics results depends substantially, not only on the body's dimensions, but also on the body's shape and the irradiation and observation directions. For example, with the glancing incidence of a wave on the flat face of a body, the edge zone occupied by the nonuniform part of the current is considerably broadened and the effect of this current becomes substantial. Therefore, physical optics gives qualitatively incorrect results for the field scattered by flat plates with glancing irradiation independent of the ratio between their dimensions and the wavelength. The effect of the nonuniform part of

the current becomes noticeable also in those directions where, according to physical optics, the fringing field must be equal to zero or have a small value.

The problem of diffraction of a plane wave with its incidence on a cone along its axis (§ 17) serves as a clear example of how important the above-indicated factors are. Although in this case the nonuniform part of the current, concentrated near the cone's vertex, has practically no influence on the scattering, nevertheless, the physical optical approach gives values for the radar thickness which are tens of decibels smaller than the experimental values, even with large dimensions of the cone. The deciding factor here is the nonuniform part of the current flowing in the vicinity of the sharp circular base rim of the conical surface; the nonuniform part of the current has an especially large value for sharply pointed cones.

Another interesting example of a similar nature is the scattering of a plane wave by a finite paraboloid of rotation (§ 18) where the physical optics approach leads to qualitatively incorrect results. The effective scattering area calculated in this approach turns out to be a periodic function of the paraboloid length, and with certain lengths it becomes zero which most certainly does not correspond to reality.

The investigation of the diffraction of edge waves shows (Chapter V) that for flat plates one may limit oneself to consideration of secondary diffraction, if their linear dimensions are one-and-a-half to two times larger than the wavelength.

Let us note that we attempted to obtain equations for the scattering characteristics which would possess physical visualizability and which would be convenient for making calculations. In keeping with this, we were obliged to introduce various kinds of interpolation equations and simplified equations which satisfy the formulated requirements, but in return are not in the general case the dominant terms of the rigorous asymptotic expansion in powers of the small parameter λ/a.

Our purpose was not to calculate the current on the body's surface, the field in the near zone, or the integral scattering thickness. These questions are investigated in a number of other works based on the physical theory of diffraction which were already enumerated in § 25. In them, in particular, the first terms of asymptotic expansions in powers of λ/a were obtained for the integral thickness which characterizes the total power scattered by a body. However, in these works, as a rule, equations are missing for the scattering characteristics which are valid with any direction of irradiation and observation. Therefore, the results of this book and the indicated works mutually supplement one another.

At present, only a limited number of diffraction problems have yielded to theoretical studies, as a result of which experimental studies of diffraction by various bodies have taken on great importance. In Chapter VI an experimental method was discussed which enabled one to isolate in a "pure form", and to measure, the field from the nonuniform part of the current excited by a plane wave on a metal body of any shape. In the same chapter, it was shown that the well-known phenomenon of depolarization of the wave reflected from a body which is found in free space is produced by the nonuniform part of the current, or, in other words, by the surface distortion.

The investigation carried out in Chapter VII for the problem of diffraction by a thin, finite length cylindrical conductor represents a natural development and completion of the method of considering the multiple diffraction of edge waves which was applied in Chapter V. In Chapter VII equations were derived for the scattering diagram which are suitable for vibrators of an arbitrary length with any irradiation and observation directions.

The results obtained in this book show the fruitfulness of physical diffraction theory, and enable one to arrive at the solution of other more complicated problems. Such problems may be divided into two classes. Problems which may now already be solved on the basis of the known results of diffraction theory are related to the

first class. As an example of such a problem, one may point to the problem of diffraction of a plane wave by a frustum of a cone or by an infinitely long cylinder with a polygonal transverse cross section. Those problems whose solution requires obtaining (using the methods of mathematical diffraction theory) a whole series of new results must be referred to the second class. In particular, in order to give a complete solution to the diffraction problem of a finite cone, it is necessary to have more precise knowledge on the diffraction laws of a semi-infinite cone.

Summing up, one may say that physical diffraction theory aids one in analyzing and sorting out the diffraction phenomena for complex bodies, poses problems for treatment by mathematical diffraction theory, and enables one to effectively apply the rigorous results of mathematical diffraction theory for the solution of new problems.

In conclusion, I express my deep thanks to L. A. Vaynshteyn for his valuable advice and regular discussion of the questions to which this book is devoted, and also for his attentive reading of the manuscript and for a number of useful remarks. I also take this opportunity to express sincere thanks to M. L. Levin for his interest in this work and his helpful remarks.

REFERENCES

1. Фок В. А. Обобщение отражательных формул на случай отражения произвольной волны от поверхности произвольной формы. ЖЭТФ, 20, 961, 1950.

2. Антенны сантиметровых волн, ч. I. Пер. с англ. под ред. Я. Н. Фельда. Изд-во «Советское радио», 1950.

3. Мейкер Дж. Р. Дифракция и рассеяние радиоволн. Пер. с англ. под ред. Л. А. Вайнштейна. Изд-во «Советское радио». 1958.

4. Вайнштейн Л. А., Электромагнитные волны. Изд-во «Советское радио», 1957.

5. Потехин А. И. Некоторые задачи дифракции электромагнитных волн. Изд-во «Советское радио», 1948.

6. Baker B. B. and Copson E. T. The mathematical theory of Huygens' principle. Oxford, 1939.

7. Уфимцев П. Я. Приближенный расчет дифракции плоских электромагнитных волн на некоторых металлических телах, ч. I. Дифракция на клине и ленте. ЖТФ, 27, № 8, 1810—1819, 1957.

8. Уфимцев П. Я. Приближенный расчет дифракции плоских электромагнитных волн на некоторых металлических телах. ч. II. Дифракция на диске и конечном цилиндре. ЖТФ, 28, № 11, 2601—2616, 1958.

9. Уфимцев П. Я. Вторичная дифракция на ленте. ЖТФ, 28, № 3, 569—582, 1958.

10. Уфимцев П. Я. Вторичная дифракция на диске. ЖТФ, 28, № 3, 583—591, 1958.

11. Уфимцев П. Я. Симметричное облучение конечных тел вращения. «Радиотехника и электроника», 6, № 4, 559—567, 1961.

12. Майзельс Е. Н., Уфимцев П. Я. Отражение электромагнитных волн круговой поляризации от металлических тел. «Радиотехника и электроника», 5, № 12, 1925—1928, 1960.

13. Уфимцев П. Я. Об отражении металлическими телами радиоволн круговой поляризации. «Радиотехника и электроника», № 12, 2094, 1961.

14. Уфимцев П. Я. Дифракция плоских электромагнитных волн на тонком цилиндрическом проводнике. «Радиотехника и электроника», 7, № 2, 260—269, 1962.

15. Schwarzschild K. Beugung und Polarisation des Lichts. Mathematische Annalen. 55, 177, 1902.

16. Франк Ф. и Мизес Р. Дифференциальные и интегральные уравнения математической физики. ОНТИ. 1937.

17. Фок В. А. Распределение токов, возбуждаемых плоской волной на поверхности проводника. ЖЭТФ, 15, № 12, 693—702, 1945.

18. Фок В. А. Дифракция радиоволн вокруг земной поверхности. М.-Л. Изд-во АН СССР, 1946.

19. Вайнштейн Л. А. Дифракция электромагнитных и звуковых волн на открытом конце волновода. Изд-во «Советское радио», 1953.

20. Oberhettinger F. On the diffraction and reflection on waves and pulses by wedges and corners. Journ. Research NBS, 61, № 5, 343—365, 1958.

21. Ватсон Г. Н. Теория бесселевых функций. Часть первая. И. Л., 1949.

22. Pauli W. On asymptotic series for functions in the theory of diffraction of light. Physical Review, 54, № 11, 924—931, 1938.

23. Мак-Лахлан Н. В. Теория и приложение функций Матье. И. Л., 1953.

24. Meixner J. and Andrejewski W. Strenge Theorie der Beugung ebener elektromagnetischer Wellen an der vollkommen leitenden Kreisscheibe und an der kreisförmigen Öffnung im vollkommen leitenden ebenen Schirm. Annalen der Physik, 7, № 3—4, 157, 1950.

25. Andrejewski W. Die Beugung elektromagnetischer Wellen an der leitenden Kreisscheibe und an der kreisförmigen Öffnung im leitenden ebenen Schirm Zeits. für angewandte Physik, 5, № 5, 178, 1953.

26. Meixner J., und Schäfke F. W. Mathieusche Funktionen und Sphäroidfunktionen. Springer-Verlag, 1954.
27. Ландсберг Г. С. Оптика. ГИТТЛ, 1954
28. Braunbek W. Neue Näherungsmethode für die Beugung am ebenen Schirm. Zeits für Physik, 127, 1, 381—390, 1950.
29. Braunbek W. Zur Beugung an der Kreisscheibe. Zeits. für Phys., 127, 4, 405—415, 1950.
30. Braunbek W. Zur Beugung an der kreisförmigen Öffnung. Zeits. für Physik, 138, 1, 80—88, 1954.
31. Braunbek W. Zur Beugung an Öffnungen in nichtebenen Schirmen. Zeits. für Physik, 156, 1, 65, 1959.
32. Frahn W. E. Beugung elektromagnetischer Wellen in Braunbekscher Näherung. I. Zeits. für Physik, 156, 1, 78, 1959.
33. Frahn W. E. Beugung elektromagnetischer Wellen in Braunbekscher Näherung. II. Zeits. für Phys., 156, № 2, 99, 1959.
34. Белкина М. Г. Дифракция электромагнитных волн на диске. В сб. «Дифракция электромагнитных волн на некоторых телах вращения». Изд-во «Советское радио», 1957, (стр. 148—174).
35. Иванов В. И. Коротковолновая асимптотика дифракционного поля в тени идеально проводящего параболического цилиндра. «Радиотехника и электроника», 5, № 3, 393—402, 1960.
36. Иванов В. И. Дифракция коротких плоских электромагнитных волн на гладком выпуклом цилиндре при наклонном падении. «Радиотехника и электроника», 5, № 3, 524—528, 1960.
37. Горянов А. С. Асимптотическое решение задачи о дифракции плоской электромагнитной волны на проводящем цилиндре. «Радиотехника и Электроника», 3, № 5, 603—614, 1958.
38. Felsen L. B. Backscattering from wide-angle and narrow-angle cones Journ. Appl. Phys. 26, № 3, 138—151, 1955.
39. Siegel K. M. Crispin J. W. and Schensted C. E Electromagnetic and acoustical scattering from a semi-infinite cone Journ. Appl. Phys., 26, № 3, 309—313, 1955.
40. Горянов А. С. Дифракция плоской электромагнитной волны, распространяющейся вдоль оси конуса. «Радиотехника и электроника», 6, № 1, 47—57, 1961.
41. Siegel K. M., Goodrich R. F., Weston V. H. Comments on far field scattering from bodies of revolution. Appl. Sci. Res., Section B. volume 8, p. 8, 1959.
42. Keller J. B. Diffraction by a convex cylinder. Trans. IRE, AP-4, № 3, 312—321, 1956.
43. Keller J. B. Diffraction by an aperture, I. Journal of Appl. Phys., 28, № 4, 426—444, 1957. Diffraction by an aperture, II. Journ. Appl. Phys., 28, № 5, 570—579, 1957.
44. Keller J. B. Backscattering from a finite coue. Trans. IRE, AP-8, № 2, 175—182, 1960. Backscattering from a finite cone—comparison of theory and experiment, Trans. IRE, AP-9, № 4, 411, 1961.
45. Schensted C. E. Electromagnetic and acoustic scattering by a semi-infinite body of revolution. Journ. Appl. Phys., 26, № 3, 306—308, 1955.
46. Clemmow P. C. Edge currents in diffraction Theory. Transactions IRE, Antennas and Propagation, AP-4, № 3, 282—287, 1956.
47. Millar R. F. An approximate theory of the diffraction of an electromagnetic wave by an aperture in a plane screen. Proc. Inst. Electrical Enges., Part C, 103, № 3, 177, 1956.
48. Millar R. F. The diffraction of an electromagnetic wave by a circular aperture. Proc. Inst. Electrical Engrs., Part C, 104, № 5, 1957.
49. Millar R. F. The diffraction of an electromagnetic wave by a large aperture. Proc. Inst. Electrical Engrs., Part C, 104, № 6, 1957.
50. Handbuch der Physik. Bd 25/1. Kristalloptik. Beugung. Berlin, Springer, 1961. H. Hönl, A. W. Maue, K. Westpfahl. Theorie der Beugung (S. 218—592).
51. Karp S. N. and Russek A. Diffraction by a wide slit, Journal of Applied Physics, 27, № 8, 886—891, 1956.
52. Buchal R. N. and Keller J. B. Boundary Layer Problems in Diffraction Theory. Commun. Pure and Appl. Mathem., 13, № 1, 85—114, 1960.

53. Гринберг Г. А. Новый метод решения задачи дифракции электромагнитных волн на плоскости с бесграничной прямолинейной щелью и родственных ей проблем. ЖТФ, 27, № 11, 2595—2605, 1957.

54. Гринберг Г. А. Метод решения дифракционных задач для плоских идеально проводящих экранов, основанный на изучении наводимых на экранах теневых токов. ЖТФ, 28, № 3, 542—554, 555—568, 1958.

55. Гринберг Г. А. О дифракции электромагнитных волн на полосе конечной ширины. ДАН СССР, 129, № 2, 295—298, 1959.

56. Гринберг Г. А. и Пименов Ю. В. К вопросу о дифракции электромагнитных волн на идеально проводящей плоскости с круглым отверстием. Ж. Т. Ф. 29, № 10, 1206—1211, 1959.

57. Гринберг Г. А. и Колесникова Э. М. К вопросу о дифракции электромагнитных волн на идеально проводящем плоском кольце. ЖТФ, 31, № 1, 13—17, 1961.

58. Millar R. F. Diffraction by a wide slit and complementary strip. Proc. Cambridge Philosophical Society, 54, 1, 479—496, 497—511, 1958.

59. Кинг Р. и Тай-Цзунь. Рассеяние и дифракция электромагнитных волн. Перевод с английского под редакцией Э. Л. Бурштейна. Изд-во иностранной литературы, 1962.

60. Кинбер Б. Е. О боковом излучении зеркальных антенн «Радиотехника и электроника», № 1, 515—558, 1961.

61. Кинбер Б. Е. Развязка между близко расположенными зеркальными антеннами. «Радиотехника и электроника», 6 № 6, 907—916, 1961.

62. Кинбер Б. Е. О дифракции электромагнитных волн на вогнутой поверхности кругового цилиндра. «Радиотехника и электроника», 6, № 8, 1273—1283, 1961.

63. Кинбер Б. Е. О дифракции электромагнитных волн на вогнутой поверхности сферы. «Радиотехника и электроника», 6, № 10, 1652—1657, 1961.

64. Фок В. А. Теория дифракции от параболоида вращения. Сборник «Дифракция электромагнитных волн на некоторых телах вращения». Изд-во «Советское радио», 1957.

65. Фок В. А. и Федоров А. А. Дифракция плоской электромагнитной волны на идеально проводящем параболоиде вращения. ЖТФ, 28, № 11, 2518—2566, 1958.

66. Фок В. А. Поле от вертикального и горизонтального диполя, приподнятого над поверхностью земли. ЖЭТФ, 19, № 10, 916—929, 1949.

67. Леонтович М. А. Об одном методе решения задач о распространении электромагнитных волн вдоль поверхности земли. Изв. АН СССР, сер. физ. 8, 16—22, 1944.

68. Леонтович М. А. и Фок В. А. Решение задачи о распространении электромагнитных волн вдоль поверхности земли по методу параболического уравнения. ЖЭТФ, 16, № 7, 557—573, 1946.

69. Фок В. А. Теория распространения радиоволн в неоднородной атмосфере для приподнятого источника. Изв. АН СССР, 14, № 1, 70—94, 1950.

70. Фок В. А. Поле плоской волны вблизи поверхности проводящего тела. Изв. АН СССР, сер. физ. 10, № 2, 171—185, 1946.

71. Вайнштейн Л. А., Федоров А. А. Рассеяние плоских и цилиндрических волн на эллиптическом цилиндре и концепция дифракционных лучей. «Радиотехника и электроника», 6, № 1 31—46, 1961.

72. Малюжинец Г. Д. и Вайнштейн Л. А. Поперечная диффузия при дифракции на импедансном цилиндре большого радиуса. ч. I. Параболическое уравнение в лучевых координатах «Радиотехника и электроника», 6, № 8, 1247—1258, 1961.

73. Вайнштейн Л. А., Малюжинец Г. Д. Поперечная диффузия при дифракции на импедансном цилиндре большого радиуса. ч. II. Асимптотические законы дифракции в лучевых координатах. «Радиотехника и электроника», 6, № 9, 1189—1195, 1961.

74. Федоров А. А. Асимптотическое решение задачи о дифракции плоской электромагнитной волны на идеально проводящей

сфере. «Радиотехника и электроника», 3, № 12, 1451—1462, 1958
75. Chytil B. The depolarisation of electromagnetic waves backscattering from certain bodies. Práce URE—ČSAV, № 17, Praha, 1961.
76. Chytil B. Depolarisation by randomly spaced scatterers. Práce URE—ČSAV, № 20, Praha, 1961.
77. Chytil B. Polarisation dependent scattering cross-sections. Práce URE—ČSAV, № 21, Praha, 1961.
78. Beckmann P. The depolarisation of electromagnetic waves by inclined planes. Práce URE—ČSAV, № 19, Praha, 1961.
79. Landroth K. Reflection of electromagnetic waves from thin metal strips. Trans. Roy. Inst. of Technol., Stockholm, Sweden, № 91, 1955.
80. Hallén E. Theoretical investigations into the transmitting and receiving qualities of antennae. Nova Acta Roy. Soc. Sci., Upsala (4), vol. 11, Ser. IV, 1938.
81. Вайнштейн Л. А. Волны тока в тонком цилиндрическом проводнике. I. Ток и импеданс передающего вибратора. ЖТФ, 29, № 6, 673—688, 1959.
82. Вайнштейн Л. А. Волны тока в тонком цилиндрическом проводнике. II. Ток в пассивном вибраторе и излучение передающего вибратора. ЖТФ, 29, № 6, 689—699, 1959.
83. Вайнштейн Л. А. Волны тока в тонком цилиндрическом проводнике. III. Вариационный метод и его применение к теории идеального и импедансного проводов. ЖТФ, 31, № 1, 29—44, 1961.
84. Вайнштейн Л. А. Волны тока в тонком цилиндрическом проводнике. IV. Входной импеданс вибратора и точность формул. ЖТФ, 31, № 1, 45—50, 1961.
85. Леонтович М. А. и Левин М. Л. К теории возбуждения колебаний в вибраторах антенн. ЖТФ, 14, № 9, 481—506, 1944.
86. Van Vleck J. H., Bloch F. and Hamermesh M. Theory of radar reflection from wires or thin metallic strips. Journ. Appl. Phys., 18, № 3, 274—294, 1947.
87. Tai C. T. Electromagnetic back-scattering from cylindrical wires. Journ. Appl. Phys., 23, № 9, 903—916, 1952.
88. Капица П. Л., Фок В. А. и Вайнштейн Л. А. Симметричные колебания идеально проводящего полого цилиндра конечной длины. ЖТФ, 29, № 10, 1188—1205, 1959.
89. Говорун Н. Н. Численное решение интегрального уравнения первого рода для плотности тока в антенне — теле вращения. «Журнал вычислительной математики и математической физики», 1, № 4, 664—679, 1961.
90. Hallén E. Exact Solution of the Antenna Equation. Transactions of the Royal Institute of Technology, Stockholm, Sweden, Nr 193, 1961.
91. Duncan R. H. and Hinchey F. A. Cylindrical Antenna Theory. J. Research Nat. Bur. Standards 64D, 569, 1960.
92. Вайнштейн Л. А. Статические задачи для полого цилиндра конечной длины (II. Численные результаты; III. Приближенные формулы). ЖТФ, 32, № 10, 1962

SYMBOL LIST

Russian	Typed	Meaning
Ц	c	cylindrical
Д	d	disk